

Some pages of this thesis may have been removed for copyright restrictions.

If you have discovered material in Aston Research Explorer which is unlawful e.g. breaches copyright, (either yours or that of a third party) or any other law, including but not limited to those relating to patent, trademark, confidentiality, data protection, obscenity, defamation, libel, then please read our [Takedown policy](#) and contact the service immediately (openaccess@aston.ac.uk)

**DOWN-REGULATION OF CENTRAL
GLUCOCORTICOID RECEPTOR EXPRESSION USING
ANTISENSE OLIGONUCLEOTIDE TECHNOLOGY**

AMINUL ISLAM

Doctor of Philosophy

ASTON UNIVERSITY

November 2000

This copy of the thesis has been supplied on condition that anyone who consults it is understood to recognise that its copyright rests with its author and that no quotation from this thesis and no information derived from it may be published without proper acknowledgement.

Dedicated to my mum and dad

ASTON UNIVERSITY

DOWN-REGULATION OF CENTRAL GLUCOCORTICOID RECEPTOR EXPRESSION USING ANTISENSE OLIGONUCLEOTIDE TECHNOLOGY

AMINUL ISLAM

Doctor of philosophy

November 2000

SUMMARY

Endogenous glucocorticoids and serotonin have been implicated in the pathophysiology of depression, anxiety and schizophrenia. This thesis investigates the potential of downregulating expression of central Type II glucocorticoid receptors (GR) both *in vitro* and *in vivo*, with empirically-designed antisense oligodeoxynucleotides (ODN), to characterise GR modulation of 5-HT_{2A} receptor expression using quantitative RT-PCR, Western blot analysis and radioligand binding. The functional consequence of GR downregulation is also determined by measuring 1-(2,5-dimethoxy 4-iodophenyl)-2-amino propane hydrochloride (DOI) mediated 5-HT_{2A} receptor specific headshakes. Using a library of random antisense ODN probes, RNase H accessibility mapping of T7-primed, *in vitro* transcribed GR mRNA revealed several potential cleavage sites and identified an optimally effective GR antisense ODN sequence of 21-mer length (GRAS5). *In vitro* efficacy studies using rat C6 glioma cells showed a 56% downregulation in GR mRNA levels and 80% downregulation in GR protein levels. In the same cells a 29% upregulation in 5-HT_{2A} mRNA levels and 32% upregulation in 5-HT_{2A} protein levels was revealed. This confirmed the optimal nature of the GRAS5 sequence to produce marked inhibition of GR gene expression, and also revealed GR modulation of the 5-HT_{2A} receptor subtype in C6 glioma cells to be a tonic repression of receptor expression. The distribution of a fluorescently-labelled GRAS5 ODN was detected in diverse areas of the rat brain after single ICV administration, although this fluorescence signal was not sustained over a period of 5 days. However, fluorescently-labelled GRAS5 ODN, when formulated in polymer microspheres, showed diverse distribution in the brain which was maintained for 5 days following a single ICV administration. This produced no apparent neurotoxic effects on rat behaviour and hypothalamic-pituitary-adrenal (HPA) axis homeostasis. Furthermore, a single polymer microsphere injection ICV proved to be an effective means of delivering antisense ODNs and this was adopted for the *in vivo* efficacy studies. *In vivo* characterisation of GRAS5 revealed marked downregulation of GR mRNA in rat brain regions such as the frontal cortex (26%), hippocampus (35%), and hypothalamus (39%). Downregulation of GR protein was also revealed in frontal cortex (67%), hippocampus (76%), and hypothalamus (80%). In the same animals upregulation of 5-HT_{2A} mRNA levels was shown in frontal cortex (13%), hippocampus (7%), and hypothalamus (5%) while upregulation in 5-HT_{2A} protein levels was shown in frontal cortex (21%). This upregulation in 5-HT_{2A} receptor density as a result of antisense-mediated inhibition of GR was further confirmed by a 55% increase in DOI-mediated 5-HT_{2A} receptor specific headshakes. These results demonstrate that GR is involved in tonic inhibitory regulation of 5-HT_{2A} receptor expression and function *in vivo*, thus providing the potential to control 5-HT_{2A}-linked disorders through corticosteroid manipulation. These experiments have therefore established an antisense approach which can be used to investigate pharmacological characteristics of receptors.

KEYWORDS: Antisense oligonucleotides, GR, 5-HT_{2A}, CNS delivery, antisense design.

ACKNOWLEDGEMENTS

The work in this thesis was jointly funded by a case award from the Engineering and Physical Sciences Research Council (EPSRC) and BASF Pharma, Research and Development, Nottingham.

I gratefully acknowledge and thank my supervisor Dr. Sheila Handley for all her help and selfless efforts in steering me in the right direction and giving me invaluable advice, encouragement and critique at a personal level which I hope will make me a better, more rounded research scientist. Only time will tell. Like she predicted, my time at aston under her guidance was like an old fashioned apprenticeship which has definitely benefited me and has equip me with the necessary skills to face the unpredictable, but exciting world of research.

I thank my external supervisor Dr. Kevin Thompson for all his genuine interest, enthusiasm, help and advice beyond the call of duty and therefore making my studies a most enjoyable and productive experience. I also greatly appreciate the help and advice from the people at BASF pharma during my time there, in particular Dr. Sue Aspley, Dr. Sharon Cheetham and Mrs Jean Viggers.

I acknowledge my co-supervisor Dr. Saghir Akhtar for his help, expertise and for his own particular brand of supervision and assistance throughout my time at aston. I also kindly acknowledge the following people for their advice and assistance with the technical aspects of my thesis: Alan Richardson and Chris Bache for general laboratory matters, Leslie Tompkinson for immuno-electron microscopy, Mel Gamble, Brian Burford and the gang for animal house related studies, Dr. David Poyner for radioligand binding assay and last but by no means least, Graham Smith for high quality reprographics.

Finally, I would like to thank all my laboratory friends, colleagues and associates for all their help, good humour and witty sarcasm over the past 3 years.

LIST OF CONTENTS

TITLE PAGE	1
THESIS SUMMARY	3
ACKNOWLEDGEMENTS	4
LIST OF CONTENTS	5
LIST OF FIGURES	10
LIST OF TABLES	19
LIST OF ABBREVIATIONS	21
CHAPTER ONE: GENERAL INTRODUCTION	
1.1 Introduction	23
1.2 Application of Antisense Technology	23
1.3 Antisense Technology	24
1.4 Antisense ODN Stability and Analogue Selection	27
1.5 Antisense Strategies in Studying Receptor Function	28
1.6 Antisense Selection and Delivery	29
1.6.1 Cellular Delivery of ODNs	29
1.6.2 Selecting Optimal Antisense Sequences	35
1.7 The Hypothalamic-Pituitary-Adrenal (HPA) Axis	37
1.7.1 Organisation of the HPA Axis	37
1.7.2 Regulation of the Circadian Rhythm in HPA Axis Activity	37
1.7.3 Regulation of Stress-Induced HPA Axis Activity	39
1.7.4 Central Corticosteroid Receptor Types	40
1.7.5 MR and GR Regulation of the HPA axis	41
1.7.6 Molecular Mechanisms of MR and GR Action	42
1.8 Regulation of 5-HT Receptors and the HPA Axis	45
1.8.1 CNS Serotonergic System	45
1.8.2 Central 5-HT _{1A} and 5-HT _{2A} Receptors	46
1.8.3 Serotonin and HPA Axis Function	48
1.8.4 5-HT _{1A} Receptors and the HPA Axis	49
1.8.5 5-HT _{2A} Receptors and the HPA Axis	51
1.8.6 Cellular Regulation of 5-HT _{2A} Receptor mRNA	52
1.8.7 Central 5-HT _{2A} Receptor Functions	53
1.8.8 GR-HPA Axis Related Gene Expression Studies	54
1.8.9 GR Control of 5-HT _{2A} Receptor Gene Expression	57
1.9 Analysis of Antisense Studies	58
1.10 Antisense Oligonucleotide Clinical Trials	61
1.11 Aims and Objectives	62

CHAPTER TWO: MATERIALS AND METHODS

2.1	Materials	64
2.2	Methods	64
2.2.1	Cell Culture Techniques	64
2.2.1.1	Cell Line	64
2.2.1.2	Passaging Attached Cells	65
2.2.1.3	Freezing Cell Lines in Liquid Nitrogen	65
2.2.1.4	Recovery of Cell Lines from Liquid Nitrogen	66
2.2.1.5	Determining Total Cell Counts and Viable Cell Number	66
2.2.2	Oligodeoxynucleotide Synthesis and Purification	67
2.2.2.1	Preparation of the Automated DNA/RNA Synthesiser	67
2.2.2.2	Phosphorothioate Oligodeoxynucleotide Synthesis	68
2.2.2.3	Calculation of Coupling Efficiency and Overall Yield of ODN Synthesis	69
2.2.2.4	Purification of Oligodeoxynucleotides	70
2.2.2.5	Quantification of Oligodeoxynucleotides	70
2.2.3	Labelling of Synthesised Nucleic Acids	72
2.2.3.1	5'-End [³² P] Radiolabelling of Oligodeoxynucleotides	72
2.2.3.2	5'-End Fluorescein Labelling of Oligodeoxynucleotides	72
2.2.3.3	5'-End Biotinylation of Oligodeoxynucleotides	73
2.2.4	Purification of Labelled Oligodeoxynucleotides	73
2.2.4.1	Polyacrylamide Gel Electrophoresis (PAGE)	73
2.2.4.2	Autoradiography	75
2.2.4.3	Radiolabelled Oligodeoxynucleotide Purification by PAGE	75
2.2.5	Cell Association/Uptake Studies	76
2.2.5.1	Cell Association/Uptake of Oligodeoxynucleotides	76
2.2.5.2	Liquid Scintillation Counting	77
2.2.5.3	The Effect of Cell Concentration on Cellular Association/Uptake	77
2.2.5.4	The Effect of Time on Cellular Association/Uptake	77
2.2.5.5	The Effect of pH on Cellular Association/Uptake	77
2.2.5.6	The Effect of Temperature on Cellular Association/Uptake	78
2.2.6	Cellular Efflux Studies	78
2.2.7	Fluorescent Localisation Studies	78
2.2.7.1	Preparation of Fluorescent Materials	78
2.2.7.2	Cell Association of Fluorescently Labelled Probes	79
2.2.7.3	Fluorescence Microscopy	80
2.2.8	Ultrastructural Studies	80
2.2.8.1	Ultrastructural Localisation of Biotinylated Materials	80
2.2.8.2	Incubation of Cells for Immunocytochemical Studies	81
2.2.8.3	Fixation for Immunoelectron Microscopy	82
2.2.8.4	Dehydration of Fixed Cells by the Progressive Lowering Temperature (PLT) Method	82
2.2.8.5	Embedding and Sectioning of Dehydrated Cells in Acrylic Resin	83
2.2.8.6	Immunocytochemical Labelling of Biotin Antigens within Cell Section	84
2.2.8.7	Cell Staining and Examination by Electron Microscopy	86
2.2.9	Lipid Mediated Delivery of Oligodeoxynucleotides	86
2.2.9.1	Preparation of Lipid- Oligodeoxynucleotide Complexes (Lipoplexes)	86
2.2.9.2	Calculation of Lipid- Oligodeoxynucleotide Charge Ratios	87

2.2.9.3	The Effect of Different Charge Ratios on Cellular Association/Uptake	87
2.2.9.4	The Effect of Different Lipid Concentrations on Cellular Viability	88
2.2.9.5	The Effect of Different ODN Concentrations on Cellular Association/Uptake	88
2.2.9.6	The Effect of Time on Lipid-ODN Complex Cellular Association/Uptake	88
2.2.9.7	The Effect of Optimised Lipid-ODN Ratio on Cellular Viability	88
2.2.10	Radioligand Binding Assays	89
2.2.10.1	Preparation of the Separating Columns for Glucocorticoid Receptor (GR) Competition Binding Studies	89
2.2.10.2	Competition Binding Assay for Glucocorticoid Receptors (GR)	90
2.2.10.3	5-HT _{2A} Receptor Membrane Preparation from C6 Glioma Cells	90
2.2.10.4	5-HT _{2A} Receptor Membrane Preparation from Rat Brain Tissue	91
2.2.10.5	Saturation Binding Assay for 5-HT _{2A} Receptors	91
2.2.11	Western Blot Analysis of Glucocorticoid Receptor Protein Levels	91
2.2.11.1	Preparation of Protein Samples	92
2.2.11.2	Electrophoretic Separation and Western Blotting	92
2.2.11.3	Detection of Glucocorticoid Receptor (GR) Protein	93
2.2.11.4	Detection of Total Protein Blotted onto Nitrocellulose Membrane	93
2.2.11.5	Detection of Total Protein in Electrophoresis Gels	93
2.2.12	Protein Determination	94
2.2.13	Reverse Transcriptase Polymerase Chain Reaction (RT-PCR) Analysis of GR, 5-HT _{2A} Receptor and β -actin mRNA Expression	94
2.2.13.1	Extraction of RNA	94
2.2.13.2	Agarose Gel Electrophoresis	95
2.2.13.3	Oligonucleotide PCR Primers	95
2.2.13.4	Reverse Transcription (RT)	96
2.2.13.5	Quantitative Competitive Polymerase Chain Reaction (PCR)	97
2.2.14	Probing Accessible Sites for Antisense Oligonucleotides on GR mRNA	97
2.2.14.1	Antisense ODNs and ODN Library Synthesis	97
2.2.14.2	T7 Promoter Site RT-PCR	98
2.2.14.3	<i>In Vitro</i> Transcription	98
2.2.14.4	RNAse H Mapping of Antisense ODN Accessible Sites	99
2.2.14.5	<i>In Vitro</i> Treatment of C6 Glioma Cells with Designed Antisense ODNs	99
2.2.15	Preparation of ODN Loaded Microspheres	99
2.2.15.1	Double Emulsion Method of Preparing Loaded Microspheres	100
2.2.15.2	Scanning Electron Microscopy (SEM) of Microspheres	100
2.2.15.3	Microsphere Particle Size Determination	101
2.2.16	Surgical Procedure for ICV Administration	101
2.2.17	Cryostat Sectioning of Rat Brain	102
2.2.18	Preparation of Tissue Sections for Fluorescence Microscopy	102
2.2.19	Staining of Tissue Sections for Microscopy	103
2.2.19.1	Cresyl Fast Violet Technique for Nissl Substance	103
2.2.19.2	Intracerebroventricular (ICV) Injection of Fluorescent Probes	103
2.2.20	Animal Post-operative Well-being Assessment	104
2.2.21	DOI Induced Rat Head-Shake Observations	106
2.2.22	<i>In Vivo</i> ODN Stability Studies	107
2.2.23	Statistics	107

CHAPTER THREE: UPTAKE AND SUB-CELLULAR TRAFFICKING OF ANTISENSE OLIGODEOXYNUCLEOTIDES

3.1	Introduction	108
3.2	Methods	111
3.3	Results	112
3.3.1	Cell Association/Uptake Studies	112
3.3.2	Lipid Mediated Delivery of Oligodeoxynucleotides	115
3.3.2.1	Cellular Association/Uptake of Lipid-ODN Complexes	115
3.3.2.2	Effect of Time on Lipid-ODN Complex Cellular Association and Cytotoxicity	116
3.3.2.3	Effect of Different Lipid Concentrations on Cellular Viability	118
3.3.3.1	Effect of Different ODN Concentrations on Cellular Association/Uptake	118
3.3.3.2	Cellular Efflux Studies	119
3.3.4	Fluorescent Localisation Studies	121
3.3.4.1	Time-dependent Subcellular Trafficking of Fluorescein-labelled Lipid-ODN Complexes	125
3.3.5	Ultrastructural Trafficking of Biotin-Labelled Lipid-ODN Complexes	127
3.4	Discussion	131

CHAPTER FOUR: DESIGN AND SELECTION OF ANTISENSE OLIGODEOXYNUCLEOTIDES

4.1	Introduction	135
4.2	Methods	137
4.3	Results	137
4.3.1	Synthesis of GR cDNA Template	137
4.3.2	PCR Product Verification Using Single Strand Sequencing	139
4.3.3	Synthesis of 5'-Radiolabelled GR RNA Transcript	139
4.3.4	Identification of RNase H Accessible Sites	139
4.3.5	Design and <i>In Vitro</i> Screening of Antisense ODNs	141
4.3.6	Assessment of Mapping and <i>In Vitro</i> RNase H Experimental Conditions	144
4.3.7	Optimisation of Antisense ODN Length in Mapping and <i>In Vitro</i> RNase H Reactions	148
4.3.8	Assessment of the Activity of Selected GR Antisense Designs	149
4.3.9	Assessment of Alternative GR mRNA Accessible Sites	151
4.3.10	Design and Assessment of Control Antisense ODN Sequences Using Mapping and <i>In Vitro</i> RNase H Reactions	153
4.3.11	Comparison of Actual and <i>mfold</i> Computer mRNA folding Algorithms on Accessible Sites in the T7-GR mRNA Transcript.	154
4.3.12	Analysis of Antisense Design Sequences	157
4.4	Discussion	158

CHAPTER FIVE: *IN VITRO* EFFECTS OF ANTISENSE

OLIGODEOXYNUCLEOTIDES TARGETING THE GLUCOCORTICOID RECEPTOR

5.1	Introduction	160
5.2	Methods	162
5.3	Results	163
5.3.1	<i>In Vitro</i> Stability of PS Oligodeoxynucleotides	163
5.3.2	Effect of Different GRAS5 ODN Concentrations on Cellular Viability	164
5.3.3	<i>In Vitro</i> Assessment of ODN Treatment on GR mRNA Expression Using Quantitative RT-PCR	165
5.3.4	<i>In Vitro</i> Assessment of ODN Treatment on 5-HT _{2A} Receptor mRNA Expression Using Quantitative RT-PCR	168
5.3.5	<i>In Vitro</i> Assessment of ODN Treatment on GR Protein Expression Using Radioligand Binding Assays	169
5.3.6	<i>In Vitro</i> Assessment of ODN Treatment on 5-HT _{2A} Receptor Protein Expression Using Radioligand Binding Assays	171
5.4	Discussion	173

CHAPTER SIX: *IN VIVO* EFFECTS OF ANTISENSE

OLIGODEOXYNUCLEOTIDES TARGETING THE GLUCOCORTICOID RECEPTOR

6.1	Introduction	177
6.2	Methods	180
6.3	Results	181
6.3.1	Oligonucleotide Synthesis and Preparation of Microspheres	181
6.3.2	Preliminary Assessment of GRAS5 ODN Treatment	183
6.3.2.1	Preliminary Well-being Assessments	184
6.3.2.2	Histological Examination	184
6.3.2.3	<i>In Vivo</i> Oligonucleotide Stability	192
6.3.2.4	<i>In Vivo</i> Fluorescent Localisation Studies	193
6.3.3	<i>In Vivo</i> Assessment of GRAS5 ODN Treatment	200
6.3.3.1	<i>In Vivo</i> Treatment Design and Groups	200
6.3.3.2	Animal Post-operative Well-being Assessment	201
6.3.3.3	<i>In Vivo</i> Assessment of GRAS5 Treatment Using Quantitative RT-PCR	204
6.3.3.4	<i>In Vivo</i> Assessment of GRAS5 Treatment Using Radioligand Binding Assays	208
6.3.4	Functional Consequences of GRAS5 ODN Treatment Assessed by Behavioural Observations	211
6.3.4.1	Animal Post-operative Well-being Assessment	212
6.3.4.2	<i>In Vivo</i> Assessment of GRAS5 Treatment Using Western Blot Analysis	213
6.3.4.3	DOI Induced Rat Head-Shake Observations	217
6.4	Discussion	221

CHAPTER SEVEN: GENERAL DISCUSSION

APPENDIX I: Publications

REFERENCES

228
240
241

LIST OF FIGURES

1.1	Some potential sites of oligonucleotide directed sequence specific inhibition of the flow of information from DNA to protein.	25
1.2	The structures of the common nucleic acid analogues.	26
1.3	Illustration representing the mechanisms necessary for successful cellular uptake of antisense ODNs using cationic liposomes.	32
1.4	Schematic representation of the degradation of polymer microspheres and subsequent release of entrapped antisense ODN molecules.	33
1.5	Schematic representation of the main mechanisms associated with antisense ODN activity.	36
1.6	The complex network of physiological regulation by glucocorticoids within the HPA axis.	38
1.7	Location of functional regions in a typical steroid receptor.	43
1.8	Molecular pathway for steroid hormone action.	43
1.9	Adaptation illustrating the distribution of the main 5-HT containing pathways and the 5-HT containing midline raphe nuclei in the rat brain.	46
1.10	Illustration representing the pathways that leads to increases in the levels of 5-HT _{2A} receptor mRNA in cells.	52
3.1	Effect of C6 glioma cell concentration on the cellular association/uptake of 1 μ M 15-mer PS ODN in SFM at 37°C and incubated for 1 hour at pH 7.2.	112
3.2	Graph showing percentage cellular association/uptake of 1 μ M 15-mer PS ODN in SFM at 37°C and incubated for 1 hour at pH 7.2 per C6 glioma cell.	113
3.3	Effect of incubation times on C6 glioma cellular association/uptake of 1 μ M 15-mer PS ODN in SFM at 37°C and pH 7.2 using 2.5x10 ⁵ cells/mL.	113
3.4	Effect of pH on C6 glioma cellular association/uptake of 1 μ M 15-mer PS ODN in SFM at 37°C and 1 hour incubation using 2.5x10 ⁵ cells/mL.	114
3.5	Effect of temperature on C6 glioma cellular association/uptake of 1 μ M 15-mer PS ODN in SFM at 37°C and 1 hour incubation using 2.5x10 ⁵ cells/mL.	114

3.6	Effect of Lipofectamine:ODN charge ratio on the cellular association/uptake of ODN.	115
3.7	Effect of time on the cellular association/uptake (A) and viability (B) of Lipofectamine:ODN complex at 1:1 charge ratio.	117
3.8	Effect of Lipofectamine concentrations on C6 glioma cellular viability in SFM at 37°C and pH 7.2 during 1 hour incubation using 2.5×10^5 cells/mL.	118
3.9	Effect of ODN concentrations on C6 glioma cellular association/uptake of 15-mer PS ODN in SFM at 37°C and pH 7.2 during 1 hour incubation using 2.5×10^5 cells/mL.	119
3.10	Graph demonstrating the rate of loss of radiolabelled compounds from cells over a 5 hour time period following 2 hours steady state accumulation.	120
3.11	Phase contrast images of C6 glioma cells incubated for 4 hours in SFM at 37°C.	121
3.12	Fluorescence detection of 5µM free FITC label associated with C6 glioma cells during 4 hours incubation at 37°C in SFM.	123
3.13	Fluorescence detection of 5µM RITC-dextran associated with C6 glioma cells during 4 hours incubation at 37°C in SFM.	124
3.14	Fluorescence detection of 5µM FITC-labelled 15-mer PS ODN associated with C6 glioma cells during 4 hours incubation at 37°C in SFM.	124
3.15	Fluorescence detection of 5µM FITC-labelled 15-mer PS ODN in the lipid-ODN complex at 1:1 charge ratio after 15 minutes incubation at 37°C in SFM.	125
3.16	Fluorescence detection of 5µM FITC-labelled 15-mer PS ODN in the lipid-ODN complex at 1:1 charge ratio after 60 minutes incubation at 37°C in SFM.	126
3.17	Transmission electron micrographs visualising ultrastructural features of C6 glioma cells.	127
3.18	Transmission electron micrographs visualising the uptake and subcellular trafficking of biotinylated PS ODNs in C6 glioma cells.	128
3.19	Transmission electron micrographs visualising the uptake and sub-cellular trafficking of biotinylated PS ODNs in C6 glioma cells.	129
3.20	Transmission electron micrographs visualising release of biotinylated PS ODN from a disrupted (arrow head) endosomal vesicular body (vb) in C6 glioma cells.	130

4.1	Representative gel electrophoresis of total RNA (1µg per lane) isolated from C6 glioma cells.	138
4.2	Representative gel electrophoresis of T7-GR RT-PCR products (12µg of cDNA per lane) obtained.	138
4.3	The nucleotide sequence of the generated GR cDNA fragment as verified by single stranded sequencing.	138
4.4	Autoradiogram of <i>in vitro</i> transcribed GR RNA fragment (0.1µmole per lane) subjected to 6% denaturing PAGE at 25 watts for 2.5 hours.	139
4.5	Autoradiogram of GR RNA fragments showing RNase H mediated cleavage at accessible sites A-D due to ODN:RNA hybridisation.	140
4.6	Densitometric analysis of cleavage bands, relative to intact GR mRNA transcript, corresponding to accessible sites A-D as shown in figure 4.5.	140
4.7	Antisense ODN designs GRAS1-10 designed against the GR mRNA sequences around accessible site D. Predicted cleavage site is approximated to occur at base 1170 and is indicated by the scissors.	141
4.8	Autoradiogram of GR RNA fragments showing cleavage potency by the GRAS designs shown in figure 4.7.	143
4.9	Densitometric analysis of cleavage bands, relative to intact GR mRNA transcript, illustrating RNA cleavage potency by 21-mer PS ODN GR antisense (GRAS) designs as shown in figure 4.8.	143
4.10	Autoradiogram of GR RNA fragments showing RNase H concentration dependent cleavage in the presence of GRAS5 due to ODN:RNA hybridisation.	144
4.11	Densitometric analysis of cleavage bands, relative to intact GR mRNA transcript, illustrating effect of RNase H concentration on cleavage efficiency as shown in figure 4.10.	144
4.12	Autoradiogram of GR RNA fragments showing RNase H concentration dependent cleavage at accessible site D due to ODN:RNA hybridisation.	145
4.13	Densitometric analysis of cleavage bands, relative to intact GR mRNA transcript, illustrating effect of RNase H concentration on cleavage efficiency as shown in figure 4.12.	145
4.14	Autoradiogram of GR RNA fragments showing incubation time dependent cleavage in the presence of GRAS5 due to ODN:RNA hybridisation.	146

4.15	Densitometric analysis of cleavage bands, relative to intact GR mRNA transcript, illustrating effect of incubation times on cleavage efficiency as shown in figure 4.14.	146
4.16	Autoradiogram of GR RNA fragments showing GRAS5 concentration dependent cleavage due to ODN:RNA hybridisation.	147
4.17	Densitometric analysis of cleavage bands, relative to intact GR mRNA transcript, illustrating effect of GRAS5 concentration on cleavage efficiency as shown in figure 4.16.	147
4.18	Antisense ODNs of varying lengths designed against the GR cDNA sequences corresponding to accessible site D.	148
4.19	Autoradiogram of GR RNA fragments showing sequence length dependent cleavage due to ODN:RNA hybridisation.	149
4.20	Densitometric analysis of cleavage bands, relative to intact GR mRNA transcript, illustrating effect of antisense sequence length on cleavage efficiency as shown in figure 4.19.	149
4.21	Autoradiogram of GR RNA fragments showing GRAS design sequence dependent cleavage due to ODN:RNA hybridisation.	150
4.22	Densitometric analysis of cleavage bands, relative to intact GR mRNA transcript, illustrating effect of antisense design sequence on cleavage efficiency as shown in figure 4.21.	150
4.23	Alignment of antisense sequences listed in tables 4.3 and 4.4 on the predicted nucleotide sequence of the rat GR mRNA/cDNA.	151
4.24	Autoradiogram of GR RNA fragments showing GRAS design sequence dependent cleavage due to ODN:RNA hybridisation.	152
4.25	Densitometric analysis of cleavage bands, relative to intact GR mRNA transcript, illustrating effect of antisense design sequence on cleavage efficiency as shown in figure 4.24.	152
4.26	Autoradiogram of GR RNA fragments showing GRAS design sequence dependent cleavage due to ODN:RNA hybridisation.	153
4.27	Squiggle plot showing the secondary structure of the T7 <i>in vitro</i> transcribed Rat GR mRNA transcript (bases 921-1421), folded using the RNA <i>mfold</i> algorithm.	156
5.1	Autoradiogram of 5'-end ³² P-labelled ODNs showing stability of 21-mer PS GRAS5 ODN (1µM) incubated with C6 glioma cells over 24 hours at 37°C.	163

5.2	Effect of GRAS5 ODN concentrations on C6 glioma cell viability during the 5 day treatment period.	164
5.3	(A) Representative gel electrophoresis of RT-PCR products obtained. (B) Densitometric analysis of GR bands standardised to the mean β -actin band density, illustrating the effect of ODN sequence and dose on the expression of GR mRNA in C6 glioma cells.	165
5.4	(A) Representative gel electrophoresis of RT-PCR products obtained. (B) Densitometric analysis of GR bands standardised to mean β -actin band density, illustrating the effect of ODN sequence on the expression of GR mRNA in C6 glioma cells.	167
5.5	(A) Representative gel electrophoresis of RT-PCR products obtained. (B) Densitometric analysis of 5-HT _{2A} receptor bands standardised to mean β -actin band density, illustrating the effect of ODN sequence and concentration on the expression of GR mRNA in C6 glioma cells.	168
5.6	GR binding in C6 glioma cells following treatment with various ODN sequences.	169
5.7	GR binding in C6 glioma cells following treatment with various ODN sequences.	170
5.8	5-HT _{2A} receptor binding in C6 glioma cells following treatment with various ODN sequences.	171
6.1	Representative scanning electron micrographs of poly D,L-lactide co-glycolide (PL-GA) polymer microspheres containing GRAS5 ODN at different viewing fields.	182
6.2	Representative particle size distribution range for ODN loaded microspheres as measured using a Malvern Mastersizer.	183
6.3	(A) Illustration of ICV administration to left lateral ventricle using coronal section of rat brain highlighting common anatomical regions. (B) the left lateral ventricle using cresyl violet staining. (C) needle tract made by ICV administration of AS treatment using stereotaxic co-ordinates entering the left lateral ventricle.	185
6.4	Representative light microscope photographs of coronal sections of rat brain showing an area of frontal cortex using cresyl violet staining.	186
6.5	Representative light microscope photographs of coronal sections of rat brain showing an area of hippocampus using cresyl violet staining.	187
6.6	Representative light microscope photographs of coronal sections of rat brain showing an area of hypothalamus using cresyl violet staining.	188

6.7	Representative light microscope photographs of coronal sections of rat brain showing an area of cerebellum using cresyl violet staining.	189
6.8	Representative light microscope photographs of coronal sections of rat brain showing an area of striatum using cresyl violet staining.	190
6.9	Representative light microscope photographs of coronal sections of rat brain showing an area of corpus callosum using cresyl violet staining.	191
6.10	Autoradiogram of 5'-end ³² P-labelled ODNs electrophoresed by 20% denaturing PAGE showing stability of 21-mer PS GRAS5 ODN administered ICV in the polymer-complexed form to male Wistar rats and retrieved 24 hours or 5 days following administration.	192
6.11	Autoradiogram of 5'-end ³² P-labelled ODNs electrophoresed by 20% denaturing PAGE showing stability of 21-mer PS GRAS5 ODN administered ICV in the free form to male Wistar rats and retrieved 24 hours following administration.	192
6.12	Fluorescent photomicrograph of a coronal section of rat brain (left hemisphere) 5 days after ICV administration of FITC-labelled GRAS5 ODN.	193
6.13	Fluorescence photomicrographs of coronal sections of rat brain 1 day after ICV administration of FITC-labelled GRAS5 ODN in polymer complexed form.	194
6.14	Fluorescence photomicrographs of coronal sections of rat brain showing fluorescence signal detected in an area of frontal cortex.	195
6.15	Fluorescence photomicrographs of coronal sections of rat brain showing fluorescence signal detected in an area of cerebellum.	195
6.16	Fluorescence photomicrographs of coronal sections of rat brain showing fluorescence signal detected in an area of striatum.	195
6.17	Fluorescence photomicrographs of coronal sections of rat brain showing fluorescence signal detected in an area of frontal cortex 5 days after ICV administration of FITC-labelled GRAS5 ODN in polymer complexed form.	197
6.18	Fluorescence photomicrographs of coronal sections of rat brain showing fluorescence signal detected in an area of hippocampus 5 days after ICV administration of FITC-labelled GRAS5 ODN in polymer complexed form.	198
6.19	Fluorescence photomicrographs of coronal sections of rat brain showing fluorescence signal detected in an area of hypothalamus 5 days after ICV administration of FITC-labelled GRAS5 ODN in polymer complexed form.	199

6.20	Mean body weight measured daily over a 5 day period following ICV administration of AS and FAS treatment groups.	202
6.21	Mean body weight measured daily over a 5 day period following ICV administration of SH, PL, AS and MM treatment groups.	202
6.22	Mean adrenal gland weight 5 days after ICV administration of AS and FAS treatment groups.	203
6.23	Mean adrenal gland weight 5 days after ICV administration of SH, PL, AS and MM treatment groups.	203
6.24	Representative gel electrophoresis of RT-PCR products obtained. (A) Lanes illustrating GR (509 nucleotides) and control β -actin (244 nucleotides) cDNA product bands corresponding to the respective treatment groups shown on the x-axis of the graph below. (B) Lanes illustrating 5-HT _{2A} receptor (216 nucleotides) and control β -actin (244 nucleotides) cDNA product bands corresponding to the respective treatment groups shown on the x-axis of the graph below. (C) Densitometric analysis of GR and 5-HT _{2A} receptor bands standardised to the mean β -actin band density illustrating the effect of treatment group on the expression of GR (black bars) and 5-HT _{2A} receptor (white bars) mRNA in the hypothalamic region of male Wistar rats.	204
6.25	Representative gel electrophoresis of RT-PCR products obtained. (A) Lanes illustrating GR (509 nucleotides) and control β -actin (244 nucleotides) cDNA product bands corresponding to the respective treatment groups shown on the x-axis of the graph below. (B) Lanes illustrating 5-HT _{2A} receptor (216 nucleotides) and control β -actin (244 nucleotides) cDNA product bands corresponding to the respective treatment groups shown on the x-axis of the graph below. (C) Densitometric analysis of GR and 5-HT _{2A} receptor bands standardised to the mean β -actin band density illustrating the effect of treatment group on the expression of GR (black bars) and 5-HT _{2A} receptor (white bars) mRNA in the frontal cortex region of male Wistar rats.	205
6.26	Representative gel electrophoresis of RT-PCR products obtained. (A) Lanes illustrating GR (509 nucleotides) and control β -actin (244 nucleotides) cDNA product bands corresponding to the respective treatment groups shown on the x-axis of the graph below. (B) Lanes illustrating 5-HT _{2A} receptor (216 nucleotides) and control β -actin (244 nucleotides) cDNA product bands corresponding to the respective treatment groups shown on the x-axis of the graph below. (C) Densitometric analysis of GR and 5-HT _{2A} receptor bands standardised to the mean β -actin band density illustrating the effect of treatment group on the expression of GR (black bars) and 5-HT _{2A} receptor (white bars) mRNA in the hippocampal region of male Wistar rats.	206

6.27	Representative gel electrophoresis of RT-PCR products obtained. (A) Lanes illustrating GR (509 nucleotides) and control β -actin (244 nucleotides) cDNA product bands corresponding to the respective treatment groups shown on the x-axis of the graph below. (B) Lanes illustrating 5-HT _{2A} receptor (216 nucleotides) and control β -actin (244 nucleotides) cDNA product bands corresponding to the respective treatment groups shown on the x-axis of the graph below. (C) Densitometric analysis of GR and 5-HT _{2A} receptor bands standardised to the mean β -actin band density illustrating the effect of treatment group on the expression of GR (black bars) and 5-HT _{2A} receptor (white bars) mRNA in the hypothalamic region of male Wistar rats.	207
6.28	GR binding in hypothalamic region of male Wistar rats 5 days after ICV administration of AS (black bars) and FAS (white bars) treatment groups.	208
6.29	GR (black bars) and 5-HT _{2A} receptor (white bars) binding in frontal cortex of male Wistar rats.	209
6.30	GR (black bars) and 5-HT _{2A} receptor (white bars) binding in hippocampi of male Wistar rats.	210
6.31	GR binding in the hypothalami of male Wistar rats.	210
6.32	Mean body weight measured daily over a 5 day period following ICV administration of SH, PL, AS and MM treatment groups.	212
6.33	Mean adrenal gland weight 5 days after ICV administration of SH, PL, AS and MM treatment groups.	213
6.34	Effects of treatment groups on GR protein expression measured by Western blot analysis. (A) Representative Western blot illustrating GR (94 kDa) and control β -actin protein levels in AS and FAS treatment group animals 5 days following ICV administration. (B) Densitometric analysis of GR bands standardised to the mean β -actin band density illustrating the effect of treatment group on the expression of GR protein.	214
6.35	Effects of treatment groups on GR protein expression measured by Western blot analysis. (A) Representative Western blot illustrating GR (94 kDa) and control β -actin protein levels in SH, PL, AS and MM treatment group animals 5 days following ICV administration. (B) Densitometric analysis of GR bands standardised to the mean β -actin band density illustrating the effect of treatment group on the expression of GR protein.	215
6.36	Effects of treatment groups on GR protein expression measured by Western blot analysis. (A) Representative Western blot illustrating GR (94 kDa) and control β -actin protein levels in SH, PL, AS and MM treatment group animals 5 days following ICV administration. (B) Densitometric analysis of GR bands standardised to the mean β -actin band density illustrating the effect of treatment group on the expression of GR protein.	216

6.37	Effect of DOI at varying dose (0.3-3mg/kg) on the number of DOI-head-shakes measured at 5 minute intervals over a total 60 minute post-treatment period.	217
6.38	Effect of SH, PL, AS and MM treatment groups on DOI-induced head-shake frequency measured at +10-20 minute time bin.	219
6.39	Effect of SH, PL, AS and MM treatment groups on DOI-induced head-shake frequency measured at +10-20 minute time bin.	219

LIST OF TABLES

1.1	Advantages and disadvantages of antisense oligonucleotides for the investigation of specific receptor function.	28
1.2	Selected examples of delivery strategies for antisense oligonucleotides.	31
1.3	Advantages and disadvantages of using cationic liposomes as delivery systems for antisense ODNs in the central nervous system (CNS).	32
1.4	A summary of the main characteristics associated with microsphere delivery systems and other traditional delivery methods relevant to CNS administration.	34
1.5	Mechanisms used to identify single-stranded mRNA accessible sites for ODN hybridisation.	35
1.6	Common characteristic features exhibited by central corticosteroid receptors MR and GR.	41
1.7	Main mechanism by which the glucocorticoid receptor (GR) controls transcription.	44
1.8	Neuropsychiatric disorders associated with the 5-HT neurotransmitter.	47
1.9	Operational characteristics of 5-HT _{1A} and 5-HT _{2A} receptors.	48
1.10	Examples of <i>in vitro</i> and <i>in vivo</i> liposomal delivery systems of antisense compounds.	58
1.11	Examples of <i>in vitro</i> and <i>in vivo</i> biodegradable polymer delivery systems of antisense compounds.	59
1.12	Examples of <i>in vivo</i> antisense studies carried out in the central nervous system (CNS).	60
1.13	A summary of ongoing human clinical trials with antisense oligonucleotides.	62
2.1	Conditions for Dehydration of Fixed Cells by the PLT Method.	83
2.2	Rat Behaviour Assessment Sheet.	104

3.1	Mean number of gold particles visualised in different fields of TEM micrographs illustrating the distribution of biotinylated PS ODNs (10 μ M) within C6 glioma cells in the presence and absence of an optimised Lipid-ODN complex.	130
4.1	Antisense oligodeoxynucleotide sequences designed using optimal accessible site D.	141
4.2	Antisense oligodeoxynucleotide sequences of varying lengths designed using accessible site D.	148
4.3	Antisense oligodeoxynucleotide sequences designed against accessible sites A, B, C and D.	151
4.4	Control 21-mer phosphorothioate oligodeoxynucleotide design sequences.	153
4.5	BLAST search alignment results for empirically determined design and control sequences.	157
5.1	Phosphorothioate oligodeoxynucleotide sequences used in rat C6 glioma cell cultures.	162
5.2	The effect on 5-HT _{2A} receptor expression in C6 glioma cells following optimal GRAS5 antisense ODN treatment targeting the GR as determined using quantitative RT-PCR and radioligand binding assay.	172
6.1	Developed oligodeoxynucleotide sequences used in male Wistar rats as polymer formulations.	180
6.2	Two day block design treatment schedule for optimal GRAS5 antisense ODN-loaded polymer microspheres (AS) and free GRAS5 antisense ODN (FAS) administered using single ICV injections.	200
6.3	Four day block design treatment schedule for sham injection (SH), saline-loaded polymer microspheres (PL), optimal GRAS5 antisense ODN-loaded polymer microspheres (AS) and mismatch ODN-loaded polymer microspheres (MM) administered using single ICV injections.	201
6.4	Raw data of DOI-head-shakes measured at +10-20 minute time-bin following ICV administration of SH, PL, AS and MM treatment groups.	218
6.5	Summary of the <i>in vivo</i> antisense experiments and the parameters determined in each experiment.	220

LIST OF ABBREVIATIONS

A, G, C, T, U	adenine, guanine, cytidine, thymidine, uridine
Ab	antibody
ACTH	adrenocorticotrophin hormone
ADP	adenosine diphosphate
AS	antisense sequence
ATP	adenosine triphosphate
AVP	arginine vasopressin
BBB	blood brain barrier
Bmax	maximum number of binding sites
BSA	bovine serum albumin
cAN	central amygdaloid nucleus
cm, mm, μ m, nm	centimetre, millimetre, micrometre, nanometre
$^{\circ}$ C	degrees Celcius
cDNA	complementary deoxyribonucleic acid
CE	cianoethyl
CNS	central nervous system
CO ₂	carbon dioxide
cpm	counts per minute
CRF	corticotrophin releasing factor
CRH	corticotrophin releasing hormone
CSF	cerebrospinal fluid
ddH ₂ O	double distilled water (sterile)
DBD	DNA-binding domain
DEPC	diethylpyrocarbonate
DMEM	dulbecco's modified eagle's medium
DMSO	dimethylsulphoxide
DNA	deoxyribonucleic acid
DOI	1-(2,5-dimethoxy-4-iodophenyl)-2-amino propane hydrochloride
DOPE	dioleoyl phosphatidylethanolamine
DOSPA	N-[2-({2,5-bis[3-aminopropyl]amino}-1-oxypentyl)amino)ethyl]-N,N-dimethyl-2,3-bis(9-octadecenyloxy)-1-propanaminium trifluoroacetate
DTT	dithiothreitol
ECACC	european collection of animal cell cultures
EDTA	ethylenediaminetetra aceitic acid
FBS	foetal bovine serum
FCS	foetal calf serum
FITC	fluoroscein isothiocyanate
GR	glucocorticoid receptor
GRE	glucocorticoid receptor-responsive elements
HBSS	Hank's balanced salt solution
Hepes	N-(2-Hydroxyethyl)piperazine-N'-(2-ethane sulfonic acid)
HPA	hypothalamo-pituitary-adrenal
HPLC	high performance liquid chromatography

HRP	horseradish peroxidase
hsp	heat shock proteins
5-HT	serotonin
ICV	intra-cerebroventricular
ip	intra-peritoneal
iv	intravenous
kDa	kilo Daltons
LBD	ligand-binding domain
LSC	liquid scintillation counting
mL, μ L, μ Ci	millilitres, microlitres, micro Curies
MP	methylphosphonates
MR	mineralocorticoid receptor
mRNA	messenger ribonucleic acid
mw	molecular weight
OD	optical density
ODN	oligodeoxynucleotide
PAGE	polyacrylamide gel electrophoresis
PBS	phosphate buffered saline (sterile)
PKC	protein kinase C
PCR	polymerase chain reaction
PLGA	polylactide-co-glycolide
PLT	progressive lowering of temperature
PMSF	phenylmethylsulphonylamide
PO	phosphodiester
Pre-mRNA	unspliced messenger ribonucleic acid
PS	phosphorothioate
PVN	paraventricular nucleus
RITC	rhodamine isothiocyanate
RNA	ribonucleic acid
RNAse H	ribonuclease H
rpm	revolutions per minute
RT	reverse transcriptase
SD	standard deviation
SDS	sodium dodecyl sulphate
SEM	scanning electron microscopy
SFM	serum free media
SH	sham
SON	supraoptic nuclei
$t_{1/2}$	half-life
TBE	tris-borate-EDTA buffer
TEM	transmission electron microscopy
TEMED	N,N,N',N'-tetramethylethylenediamine
Tris	tris(hydroxymethyl)amino methane
Triton x-100	octyl phenoxy polyethoxyethanol
UTR	untranslated region
UV	ultraviolet light (absorbance)
v/v	volume per volume
w/v	weight per volume
w/w	weight per weight

CHAPTER ONE

GENERAL INTRODUCTION

1.1 Introduction.

This thesis is a study of the use of exogenously delivered antisense oligonucleotides as a means of investigating the relationship between two receptors (i.e. GR and 5-HT_{2A}) in the brain, in terms of their function and expression. This chapter will therefore cover aspects in the rationale of using synthesised antisense oligonucleotides in order to mediate receptor function elucidation and also the importance and significance of investigating the relationship between the GR and 5-HT_{2A} receptors in the CNS.

1.2 Application of Antisense Technology.

The possible applications of antisense oligonucleotides are very wide ranging because of the universality of the principle on which they are based. They can be applied in fundamental, investigative, and therapeutic forms of research. However research is most advanced in the areas of virology to inhibit the replication of viruses such as HIV (Agrawal *et al*, 1988) and oncology to inhibit malignant cell proliferation (Gill and Lazar, 1981). Antisense oligonucleotides have only recently emerged as suitable candidates in the role of investigative biological tools. They have been used to study a diverse range of receptor proteins throughout the body including the fields of neuropsychiatry and neuropharmacology with great advances being made as a reliable method for investigating receptor subtypes and orphan receptors which have been identified using molecular biological techniques (Akhtar and Agrawal, 1997).

1.3 Antisense Technology.

Novel drugs are usually not discovered by rational drug design, instead empirical methods are employed to discover new active substances which are directed against specific proteins such as enzymes, hormones, receptors, or ion channels. This can be both time consuming and expensive producing few products of varying levels of specificity. One way to possibly overcome this is to offer mechanistic intervention at the level of the nucleic acid.

All proteins are synthesised from unique mRNA sequences, which carry a specific 'blueprint' for the protein from the chromosomal DNA to the sites of protein synthesis (Alberts *et al*, 1989). If a cell produces too much or too little of a specific protein, the activity of the cell will be different from that of cells with the normal amount of protein. Variations in the expression of particular proteins between cells are often the basis of disease (Bradley *et al*, 1992). Another possible cause of disease is damage (or mutation) to the genetic 'blueprint' (the chromosomal DNA) which encodes a particular protein. This can result in the production of defective proteins which, in turn, can disrupt normal cell function.

Recent advances in molecular biology and chemistry have culminated in a potentially powerful group of techniques which may be used for determining gene function and provide the basis for a new generation of therapeutic and investigative agents. The 'antisense' concept is based on the idea of restricting or blocking the flow of information from the DNA of a specific gene to its protein product, thereby ablating phenotypic expression of the target gene (see Figure 1.1). Antisense originally referred to effects resulting from the binding via Watson-Crick base pairing of DNA to the mRNA or pre-mRNA of a target gene. Recently the term has been broadened to include any regulatory action obtained with nucleic acids and analogue structures (Crooke, 1992).

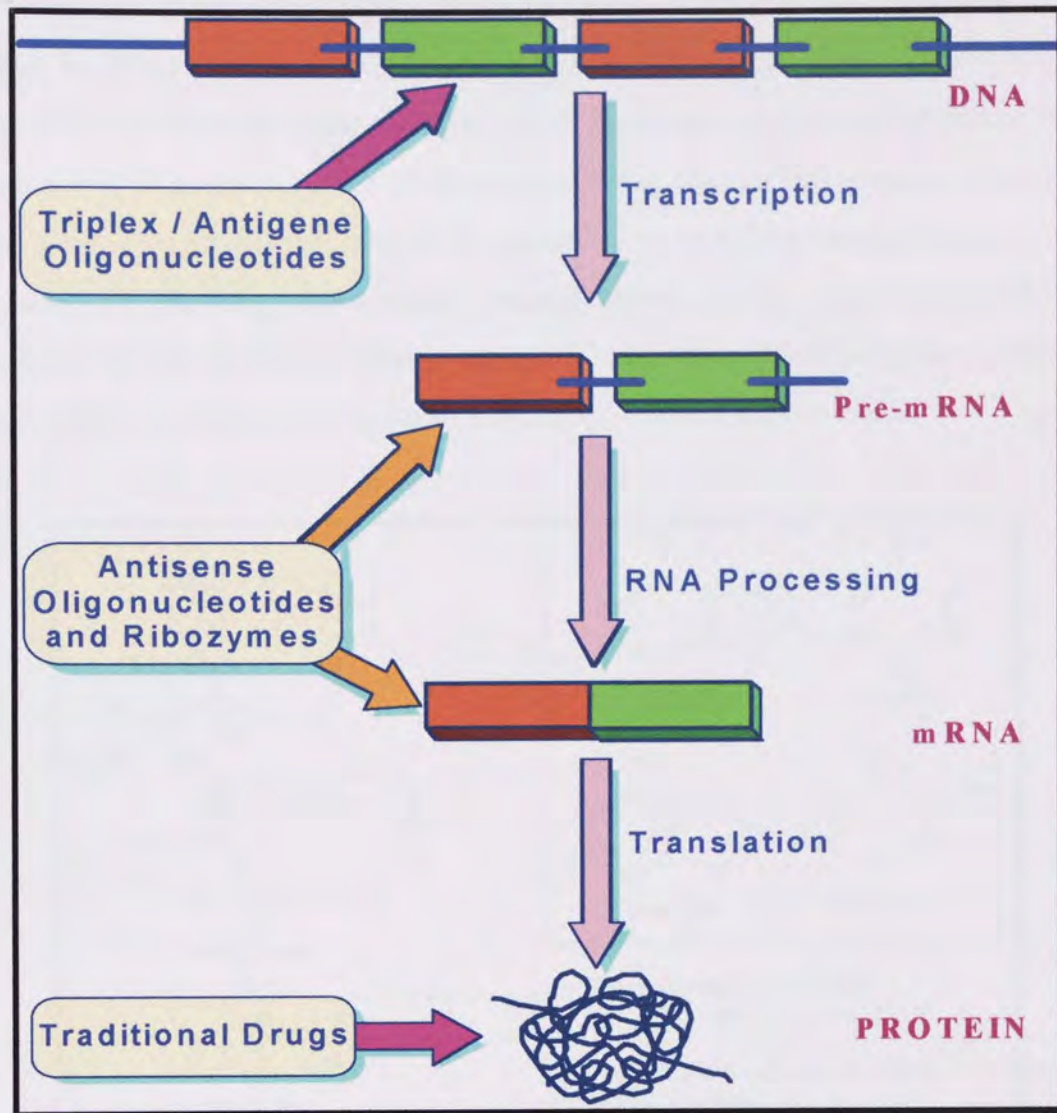


Figure 1.1 Some potential sites of oligonucleotide directed sequence specific inhibition of the flow of information from DNA to protein. Antisense ODNs bring about translational arrest by blockade of pre-mRNA or mRNA expression.

Various strategies exist for inhibiting gene expression with nucleic acids, which may be subdivided by their chemistry, either synthetic or biological, and by the type of target within the cell, which may be genomic DNA, mRNA, or protein. These approaches have been extensively reviewed (Van der Krol *et al*, 1988; Uhlmann and Peyman, 1990; Dolnick, 1991). The focus of this introduction will be on synthetic oligodeoxynucleotides (ODNs) and analogues that achieve effects via binding to mRNA.

Zamecnik and Stephenson (1978) were the first to propose the use of synthetic antisense ODNs for therapeutic purposes and it has now been widely accepted that synthetic ODNs are able to cross the external membrane of eukaryotic cells and exert specific, inhibitory effects on

gene expression. Antisense ODNs anneal to their complementary (antisense) mRNA sequences via Watson-Crick base pairing to form (anti-parallel) antisense/mRNA duplexes bringing about translational arrest (Gibson, 1994). Since the specificity of antisense ODNs is governed primarily by the sequence of the target mRNA, the principles learned from working with one genetic target can theoretically be applied to an indefinite number of genetic targets (Agrawal, 1996). Therefore the antisense strategy allows a more rational approach to drug development than the traditional 'blanket screening' of drug candidates against protein targets and also provides a unique opportunity to investigate protein function itself.

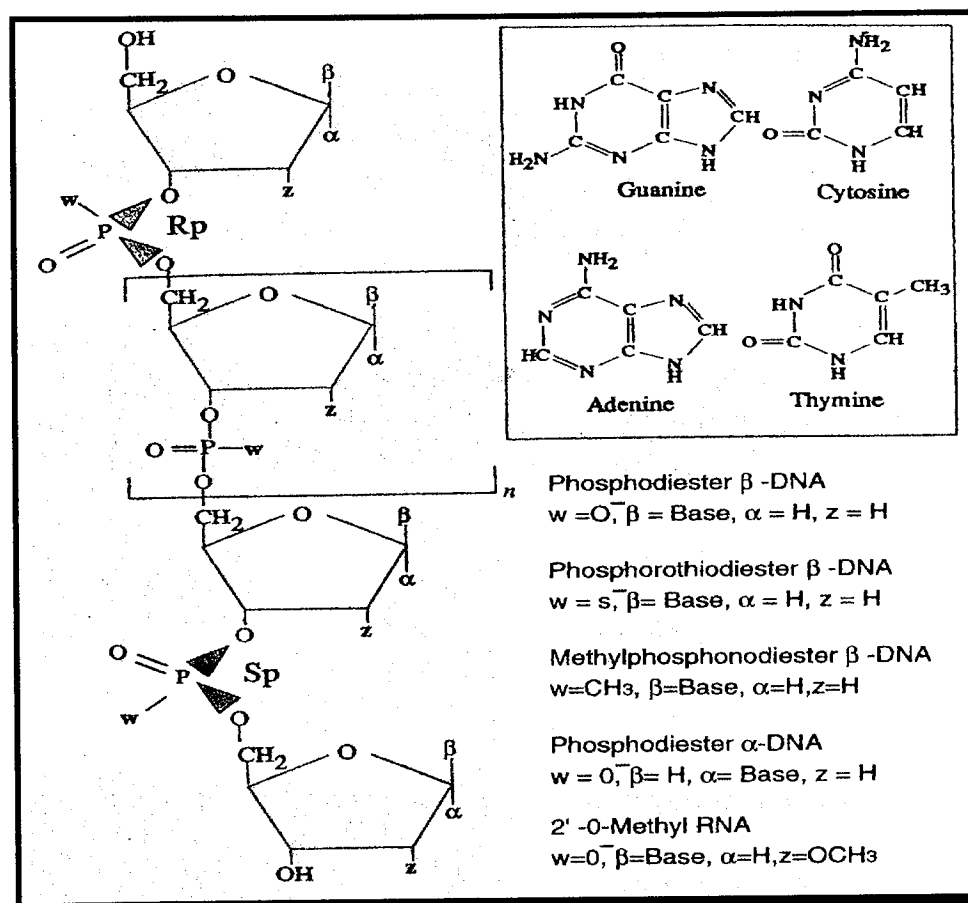


Figure 1.2 The structures of the common nucleic acid analogues. The natural DNA is modified at the positions indicated by, w , α , β , and z . The groups present at these positions are indicated for phosphodiester, phosphorothioate, methylphosphonate and α -anomeric DNA structures, and for the 2'-O-methyl RNA analogue. The four natural DNA bases are illustrated in the inset.

The precise mechanism of 'antisense action' remains a matter of debate although it is known to be dependant upon the type of oligonucleotide analogue used. Antisense oligonucleotide analogues (see Figure 1.2) can be placed into two broad groups with regard to their mechanism of action: One group, which includes unmodified phosphodiester (PO) ODNs and

those containing phosphorothioate (PS) inter-nucleotide bonds, are thought to inhibit mRNA translation by facilitating the destruction of the antisense/mRNA duplexes by ribonuclease H (Tidd, 1996; Akhtar and Agrawal, 1997). Ribonuclease H (RNase H) is an ubiquitous intracellular enzyme which cleaves the RNA portion of RNA/DNA duplex hybrids (Helene and Toulme, 1990). The second group of analogues, which includes ODNs containing methylphosphonate inter-nucleotide linkages (MP-ODNs) and oligoribonucleotides (ORNs), form antisense/mRNA duplexes which are more RNase H resistant (Kole *et al*, 1991). However they are still able to down-regulate protein translation (Krystal, 1992). Hence, physical blocking of mRNA translation at the ribosomes offers a likely explanation for the mechanism by which this second group of oligonucleotides exert their effects (Krystal, 1992; Rossi, 1995).

1.4 Antisense ODN Stability and Analogue Selection.

Modifications shown in Figure 1.2 have been necessary to impart biological stability to antisense ODNs that in their natural PO form are subjected to degradation to ubiquitous endo- and exonucleases (Eckstein, 1985; Woolf *et al*, 1990). Modifications to the base, sugar moieties and the conjugation terminal groups have also been performed for the same reasons (Uhlmann *et al*, 1997; Milligan *et al*, 1993). It is apparent that use of unmodified antisense ODNs in many experiments would be limited as PO ODNs have a half-life of about 30 minutes in serum (Wickstrom, 1986). However, in cerebral spinal fluid (CSF) the half life is considerably longer and recovery of undegraded oligonucleotide 24 hours after infusion has been shown (Ogawa *et al*, 1995). It is therefore accepted that modifications made to antisense ODNs increases the resistance of the ODN to nuclease activity by dia-sterioisomeric stability (Uhlmann *et al* 1997) and therefore increases its half life in serum and biological tissues. The majority of experiments today are carried out using PS ODNs which are effective at low, micromolar concentrations and are very stable having a half life of about 24-48 hours in serum (Agrawal *et al*, 1991). The PS ODN synthesis is automated and they are soluble in aqueous solutions making them more suitable for *in vivo* experiments. PS ODNs have been reported to show higher levels of toxicity (Le Corre *et al*, 1997), but various steps have been taken to reduce the non-specific effects of the sulphur moiety in the phosphate backbone (Toulme, 1992; Brysch and Schlingensiepen, 1994; Agrawal and Zhao, 1998). The length of ODN used

in experiments, is dictated by the minimum number of bases required for specific binding and the maximum number of bases that can efficiently cross cell membranes. ODNs of around 15 bases have a high probability of binding to a single cellular mRNA (Crooke, 1992) and the specific mechanisms that govern the uptake into cells limits ODN length to 20-25 bases. Consideration of such factors along with the use of rational design of antisense ODNs (see section 1.6.2) should successfully lead to the development of highly selective antisense sequences with little or no toxicity.

1.5 Antisense Strategies in Studying Receptor Function.

Traditionally the investigation of the function of a receptor has relied on the costly development and use of selective antagonists in preventing the biochemical and functional role of the receptor in question. This enables the researcher to elucidate the particular roles associated with that receptor. Another approach is the use of ‘knockout’ animals where a selected receptor gene is purposely disrupted. But these animals develop in the absence of the receptor and compensatory mechanisms are likely to occur. In contrast to these methods specificity of antisense inhibition has been demonstrated as a technique for deducing the function of specific receptor gene products (Weiss *et al*, 1997). Antisense oligonucleotides can be designed and tested once a receptor protein has been cloned and the gene sequence identified . Table 1.1 lists some of the advantages and disadvantages of receptor knockdown using antisense oligonucleotide inhibition (Wahlestedt, 1994).

Table 1.1 Advantages and disadvantages of antisense oligonucleotides for the investigation of specific receptor function.

ADVANTAGES	DISADVANTAGES
The effect is reversible	Potential toxic effects when using PS ODNs
Offers therapeutic potential	Poor cell membrane transfer
Low developmental costs	Continuous or repeated administration necessary
Available to use in any species	Limited stability
Produces selective and specific effects	Compensatory mechanisms and secondary effects may complicate results

Despite the complexities associated with the antisense approach, it does however provide a unique means of determining the functional role of different receptor proteins and their individual physiological and pathophysiological significance especially in the absence of selective ligands.

1.6 Antisense Selection and Delivery.

Despite the rapid entry of antisense technology into the clinical research arena (see section 1.10), its use as a biological tool *in vitro* and *in vivo* has somewhat been hampered by certain problems. These have included the poor biological stability of nucleic acids (which has been addressed in section 1.4), non-antisense mediated toxic effects, and poor cellular delivery and targeting (Akhtar, 1995). However, key developments in two areas of antisense technology, namely cellular delivery and target selection (finding optimally acting antisense ODNs), look set to revolutionise this technology.

1.6.1 Cellular Delivery of ODNs.

Exogenously administered ODNs enter cells crossing the cell membrane barrier, albeit rather poorly due to their polar nature and relatively large molecular size, by a combination of different endocytic mechanisms including fluid-phase (pinocytosis), adsorptive and ‘binding-protein’ or ‘receptor-mediated’ endocytosis (Akhtar and Juliano, 1992). The precise mechanisms involved are dependent on ODN chemistry, conformation and concentration, cell type, cell cycle, degree of cell differentiation, passage number as well as cell culture conditions used (e.g. pH and cation concentration) (Akhtar and Juliano, 1992). Fluorescently labelled ODNs have indicated that entry by endocytosis invariably leads to endosomal/lysosomal accumulation within the cells (Akhtar, 1998). Their escape from these compartments, a prerequisite for antisense activity, may require active assistance in the form of endosomal disruption agents such as cationic lipids (Bennett, 1995; Wyman *et al*, 1997) or molecules which can alter the sub-cellular sorting and trafficking of oligonucleotides (Pichon *et al*, 1997). The precise mechanisms by which such ODN conjugates or complexes can gain entry to the cytosol or nucleus for efficacy, however, remains poorly understood.

Various techniques have been employed to improve cellular delivery of ODNs mainly in an *in vitro* setting. Table 1.2 sets out these cellular delivery strategies. The strategies highlighted should not be taken in isolation as there is a degree of overlap in the mechanism(s) by which cellular ODN delivery is improved (Akhtar, 1998).

It seems that cationic liposomes (microscopic lipid vesicles) are probably the most successful in obtaining biological effects with antisense ODNs in cultured cells and commercial preparations such as lipofectin and lipofectamine have been extensively used. These preparations have the dual advantage that they can improve adsorptive endocytosis, and also facilitate endosomal exit via a proposed lipid-exchange mechanism (Zelphati and Szoka, 1996). The effectiveness of cationic lipids is dependent on several variables including cell type, ODN chemistry and charge ratio (Coulson and Akhtar, 1997) which means that conditions have to be optimised for a given cell nucleic acid system. In addition, cationic lipids are toxic and generally ineffective in the presence of serum proteins which consequently has limited their application, mainly, to cells in culture.

Figure 1.3 shows the mechanism required for successful cellular delivery of ODNs using cationic lipids while Table 1.3 lists the advantages and disadvantages of using cationic liposomes as a delivery system for antisense ODNs in the CNS (Felgner *et al*, 1995).

Table 1.2 Selected examples of delivery strategies for antisense oligonucleotides.

STRATEGY	REFERENCES
(A) Strategies for improving cell uptake	
1) Receptor targeted delivery	
Mannose	Akhtar <i>et al</i> , 1995; Rojanasakul <i>et al</i> , 1997
Transferrin	Citro <i>et al</i> , 1994; Walker <i>et al</i> , 1995
Immunoliposomes	Yamada <i>et al</i> , 1996; Aoki <i>et al</i> , 1997
2) Non-specific lipophiles	
Lipids	Shea <i>et al</i> , 1990
Cholesterol	Alahari <i>et al</i> , 1996; Kreig <i>et al</i> , 1993
3) Poly-lysine and other cations	Chiou <i>et al</i> , 1994; Wu-Pong <i>et al</i> , 1994
4) Particulates, cells and supramolecular structures	
Liposomes	Thiery and Tackle, 1995
Polymer microspheres	Akhtar and Lewis, 1997; Lewis <i>et al</i> , 1998
Human erythrocytes	Grimaldi <i>et al</i> , 1997
Dendrimers	Bielinksa <i>et al</i> , 1996
(B) Strategies for improving endosomal exit	
1) pH sensitive peptides	Wyman <i>et al</i> , 1997
2) Cationic lipids	Bennett <i>et al</i> , 1992; Williams <i>et al</i> , 1996
(C) Strategies for improving targeting to sub-cellular sites	
1) Endoplasmic reticulum via ODN conjugates	Pichon <i>et al</i> , 1997
(D) Strategies by-passing endocytosis by membrane disruption/pore formation	
1) Electroporation	Bergan <i>et al</i> , 1993
2) Microinjections	Chin <i>et al</i> , 1990; Leonetti <i>et al</i> , 1991
(E) Strategies for providing sustained-delivery	
1) Liposomes	Akhtar and Juliano, 1992; Thiery and Tackle, 1995
(F) Biodegradable polymer matrices	
1) Thin films	Lewis <i>et al</i> , 1995; Hudson <i>et al</i> , 1996
2) Microspheres	Akhtar and Lewis, 1997; Lewis <i>et al</i> , 1998

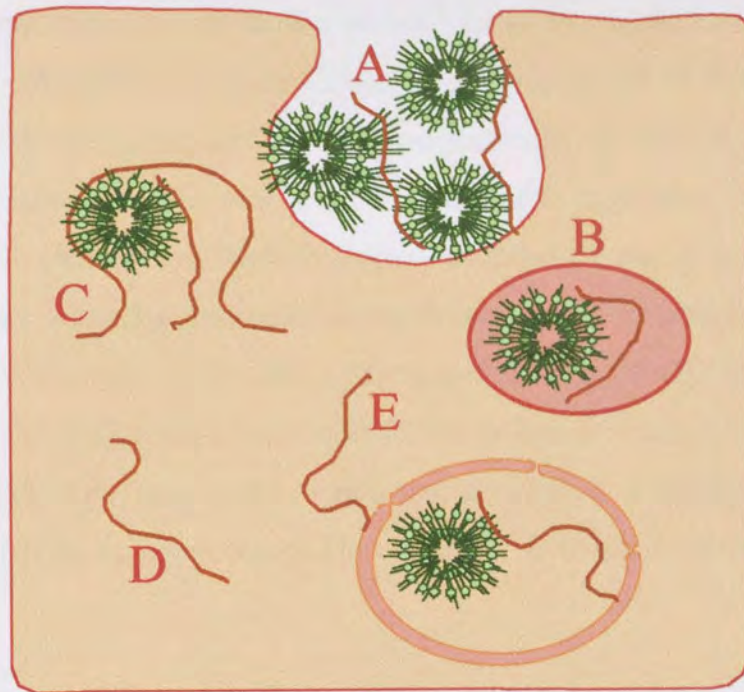


Figure 1.3 Illustration representing the mechanisms necessary for successful cellular uptake of antisense ODNs using cationic liposomes. [A] formation of liposomal-ODN complex (lipoplex), [B] entry of lipoplex into cellular endosome across the cell membrane, [C] release of lipoplex from endosome, [D] dissociation of the ODN from the cationic liposome, [E] migration of free ODN to the site of action (cytoplasm and/or nucleus).

Table 1.3 Advantages and disadvantages of using cationic liposomes as delivery systems for antisense ODNs in the central nervous system (CNS).

ADVANTAGES	DISADVANTAGES
Biologically safe	Stability of expression unknown
Virtually no size limitations	Cytotoxicity of certain cationic lipids
Imparts stability to ODN structure	Low efficiency of transaction
Potential of providing cell-specific delivery	Mechanism of action unknown
Potential to produce sustained and controlled release formulation	Molecular organisation of complexes unknown

As cationic liposomes have proven to be unsuitable for *in vivo* applications (Akhtar, 1998), it seems that most work particularly in the CNS has relied on the use of direct administration of antisense ODNs into the brain, both intracerebroventricular (ICV) and local administration into the brain parenchyma, has been used to inhibit the expression of receptor proteins (Wahlestedt, 1994). Other related techniques have included the use of subcutaneously placed osmotic minipumps delivering antisense ODNs at a constant concentration over a specific period of time (Wahlestedt *et al*, 1993; Zhang and Creese, 1993). In light of this, new methodology for the application of antisense ODNs *in vivo* is constantly emerging (Crooke, 1992; Akhtar, 1998). One such novel *in vivo* delivery tool is biodegradable polylactide-co-glycolide (PLGA) polymer microspheres (Lewis *et al*, 1995; Cleek *et al*, 1997; Akhtar and Lewis, 1997).

Microspheres are spherical, microscopic, matrices of polymer. Antisense compounds are dispersed within the polymer matrix, and released in a predictable and controlled manner to the exogenous medium (see Figure 1.4). Like cationic liposomes, microspheres encapsulate antisense molecules and are a means of ODN delivery across cell membranes without the inherent toxicity associated with cationic liposomes (Lewis *et al*, 1995; Cleek *et al*, 1997).

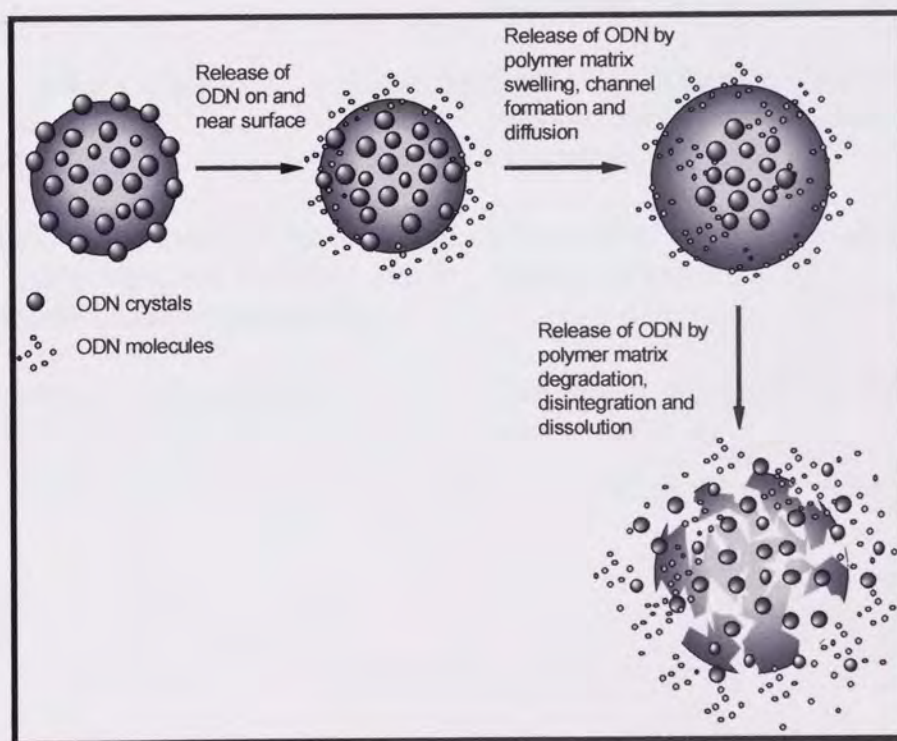


Figure 1.4 Schematic representation of the degradation of polymer microspheres and subsequent release of entrapped antisense ODN molecules.

Polymer microspheres have the potential to provide ODNs with protection from nuclease degradation (Lewis *et al*, 1995) and can be designed to provide a required release profile. The rate of drug release from microspheres depends on many factors including polymer matrix, co-polymer ratio, drug load and particle size (Akhtar and Lewis, 1997). As microspheres have been developed to act as sustained release systems which can be implanted at a desired site for ODN release, followed by biodegradation into biocompatible products, it is clear that such characteristics can be of great advantage to researchers in the realms of neuropharmacology and other CNS related disciplines. Table 1.4 compares the microsphere delivery system with the traditional direct CNS administration methods discussed previously.

Table 1.4 A summary of the main characteristics associated with microsphere delivery systems and other traditional delivery methods relevant to CNS administration.

MICROSPHERES	TRADITIONAL METHODS
Utilises less traumatic forms of stereotaxic surgery	Normally requires more complicated forms of stereotaxic surgery
Reduces the concentration of ODN necessary	Site specific delivery gives rise to potential of reducing ODN concentration
Allows single administration regimens	Requires repeated administration regimens unless using osmotic minipump system
Inherently allows tailored continuous delivery of ODN following single administration	Continuous delivery of ODN achieved using osmotic minipump infusions or repeated site-specific injections
Advantageous in analysis of stress-related molecular and behavioural functions due to the less stressful nature of administration	Allows ODN dosing to be terminated at any point in the experiment
Imparts stability to ODN molecules	Distribution of ODN in the CNS well documented

1.6.2 Selecting Optimal Antisense Sequences.

To achieve antisense-mediated efficacy with ODNs requires the rational design of effective ODN sequences complementary to the mRNA of the targeted gene. It would appear to be a simple task whereby accessible sites (single-stranded regions) for ODN hybridisation on the target mRNA are selected from computer predicted folding of RNA. However this has proven to be an inappropriate form of target selection as such sequences have failed to bring about antisense effects, thus leading to scepticism in this technology. This is due to RNA molecules exhibiting a high degree of secondary and tertiary structure which cannot be readily predicted from current computer algorithms for assessing RNA folding and the presence of RNA-binding proteins inside cells which may further prevent ODN hybridisation to single-stranded RNA sites. Poor target selection also favours the non-specific and non-antisense mediated effects seen with PS ODN analogues (Akhtar, 1998). Though this has to be balanced with the knowledge that certain ODN sequence motifs, depending on the sequence context, can have defined, but non-antisense mediated physiological actions such as immune stimulation (Krieg *et al*, 1993; Yamamoto *et al*, 1994) or inhibition of receptor tyrosine kinase activity (Bergan *et al*, 1995; Coulson *et al*, 1996).

It has therefore been the focus of recent research to develop methods for finding optimally acting antisense sequences by identifying the ‘open’ and ‘accessible’ structure of RNA and these techniques are listed in Table 1.5. Mechanisms of these techniques vary, but essentially work on the principles relating to the mechanism of action of antisense ODNs.

Table 1.5 Mechanisms used to identify single-stranded mRNA accessible sites for ODN hybridisation.

MECHANISM	mRNA TARGET	REFERENCES
1) Empirical ‘walk-the-gene’ strategy	C-raf kinase Murine α tumour necrosis factor	Monia <i>et al</i> , 1996 Stull <i>et al</i> , 1996
2) Scanning antisense ODN arrays (DNA chip technology)	Rabbit β -globulin Bacterial genes	Milner <i>et al</i> , 1997 Saizieu <i>et al</i> , 1998
3) RNase H-mapping of target mRNA	Hepatitis C virus Angiotensin type-1 receptor	Lima <i>et al</i> , 1997 Ho <i>et al</i> , 1998

Antisense ODNs are reported to essentially bring about sequence-specific inhibition of gene expression by interacting with the mRNA and causing steric hindrance of ribosomal read-through or, in the case of PS and PO ODNs, by activation of RNase H to selectively destroy the RNA component of the DNA/RNA duplex (Figure 1.5). It is the latter of these mechanisms which the RNase H-mapping technique manipulates in order to select optimally acting antisense sequences. The application of this technique is to be the focus of this introduction.

The RNase H-mapping technique relies on the ability of the ubiquitous enzyme RNase H to recognise and selectively cleave the mRNA at sites within the hybridised ODN:mRNA duplex. Sites accessible for hybridisation, as determined by mRNA cleavage fragments produced by the enzyme, are selected by combining the targeted mRNA transcript with a random, or semi-random, library of chemically synthesised ODNs. Subsequent sequencing of the RNase H cleaved fragments identifies the 'open' mRNA sites for targeting of antisense ODNs (Ho *et al*, 1996; Lima *et al*, 1997).

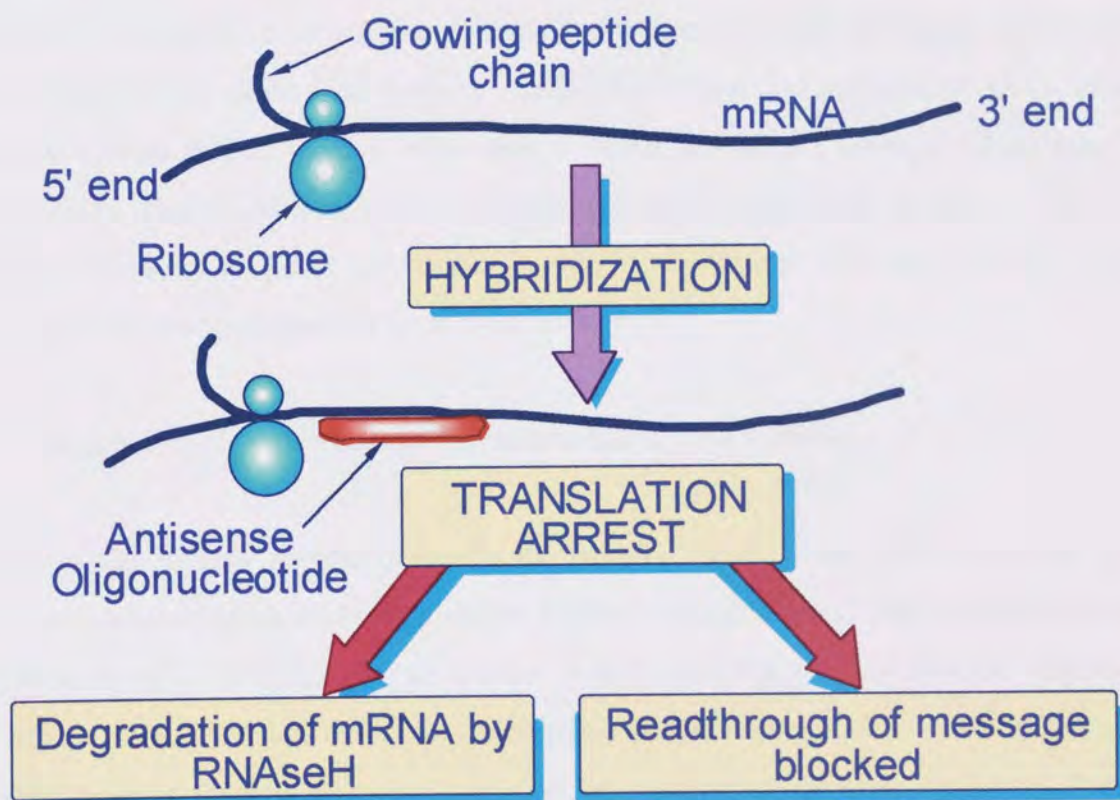


Figure 1.5 Schematic representation of the main mechanisms associated with antisense ODN activity.

1.7 The Hypothalamic-Pituitary-Adrenal (HPA) Axis.

1.7.1 Organisation of the HPA Axis.

The HPA axis is physiologically composed of neuroendocrinological components which comprise of the hypothalamic regions of the brain, the anterior portion of the pituitary gland and the adrenal cortex (Jacobson and Sapolsky, 1991). This forms a cascade type mechanism which is involved in the regulation of various functions ranging from stress, inflammation and complex behaviour (Reichardt and Schutz, 1998). The HPA axis is depicted schematically in Figure 1.6. The system is mainly regulated via circulating levels of glucocorticoids (cortisol in humans and corticosterone in rats) and variations in its level and therefore its complex interactions as dictated by periods of stress and circadian rhythm forms the basis for HPA axis function. The HPA axis generally follows a distinct chain of events which occurs with signals originating from higher brain areas such as the hippocampus or amygdala which modulate synthesis and release of corticotropin-releasing factor (CRF) and arginine vasopressin (AVP) from the hypothalamus (paraventricular (PVN) and supraoptic (SON) nuclei), which then results in the generation of an adrenocorticotrophic hormone (ACTH) signal in the anterior lobe of the pituitary gland. This leads to increased synthesis and secretion of glucocorticoids from the adrenal cortex, thereby influencing a variety of different biological functions (Fink, 1997). These glucocorticoids and their specific receptor interactions regulate the HPA axis through a negative feedback mechanism in which they repress CRF and ACTH, therefore blocking their own synthesis (for review see Fink, 1997).

1.7.2 Regulation of the Circadian Rhythm in HPA Axis Activity.

The circadian rhythm roughly parallels the activity cycle of the HPA axis and plasma glucocorticoids are typically highest before waking (circadian peak) and lowest before sleep (circadian trough), corresponding in humans to early morning and late evening, respectively, and to the reverse in rats which are nocturnally active (Krieger, 1977). The HPA axis is thought to control this biological variation in corticosteroid level by inputs from the hippocampus which is thought to exert an inhibitory influence on the HPA axis and ultimately

affect circadian trough and peak ACTH secretion leading to changes in plasma glucocorticoid levels (Jacobson and Sapolsky, 1991).

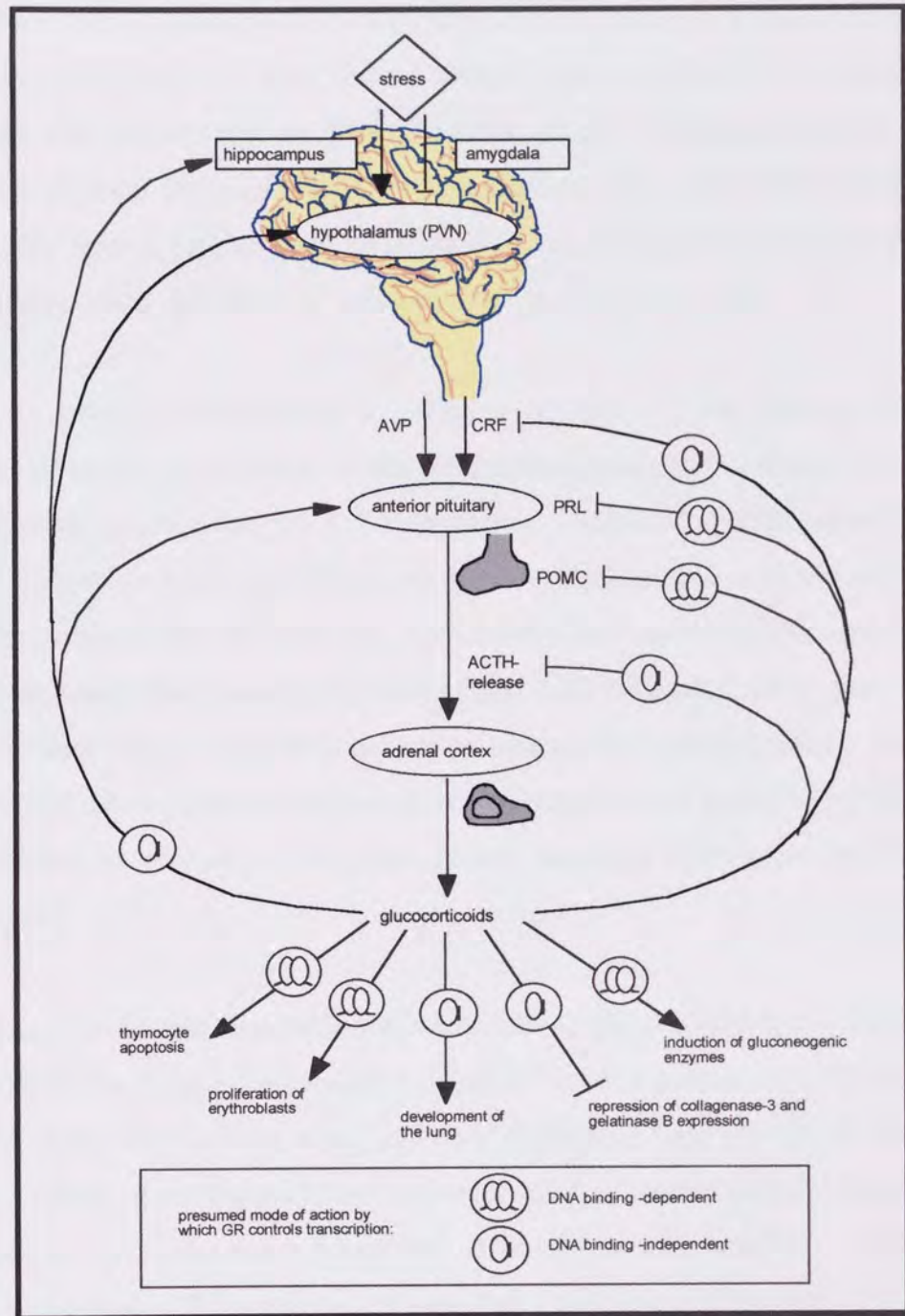


Figure 1.6 The complex network of physiological regulation by glucocorticoids within the HPA axis. The release of glucocorticoids from the adrenal gland is controlled by a neuroendocrine cascade which is under negative feedback control via the GR and MR. Signals originating in the CNS and interactions with the immune system further contribute to the complexity of this system. DNA binding-dependent and DNA binding-independent activation and repression of gene expression in target organs are indicated above (adapted from Reichardt and Schutz, 1998). Abbreviations: PVN, paraventricular nucleus; AVP, arginine vasopressin; CRF, corticotrophin-releasing factor; PRL, prolactin; POMC, proopiomelanocortin; ACTH, adrenocorticotrophic hormone.

1.7.3 Regulation of Stress-Induced HPA Axis Activity.

Stress constitutes any perturbation of homeostasis and may be physiological and psychological in nature. Measures of autonomic nervous system arousal, changes in endocrine function, and disruption in coping behaviour have all been used as indices of stress. However many authors have agreed that an increase in plasma glucocorticoid concentration is the definitive characteristic of stress (Selye, 1952; Green and Curzon, 1968). The HPA axis is the classic neuroendocrine system that responds to stress in its manifestation as increased synthesis and secretion of glucocorticoids from the adrenal cortex (Lopez *et al*, 1991).

Inhibition of stress responsiveness is achieved in part by the binding of circulating glucocorticoids to specific cytoplasmic receptors in the hypothalamus, where they inhibit CRF and consequently pituitary derived ACTH secretion. Additional modulation of the system is apparently achieved in limbic structures, specially the hippocampus, a structure that is linked to the hypothalamus through neuronal connections that converge on the PVN of the hypothalamus, where the stress responsive CRF and AVP neurons reside (Lopez *et al*, 1991). There are several reports suggesting the importance of the hippocampus for HPA feedback mechanisms and this is predominantly in the form of hippocampal inhibition of HPA responses to stress leading to a cessation of glucocorticoid secretion (for review see Jacobson and Sapolsky, 1991).

In acute stress it is thought that the increased circulating glucocorticoids due to stimulation of the HPA axis by the stress stimuli causes a negative feedback control of the HPA response to stress at all levels of the HPA axis, but with a different time course at different levels (Checkley, 1996). Fast feedback is operated by the corticosteroid receptors in the hippocampus which in response to rising levels of glucocorticoids bring about inhibition of the HPA axis by inhibiting CRF synthesis and secretion (Jacobson and Sapolsky, 1991; Young *et al*, 1991). Fast feedback operates over a time scale of minutes and is proportional to the rate of change in plasma glucocorticoids (Keller-Wood and Dallman, 1984). In comparison, delayed feedback takes place over a time scale of hours and is proportional to the mean plasma glucocorticoid concentration over that time and not to the rate of its change. This is thought to occur at the level of the pituitary gland (Miller *et al*, 1992). In the presence of

chronic stress however, specific changes and alterations in the activity at all three levels of the HPA axis seems to occur leading to an impairment of the feedback (fast and delayed) mechanisms (Lopez *et al*, 1991; Chalmers *et al*, 1993). This impaired feedback following chronic stress is associated with a reduction of both the mineralocorticoid (MR) and glucocorticoid (GR) receptors within the HPA axis, particularly in the hippocampus which is the main site responsible for fast feedback inhibition (Brooke *et al*, 1994; Herman *et al*, 1995). These receptors form an integral part in the regulation and functioning of the HPA axis mediated by the circulating glucocorticoid concentration.

1.7.4 Central Corticosteroid Receptor Types.

In man the glucocorticoid cortisol is a lipophilic molecule that readily enters neuronal cells and exerts many of its functions by binding to intracellular MR and GR. MR and GR belong to the superfamily of steroid receptors and show striking similarities in structure and mechanism of action (Evans, 1988; Beato, 1989). However as a consequence of differences in distribution and pharmacology, and because of some crucial molecular characteristics, activation of MR and/or GR may result in quite different effects on neuronal function (Meijer and de Kloet, 1998). Table 1.6 summarises these characteristics of both MR and GR (Meijer and de Kloet, 1998). MR has a much higher affinity to glucocorticoids resulting in almost complete occupancy under basal conditions. In contrast, the affinity constant of GR is within the range of physiological glucocorticoid concentrations, however the strength of signalling varies in response to altered hormone levels (Beato *et al*, 1995). MR are located almost exclusively in the limbic brain areas (hippocampus, septum, amygdala) and are functionally involved in the regulation of HPA axis activity under basal and stress conditions (Reul and de Kloet, 1985) while the GR is widely distributed within the brain (hypothalamus, hippocampus, brainstem) and is thought to play a central role in the mediation of the negative feedback signal of elevated glucocorticoid levels in response to stress (Reul and de Kloet, 1985; Dallman *et al*, 1987).

Table 1.6 Common characteristic features exhibited by central corticosteroid receptors MR and GR.

	MR	GR
Affinity for glucocorticoids	High (Kd = 0.5 nM)	Low (Kd = 2-5 nM)
CNS distribution	Hippocampus, amygdala, septum,	Hypothalamus, hippocampus, brainstem, amygdala, septum, cerebral cortex, noradrenergic and serotonergic cell bodies
Receptor occupancy	High at circadian troughs (basal conditions)	High at circadian peaks and under stress conditions
Chronic treatment of exogenous dexamethasone	Upregulation (Reul <i>et al</i> , 1989)	Downregulation (Reul <i>et al</i> , 1989)
Highest density of receptors	Hippocampus	Hippocampus, hypothalamus

1.7.5 MR and GR Regulation of the HPA axis.

It seems that both MR and more importantly GR are essentially involved in the feedback mechanisms controlling the HPA axis during homeostatic imbalance (Jacobson and Sapolsky, 1991). At basal levels of circulating glucocorticoids, the MR is approximately 80% occupied compared to 10% of GR occupation (Reul and de Kloet, 1985) therefore suggesting that MR mediates the effects of, and possibly controls, low basal circadian levels of glucocorticoids by a tonic inhibitory effect on HPA axis activity at the level of the hippocampus (Mason, 1958; Bouille and Bayle, 1973; Fischette *et al*, 1980). As a consequence it would seem that the amount of MR protein is an important determinant of MR-mediated glucocorticoid signal at both basal (de Kloet and Reul, 1987) and elevated (Oitzl *et al*, 1994) levels of glucocorticoids. At peak levels of circulating glucocorticoids, as seen during circadian peaks and stress conditions, the GR also becomes extensively occupied and is thought to be mainly responsible for the negative feedback effects of glucocorticoids on the HPA axis with possible assistance from MR (Bradbury and Dallman, 1989). GR mediated inhibitory action on HPA activity occurs at the level of the hippocampus, hypothalamus and pituitary gland (Reul and de Kloet, 1985; Jacobson *et al*, 1989; de Kloet, 1991) by their respective onset (delayed or fast) of the

feedback mechanisms. Unlike the MR, the concentration of glucocorticoids seems to be the main determinant for the GR-mediated signal (Meijer and de Kloet, 1998).

Under chronic stress conditions (as seen in depression and anxiety) it would seem that the cascade of effects which control feedback inhibition of the HPA axis constituting the adaptive response to stress (increased levels of circulating corticosteroids) becomes somewhat dysfunctional (Plotsky *et al*, 1998). This is thought to take place through diminished levels of the corticosteroid receptors in the brain and pituitary gland, caused possibly by a malfunctioning of the systems involved in the regulation of the receptor gene expression (Barden, 1999). Studies have shown that GR levels have been downregulated under chronic exposure to elevated levels of exogenous glucocorticoids (dexamethasone) at the level of the hippocampus and hypothalamus (Reul *et al*, 1987; Reul *et al*, 1989). This reduction in GR if replicated in stressed animal models would lead to a reduction of limbic-hippocampal GR-mediated inhibitory tone on the hypothalamic limb of the HPA axis (Sapolsky and Plotsky, 1990; Sapolsky *et al*, 1990) causing a prolongation in the elevated corticosteroid levels and in turn the stress condition. Work involving the study of MR under these conditions is somewhat limited although a decrease in MR expression levels has been reported after chronic stress (Herman *et al*, 1995). This reduction might additionally contribute to prolongation of stress conditions by further diminishing GR-mediated feedback (Wilson *et al*, 1980; Bradbury and Dallman, 1989). Under acute stress it is thought that both hippocampal MR and GR concentrations increase as a direct consequence of the single stressor to normalise corticosteroid levels (van Dijken *et al*, 1993). It is however, clear that further studies using well designed experimental models are needed to look at the expression of these two important receptors under acute and chronic stress conditions.

1.7.6 Molecular Mechanisms of MR and GR Action.

Glucocorticoids exert numerous effects on metabolism, reproduction, inflammation, immunity, and structure (Munck and Holbrook, 1984; McEwen *et al*, 1986). Additional influence is found upon neurogenesis, apoptosis in the developing and adult hippocampus, and regulation of the HPA axis via the MR and GR (McEwen and Magarinos, 1997). Modes of action of MR and GR are similar in that both upon binding to corticosteroids, are 'activated' and

translocated from the cytosol to the nucleus to act as transcription factors (Meijer and de Kloet, 1998). Both GR and MR have a modular structure, consisting of a DNA-binding domain (DBD), a ligand-binding domain (LBD) and two activating functions (Figure 1.7). In the absence of ligand, these receptors are found as an inactive cytosolic complex associated with preformed complexes of proteins called heat shock proteins (hsp) (Smith and Toft, 1993). Ligand binding leads to a conformational change resulting in dissociation of the hsp, receptor dimerisation and translocation of this complex to the nucleus followed by binding to specific steroid response elements in the promoter and enhancer regions of responsive genes (DNA). It is by this process (Figure 1.8) that transcriptional activity of target genes is modulated via different mechanisms (Reichardt and Schutz, 1998).



Figure 1.7 Location of functional regions in a typical steroid receptor. [A/B] represents the region N-terminal to the DNA-binding domain (transactivation region), [C] contains the DNA-binding domain, [D] contains the hinge region, [E] contains the ligand-binding domain, [F] is a region that can be deleted without eliminating hormone binding.

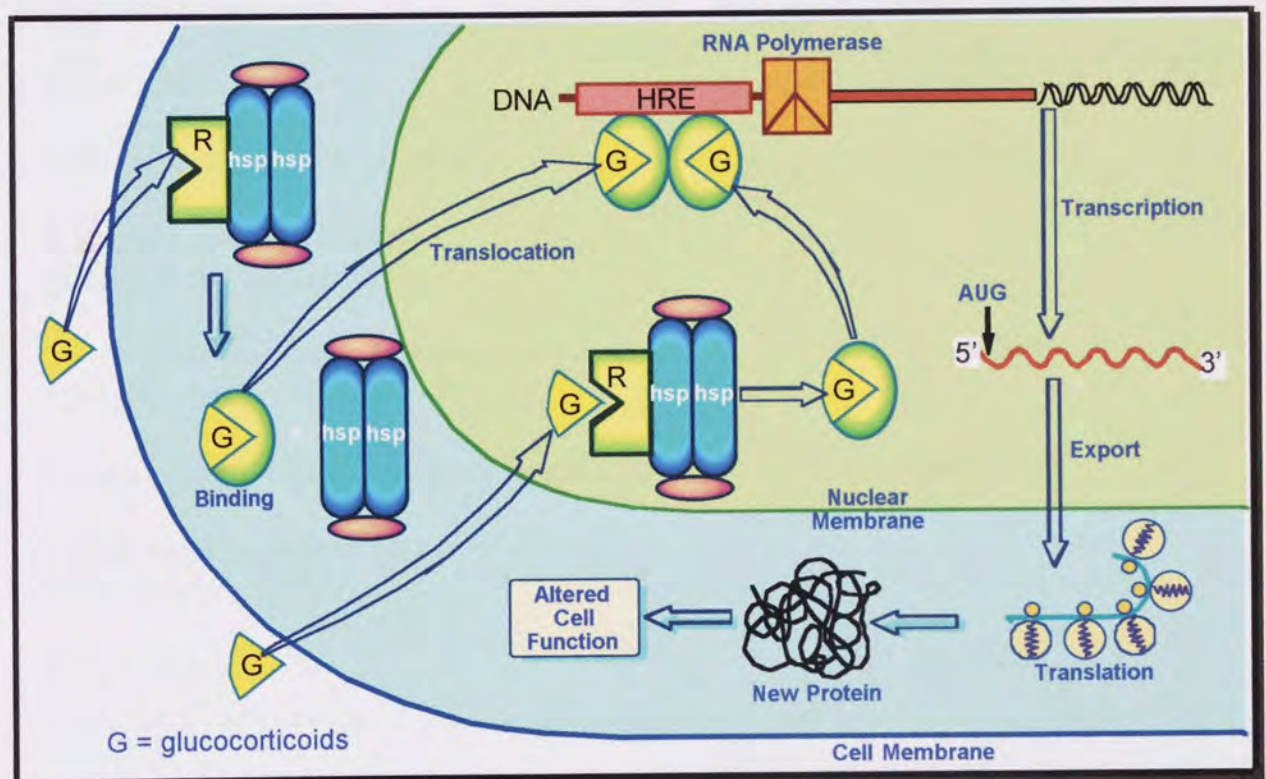


Figure 1.8 Molecular pathway for steroid hormone action. The steroid passively diffuses into target cells where it binds to an intracellular receptor located either in the cytoplasm or the nucleus. The occupied receptor then associates with the specific steroid responsive sequences in target genes (HRE) and alters the rate of RNA polymerase activity. The ensuing transcriptional and translational events lead to phenotypic alterations within the cell (adapted from McDonnell *et al*, 1993).

Activated MR and GR in the nucleus bind to specific DNA elements (nucleotide sequences), known as glucocorticoid receptor-responsive elements (GREs) and bring about differential effects on the function of the cells, depending on whether its effects are mediated by MR, GR, or both receptor types (de Kloet, 1991). MR and GR must therefore differ in the way gene transcription is influenced. The mechanisms of transcriptional modulation falls mainly into the categories of DNA binding-dependent interactions, protein-protein interactions, and non-ligand receptor phosphorylation (Weigel, 1996) and their modes of action is summarised in Table 1.7.

Table 1.7 Main mechanism by which the glucocorticoid receptor (GR) controls transcription.

MECHANISM	EFFECT ON TRANSCRIPTION
1) DNA binding-dependent interactions (Meijer and de Kloet, 1998)	
GR homodimers	Activation (++++)
GR-MR heterodimers	Activation (++)
MR homodimers	Activation? (+)
GR or MR binding to negative GRE	Repression
2) Protein-protein interactions (Reichardt and Schutz, 1998)	
GR interactions with transcription factors: AP-1, NF- κ B, GATA-1, CREB	Repression
GR interactions with transcription factor Stat5	Activation
3) Non-ligand receptor phosphorylation (Bodwell <i>et al</i> , 1991)	
GR phosphorylation	Repression

1.8 Regulation of 5-HT Receptors and the HPA Axis.

The HPA axis is the classical neuroendocrine system that responds to stress and whose final product, corticosteroids, targets components of the limbic system, particularly the hippocampus (Lopez *et al*, 1997). There are however reports of 5-HT receptor changes observed in brains following chronic stress conditions (i.e. depression, anxiety, and schizophrenia) suggesting a possible role for 5-HT receptors in controlling affective states by corticosteroid modulation. This would provide a potential mechanism by which these steroid hormones may regulate mood (Lopez *et al*, 1997).

1.8.1 CNS Serotonergic System.

Serotonin (5-HT) seems to be the most closely involved monoamine neurotransmitter with neuropsychopharmacology. Only about 1-2% of the 5-HT in the whole body is found in the brain (Cooper *et al*, 1996). As 5-HT cannot cross the blood brain barrier (BBB) the brain cells have to synthesise it from dietary tryptophan (for review see Udenfriend *et al*, 1955). Serotonergic cell bodies that project rostrally throughout the brain are located in the median and dorsal raphe nuclei (clusters of cells) in the brain stem (for review see Jacobs and Azmitia, 1992). These serotonin containing neurones are specifically restricted to nuclei lying in or near the midline raphe region of the midbrain and pons. Nine such clusters have been described and have been termed nuclei B1-B9 (Dahlstrom and Fuxe, 1965; see Figure 1.9) which show extensive projections into various parts of the brain. Due to these widespread projections gross manipulation of the central 5-HT function may modulate a range of behavioural and physiological events associated with different areas of the brain.

The hippocampus, in particular, is an anatomical region in which there is a rich representation of the 5-HT system since as many as $2-3 \times 10^6$ serotonergic varicosities per mm^3 are present throughout the hippocampus (Jacobs and Azmitia, 1992). This leads to an estimated number of 20-130 serotonergic terminals per hippocampal granule or pyramidal cell, indicating a strong modulatory influence of 5-HT on hippocampal functioning (Oleskevich and Descarries, 1990). As the hippocampus is also a prime region for HPA axis representation and activity, it would therefore not only provide an ideal anatomical region to study HPA axis and 5-HT

system relationships, but also support the possible neurobiological link between these two systems.

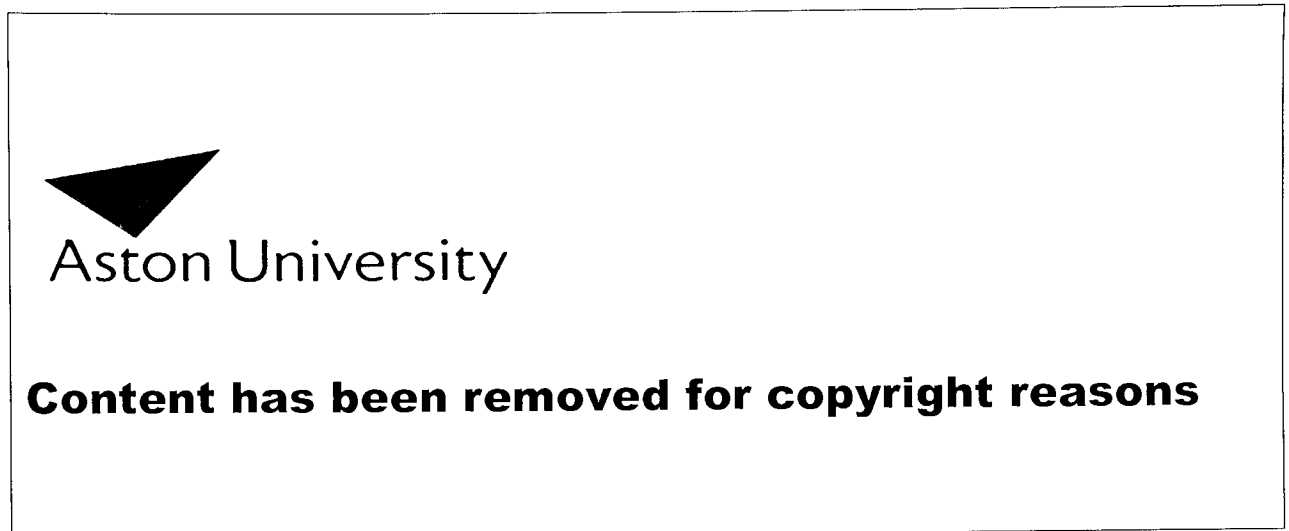


Figure 1.9 Adaptation illustrating the distribution of the main 5-HT containing pathways and the 5-HT containing midline raphe nuclei in the rat brain (Breese, 1975).

1.8.2 Central 5-HT_{1A} and 5-HT_{2A} Receptors.

Altered serotonergic function is associated with a number of CNS related pathological conditions (see Table 1.8), the most studied of the 5-HT receptors in terms of neuropsychiatric disorders is the 5-HT_{1A} receptor. These receptors are mainly found in the hippocampus, the septum, the hypothalamus, the frontal cortex, the spinal cord and the raphe nuclei. Many of these regions are components of the pathways involved in the modulation of emotion and behaviour, and thus 5-HT_{1A} receptors are thought to mediate emotional and behavioural mechanisms (Iversen, 1984; Tricklebank, 1985). In the raphe nuclei 5-HT_{1A} receptors are located presynaptically on serotonergic cell bodies and function as somato-dendritic autoreceptors negatively controlling serotonergic nerve firing, 5-HT synthesis, and 5-HT release (for review see de Montigny and Blier, 1992). The main characteristics of 5-HT_{1A} receptors are summarised in Table 1.9.

Table 1.8 Neuropsychiatric disorders associated with the 5-HT neurotransmitter.

NEUROPSYCHIATRIC DISORDERS	REFERENCE
Affective disorders	Meltzer and Lowry, 1987
Aggressive behaviour	Wetzler <i>et al</i> , 1991
Anxiety disorders	Nut and George, 1990
Autism	Cook, 1990
Schizophrenia	Csernansky <i>et al</i> , 1992
Sleep disorders	Koella, 1988
Suicidal behaviour	Mann <i>et al</i> , 1990
Tourette syndrome	Schweitzer and Friedhoff, 1988

The other main serotonin receptor proposed to be closely associated with neuropsychiatric functions is the 5-HT_{2A} receptor. These receptors are widely distributed in the brain and the spinal cord. They are enriched in the cortex, the tuberculum olfactorium, the substantia nigra and the hypothalamus. It is suggested that 5-HT_{2A} receptors play a key role in the regulation of the sleep-waking cycle, in anxiety and schizophrenia, in drug-induced hallucinations, and in numerous neuroendocrine and autonomic functions (Chaouloff, 1995). The main characteristics of 5-HT_{2A} receptors are summarised in Table 1.9. It is only fairly recently that a lot of interest has been focused on the 5-HT_{2A} receptor subtype in its role as mediator of HPA axis regulation and function. This is in light of the availability of suitable ligands, biological tools and experimental techniques allowing analysis of direct corticosteroid effects upon 5-HT receptors. But it is clear that a lot more work is still required before it is known what effects corticosteroids exert on 5-HT receptor-mediated functions, including those related to neuropsychiatric disorders such as stress, depression, anxiety and schizophrenia.

Table 1.9 Operational characteristics of 5-HT_{1A} and 5-HT_{2A} receptors. The rank of agonists/antagonists potencies for each receptor is found in the adjacent brackets and is determined from their relative equieffective molar concentration ratios (Hoyer *et al*, 1994).



Aston University

Content has been removed for copyright reasons

1.8.3 Serotonin and HPA Axis Function.

It is thought that certain mechanisms are involved in corticosteroid modulatory control of 5-HT biosynthesis/metabolism under 'normal' and 'stressed' conditions (Chaouloff, 1993). This is primarily controlled peripherally through liver tryptophan pyrolyase activity (the rate limiting enzyme in 5-HT biosynthesis) and BBB permeability which ultimately regulates central 5-HT synthesis (Azmitia *et al*, 1970; Long and Holaday, 1985). Adrenalectomy in rats has been shown to decrease the activity of tryptophan pyrolyase (Kizer *et al*, 1976) and decrease 5-HT turnover (Van Loon *et al*, 1981) which is reversible by substitution of glucocorticoids (Meijer and de Kloet, 1998). Corticosteroid administration to intact rats has been shown to increase uptake of tryptophan (5-HT precursor) and 5-HT synthesis into serotonergic neurones (Neckers and Sze, 1975). These events are thought to apply to stress conditions as shown by permissive (GR-mediated) involvement of glucocorticoids in sound stress-induced hyperactivity of tryptophan pyrolyase (Singh *et al*, 1989). During acute stress

conditions resulting in HPA axis overactivity and increased circulating glucocorticoids causing maximal GR receptor occupation, there is a GR-mediated increase in 5-HT synthesis in serotonergic neurones (Singh *et al*, 1989). However, under chronic stress conditions it has been reported that the activity of serotonergic neurons is suppressed with a lowering of 5-HT synthesis (Azmitia *et al*, 1993; Kitayama *et al*, 1989). It is this relationship between the 5-HT system and the HPA axis (MR and/or GR mediated) in terms of their regulatory functions under these chronic stress conditions which prove to be of most interest.

Besides considering the modulatory impact of corticosteroids upon 5-HT biosynthesis and metabolism, the influence of corticosteroids upon 5-HT receptors is very important as regards HPA axis driven modulation of the central serotonergic system. Release of ACTH from the pituitary is strongly and acutely stimulated by 5-HT via an action mediated by 5-HT_{1A} and 5-HT_{2A} receptors in the hypothalamus (Fuller, 1992). Some evidence suggests that stimulation of GR expression in the hippocampus is mediated via 5-HT_{2A} receptors (Meany *et al*, 1994). Due to the parallels seen in the distribution of both MR, GR, 5-HT_{1A} and 5-HT_{2A} receptors particularly in the hippocampus, it can be assumed that the hippocampus represents a key anatomical structure involved in the central control of HPA axis function and limbic circuitry (Lopez *et al*, 1991). As such, this region provides a unique anatomical environment in which to study the molecular interplay between serotonergic systems and corticosteroids. Hence these two 5-HT receptor subtypes will be the focus of this introduction in terms of HPA axis regulation and function.

1.8.4 5-HT_{1A} Receptors and the HPA Axis.

Experiments exhibiting physiological levels of steroid i.e. those involving adrenalectomy followed by administration of low dose corticosterone produces partial reversal of adrenalectomy-induced upregulation of hippocampal 5-HT_{1A} receptors (Chalmers *et al*, 1994; Chalmers and Watson, 1991). This would indicate that in such circulating corticosteroid conditions it is the MR that is selectively occupied, and therefore 5-HT_{1A} receptors are under tonic inhibition (MR-mediated) by corticosteroids. Such MR modulation of 5-HT_{1A} receptors under basal conditions has been reported in many studies (Kuroda *et al*, 1994; Meijer and de Kloet, 1994; Lopez *et al*, 1997).

Under conditions exhibiting persistent HPA activation (chronic unpredictable stress paradigm) causing persistent elevation of circulating corticosteroids, 5-HT_{1A} mRNA and receptor densities were significantly reduced in the hippocampus, relative to control animals following two weeks of chronic stress (Lopez, 1994; Lopez *et al*, 1997). This would suggest that such 5-HT_{1A} receptor downregulation is influenced by simultaneous corticosteroid occupation of both MR and GR. Imipramine (antidepressant) administration concomitantly to chronically stressed animals prevents both the downregulation of 5-HT_{1A} receptors and the stress-induced increase in plasma corticosteroids (Watanabe *et al*, 1993). This indicates that attenuation of elevated corticosterone using imipramine produces 5-HT_{1A} receptor downregulation via reduction of HPA hyperactivity. Lopez *et al*, (1997) have investigated whether such 5-HT_{1A} receptor downregulation observed is a consequence of the increased plasma corticosterone or mediated by a central mechanism. In this study the effect of chronic unpredictable stress in adrenalectomised rats with and without corticosterone replacement was assessed. It was found that in sham-stressed animals, chronic stress caused a consistent decrease in 5-HT_{1A} mRNA in all hippocampal subfields. No 5-HT_{1A} mRNA downregulation was observed in the adrenalectomy stress or cortisone-replaced stress groups. Therefore, elimination of the corticosterone rise after stress prevented the decrease in hippocampal 5-HT_{1A} mRNA. This would indicate 5-HT_{1A} downregulation observed after chronic stress is mostly mediated by increases in plasma corticosterone levels.

Due to the abundance of MR and GR in the hippocampal region of the brain, corticosteroid-induced downregulation of 5-HT_{1A} is likely to be an effect specific to the hippocampal formation. Regulation of 5-HT_{1A} receptors may be different in different brain regions. For example, hippocampal 5-HT_{1A} receptors due to their colocalisation with MR and GR, may be more sensitive to circulating steroids, whereas receptors in the prefrontal cortex may be less responsive to steroids and more responsive to changes in local 5-HT levels (de Kloet *et al*, 1986; Joels *et al*, 1991; Chalmers and Watson, 1991).

The studies mentioned above mainly suggest that corticosteroids, by interacting with the 5-HT_{1A} receptor, may play an important role in the relationship among stress, depression and perhaps suicide (McEwen, 1987). Because hypersecretion of endogenous corticosteroids in animal models can decrease 5-HT_{1A} receptor expression, it may be possible that the

hypercortisolemia found in depressed patients can exacerbate disturbances in affective states associated with 5-HT_{1A} receptor function. If this is the case, then antidepressant medications, in addition to directly correcting a central monoaminergic disturbance, may act to improve serotonergic function indirectly by decreasing corticosteroid hypersecretion (Lopez *et al*, 1997).

1.8.5 5-HT_{2A} Receptors and the HPA Axis.

An increase in 5-HT_{2A} receptor number in the prefrontal cortex of suicide victims has been reported by several investigators (Mann *et al*, 1986; Arango *et al*, 1992; Hrdina *et al*, 1993). Also chronic antidepressant treatment causes opposite changes of those found in suicide, that is, downregulation of cortical 5-HT_{2A} receptors (Peroutka and Snyder, 1980). Animal studies have shown that 5-HT_{2A} receptors can be regulated by steroids and by stress thus linking them to HPA axis modulation. Chronic social stress increases 5-HT_{2A} receptor binding in the parietal cortex of subordinate rats (McKittrick *et al*, 1995). Administration of ACTH for 10 consecutive days decreased 5-HT_{2A} receptor binding in the neocortex of the rat forebrain (Kuroda *et al*, 1992). This effect is abolished by adrenalectomy and mimicked by corticosterone administration for 10 days (Kuroda *et al*, 1992). Dexamethasone treatment for the same amount of time also causes a dose-dependent increase in 5-HT_{2A} receptor binding in the cortex (Kuroda *et al*, 1993), suggesting that this effect is mediated by the GR. These effects of stress and steroids on cortical 5-HT_{2A} receptors are again in the direction expected if stress and HPA activation are contributing to the 5-HT receptor changes observed in suicide victims. The effect of corticosteroids on 5-HT_{2A} receptor number seems to be specific for the cortex as neither chronic social stress (McKittrick *et al*, 1995), nor dexamethasone administration (Kuroda *et al*, 1993) altered 5-HT_{2A} receptor binding in the rat hippocampus or hypothalamus. Given the abundance of both MR and GR in the hippocampus, and the lack of MR in the cortex, it is plausible that 5-HT receptor regulation in the cortex is mediated through different mechanisms than in the hippocampus. This may involve 5-HT_{2A} receptors being more responsive to antecedent changes in the endogenous 5-HT ligand than to direct regulation by corticosteroids, as occurs with hippocampal 5-HT_{1A} receptors (Lopez *et al*, 1997). This therefore highlights the importance of carrying out further detailed studies investigating the steroidal modulation of 5-HT_{2A} receptors.

1.8.6 Cellular Regulation of 5-HT_{2A} Receptor mRNA.

The 5-HT_{2A} receptor is a G-protein linked receptor coupled to activation of phospholipase C (PLC) and the hydrolysis of membrane phosphoinositides with the subsequent generation of the second messengers inositol triphosphate (IP₃) and diacylglycerol (DAG). Upon stimulation of cells with 5-HT (see Figure 1.10), PLC is activated resulting in hydrolysis of membrane phosphoinositides (PI). PI hydrolysis leads to the generation of IP₃ and DAG which act as second messengers leading to a rise in levels of intracellular calcium and activation of protein kinase C (PKC). This activated PKC isoform translocates from the membrane to the cytosol where it causes increases in the levels of 5-HT_{2A} receptor mRNA and imparts stability by interactions with the nuclear gene expression machinery (Wohlpert and Molinoff, 1997). This activation process is typical of G-protein linked receptors whereby the agonist binding to the G-protein coupled receptors promotes a conformational change in the receptor that facilitates physical coupling between receptor and G-protein in a bound inactive form consisting of a ternary complex between agonist, receptor and G-protein. Agonists promote receptor G-protein coupling upon binding leading eventually to enhanced levels of the receptor protein.

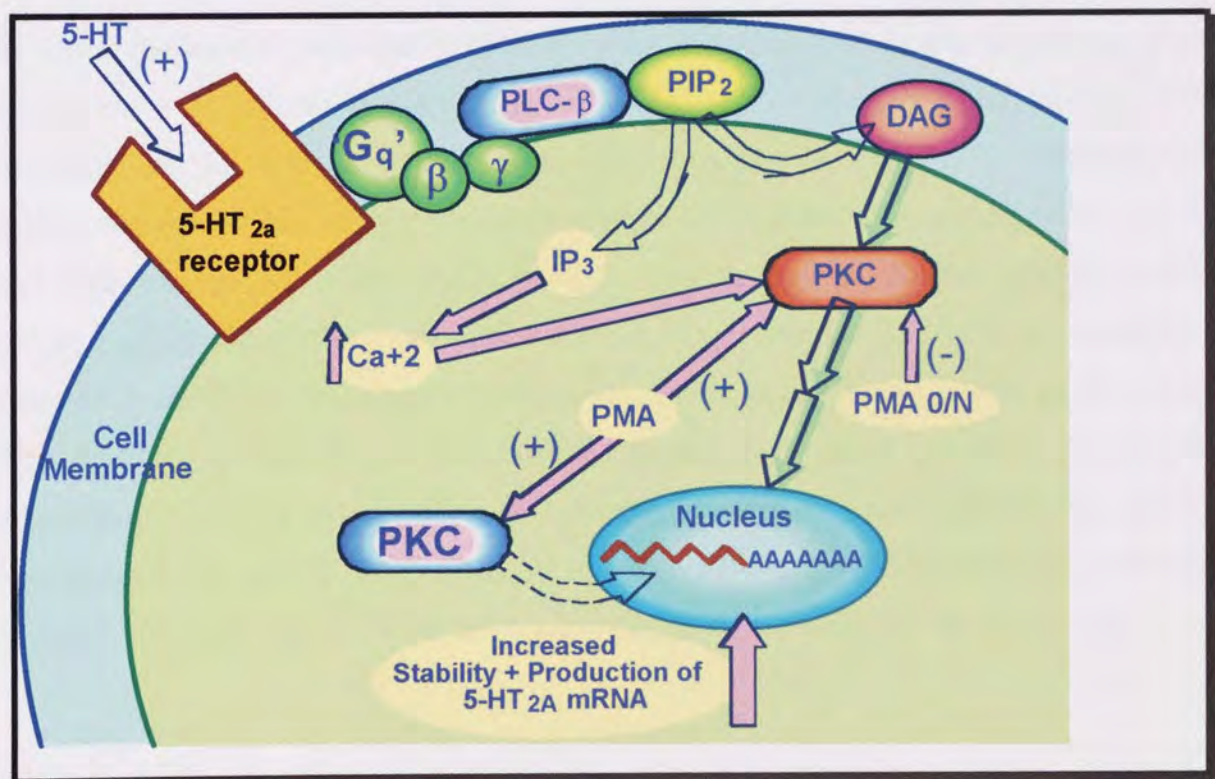


Figure 1.10 Illustration representing the pathways that leads to increases in the levels of 5-HT_{2A} receptor mRNA in cells.

1.8.7 Central 5-HT_{2A} Receptor Functions.

5-HT_{2A} receptors have been proposed to play a key role in the regulation of the sleep-waking cycle, in anxiety and schizophrenia, in drug-induced hallucinations, and in numerous neuroendocrine and autonomic functions (Chaouloff, 1995). Increased levels of the receptor have been measured in the brains of depressed individuals who committed suicide (Stanley and Mann, 1983). The 5-HT_{2A} receptor is also thought to be one of the sites of action of the atypical anti-psychotic drugs, such as clozapine (5-HT_{2A} binding site antagonist), which are useful in treating schizophrenia resistant to traditional anti-psychotic drugs (Meltzer and Nash, 1991). Moreover, this receptor is one of the sites of action of lysergic acid diethylamide (LSD) and other hallucinogenic drugs (Glennon, 1990), indicating 5-HT_{2A} receptors having a role in sensory processing. An involvement of 5-HT_{2A} receptor dependent mechanisms in cognition, short term memory and other higher cerebral functions is indicated by the decrease in the number of 5-HT_{2A} binding sites in dementia patients (Meltzer and Nash, 1991). In addition, stimulation of 5-HT_{2A} receptors by agonists such as 1-(2,5-dimethoxy-4-iodophenyl)-2-aminopropane (DOI) elicits 5-HT_{2A} receptor specific behavioural effects such as head-twitches in mice and head- and body-shakes in rats (Chaouloff, 1995).

In animal studies, the number of 5-HT_{2A} receptor binding sites is decreased in the rat frontal cortex following chronic administration of antidepressants (Pertouka and Snyder, 1980), indicating that the mode of action of antidepressants may involve 5-HT_{2A} receptors. Also 5-HT_{2A} receptor binding density was found to be increased in the post-mortem brain of suicide and depressed subjects suggesting a possible compensatory mechanism involving 5-HT_{2A} receptor up-regulation, due to the lowered levels of serotonergic activity in these conditions (Kuroda *et al*, 1992). Stimulation of 5-HT_{2A} receptors promotes an increase in GR binding capacity both in hippocampal and cortical regions of the brain (Meaney *et al*, 1994). Alternatively, prior blockade of 5-HT_{2A} receptors prevents stress-induced increases in hippocampal GR density (Mitchell *et al*, 1990). This therefore highlights the interaction between 5-HT_{2A} receptors and the HPA axis, being mediated primarily through the GR.

1.8.8 GR-HPA Axis Related Gene Expression Studies.

In the last few years, antisense ODNs and transgenic animal models have become commonly used tools for blocking of gene expression in mammalian CNS. As regards the HPA axis, a lot of work using transgenic mice have been carried out to examine genetic causation to conditions such as depression (Barden, 1996; 1999). In these studies the transgenic mice express GR antisense RNA due to the introduction of antisense gene constructs into the germ line of mice. This specifically produces animals with decreased GR in the brain (Pepin *et al*, 1992). Such animals have been shown to exhibit increased HPA axis activity (increased circulating corticosterone) with corresponding behavioural and cognitive deficits (Barden, 1999), thus suggesting the active involvement of GR for a normally functioning HPA axis. In addition these GR-deficient transgenic mice show resistance to suppression of adrenocortical secretions by dexamethasone with eventual adrenocortical hypertrophy, as seen in chronic depression states (Stec *et al*, 1994). Using this imbalance in GR system as a model, it was shown that antidepressant therapy (desipramine/amitriptyline) in transgenic mice produced increased GR mRNA density and GR binding in several areas of the brain including the hippocampus and hypothalamus (Barden, 1996). These changes coincided with a decrease in plasma ACTH and corticosterone concentrations suggesting a mechanism for the restoration of the hyperactive HPA system to normality (Barden, 1999). As there is an antidepressant-induced increase in GR expression in these transgenic mice, it is possible that central GR gene expression could be part of the HPA system which becomes more sensitive to circulating corticosteroid hormones, thereby reducing the over-reactivity of the HPA axis in depression states through the appropriate HPA centres (hippocampus/hypothalamus) regulating the negative feedback mechanisms (Barden, 1999). Such studies highlight the importance of examining GR expression and regulation for the mechanistic understanding of neuropsychiatric disorders and provides potential for possible future therapeutic interventions. However there are certain disadvantages associated with this transgenic mice model as a neuropharmacological tool. This mainly includes the irreversible nature of the technique which can lead to compensatory mechanisms being operative giving rise to abnormal physiological conditions. This is seen in the Barden transgenic model where the GR antisense transgenic mice have pituitary glands sensitive to CRH stimulation and adrenal gland hypertrophy leads to refractory stimulation by ACTH. In affective disorders the opposite is true (Barden, 1999).

In comparison, there are fewer antisense ODN studies looking at GR involvement in the regulation of normal HPA function. This can be partly due to the problems of selecting highly specific antisense sequences and ensuring adequate sustained cellular delivery to target organelles (Akhtar, 1998). Conventional GR antagonists such as mifepristone are available, but they are not sufficiently selective enough to provide a reliable assessment of CNS GR regulation and function and therefore the need for such antisense studies are essential.

Korte *et al* (1996), used 18-mer PS antisense ODNs (2nmol) to downregulate GR in hippocampal dentate gyrus of male Wistar rats via direct single bilateral infusion to this region. This antisense treatment produced a significant reduction in GR expression (by 15%) compared to controls as measured by immunolabeling. When the treated animals were exposed to the forced swim test 6 and 30 hours post-treatment to measure the possible consequence of inhibition of GR expression on immobility behaviour, it was found that the antisense groups produced a significantly reduced time spent in immobility behaviour compared to controls. Time spent in immobility behaviour is used to examine GR-mediated depression behaviour (de Kloet *et al*, 1988). Such an effect was also noticed with animals treated with the GR antagonist RU38486 (2.5mg/100g bodyweight). This would suggest that GR is involved in the display of immobility behaviour and this is mediated by its influence on the HPA axis and interactions with circulating corticosteroids.

Liebsch *et al* (1995), studied the role of central amygdala corticotrophin-releasing factor (CRF) receptors in behavioural responses to anxiogenic stimuli using antisense ODNs. They used 15-mer PS endcapped ODNs designed against the CRF receptor mRNA and gave male Wistar rats chronic antisense infusions via osmotic minipumps (0.25µg/0.5µL/hour) for 4 days directly to the central amygdaloid nucleus (cAN). This antisense treatment produced low expression and density of CRF receptors in the cAN as detected using in situ hybridisation compared to controls. When the animals were subjected to behavioural testing, it was seen that the antisense-treated animals spent significantly more time exploring the open arms of the plus-maze than control groups. The elevated plus maze test originally developed by Handley and Mithani (1984), has been validated for the detection of emotional responses to anxiogenic and anxiolytic substances (Pellow *et al*, 1985) and stressful external stimuli such as social defeat (Heinrichs *et al*, 1992). Therefore the increased open-arm exploration, as seen with the

antisense group, would indicate a reduction in anxiety in this treatment group. This would suggest that CRF receptors are involved in the mediation and expression of anxiety-related behaviour. Due to the potent anxiogenic nature of CRF itself, the effect is possibly driven by non-HPA related CRF receptor interactions.

Engelmann *et al* (1998), have reported the use of 18-mer antisense PS ODNs to significantly reduce the binding of MR by 28% and GR by 23% in the hippocampus of male Brown Norway rats following 7 days ICV administration using an osmotic minipump (1µg/0.5µL/hour). The specificity of antisense ODNs is shown in this study by the way that rats treated with MR-antisense did not show any changes in GR and vice versa. However it was found that these levels of downregulation (20-30%) achieved using antisense technology did not produce any behavioural effects in terms of spatial navigation abilities using the Morris water maze. This may be accounted for by the fact that the extent of receptor downregulation achieved in this study may not be high enough to allow for the detection of such defined behavioural effects. Such poor levels of receptor downregulation may be due to the authors not fully addressing the antisense design and delivery factors discussed in section 1.6.

Reul *et al* (1997), investigated the role of MR in the regulation of neuroendocrine and behavioural responses during ongoing and stressful conditions. They used an 18-mer PS endcapped antisense ODN directed against the MR mRNA in male Wistar rats. The ODN solution was administered ICV for 7 days via an osmotic minipump (1µg/0.5µL/hour). The MR-antisense treatment produced a 21% decrease in hippocampal MR binding with no change in hippocampal GR density. When these animals were subjected to elevated plus-maze assessment, no changes in the anxiety-like behaviour were observed in antisense treated animals. However, after the behavioural tests these antisense treated animals had markedly higher plasma ACTH, but not corticosterone, levels than the control groups. This study therefore highlights that the downregulation of brain MR produces enhanced responsiveness of ACTH to stressful situations which appears to be accompanied by reduced sensitivity of the adrenal gland to ACTH resulting in lowered circulating corticosteroid concentrations.

1.8.9 GR Control of 5-HT_{2A} Receptor Gene Expression.

The 5-HT_{2A} receptor has been implicated in the pathophysiology of several psychiatric disorders, including depression and schizophrenia. In severely depressed, suicidal patients elevated levels of 5-HT_{2A} receptors have been measured in platelets as well as in frontal cortex (Stanley and Mann, 1983; Pepin *et al*, 1992; Hrdina *et al*, 1993). Other studies have also reported that under increased HPA activity as in depression changes in the serotonin system occurs with the presence of increased postsynaptic 5-HT_{2A} receptors (Kuroda *et al*, 1992). These reports have led to the assumption that glucocorticoids via their interactions with the GR may be involved in controlling the expression of the 5-HT_{2A} receptor gene. This assumption is further supported by the fact that the 5-HT_{2A} receptor gene promoter region has an 11 out of 15 nucleotide sequence match to the GRE which is involved in steroid induced transcription initiation (Garlow and Ciaranello, 1995).

Evidence of this GR regulatory relationship exists mainly in *in vitro* studies (Garlow and Ciaranello, 1995) which have sought to determine whether the GR could influence the expression of the promoter for the 5-HT_{2A} receptor gene. By transfecting different cell lines with a sub-cloned 5-HT_{2A}-luciferase promoter-reporter plasmid (Garlow *et al*, 1994) which served as a positive control for steroid responsiveness, the authors investigated this GR regulation of 5-HT_{2A} receptor gene expression (Garlow and Ciaranello, 1995). It was found that activating GR, using dexamethasone administration, inhibited transcription from the 5-HT_{2A} receptor promoter in two different glucocorticoid responsive cell lines (CCL-39 Chinese hamster lung fibroblasts and RS-1 cells derived from PC-12 cells). In Neuro-2a cells (derived from mouse neuroblastoma) however, dexamethasone induced GR activation, stimulated transcription from the 5-HT_{2A} receptor promoter. This suggests that steroid mediated effects on the 5-HT_{2A} receptor promoter is subject to cell-type specific regulation and such positive and negative responses may be mediated through different promoter elements with possible influence from additional transcription factors (Garlow and Ciaranello, 1995). As there is a lack of information regarding those factors regulating 5-HT_{2A} receptor gene expression *in vivo*, it is essential such studies are carried out to highlight the functionality and importance of these regulatory mechanisms in the understanding of associated neuropsychiatric conditions. Such a task will therefore require the use of either transgenic or antisense strategies.

1.9 Analysis of Antisense Studies.

The main experimental success in using antisense ODNs *in vivo* tends to be the effective reduction in the expression of specific genes. This is measured normally using techniques such as radioligand binding, RT-PCR, Western and Northern blot analysis (Englehard *et al*, 1996). But in obtaining gene inhibition, *in vivo*, the following needs to be quantified: stability of ODN in the medium, ODN uptake by cells, ODN toxicity, ODN specificity and mechanism of ODN function. Most of the studies carried out in the CNS are well controlled and clearly demonstrate antisense efficacy in inhibiting gene expression (for a review see Szklarczyk and Kaczmarek, 1999). The following are tables highlighting recent antisense studies carried out specifically in the CNS and those antisense studies carried out *in vitro* as well as *in vivo*, with the aid of delivery tools such as liposomes and biodegradable polymers.

Table 1.10 Examples of *in vitro* and *in vivo* liposomal delivery systems of antisense compounds.

GENETIC TARGET (reference)	ANTISENSE AGENT	DELIVERY METHOD	CELL LINE OR ANIMAL MODEL	COMMENTS
mdr-1 mRNA (Kiehntopf <i>et al</i> , 1994)	42-mer chimeric 2'-fluoro-modified ribozyme	Cationic lipid complex (DOTMA)	PXF118 human pleural mesothelioma cells	93% reduction in protein levels. Reverse of drug-resistant phenotype after 72 hours.
CD44 mRNA (Ge <i>et al</i> , 1995)	38-mer all-RNA ribozyme	Cationic lipid complex (DOSPA)	SNB-19 human glioma cells	Expression of CD44 adhesion protein decreased in up to 30% of cells after 48 hours.
<i>c-myc</i> mRNA (Williams <i>et al</i> , 1996)	18-mer PS ODN	Lipofectamine lipid complex	Burkitts lymphoma cells	35% decrease in cell proliferation with a 60% reduction in intracellular <i>c-myc</i> protein levels.
TNF- α mRNA (Kisich <i>et al</i> , 1995)	36-mer all-RNA ribozyme	i.p. injection of ribozyme / cationic lipid complex (DOSPA)	Male BALB/c mice	85% reduction in TNF- α protein secretion by peritoneal macrophages.
TNF- α mRNA (Sioud, 1996)	45-mer 5'-capped RNA ribozyme	i.p. injection of ribozyme / cationic lipid complex (DOSPA)	Male BALB/c mice	50% reduction in TNF- α protein secretion by peritoneal macrophages.

Table 1.11 Examples of *in vitro* and *in vivo* biodegradable polymer delivery systems of antisense compounds.

GENETIC TARGET (reference)	ANTISENSE AGENT	DELIVERY METHOD	CELL LINE OR ANIMAL MODEL	COMMENTS
<i>tat</i> gene in HIV (Akhtar and Lewis, 1997)	20-mer PO and PS ODNs	ODNs incorporated into PLGA 50:50 microspheres	RAW 264.7 murine macrophage cells	Cellular association of ODNs entrapped in small spheres was improved 10-fold in murine macrophages compared with free ODNs.
Rat tenascin mRNA (Cleek <i>et al.</i> , 1997)	24-mer PS ODN	ODNs encapsulated into PLGA microparticles	Vascular smooth muscles (SMC) from carotid arteries of rats	SMC proliferation studies exhibited dose-dependent growth inhibition with ODN loaded microparticles.
GAD ₆₇ mRNA (Bannai <i>et al.</i> , 1998)	15-mer PS ODN	ODN incorporated in water-absorbent polymer (WAP) hydro-gels	Site specific CNS cannula injections in male Wistar-Imamichi rats	ODNs are effectively incorporated by all CNS cell types examined and suppress the synthesis of the GAD ₆₇ protein.
<i>env</i> mRNA of Friend retrovirus (Fattal <i>et al.</i> , 1998)	15-mer oligothymidylate ODN	ODNs absorbed onto polyalkylcyanoacrylate nanoparticles (isobutylcyanoacrylate and isohexylcyanoacrylate)	i.v. administration to male OF1 mice	Pharmacokinetic studies showed tissue distribution of nanoparticles was significantly modified. Stability of ODN <i>in vivo</i> in the plasma and liver was also improved for adsorbed ODN.
<i>env</i> mRNA of Friend retrovirus (Aynie <i>et al.</i> , 1999)	15-mer PO/poly-L-lysine complex	ODNs encapsulated into alginate nanoparticles	Male OF1 mice	Biodistribution was modified following i.v. administration, compared to free ODN with radioactivity detected in lungs, liver and spleen.
<i>Ha-ras</i> gene (Schwab <i>et al.</i> , 1994)	Unmodified PO ODN	ODN absorbed onto PHCA nanoparticles	s.c. administration to male nude mice	Produced significant inhibition of <i>H-ras</i> dependant tumour growth in nude mice.

Table 1.12 Examples of *in vivo* antisense studies carried out in the central nervous system (CNS).

GENETIC TARGET (reference)	ANTISENSE AGENT	DELIVERY METHOD	ANIMAL MODEL	COMMENTS
GABA _A receptor mRNA (Karle <i>et al</i> , 1997)	PS ODN	Intrahippocampal and Intrastriatal infusion	Male Wistar rats	Significant reductions in GABA receptor binding observed in both hippocampal and striatal regions.
5-HT _{1A} receptor mRNA (Le-Corre <i>et al</i> , 1997)	PS ODN	ICV administration	Male Wistar rats	limited reduction in 5-HT _{1A} receptor density obtained.
α_{2C} adrenoceptor mRNA (Lu and Ordway, 1997)	15-mer PS ODN	Intrastriatal infusion	Male Wistar rats	35% reduction in α_{2C} adrenoceptor protein density in the striatum.
CRF mRNA (Wu <i>et al</i> , 1997)	PS ODN	Direct hippocampal injections	Male Wistar rats	Quantitative RT-PCR determined reductions in CRF mRNA in specific brain regions accompanied with impairment in memory retention and an increase in exploration behaviour.
D2 dopamine receptor mRNA (Zhou <i>et al</i> , 1996)	PS ODN	Intrastriatal injections	Mice	Antisense treatment caused specific inhibition of rotational behavioural responses which are mediated by the D2 dopamine receptor.
NMDA-R1 receptor mRNA (Zapata <i>et al</i> , 1997)	PO ODN	ICV administration	Mice	Significant reductions in NMDA-R1 receptor binding and increased time spent by mice in open arms of elevated plus-maze.
mu and delta opioid receptor mRNA (Sanchez <i>et al</i> , 1997)	PS ODN	ICV administration	Mice	Reduces opioid receptor mediated morphine dependence by diminishing the incidence of withdrawal signs of naloxone.

Table 1.12 continued.....

Growth hormone receptor (GHR) mRNA (Pellegrini <i>et al</i> , 1996)	PS ODN	ICV infusions	Male rats	GHR binding in the choroid plexus was reduced by 40%. Antisense treated dose-dependent stimulation of growth hormone release was observed in the rats.
Urokinase mRNA (Englehard <i>et al</i> , 1996)	PS ODN	ICV administration	Male rats	Northern blot analysis showed decreases in urokinase expression.
<i>c-fos</i> mRNA (Quercia and Chang, 1996)	PS ODN	Direct injections to the paraventricular hypothalamic nucleus (PVN)	Male Wistar rats	Significant decreases in the density of <i>c-fos</i> immunolabeled nuclei in the PVN.
5-HT ₆ receptor mRNA (Sleight <i>et al</i> , 1996)	PS ODN	ICV administration	Male rats	30% reduction in 5-HT ₆ receptor binding in frontal lobes with a specific behavioural syndrome of yawning, stretching and chewing observed in antisense treated animals.

1.10 Antisense Oligonucleotide Clinical Trials.

Several antisense ODNs are undergoing clinical evaluation (see Table 1.13), and the first antisense drug has recently been approved for marketing. Vitravene™ (Formivirsen), which received FDA-approval in July 1998, is an antisense compound delivered locally to the eye to treat cytomegalovirus (CMV) induced retinitis in AIDS patients. Other antisense ODN compounds are being screened for anti-cancer, anti-inflammatory and anti-HIV applications (for a review see Akhtar and Agrawal, 1997). Despite the fact that many of the other ongoing clinical trials with ODNs employ systemic routes of administration, local delivery to sites of disease can offer various advantages. The appropriate choice of an efficient ODN delivery strategy may not improve efficacy, but help reduce side effects, and ultimately reduce drug costs. Considerable advances in manufacturing ODNs have been made and continued success in this area will undoubtedly make ODN-based therapeutics cost effective. The issue of toxicity has to be balanced with the severity of the condition being treated. Some degree of

non-specific toxicity would be tolerable to life threatened AIDS or cancer patients provided that the ODN is therapeutically efficacious.

Table 1.13 A summary of ongoing human clinical trials with antisense oligonucleotides.

TARGET	DISEASE	STATUS	OWNERSHIP
Vitravene™ Vision	CMV retinitis (AIDS)	Approved	Isis/CIBA Vision
ISIS 2302 ICAM-1	Crohns disease Renal transplant rejection Psoriasis (topical) Ulcerative colitis	Pivotal trial Phase II IND Candidate IND Candidate	Isis/Boehringer- Ingelheim
ISIS 3521 PKC- α	Cancer	Phase II	Novartis
ISIS 5132 <i>c-raf</i> kinase	Cancer	Phase II	Novartis
ISIS 2503 <i>H-ras</i>	Cancer	Phase II	Novartis
GEMO 231	Cancer	Phase II	Hybridon
ISIS 14803 HCV	Hepatitis C	IND Candidate	Isis
TNF- α	Inflammation	Preclinical	Isis
VLA-4	Inflammation	Preclinical	Isis

1.11 Aims and Objectives.

The initial aim of this thesis was to investigate the relationship between central GR and 5-HT_{2A} receptors in terms of activated GR regulation of 5-HT_{2A} receptor expression and function both *in vitro* and *in vivo*. This was based on the findings of the *in vitro* studies carried out by Garlow and Ciaranello (1995), who discovered GR mediated control of 5-HT_{2A} receptor promoter transcription in neuronal cell lines (see section 1.8.8). It was decided that antisense ODNs and their characteristic sequence specific arrest of genetic expression would be employed as biological tools to bring about GR protein downregulation and thus allow assessment of any associated effects on 5-HT_{2A} receptor expression and function.

Thus the feasibility of the employment of antisense technology as a reliable method of providing protein receptor function elucidation in the CNS was also to be an integral part of the main objectives of this report. These aims were essentially to be carried out at both *in vitro* (rat C6 glioma cell line) and *in vivo* (male Wistar rats) experimental settings.

To fully utilise any achieved antisense effects, optimisation of cellular antisense ODN delivery and GR mRNA specific design of antisense ODNs would be carried out initially. Following this the optimal antisense sequence directed against the GR would be screened for its efficacy and any related effects on 5-HT_{2A} receptor expression in cell culture. Such effects would be analysed using molecular biological techniques and provide key information as regards to the initial design and undertaking of appropriate animal studies assessing the efficacy and any 5-HT_{2A} receptor mediated effects of the selected antisense ODNs *in vivo*.

Studies looking closely at antisense ODN distribution, stability and toxicity, especially *in vivo*, will provide much needed information regarding the exact mechanism of cellular uptake of ODNs and their intracellular fate following cell entry.

As stimulation of 5-HT_{2A} receptors by DOI elicits 5-HT_{2A} receptor specific head- and body shakes in rats, 5-HT_{2A} receptor mediated behavioural analysis in the form of DOI induced head shakes would be used as an indicator of acquired 5-HT_{2A} receptor functional changes seen as a consequence of antisense directed downregulation of GR.

These studies would not only highlight the important factors governing the possible regulation of 5-HT_{2A} receptors by central GR. But also provide mechanistic understanding of pathophysiological conditions which are associated with abnormal expression of these two functionally important CNS receptors, thus providing the potential for therapeutic interventions to GR and/or 5-HT_{2A} receptor related CNS disorders.

CHAPTER TWO

MATERIALS AND METHODS

2.1 Materials.

Sterile double distilled de-ionised water and other sterile solutions and equipment were prepared by autoclaving at 120°C for 30 minutes at 15 pounds per square inch above atmospheric pressure in a series 300 autoclave (LTE Scientific Ltd., Oldham, UK). All chemical reagents used were molecular biology grade or alternatively the highest grade available from Sigma Chemical Company (Poole, UK), unless otherwise indicated.

Cell culture reagents and media were purchased from Gibco Life Technologies Inc. (Paisley, UK). Tissue culture flasks, multiwell tissue culture plates, 15mL and 50mL polypropylene tubes were purchased from Falcon (Beckton Dickinson and Company, Plymouth, UK). Disposable pipettes, microcentrifuge tubes, and finnpipette tips were purchased from Starstedt (Leicester, UK). The 2mL Bio-freeze cryovials were obtained from Costar (Cambridge, USA).

2.2 Methods.

2.2.1 Cell Culture Techniques.

2.2.1.1 Cell Line.

The C6 rat glioma cell line was obtained from stocks held at Knoll Pharmaceuticals (Nottingham, UK). This cell line is derived from a rat glial tumour induced by N-nitrosomethylurea and known to express both 5-HT_{2A} receptors and glucocorticoid receptors (European Collection of Animal Cell Cultures Number: 85040101; Benda, 1968).

C6 glioma cells were maintained in Dulbecco's modified Eagle's media (DMEM) supplemented with 10% v/v dialysed foetal calf serum (FCS), 1% v/v penicillin/streptomycin and 2µM *L*-glutamine. The same medium, without the addition of the FCS, was used as serum free medium (SFM) in cell culture experiments.

Cells were cultured in 75cm³ plastic tissue culture flasks with 25mL of medium. The cultures were incubated at 37°C in a humidified (95%) atmosphere of 5% CO₂ in air, (Mk II Proportional Temperature Controller, LEEK Ltd., Nottingham, UK).

Stock cultures were maintained by changing the media every 72 hours and passaged with a 1:10 dilution ratio when confluent (after approximately 3 days).

2.2.1.2 Passaging Attached Cells.

Passaging was carried out by removing the medium and washing the cells with 10mL of 0.1M phosphate-buffered saline (PBS). Following this 5mL of 2X trypsin/EDTA solution (0.25% w/v trypsin + 0.2% w/v ethylenediamine tetra-acetate in PBS, pH 7.2) was added to the flask to wet the cells. Soon after, 4mL of the trypsin/EDTA solution was removed from the flask. The cells were then incubated at 37°C for 5 minutes after which the flask was tapped to dislodge the cell monolayer from the bottom. Fresh media (9mL) was added (shaking the flask gently on addition) to neutralise the remaining trypsin/EDTA solution. Finally 1mL of this cell suspension was resuspended in a newly prepared flask containing 24mL of fresh medium to give a 1:10 cell dilution ratio in a final volume of 25mL.

2.2.1.3 Freezing Cell Lines in Liquid Nitrogen.

Frozen stock cultures were prepared for long term storage. This was carried out by trypsinising exponentially growing cells (see section 2.2.1.2) and neutralising this by the addition of 10mL of fresh medium. The cell suspension was then harvested in a 15mL polypropylene tube by centrifugation (3 minutes at 500 rpm) using a Mistral 3000 I centrifuge (Sanyo MSE, Leicester, UK). The supernatant was decanted, then the cell pellet resuspended in the 'freezing medium' (10% dimethyl sulphoxide (DMSO) and 90% dialysed FCS) to give an approximate final cell concentration of 1.4×10^6 cells/mL.

1mL of this cell suspension was aliquoted into each 2mL screw capped cryovial. The cryovials were then placed in a freezer (Forma Scientific Freezer Inc., USA) at -70°C and allowed to cool slowly ($\approx -1^{\circ}\text{C}/\text{min}$). After 4-6 hours the cryovials were transferred into a liquid nitrogen cell storage vessel (-196°C).

2.2.1.4 Recovery of Cell Lines from Liquid Nitrogen.

Cryovials were taken from liquid nitrogen storage and placed at room temperature for approximately one minute before being transferred to a 37°C waterbath until fully thawed (cryovials were not fully immersed). The outside of the cryovial was swabbed with 70% v/v ethanol prior to opening. 0.5mL of pre-warmed fresh media was slowly pipetted into the cryovial and the contents were removed to a sterile 15mL polypropylene tube. A further 9mL of warmed media was added drop by drop with gentle agitation. The cell suspension was pelleted by centrifugation at 500 rpm for 3 minutes. After decanting the supernatant the cell pellet was resuspended in 10mL of fresh media and placed in a newly prepared flask containing 15mL of fresh warm media and incubated in the normal way (see section 2.2.1.1).

2.2.1.5 Determining Total Cell Counts and Viable Cell Number.

Trypan blue is one of several stains recommended for use in dye exclusion procedures for viable cell counting. The method is based on the principle that live cells do not take up certain dyes, whereas dead cells do. Thus viable cell density of stock cultures was measured by haemocytometry using a trypan blue exclusion test. 100 μL of trypan blue (4mg/mL) was mixed thoroughly with 400 μL of cell suspension (prepared by trypsinised and resuspended cells as described in section 2.2.1.2) and allowed to stand for 5 minutes. A small amount of the trypan blue-cell suspension was added to the counting chambers of a Neubauer haemocytometer (Weber Scientific International Ltd., UK) having a volume of 0.1mm³ per square. In each of the chambers cells were counted in the 5 large squares of the haemocytometer using a Nikon light microscope (model TMS-F, Japan). Since live cells do not take up trypan blue dye the number of viable (unstained) cells were counted in each square. Cell number was thus determined by obtaining the mean count per large square on the

haemocytometer. In order to calculate cell concentration and total number of cells the following equations were used:

$$\text{CELLS PER ML} = \text{average viable cell count per square} \times 10^4 \times 1.25 \text{ (dilution factor)}$$

$$\text{TOTAL CELLS} = \text{cells per mL} \times \text{original volume of cell sample suspension}$$

Non-viable cells are stained by trypan blue and can be identified when viewed under the microscope. Hence the mean total count of viable cells per square and the mean total cell count (viable + non-viable) were used to calculate the percentage of viable cells using the following equation:

$$\% \text{ CELL VIABILITY} = \text{mean viable cell count} / \text{mean total cell count} \times 100$$

2.2.2 Oligodeoxynucleotide Synthesis and Purification.

2.2.2.1 Preparation of the Automated DNA/RNA Synthesiser.

The oligodeoxynucleotides (ODNs) used in this thesis, unless otherwise stated were synthesised on an automated DNA/RNA synthesiser (Model 392, Applied Biosystems (ABI), Warrington, UK). Synthesis reagents, columns and nucleotide phosphoramidites were obtained from Cruachem Ltd. (Glasgow, UK) unless otherwise stated and were stored under argon at 4°C when not in use.

Before synthesis commenced the reagent lines on the synthesiser were purged with DNA grade acetonitrile. Reagent bottles containing acetonitrile were added to the machine in the positions normally reserved for synthesis reagents and a 'dummy' synthesis was performed as described by Brown and Brown (1991). The bottles containing acetonitrile were then replaced with the required synthesis reagents in their designated positions.

2.2.2.2 Phosphorothioate Oligodeoxynucleotide Synthesis.

Automated synthesis of ODNs has become an established technique over the past decade. Various solid phase phosphoramidite techniques have been developed (Brown and Brown, 1991). The standard method used to synthesise ODNs and other analogues employs 2-cyanoethyl chemistry. The chemistry involved in this synthesis was used for the automated synthesis of all nucleic acid analogues used in this thesis. However certain reagents and step times were varied according to the type of nucleic acid sequence synthesised.

In ODN synthesis the nucleosides at the 3'-terminus were attached by means of a succinamide linker to borosilicate CPG support beads, housed inside a polypropylene column. In the first synthesis step, the support-bound nucleosides were detritylated with 2% trichloroacetic acid (TCA). This removed the dimethoxytrityl- [DMT(r)] protecting groups, thus providing free 5'-hydroxyl groups for attachment of the second nucleotide. Quantification of the released DMT(r) groups was used to indicate the step-wise coupling efficiency and overall yield (see section 2.2.2.3). In the second step an excess of the second nucleotide, protected at the 5'-hydroxyl position to prevent self-polymerisation, was activated by tetrazole which acted as a catalyst in the protonation of the N,N-diisopropyl phosphoramidite group. In the subsequent addition step, the protonated amino group was displaced due to nucleophilic attack by the 5'-hydroxyl group of the support bound nucleoside. This addition step formed support bound dimers, bearing 5'-DMT(r) groups which prevented further nucleoside additions. In the capping step any unreacted 5'-hydroxyl groups were rendered inert to further nucleoside addition by acetylation with acetic anhydride and 1-methylimidazole, thus minimising the chain length of any impurities (i.e. failure sequences). In the oxidation step the successfully dimerised sequences were oxidised with aqueous iodine (iodine-water-pyridine in basic tetrahydrofuran) to convert the phosphite triester into a more stable pentavalent phosphate triester. After this stage the fully protected phosphotriester dimers on the solid support material were ready to enter further cycles of base addition. Synthesis cycles were repeated until the ODNs reached the required chain length.

Antisense ODN sequences designed against the rat glucocorticoid receptor cDNA nucleotide sequence (Miesfeld *et al*, 1986), was synthesised in Phosphorothioate (PS) form on the DNA/RNA synthesiser (0.2 μ mole scale column) using a pre-programmed ‘sulfur’ cycle. This cycle was a modified version of the 2-cyanoethyl phosphoramidite cycle with the presence of a sulphurisation step using tetraethyl disulphide prior to the capping step (Zon *et al*, 1990).

Following synthesis the solid support material bearing the synthesised PS ODN was manually removed from the column. The PS ODN was cleaved from the solid support material and the base protecting groups removed by treatment with 1.5mL of concentrated ammonium hydroxide and incubated at 55°C for 8 hours (deprotection).

2.2.2.3 Calculation of Coupling Efficiency and Overall Yield of ODN Synthesis.

A stock solution of 0.1M *p*-toluene sulphonic acid (19.2g in 1000mL acetonitrile) was prepared. For a 0.2 μ mole scale synthesis the contents of the collecting tubes containing the orange effluent from the detritylation were made up to 25mL with *p*-toluene sulphonic acid solution. The absorbance (i.e. optical density) of these solutions was measured in a 1cm cuvette (Hellma, UK) in a UV/visible spectrophotometer (Jenway Scientific Instruments, UK) at 495nm. The coupling efficiency and overall yield were calculated as follows:

$$\text{OVERALL YIELD} = y/x$$

$$\% \text{ OVERALL YIELD} = \text{overall yield} \times 100$$

$$\% \text{ STEPWISE YIELD (coupling efficiency)} = 100\{(\text{overall yield})^{(1/y-x)}\}$$

where $y = \text{OD}_{495\text{nm}}$ final or lowest trityl effluent collected

and $x = \text{OD}_{495\text{nm}}$ second or highest trityl effluent collected

The OD (optical density) of the first trityl fraction is ignored as this represents the first base which was attached to the column. The coupling efficiency was typically 98% for PS ODN with overall yields in the region of 70%.

2.2.2.4 Purification of Oligodeoxynucleotides.

After deprotection, the resulting ODN was purified using a commercial Nap-10, DNA Grade Sephadex G-25 column (Pharmacia Biotech, St.Albans, UK). The column was rinsed with 3 x 5mL sterile double distilled water (ddH₂O) before the application of the ODN solution (in a volume of 1mL) to the top of the column. A further 1.5mL of ddH₂O was added to the column and the eluted fraction containing the purified ODN was collected in sterile microcentrifuge tubes. The eluted samples were dried by vacuum centrifugation using a DNA Speed Vac (Savant, UK) and stored at -70°C.

The purification procedure removed salts and other impurities such as failed sequences less than 10 bases in length. ODNs were further purified, after radiolabelling, by polyacrylamide gel electrophoresis (PAGE) if required (see section 2.2.4.3).

2.2.2.5 Quantification of Oligodeoxynucleotides.

ODN samples were quantified by UV spectroscopy at 260nm (Jenway Scientific Instruments, UK). The purine and pyrimidine bases of DNA and RNA strongly absorb light with maxima near 260nm. The absorbance reading can be translated to concentration according to Beers Law, $A = \epsilon Cl$ where:

A = absorbance

ϵ = molar extinction coefficient

C = concentration

l = path length (typically 1cm)

The method used to calculate the quantities of ODN in samples from OD_{260nm} measurements was adapted from that of Brown and Brown (1991), and is as follows:

A. Estimation of the Molecular Weight of ODNs:

$$\text{Mol Wt} = \{(249 \times n_A) + (240 \times n_T) + (265 \times n_G) + (225 \times n_C) + (64 \times n-1) + 2\}$$

where: (i) n_A = number of adenine bases in the sequence etc.

(ii) n = total number of bases

(iii) $(64 \times n-1)$ accounts for the molecular weight of the phosphate groups

B. Estimation of the Molecular Extinction Coefficient (ϵ):

$$\epsilon = \{[(8.8 \times n_T) + (7.3 \times n_C) + (11.7 \times n_G) + (15.4 \times n_A)] \times 0.9\}$$

It is necessary to multiply the extinction coefficient of the sum of the individual bases by 0.9 because the base stacking interactions in the single strand suppress the absorbance of DNA. This suppression is even greater in a duplex and the multiplication factor for a self-complementary sequence is 0.8 (Brown and Brown, 1991).

C. OD_{260nm} Units Conversion into Milligrams:

$$1\text{mg} \approx \epsilon / (\text{Mol Wt} / 1000) \text{ } OD_{260nm} \text{ units}$$

$$\text{therefore } 1 \text{ } OD_{260nm} \text{ unit} \approx (\text{Mol Wt} / 1000) / \epsilon \text{ milligrams}$$

This method however, does not allow for differences in molecular weight between phosphodiester (PO) and phosphorothioate (PS) oligodeoxynucleotides. Thus in the case for PS a sulphur (Mol Wt = 32) replaces an oxygen (Mol Wt = 16) on the PO side chain. Consequently an adjustment of +16 is made for $n-1$ bases.

$$\text{i.e. Mol Wt} = \{(249 \times n_A) + (240 \times n_T) + (265 \times n_G) + (225 \times n_C) + (\underline{80} \times n-1) + 2\}$$

fluorescein phosphoramidite because of the longer coupling time which this cycle allowed. The synthesis was performed without a final detritylation step because the fluorescein phosphoramidite monomer bears no DMT(r) group and is only suitable for the addition to the 5'-terminus of a synthesised ODN. Following deprotection of the 5'-end fluorescein labelled PS ODN (see section 2.2.2.2) the ODN was then purified using Nap-10 columns (see section 2.2.2.4).

2.2.3.3 5'-End Biotinylation of Oligodeoxynucleotides.

PS ODNs were 5'-end biotinylated during automated synthesis. Biotin cyanoethyl (CE) phosphoramidite (Cruachem, UK) was reconstituted in DNA grade acetonitrile to a concentration of 0.1M and added to a spare monomer position on the DNA/RNA synthesiser (see sections 2.2.2.1 and 2.2.2.2). The Custom synthesis cycle designed for use with ribonucleoside phosphoramidites was used for the addition of the biotin phosphoramidite because of the longer coupling time which this cycle allowed. With 5'-end biotinylation of ODNs a final detritylation step was included in the synthesis cycle to remove the 5'-DMT(r) from the biotin moiety. Following deprotection of the 5'-end biotin labelled PS ODN (see section 2.2.2.2) the ODN was then purified using Nap-10 columns (see section 2.2.2.4).

2.2.4 Purification of Labelled Oligodeoxynucleotides.

2.2.4.1 Polyacrylamide Gel Electrophoresis (PAGE).

Polyacrylamide gels were prepared and polymerised as described by Sambrook *et al*, (1989) and Gait *et al*, (1991). BioRad Protean II electrophoresis systems and BioRad power sources (Hemel Hempstead, UK) were used throughout and were assembled and run according to the manufacturer's instructions.

1000mL stock solutions of native polyacrylamide gel mixtures were prepared. In general a 20% gel (200g acrylamide, 6.6g bis-acrylamide, 200mL 5X TBE, and sterile ddH₂O to 1000mL) was used for oligonucleotides up to 20 base residues in length. For oligonucleotide sequences of more than 20 base residues a 15% gel (150g acrylamide, 5.0g bis-acrylamide,

200mL 5X TBE, and sterile ddH₂O to 1000mL) was used. Gel mixtures were filtered and de-gassed and stored at 4°C in amber glass bottles. Denaturing gels were prepared by the addition of urea (8M) to the native gel mixtures.

To prepare individual gels for electrophoresis, the polymerisation reaction was initiated by the addition of 600µL ammonium persulphate (10% w/v) and 40µL TEMED (N,N,N',N'-tetraethylethylenediamine) to 50mL aliquots of the stock gel mixture. The polymerising mixture was poured between two BioRad glass plates (200mm x 200mm and 220mm x 200mm) with 1mm spacers (BioRad). A BioRad comb with 20mm slots was inserted between the plates to form sample wells. Gels were allowed to polymerise for 30 minutes at room temperature before use.

Samples to be run on native gels were diluted with an equal volume of non-denaturing loading buffer (5% v/v glycerol in 1X TBE). Samples to be run on denaturing gels were diluted with a standard loading buffer (4.2g urea, 100µL 0.5M EDTA, 10mg bromophenol blue, and sterile ddH₂O to 10mL). 1X TBE (Tris Borate/EDTA Buffer) was used as the running buffer for electrophoresis and was diluted from a 5X stock solution (54g tris base, 27.5g boric acid, 20mL 0.5M EDTA (pH 8), and sterile ddH₂O to 1000mL). Marker dyes (0.25% bromophenol blue and 0.25% xylene cyanole in 1X TBE) were used to track the progress of sample migration down the gel.

Following a 30 minute period of pre-electrophoresis at 10 watts, samples and marker dyes were loaded and gels were run for 2-3 hours at 10-20 watts and were cooled throughout to 10°C using a thermostat controlled water circulator (Sarver Instruments, UK). Usually the samples were allowed to migrate approximately two thirds down the gel (position estimated from the location of marker dyes).

2.2.4.2 Autoradiography.

Following separation of radioactive samples by PAGE, the 220mm x 200mm plate was carefully removed from the tank with the intact gel on the upper surface. The gel was covered with a single layer of Saran wrap and stored in a Hypercassette (Amersham Life Sciences, Amersham, UK) fitted with an intensifying screen. Under dark room conditions gels were exposed to Kodak HP autoradiograph film and stored at -70°C for the required exposure time. Films were developed using freshly prepared Kodak photographic reagents (i.e. developer and fixer).

2.2.4.3 Radiolabelled Oligodeoxynucleotide Purification by PAGE.

PAGE was performed as described in section 2.2.4.1. Radiolabelled ODNs were mixed with an equal volume of non-denaturing loading buffer (5% v/v glycerol in 1X TBE). For purification of radiolabelled 15-mer PS ODN a 20% native polyacrylamide gel was used to improve the molecular weight separation during electrophoresis as described by Gait *et al*, (1991). The position of the purified radiolabelled product within the gel was visualised by autoradiography (see section 2.2.4.2). For PAGE purification of non-radiolabelled ODNs, samples were loaded onto gels as described above, but additional samples of radiolabelled ODN markers of known chain length were loaded onto adjacent wells on the polyacrylamide gel to allow location of the purified, unlabelled product band by autoradiography.

Appropriate gel bands containing the purified products were excised and transferred, without crushing, to sterile 15mL polypropylene tubes containing 3mL of sterile ddH₂O. The excised bands were incubated (with gentle agitation) in ddH₂O overnight at room temperature. The supernatant solution containing the purified product was then removed and desalted using Nap-10 columns (see section 2.2.2.4) before being dried by vacuum centrifugation (Savant DNA Speed Vac) and stored at -70°C until required.

2.2.5 Cell Association/Uptake Studies.

Methods for cell association/uptake studies used throughout are detailed below. Details of amendments and additional methods used are described in the relevant sections. Each experiment was carried out in triplicate, unless otherwise stated. To grow C6 glioma cells in multiwell cell culture plates, cells were trypsinised in a culture flask and the cell number determined using a Neubauer haemocytometer (section 2.2.1.5). Cells were diluted to the appropriate number per mL using maintenance media (section 2.2.1.1). C6 glioma cells were seeded at 4.5×10^5 , 2.5×10^5 , and 1×10^5 cells per mL in 12, 24, and 96 well plates (Falcon, UK) respectively when used for cell association/uptake studies, unless otherwise stated. This dilution produced approximately 70% confluent cell cultures after 24 hours incubation, after which cells were used in association/uptake studies.

2.2.5.1 Cell Association/Uptake of Oligodeoxynucleotides.

Radiolabelled ODNs were diluted to a final concentration of $1 \mu\text{M}$ in DMEM serum free media (SFM). The use of SFM reduced the potential for enzymatic degradation of ODNs. C6 glioma cells were seeded in 24 well plates and incubated overnight (see section 2.2.5) after which the cells were washed twice with 1mL sterile PBS (warmed to 37°C) per well. The PBS was aspirated and the ODN was added to the wells in 0.5mL warmed SFM. Cells were incubated for the required time (0-6 hours) at 37°C , unless otherwise stated. Following incubation the SFM was removed from the cells and collected. Cells were then washed 4 times with 1mL ice cold PBS/azide (0.05% w/v sodium azide in phosphate buffered saline) and the washings collected. Cell monolayers were solubilised by the addition of 1mL triton-X100 (3% in ddH₂O) for 2 hours at 37°C . The cell suspension was harvested and the wells washed twice more with 1mL triton-X100 to remove any remaining cells. The cell suspension and the final triton-X100 washings were pooled and collected.

Quantities of radiolabelled ODNs in each of the three fractions (SFM, PBS/azide washes, cell suspensions) were assessed by liquid scintillation counting using a Packard 1900TR Scintillation Counter. Fractions were added to 5mL of Optiphase Hi-Safe 3 Scintillation Cocktail (Pharmacia-Wallac, St.Albans, UK) and counted for 5 minutes using an appropriate

program for the detection of ^{32}P isotope activity. Counts per minute (cpm) were recorded and compared with background values. The half life and reference date of the ^{32}P radionucleotide were used to account for decay during the experimental period.

2.2.5.2 Liquid Scintillation Counting.

The specific activities of radiolabelled samples were determined using a Packard 1900TR Scintillation Counter. Samples of known volume were added to 5mL of Optiphase Hi-Safe 3 Scintillation Cocktail (Pharmacia-Wallac, St.Albans, UK) in scintillation vials (Starstedt, UK) and counted for 5 minutes using an appropriate program for the detection of ^{32}P , ^{14}C , and ^3H isotope activity. Counts were compared with background values and the half life and reference date of the ^{32}P radionucleotide was used to account for the decay during the experimental period. Specific activities were calculated as cpm/ μL .

2.2.5.3 The Effect of Cell Concentration on Cellular Association/Uptake.

Cell association/uptake experiments (section 2.2.5.1) were conducted using C6 glioma cells which were seeded in 1mL at 2×10^4 , 2×10^5 , and 2×10^6 cells/mL in 24 well plates. The cells were incubated at 37°C for 1 hour with $1\mu\text{M}$ ^{32}P -labelled 15-mer PS ODN (section 2.2.2.2).

2.2.5.4 The Effect of Time on Cellular Association/Uptake.

Cell association/uptake experiments (section 2.2.5.1) were conducted using C6 glioma cells at a concentration of 2.5×10^5 cells/mL in 24 well plates at different incubation times (30, 60, 120, 240, and 360 minutes). The cells were incubated at 37°C with $1\mu\text{M}$ ^{32}P -labelled 15-mer PS ODN (section 2.2.2.2).

2.2.5.5 The Effect of pH on Cellular Association/Uptake.

Cell association/uptake experiments (section 2.2.5.1) were conducted using C6 glioma cells at a concentration of 2.5×10^5 cells/mL in 24 well plates at different pH (5, 6, 7, and 8). For these experiments instead of incubating in SFM, an incubation solution comprising of Hanks

balanced salt solution (HBSS) containing 0.01% phenol red, 5mM D-glucose and buffered with 25mM HEPES [(N-2-hydroxymethylpiperazine)-N'-2-ethanesulfonic acid] at pH 7 and 8 or MES [2-(N-morpholine)-ethanesulfonic acid] at pH 5 and 6 was used. The cells were incubated at 37°C with 1µM ³²P labelled 15-mer PS ODN (section 2.2.2.2).

2.2.5.6 The Effect of Temperature on Cellular Association/Uptake.

Cell association/uptake experiments (section 2.2.5.1) were conducted using C6 glioma cells at a concentration of 2.5 x 10⁵ cells/mL in 24 well plates at different incubation temperatures (37°C and 4°C). The cells were incubated for 1 hour with 1µM ³²P-labelled 15-mer PS ODN (section 2.2.2.2).

2.2.6 Cellular Efflux Studies.

To assess the efflux of labelled material from C6 glioma cells, a similar method to that of Tonkinson and Stein (1994) was used. Studies were initiated in 96 well plates as described in section 2.2.5. Cells were incubated separately with the following: 1µM ³²P -labelled PS ODN, 1µM D-[1-¹⁴C] Mannitol (Amersham Life Sciences, UK), or 1µM ³²P -labelled PS ODN and Lipofectamine (section 2.2.10.1) complex (1:1 charge ratio), for 2 hours at 37°C. Following cell loading the culture plates were placed on ice and the apical medium was removed and collected in scintillant. Cells were then re-covered in pre-warmed (37°C) SFM and incubated for the stated efflux times (5 minutes to 5 hours). Following efflux, the cells were quickly washed three times with ice cold PBS containing 1% bovine serum albumin (BSA), each efflux sample was collected in scintillant. Levels of radioactive material in each sample was determined by liquid scintillation counting (section 2.2.5.2).

2.2.7 Fluorescent Localisation Studies.

2.2.7.1 Preparation of Fluorescent Materials.

5'-FITC (fluorescein isothiocyanate) labelled ODNs were synthesised and purified as described in section 2.2.3.2. Free FITC (mixed isomers, HPLC purified) were obtained from

Sigma. Rhodamine B isothiocyanate-Dextran (0.002-0.01 moles RITC per mole of glucose, approximate Mol Wt. 10000) was obtained from Sigma and purified through Nap-10 columns (section 2.2.2.4) to remove free rhodamine. Fluorescently labelled dextrans have been characterised as an indicator of fluid phase endocytosis and are known to reside in endocytic vesicles of various types following cell entry (Amano *et al*, 1981). Unlike dextrans labelled with fluorescein, dextran labelled with fluorophores such as rhodamine demonstrate significantly less bleaching effect when exposed to light (Swanson, 1989).

2.2.7.2 Cell Association of Fluorescently Labelled Probes.

C6 glioma cells at a density of 1×10^5 cells/mL per well were seeded onto 8 well Permanox chamber slides (LAB-TEK, Naperville, USA) and incubated for 24 hours at 37°C. Following incubation cells were washed with pre-warmed sterile PBS. 5'-FITC labelled ODNs were diluted to a concentration of 5µM in SFM. Where co-localisation studies were to be performed the medium containing the fluorescein labelled ODN was supplemented with 5µM RITC-dextran. In control experiments 5µM of free FITC or 5µM of RITC-dextran in SFM were used as test samples. These media were added to the cells which were incubated for the required period (normally 4 hours) at 37°C.

Following incubation, cells were washed four times with sterile PBS to remove traces of non-cell associated fluorophores. The plastic chamber gasket was separated from the cells on the slide. Slides were mounted in Vectashield Mounting Medium (used as an anti-fading agent) for fluorescence (Vector Laboratories Inc., Peterborough, UK), and a cover slip added. The slides were then viewed using fluorescence microscopy (section 2.2.7.3).

In all studies additional wells were seeded with cells and treated with test solutions. Cells were then removed by trypsinisation and viable cell counts determined using trypan blue exclusion. Cell counts were made using a haemocytometer (section 2.2.1.5). The percentage viable cells was typically in the range of 90-95%.

2.2.7.3 Fluorescence Microscopy.

A Jenamed fluorescence microscope (Jena Instruments, Oberkochen, Germany) and a high pressure mercury HBO-50 light source (C-Z Scientific, Basingstoke, UK) were used to visualise cell associated fluorophores, using epifluorescence. The excitation and emission spectra of fluorescein and rhodamine B overlap to a small degree (Minta *et al*, 1989), therefore narrow band-pass filters were required to distinguish between the fluorophores.

A 510nm wavelength blocking filter was used for detection of fluorescein and FITC labelled probes. With reference to UV emission spectra of fluorescein and rhodamine (Minta *et al*, 1989), the use of the 510nm narrow band blocking filter should totally prevent any cross-over excitation/emission from rhodamine. For the detection of rhodamine-dextran, a 590nm wavelength narrow band blocking filter was used as recommended for the differential detection of this fluorophore (Minta *et al*, 1989). The filter sets were mounted in a mechanical filter cube positioned above the objective lens of the microscope to permit rapid switching of the filters and allow images of the fluorescence from multiple probes in the same specimen.

Cells were photographed using an Olympus camera with Jenamed adapter and Kodak Gold (colour) or Illford FP4 (black and white) film (minimum ISO 200).

2.2.8 Ultrastructural Studies.

2.2.8.1 Ultrastructural Localisation of Biotinylated Materials.

Immunocytochemistry was used to detect biotin and biotinylated compounds within ultra thin sections of C6 glioma cells. The detection method involved the use of monoclonal antibodies raised against biotin, which specifically bind to their biotin antigen within cells, provided that the antigen has not changed its structure. Monoclonal antibodies can be labelled with gold particles to permit detection in ultra thin sections using transmitted electron microscopy (TEM).

Cells prepared for electron microscopy, are generally treated with the cross-linking fixative glutaraldehyde to preserve cellular morphology. In addition cells are then dehydrated, embedded within a support material and cut into extremely thin sections. However, chemical fixatives generally have a detrimental effect on immunoreactivity because antigen structure can be chemically destroyed. In addition, the access of antibodies to their antigens is hindered by extensive protein cross linking within the cells (Wilchek and Bayer, 1990). Therefore a justifiable compromise has to be found between preservation of cellular morphology and the maintenance of immunoreactivity.

Several approaches have been used here in an attempt to limit the damage to the biotin antigen whilst maintaining cellular morphology as far as possible. Fixation damage was minimised in several ways: cell samples were fixed for a short time period (20-30 minutes) than would be routinely used if preservation of cellular morphology were the sole aim. In addition, the fixative solution contained very low levels of glutaraldehyde, which was substituted with paraformaldehyde, a less potent cross linker. Dehydration using ethanol, was performed at low temperatures in order to reduce extraction of cellular components by dehydration solvents. This technique is termed the progressive lowering of temperature (PLT) method and was followed by a low temperature embedding stage into a resin which has a low viscosity even at very low temperatures. The combination of these measures would be expected to significantly reduce damage to the biotin antigen within cell preparations.

2.2.8.2 Incubation of Cells for Immunocytochemical Studies.

Cells for electron microscopy were grown on Thermanox plastic coverslips (Inter Med, Naperville, USA) in 12 well plates. The Thermanox coverslips (sterilised by immersion in 100% analar grade ethanol for 5 minutes) were placed inside 12 well plates and C6 glioma cells were seeded at 4.5×10^5 cells/mL per well on the coverslips. Any air trapped beneath the coverslips was gently expelled using a sterile pipette tip. Following a 24 hour growth period (producing approximately 70% confluent cell cultures on the cover slips) the cells were incubated with either $10\mu\text{M}$ 5'-biotinylated ODN or $10\mu\text{M}$ biotin-dextran (Sigma, molecular biology grade, Mol Wt. 70000) in SFM at 37°C for 6 hours.

Control samples were prepared in parallel, where cells were incubated with either 10 μ M d-biotin (Sigma, molecular biology grade, Mol Wt. 244.3) in SFM or in the absence of any biotinylated agent for the same time period at 37°C. These cells served as a control of the labelling specificity of biotinylated nucleic acids, as opposed to endogenous or added biotin.

2.2.8.3 Fixation for Immunoelectron Microscopy.

Cell preparations for immunocytochemical studies were fixed for 30-40 minutes in a freshly prepared fixative solution containing 1.5% paraformaldehyde (Sigma, microscopy grade), 0.05% glutaraldehyde (Sigma, grade I) in 0.1M PBS. This is a variation of the '205' fixative which is commonly used to fix samples which are processed via the PLT method. Some of the control cell samples, which had not been incubated in the presence of any biotinylated agents were subjected to a much higher level of fixation (2.5% glutaraldehyde in 0.1M PBS). These cells were subsequently processed via the same PLT method, however the greatly increased level of cross linking fixative permitted greater preservation of cellular morphology. These cell preparations were not immuno-labelled, but were viewed under the electron microscope to assess the morphological characteristics of the C6 glioma cell line.

2.2.8.4 Dehydration of Fixed Cells by the Progressive Lowering of Temperature (PLT) Method.

Following fixation, cells were dehydrated by the PLT method which involves stepwise reduction in temperature as the concentration of the dehydrating agent is increased (Armbruster *et al*, 1982). Fixed C6 glioma cells on Thermanox coverslips were placed inside drilled chambers in sterile aluminium blocks containing ascending concentrations of ethanol for 30 minute periods, at progressively lower temperatures as indicated in table 2.1.

TABLE 2.1 Conditions for Dehydration of Fixed Cells by the PLT Method.

Ethanol Concentration	Temperature	Location / Equipment
30%	0°C	on ice
55%	-15°C	refrigerator ice box
70%	-30°C	cryostat chamber
100%	-50°C	Reichert CS Auto
100%	-50°C	Reichert CS Auto

2.2.8.5 Embedding and Sectioning of Dehydrated Cells in Acrylic Resin.

The purpose of the infiltration and embedding steps was to prepare the cells within a solid medium which would have sufficient strength to allow thin sections to be cut using an ultramicrotome.

Lowicryl HM20 (Polysciences Europe, Eppelheim, Germany) was polymerised with 'Initiator C' solution (Polysciences Europe) for a short period of time with very gentle mixing to prevent foaming. Cells were infiltrated with Lowicryl resin inside the Reichert CS Auto at -50°C. Initially cells were exposed to a 2:1 mixture of ethanol:resin for 1 hour, followed by exposure to a 1:2 mixture of ethanol:resin for a further 1 hour period. Cells were then infiltrated with 100% Lowicryl resin inside the CS Auto for a 20 hour period at -50°C. The resin solution was replenished several times throughout this period.

Cells were embedded following the addition of fresh Lowicryl resin which was polymerised at -50°C with UV light for 48 hours in the Reichert CS Auto. The Thermanox coverslips were broken away from the resin material leaving resin embedded cells. These were allowed to equilibrate to room temperature for a further 24 hours prior to sectioning. Thin cell sections (<0.1µm) were cut from the resin blocks (pyramids) using a diamond knife ultramicrotome and these sections were collected on the dull side of Formvar-coated nickel grids (Amersham, UK).

2.2.8.6 Immunocytochemical Labelling of Biotin Antigens within Cell Sections.

Four separate methods were available for the detection of biotin antigens within the prepared sections of C6 glioma cells. Each detection method relies upon the visualisation of colloidal gold particles by electron microscopy. Gold particles are highly electron dense and appear on electron micrographs as a dark dot against the cell structure if properly contrasted by the use of staining techniques (section 2.2.8.6).

Indirect labelling methods combine the use of a primary antibody raised against biotin, which is subsequently detected with a secondary gold labelled agent. Indirect methods are more time consuming than direct methods and require a greater number of controls than for direct labelling methods in order to confirm labelling specificity. There is also a great potential for non-specific reactions, especially where Protein A:gold is used as this binds indiscriminately to all antibodies. Indirect methods are more widely used because primary antibody gold conjugates are often unavailable (Wilchek and Bayer, 1990).

However, direct labelling options are commercially available for the immuno-detection of biotin within cell preparations. Historically streptavidin is an avidin compound derived from the bacteria *Streptococcus* which has a very high affinity constant for binding to biotin (Wilchek and Bayer, 1989). When conjugated with colloidal gold it has been used successfully to detect a variety of biotinylated molecules within cells (Wilchek and Bayer, 1990) including cell surface bound ODNs (Beltinger *et al*, 1995). However recent studies indicate that a primary anti-biotin Ab:gold conjugate demonstrates higher levels of sensitivity in the detection of biotin compared with streptavidin (Technical Bulletin, British BioCell International, Cardiff, UK). Fewer controls are required with direct labelling methods to ensure labelling specificity because only a single labelling step is required. Direct labelling methods are also less time consuming and the overall cost of the labelling reagents is less than that with indirect methods.

In these studies a primary goat anti-biotin antibody, conjugated to 5nm colloidal gold was used. This primary antibody preparation allows a direct, one step labelling protocol to be used in these studies. This is in contrast to previous studies where the intracellular localisation of antisense ODNs was assessed using an indirect labelling protocol (Beltinger *et al*, 1995).

Before the cell sections were exposed to the immuno-gold label, they were first exposed to sterile blocking buffer (0.2% BSA in 0.1M sterile PBS). The cell sections on the nickel grids were carefully placed, dull side down, onto 30 μ L droplets of blocking buffer for 45 minutes at room temperature. The sterile blocking buffer was a general purpose protein solution which would bind to sites on the sections which had non-specific affinity for proteins. Similar buffers have been shown to significantly reduce background labelling in other studies when combined with a suitable washing protocol (Wilchek and Bayer, 1990).

The goat anti-biotin antibody:gold conjugate (5nm gold [EM-GAB5], British BioCell International, Cardiff, UK) was diluted 1 in 50 with sterile blocking buffer. In preliminary studies this dilution was found to give optimal labelling with very low levels of background/non-specific labelling. The cell sections on the nickel grids were dried and placed, dull side down, onto 30 μ L droplets of the diluted immunolabelling solution and incubated overnight in a humidified atmosphere at 4°C.

Following immunolabelling a thorough washing protocol was required in order to remove non-specifically bound antibody:gold particles from the cell sections. The nickel grids were first floated, dull side down, on droplets of blocking buffer for 5 minutes at room temperature. This process was repeated four times using fresh droplets of blocking buffer. Grids were then floated, dull side down, on droplets of sterile distilled water for 5 minutes at room temperature, this process was again repeated four times with a fresh droplet of water.

2.2.8.7 Cell Staining and Examination by Electron Microscopy.

Two stains were used in these studies, in order to provide contrasted images of the cell sections: Uranyl acetate stain (2% uranyl acetate in 70% acetone) and Reynolds lead citrate stain (0.0133g lead nitrate, 0.0176g sodium citrate, 0.08mL 1M sodium hydroxide in 50mL sterile distilled water) were applied to the grids for 15-30 minutes each. Following the application of each stain, the nickel grids were rinsed with sterile distilled water. All cell sections were examined using a JEOL 200X Transmission Electron Microscope, micrographs were taken using Amersham EM photographic media.

2.2.9 Lipid Mediated Delivery of Oligodeoxynucleotides.

2.2.9.1 Preparation of Lipid-Oligodeoxynucleotide Complexes (Lipoplexes).

The lipid used was a commercial cationic lipid called Lipofectamine (Life Technologies, UK) which consisted of two lipid components: charged (+5) DOSPA (2'-(1'',2'')-dioleoyloxypropyldimethyl-ammonium bromide)-N-ethyl-6-amidospermine tetra trifluoroacetic acid) and neutral DOPE (dioleoylphosphatidylethanolamine) in a 3 DOSPA : 1 DOPE ratio.

To produce the correct charge ratio (section 2.2.10.2) of lipid-ODN complex the appropriate amounts of Lipofectamine and 15-mer PS ODN were mixed using a whirlmixer (Fisons, Scientific Equipment, UK) for 2 minutes. The resulting reaction mixture was pulse centrifuged using a microcentrifuge (MSE Microcentaur, Sanyo, UK) and left to stand at room temperature for 30 minutes prior to use in C6 glioma cell experiments (Stegmann and Legendre, 1997).

2.2.9.2 Calculation of Lipid-Oligodeoxynucleotide Charge Ratios.

It is known that the cationic lipid Lipofectamine expresses a net positive charge of +5 while the anionic 15-mer PS ODN had a net negative charge of -14. Therefore it was assumed that equimolar concentrations of lipid and ODN would give the following charge ratio:

$$1\mu\text{M Lipofectamine (+5)} : 1\mu\text{M 15-mer PS ODN (-14)}$$

Hence by altering the concentration of both the lipid and ODN you can obtain the required charge ratio:

$$0.2\mu\text{M Lipofectamine (+1)} : 0.071\mu\text{M 15-mer PS ODN (-1)}$$

2.2.9.3 The Effect of Different Charge Ratios on Cellular Association/Uptake.

Cell association/uptake experiments (section 2.2.5) were conducted using C6 glioma cells in 96 well plates with different Lipofectamine:ODN charge ratios (1:0.5, 1:1, 1:2, 1:4, 1:6, 1:8, and 1:10) and free ODN. These charge ratios included Lipofectamine concentrations ranging from 3 to 57 μM in 100 μL reaction mixture. The cells were incubated at 37°C for 1 hour with a 10 μM concentration of ^{32}P -labelled 15-mer PS ODN in the lipid-ODN complexes or on its own (sections 2.2.2.2 and 2.2.9.1). Cellular association/uptake studies (section 2.2.5) were also conducted with lipid-ODN complexes where a standard 20 μM concentration of Lipofectamine was used in different charge ratios and varying ODN concentrations from 4 to 71 μM in 100 μL reaction mixture.

2.2.9.4 The Effect of Different Lipid Concentrations on Cellular Viability.

Cell viability studies measured by trypan blue exclusion assay (section 2.2.1.5) were conducted using C6 glioma cells (1×10^5 cells/mL) in 96 well plates (section 2.2.5) with varying concentrations of Lipofectamine (10, 20, 40, 100, 200, and 500 μ M). The cells were incubated at 37°C for 1 hour.

2.2.9.5 The Effect of Different ODN Concentrations on Cellular Association/Uptake.

Cell association/uptake experiments as described in section 2.2.5.1 were conducted using C6 glioma cells (1×10^5 cells/mL) in 96 well plates (section 2.2.5) with different 32 P-labelled 15-mer PS ODN (section 2.2.2.2) concentrations (1, 10, 20, 40, 100, 200, and 500 μ M). The cells were incubated at 37°C for 1 hour.

2.2.9.6 The Effect of Time on Lipid-ODN Complex Cellular Association/Uptake.

Cell association/uptake experiments as described in section 2.2.5.1 were conducted using C6 glioma cells (1×10^5 cells/mL) in 96 well plates (section 2.2.5) with Lipofectamine:ODN complex at a 1:1 charge ratio (section 2.2.10.1) over different incubation time periods (1, 2, 4, 6, and 12 hours). The cells were incubated at 37°C with a 10 μ M concentration of 32 P-labelled 15-mer PS ODN in the lipid-ODN complex (section 2.2.2.2).

2.2.9.7 The Effect of Optimised Lipid-ODN Ratio on Cellular Viability.

Cell viability studies measured by trypan blue exclusion assay (section 2.2.1.5) were conducted using C6 glioma cells (1×10^5 cells/mL) in 96 well plates (section 2.2.5) with Lipofectamine:ODN complex at a 1:1 charge ratio (section 2.2.10.1) over different incubation time periods (1, 2, 4, 6, and 12 hours). The cells were incubated at 37°C with a 10 μ M concentration of 32 P-labelled 15-mer PS ODN in the lipid-ODN complex (section 2.2.2.2).

2.2.10 Radioligand Binding Assays.

Receptor binding studies are possible because of the high affinity that some agonists and antagonists have for their receptor. Consequently, at low concentrations of drug, a high proportion is bound to the receptor compared to the proportion which binds to non-receptor sites. Although only minute amounts of receptor are present in most tissues (typically less than 1pmole/mg protein), the amount of drug bound can be measured by radiolabelling it and measuring the amount of radioactivity bound to the tissue. It is essential to separate the bound drug from that which is free in solution, and this can be achieved by filtration (drug bound to the tissue is retained on the filter paper, but unbound drug passes through) or by centrifugation (in which the bound drug is trapped in the tissue pellet). The former is generally, but not always the method of choice provided that the drug does not dissociate significantly from the membranes during the process of filtration or does not bind to the filter.

2.2.10.1 Preparation of the Separating Columns for Glucocorticoid Receptor (GR) Competition Binding Studies.

Sephadex LH-20 (Pharmacia Biotech, Uppsala, Sweden) is prepared by hydroxypropylation of Sephadex G-25, a bead-formed dextran gel, and has been specifically developed for gel filtration of natural products, such as steroids, terpenoids, lipids and low molecular weight peptides, in organic solvents.

Sephadex LH-20 powder was added to excess separating buffer and allowed to swell for 3 hours at room temperature with gentle mixing. Excess buffer was then decanted to remove any unswelled, floating particles and more buffer added to make a gel slurry in a ratio of 50% settled gel to 50% buffer. 5mL of this gel slurry (during mixing) was removed and added to 10mL BioRad separation columns to produce a 2.5mL packed volume of swollen gel per column and allowed to settle. Each column was saturated with a solution of 1% BSA in separation buffer by running 10mL of this solution through the column to prevent any non-specific binding. This was then used to separate ligand bound to GR from unbound ligand, due to differences in their molecular weights.

2.2.10.2 Competition Binding Assay for Glucocorticoid Receptors (GR).

C6 glioma cells (250 μ L, equivalent to 150 μ g protein) or rat brain tissue (250 μ L, equivalent to 200 μ g protein) were rinsed with sterile PBS and harvested in 10mL TEDGM buffer (30mM Tris, 1mM EDTA, 10mM molybdate, 10% v/v glycerol and 1mM dithiothreitol in ddH₂O, pH 7.4 at 4°C) containing a cocktail of protease inhibitors (0.2mM aprotinin, 0.05mM pepstatin A, 1mM EDTA, 0.1mM antipain and 0.1mM phenylmethylsulfonyl fluoride). The resulting suspension was homogenised using a motor driven teflon pestle (8 strokes at 120 rpm) and centrifuged using an ultracentrifuge (Beckman L8-60M, USA) at 100000 g for 60 minutes at 4°C. The supernatant was discarded and the resulting pellet eluted in 500 μ L of TEDGM buffer. 250 μ L of this membrane solution was incubated for 24 hours at 4°C with 10nM [1,2,4,6,7-³H]-Dexamethasone (Amersham International plc, Buckinghamshire, UK), while non-specific binding was determined in parallel incubations containing 2 μ M of the unlabelled GR antagonist mifepristone (RU 486) obtained from Sigma (Poole, UK). To separate bound from unbound radiolabelled ligand, 250 μ L of the incubated samples were added onto the separation column (see section 2.2.10.1) and eluted with 100 μ L fractions of TEDGM buffer. 20 fractions per column were collected in separate scintillation vials containing 5mL of scintillation cocktail and counted (see section 2.2.5.2). This method was based on the protocol followed by O'Donnell *et al*, 1995.

2.2.10.3 5-HT_{2A} Receptor Membrane Preparation from C6 Glioma Cells.

Cells at confluency (40mg of cell pellet) were harvested and homogenised in ice-cold 50mM Tris-HCl buffer, pH 7.4 (at 25°C) containing 5mM MgCl₂ using a motor driven teflon pestle (8 strokes at 120 rpm). The homogenate was centrifuged at 28000 g for 10 minutes. The resulting membrane pellet was washed by resuspension in 50mM Tris-HCl buffer with 5mM MgCl₂, pH 7.4 and centrifuged at 28000 g for 10 minutes twice. The final pellet was resuspended in 50mM Tris-HCl buffer with 5mM MgCl₂, pH 7.4 and used immediately in the binding assays. All centrifugations were carried out at 4°C.

2.2.10.4 5-HT_{2A} Receptor Membrane Preparation from Rat Brain Tissue.

Brain tissue (120-240mg) were weighed individually and homogenised with a motor driven teflon pestle (8 strokes at 120 rpm) in 30 vol of sucrose buffer (0.25M sucrose in 50mM Tris HCl, pH 7.7 at 4°C). The homogenate was centrifuged at 1000 g for 10 minutes at 4°C. The supernatant was stored on ice and the resulting pellet resuspended in 15 vol sucrose buffer (0.25M sucrose in 50mM Tris HCl, pH 7.7 at 4°C). The solution was centrifuged at 850 g for 10 minutes at 4°C. Both the resultant supernatants were pooled, mixed and diluted to 80 vol with assay buffer (50mM Tris HCl, pH 7.7 at 4°C) and centrifuged at 40000 g for 10 minutes at 4°C. The pellet was washed by resuspension in 80 vol of assay buffer and centrifuged at 40000 g for 10 minutes at 4°C. The final pellet was resuspended in assay buffer and used immediately in the binding assays.

2.2.10.5 Saturation Binding Assay for 5-HT_{2A} Receptors.

C6 glioma cell membrane preparations (400µL, equivalent to 150µg protein) or rat brain tissue membrane preparations (400µL, equivalent to 200-400µg protein) were incubated, to equilibrium (15 minutes) with 8 concentrations of [³H]-ketanserin (Amersham International plc, Buckinghamshire, UK), in 50µL assay buffer, over the range 0.5-50nM, at 37°C in a final volume of 500µL. Non-specific binding was determined using 5µM methysergide for each free ligand concentration. Bound and free radioligand were separated by rapid filtration under vacuum through Skatron glass fibre filters (11734) using a Skatron Cell Harvester. The filters were rapidly washed with 8mL assay buffer (50mM Tris HCl, pH 7.7 at 4°C) and radioactivity measured by liquid scintillation counting (see section 2.2.5.2) using 1mL of Packard emulsifier scintillator MV Gold.

2.2.11 Western Blot Analysis of Glucocorticoid Receptor Protein Levels.

Protein blotting involves the immobilisation of proteins on synthetic membrane supports, followed by detection using systems specifically developed for analysing blots. One very common blotting method is the western technique, in which proteins are first resolved by gel electrophoresis. This is followed by blotting (electrophoretic transfer) of resolved proteins

from a gel onto the surface of a membrane (solid-phase support). When the protein is transferred to a membrane it becomes bound to the membrane surface and is easily accessible to many macromolecular probes (antibodies) and other detection and analysis techniques.

2.2.11.1 Preparation of Protein Samples.

C6 glioma cells (25mg cell pellet) or rat brain tissue samples (50mg) were homogenised with a motor driven teflon pestle (8 strokes at 120 rpm) in 5 vol of 0.32M sucrose. The homogenate was centrifuged at 30000 g for 30 minutes at 4°C. The supernatant was discarded with the resulting pellet resuspended in 1.5 vol of Sigma SDS sample buffer (1X) and boiled for 10 minutes in a water bath and used in the western blot assays.

2.2.11.2 Electrophoretic Separation and Western Blotting.

Prepared C6 glioma cell or rat brain tissue samples (25µL, equivalent to 50µg protein) were subjected to denaturing and reducing electrophoresis on BioRad 7.5% Tris HCl (10 well/30µL) precast Ready Gel cassettes using a BioRad Ready Gel Cell Module at 200 volts for 40 minutes in BioRad Tris glycine/SDS buffer (25mM Tris, 192mM glycine and 0.1% SDS). Prestained molecular weight markers (BioRad) enabled visual monitoring of electrophoresis progression. Following electrophoresis the cassettes were opened and the gels removed and left to equilibrate for 30 minutes in BioRad Tris glycine blotting buffer (25mM Tris, 192mM glycine and 20% methanol). The blotting sandwich was made up using the gel, nitrocellulose membrane (0.2µm, BioRad) and blotting filter paper (Whatman) as described by Towbin *et al*, (1979). The blotting sandwich was placed in a BioRad Mini Trans-Blot Module immersed with blotting buffer and electrophoretic transfer achieved by applying, with cooling to 15°C, either 32 volts overnight or 100 volts for 1 hour. Following separation of the blotting sandwich the prestained molecular weight markers provided a visual check of the efficiency of transfer of protein from gel to nitrocellulose membrane. Occasionally nitrocellulose blots (section 2.2.11.4) and gels (section 2.2.11.5) were stained to further assess the efficiency of transfer.

2.2.11.3 Detection of Glucocorticoid Receptor (GR) Protein.

Detection of the GR protein was achieved using a double antibody technique where the secondary antibody (horseradish peroxidase conjugated Donkey anti-mouse Ig, Amersham Life Science) was used to visualise the bands detected by the primary antibody (monoclonal Mouse anti-glucocorticoid receptor IgG₂, Affinity Bioreagents, Inc, USA). The nitrocellulose membrane following blotting was incubated in TBS-T (20mM Tris, 137mM NaCl and 0.1% Tween-20, pH 7.5) blocking buffer with 5% non-fat dried milk (BioRad) for 1 hour at room temperature. Membranes were washed briefly in TBS-T and incubated for 16-20 hours in primary antibody at 4°C diluted 1 in 1000 with TBS-T containing 0.5% non-fat dried milk. The membranes were then washed three times for 5 minutes with TBS-T and incubated in the secondary antibody at room temperature for 1 hour diluted 1 in 1000 with TBS-T containing 0.5% non-fat dried milk. The membranes were then washed three times for 5 minutes with TBS-T and the protein blots detected with Amersham's ECL (chemiluminescence) kit and apposed to film (ECL hyperfilm, Amersham) for 2-10 minutes. Films were developed using freshly prepared Kodak photographic reagents. In order to check accuracy of sample loading, selected blots were reprobbed and detected as described above using a β -actin secondary monoclonal antibody (Sigma) diluted 1 in 500 with TBS-T containing 0.5% non-fat dried milk. Remaining procedures were as described above.

2.2.11.4 Detection of Total Protein Blotted onto Nitrocellulose Membrane.

Nitrocellulose membranes with bound protein were stained with a solution of 1% azide black 10B (BDH) in a 20% ethanol, 7% acetic acid aqueous solution for 20-30 minutes then destained in the same solution, minus the azide black, until the background had reduced sufficiently.

2.2.11.5 Detection of Total Protein in Electrophoresis Gels.

General protein staining of gels was achieved with a staining solution of 1% Coomassie blue R250 (BDH) in 50% methanol, 10% acetic acid aqueous solution for 1.5 hours followed by destaining with 10% methanol, 10% acetic acid solution in water for up to 24 hours.

2.2.12 Protein Determination.

The protein content of C6 glioma cell or rat brain membranes was measured using the method of Bradford, (1976), using bovine serum albumin (BSA) to generate a standard curve. Protein concentrations for cell/tissue samples were determined from the standard curve following computer assisted linear regression (GraphPAD Prism, version 2.01).

2.2.13 Reverse Transcriptase Polymerase Chain Reaction (RT-PCR) Analysis of GR, 5-HT_{2A} Receptor and β -actin mRNA Expression.

RT-PCR is a highly sensitive and specific method for detecting the expression of a particular mRNA sequence in tissue or cells. It can also be used for quantification of mRNA expression level in a sample provided appropriate conditions and controls are used. It is a 3 step process requiring: (i) the careful isolation of intact mRNA, (ii) a single cycle of Reverse Transcriptase catalysed cDNA synthesis from the mRNA template, (iii) repeated cycles of DNA synthesis from the cDNA template using 2 primers specific to the sequence of interest to initiate polymerisation in the forward and reverse direction.

2.2.13.1 Extraction of RNA.

Total RNA was obtained from C6 glioma cells or rat brain tissue by treating samples with the commercially available RNeasy Total RNA isolation kit according to manufacturers instructions (Qiagen Ltd., West Sussex, UK). The yield of total RNA was determined by measuring the absorbency ratio of an aliquot of the precipitated RNA stock at wavelengths of 260 and 280nm (Jenway Scientific Instruments, UK). To check for possible DNA contamination or RNA degradation, after each extraction, 10 μ L RNA samples at a concentration of 0.1 μ g/ μ L were subjected to 1% agarose gel electrophoresis at 80 volts for 1-2 hours and ethidium bromide staining as described in section 2.2.13.2.

2.2.13.2 Agarose Gel Electrophoresis.

Agarose gels (1-2.5%) were prepared by mixing the appropriate weight of agarose with 150mL 1X TBE, warming gently in a microwave until the agarose had dissolved. The agarose solution was poured into a plastic mould (10cm x 10cm) taking care not to introduce air bubbles. A 10cm BioRad comb with 20mm slots was positioned in the liquid agarose solution at one end of the mould to form sample wells. The agarose solution was then allowed to set at room temperature, before the comb was removed. The gel was transferred to an electrophoresis tank (BioRad DNA Sub Cell) filled with 2000mL 1X TBE running buffer. RNA/DNA samples were mixed with 5 μ L of Blue/Orange 6X loading dye (Promega, USA) and loaded into the wells. A 100 base pair (1 μ g/ μ L) DNA ladder (Pharmacia Biotech, Sweden) was added in parallel wells mixed with loading dye for size determination of DNA product bands. Samples were electrophoresed using 100 volts supplied by a BioRad power source for 2-3 hours. Agarose gels were developed by soaking in 200mL 1X TBE buffer with 20 μ L ethidium bromide (10mg/mL) for 45 minutes. Specific product bands separated on the agarose gels were viewed and identified using an UV Transilluminator (UVP Inc., Upland, USA) with Grab-IT Annotating Grabber version 2.04 software (Synoptics Ltd., Cambridge, UK).

2.2.13.3 Oligonucleotide PCR Primers.

Amplification primers were custom synthesised by Gibco BRL (Life Technologies Inc., Paisley, UK). The following primer pairs were used in the RT-PCR experiments to produce their specific PCR product:

(a) Rat Glucocorticoid Receptor

Forward Primer Sequence (5' to 3'):

911-AGA TAC AAT CTT ATC AAG TCC C-932

Reverse Primer Sequence (5' to 3'):

1420-TGA CAT CCT GAA GCT TCA TCG GAG C-1395

Product Size: 1420-911= 509 base pairs

Accession Number: M14053

(b) Rat 5-HT_{2A} Receptor

Forward Primer Sequence (5' to 3'):
1031–GCT GGG CAT CGT GTT CTT CC–1040

Reverse Primer Sequence (5' to 3'):
1247–CTG AAT GTA CCT TGA GAA GG –1228

Product Size: 1247–1031= 216 base pairs
Accession Number: M30705

(c) Porcine β -actin Protein

Forward Primer Sequence (5' to 3'):
1–GTG GGC CGC TCT AGG CAC CA–20

Reverse Primer Sequence (5' to 3'):
245–CGG TTG GCC TTA GGG TTC AGG GGG G –221

Product Size: 245–1= 244 base pairs
Accession Number: AF054837

2.2.13.4 Reverse Transcription (RT).

All reagents, including buffers, that were used for RT-PCR were obtained from Promega (Madison, USA) unless otherwise stated. Total RNA (25ng/ μ L) samples in RNase free diethyl pyrocarbon (DEPC) treated ddH₂O (see section 2.2.13.1) were incubated in a thermal cycler (Hybaid, UK) with Moloney murine leukemia virus (MMLV) reverse transcriptase (200units/ μ L, Gibco BRL, UK) for 1 hour at 42°C and 3 minutes at 94°C in a total reaction volume of 20 μ L containing 10X thermophilic buffer (10mM), MgCl₂ (25mM), RNase inhibitor (40units/ μ L), 10mM of each deoxynucleotide triphosphate (dNTP) and oligo(dT) random hexamer primer (0.5 μ g/ μ L, Gibco BRL, UK). The resulting RT samples were cooled on ice for 5 minutes before being used in the PCR step.

2.2.13.5 Quantitative Competitive Polymerase Chain Reaction (PCR).

20 μ L of the RT sample was mixed with amplitaq DNA polymerase (5units/ μ L, Gibco BRL, UK) in a total reaction volume of 120 μ L containing 10X thermophilic buffer (10mM), MgCl₂ (25mM) and the appropriate test amplification primers (50 μ g/mL per primer) with the control β -actin primers (10 μ g/mL per primer) as described in section 2.2.13.3. The samples were made up to volume with DEPC ddH₂O and covered with 30 μ L of mineral oil (Sigma, UK). PCR cycles were performed in an automated thermal cycler (Hybaid, UK) with the following temperature profile: denaturation at 94°C for 45 seconds, primer annealing at 60°C for 45 seconds and primer extension at 72°C for 1.5 minutes. After an initial denaturation step (94°C for 5 minutes), the cycle was repeated 30 times. The last cycle was followed by a final extension step of 10 minutes at 72°C. Following PCR 20 μ L of the resulting samples were electrophoresed on a 2.5% agarose gel and stained with ethidium bromide as described in section 2.2.13.2. Quantification of the PCR product bands were normalised to the control β -actin bands using a densitometry package with Scion NIH image analysis software (Scion Corporation, Maryland, USA).

2.2.14 Probing Accessible Sites for Antisense Oligonucleotides on GR mRNA.

A major hurdle to the wider application of antisense ODNs is the identification of active antisense sequences which are effective in their ability to inhibit protein synthesis. Thus an empirical selection and screening method in the form of RNase H accessibility mapping was adopted. This involved probing the RNA transcript of interest with a random library of antisense ODNs. Regions on the RNA accessible to hybridisation with members of the ODN library were cleaved using the enzyme RNase H (which acts on RNA-DNA duplexes). These regions are then used to design and optimise antisense ODNs.

2.2.14.1 Antisense ODNs and ODN Library Synthesis.

Phosphorothioate 21-mer antisense ODNs and phosphodiester 12-mer random ODN libraries were chemically synthesised on an ABI 392 automated RNA/DNA synthesiser (Applied Biosystems, UK) using phosphoramidite chemistry, with tetraethyl thiuram disulphide as the

sulphurising reagent. The ODNs were desalted using sephadex G25 gel-filtration (Pharmacia Biotech, UK).

2.2.14.2 T7 Promoter Site RT-PCR.

A 509 base pair fragment of GR cDNA with a 23 base pair T7 promoter site (TTC TAA TAC GAC TCA CTA TAG GG) attached to the 5'-end was generated by performing a RT-PCR as described in section 2.2.13 with the incorporation of a T7-GR forward primer (5'-TTC TAA TAC GAC TCA CTA TAG GGA GAT ACA ATC TTA TCA AGT CCC-3', Gibco BRL, UK) and GR reverse primer (section 2.2.13.3) in the PCR step at concentrations of 50µg/mL in the absence of the control β-actin primers. The integrity of the resulting product was determined by 2.5% agarose gel electrophoresis with ethidium bromide staining (section 2.2.13.2). The T7 GR cDNA fragment was used as the template for generating a GR RNA transcript using an *in vitro* transcription reaction (section 2.2.14.3).

2.2.14.3 In Vitro Transcription.

A 515 base pair GR RNA transcript, [³²P]-radiolabelled at the 5'-end, was generated to act as the substrate for the RNase H accessibility mapping reactions using a SP6/T7 Transcription Kit (Boehringer Mannheim, UK). T7 GR cDNA (0.3µg/µL) samples in DEPC ddH₂O (see section 2.2.14.2) were incubated in a thermal cycler (Hybaid, UK) with T7 RNA polymerase (10units/µL) for 1 hour at 30°C in a total reaction volume of 20µL containing 10X transcription buffer (10mM), RNase inhibitor (20units/µL), 10mM of each ribonucleotide triphosphate (rNTP) and [γ-³²P] guanine triphosphate (GTP) (400 Ci/mmol, Amersham Life Sciences, UK). Following transcription the samples were incubated with DNase I (10units/µL) for 15 minutes at 37°C to remove cDNA template fragments. Samples were finally purified using the RNeasy Total RNA isolation kit (Qiagen Ltd, UK) and used in the RNA accessibility mapping experiments.

2.2.14.4 RNase H Mapping of Antisense ODN Accessible Sites.

Each mapping reaction contained 0.1 μM 5'-³²P-labelled RNA transcript, 50mM Tris HCl, 10mM MgCl₂, 50mM KCl, 10mM DTT, RNase inhibitor (20units/ μL), 0.5nM random 12-mer ODN library or specifically designed PS antisense ODN and RNase H (25units/ μL , Boehringer Mannheim, UK) in a total reaction volume of 10 μL . The mixture was incubated for 30 minutes at 37°C and analysed by 6% denaturing (7M urea) PAGE at 25 watts for 2.5 hours as described in section 2.2.4.1. Autoradiography was performed as described in section 2.2.4.2. The cleaved RNA fragments were sized using the RiboMark labelling system (Promega, USA).

2.2.14.5 *In Vitro* Treatment of C6 Glioma Cells with Designed Antisense ODNs.

The chosen 21-mer PS antisense ODN was complexed with Lipofectamine to produce a lipid-ODN complex (lipoplex) at a charge ratio of 1:1 (section 2.2.10). C6 glioma cells were seeded at 1 x 10⁴ cells/mL/well in 24 well plates and allowed to settle for 12 hours at 37°C in normal maintenance medium (section 2.2.1.1). The cells were then incubated with the lipid-ODN complex at a specified concentration in 1mL of SFM at 37°C for 4 hours. Following incubation the medium was removed and the cells washed with sterile PBS (warmed to 37°C) and replenished with maintenance medium at 37°C. The cells were incubated for a further 20 hours at 37°C. This step of lipoplex treatment for 4 hours followed by its withdrawal for 20 hours was repeated a further 4 times, totalling a period of 5 days of continued cell growth. After this period the cells were harvested for the measurement of GR or 5-HT_{2A} receptor expression. Each treatment was carried out in triplicate (n=3).

2.2.15 Preparation of ODN Loaded Microspheres.

Microspheres can be defined as microporous spherical matrix systems where the drug is uniformly dispersed throughout the polymer. They have the advantage of being used for a wide number of delivery routes depending on their desired application. Microspheres can be prepared by several different methods. Solvent evaporation is the most common where the polymer is dissolved in a volatile organic solvent (e.g. dichloromethane). The drug to be

incorporated is either dissolved or suspended in the polymer solution and the resulting mixture is emulsified in an aqueous phase containing an emulsifier. Evaporation of the solvent occurs during stirring, forming solid drug-loaded microparticles.

2.2.15.1 Double Emulsion Method of Preparing Loaded Microspheres.

A 90 μ L aliquot of aqueous ODN solution of known concentration was mixed with 10 μ L 4% poly vinyl alcohol (PVA) and added dropwise to 500mg of polymer [Poly D,L-lactide co-glycolide 50:50 P(LA:GA), Mw. 3000 (ref RG 502) obtained from Boehringer Ingelheim, Germany] dissolved in 5mL of dichloromethane and stirred at 4000 rpm using a Silverson SL2T mixer (Silverson Machines Ltd., UK) for 2 minutes at room temperature. This formed the primary emulsion and was later added to 160mL of aqueous external phase (0.9%w/v NaCl and 4%w/v PVA in sterile ddH₂O) at 4°C and stirred using a Silverson SL2T mixer at 6000 rpm for 5 minutes at room temperature. The mixture was then left stirring gently (in a beaker covered with punctured parafilm) overnight on a magnetic stirrer (Stuart Scientific, UK). The resulting spheres were centrifuged at 4000 rpm for 10 minutes (43124-704 rotor, Mistral 3000 I centrifuge, MSE Ltd., UK). The supernatants were discarded and the polymer pellet washed by resuspension in sterile ddH₂O and centrifugation as above. This wash protocol was carried out a total of three times to remove any emulsifier and non-encapsulated ODN. The washed microsphere pellet was finally resuspended in 3mL of sterile ddH₂O and frozen at -70°C, followed by freeze drying for 1-2 days (Edwards/Modulyo Freeze Dryer, BOC Ltd., UK).

2.2.15.2 Scanning Electron Microscopy (SEM) of Microspheres.

The surface morphology of polymer microspheres was examined using a Cambridge Instruments Stereoscan 90 Scanning Electron Microscope connected to a computer imaging system. The samples were thoroughly dried and embedded in carbon adhesive on aluminium stubs and gold coated in an Emscope SC 500 sputter coater, in order to obtain a conducting specimen surface. Microsphere images were recorded using the computer imaging software.

2.2.15.3 Microsphere Particle Size Determination.

Approximately 10mg of polymer microspheres were added to 10mL of 0.2µm filtered water and injected into a Malvern Mastersizer E, Class 1 particle sizer (Malvern Instruments, UK). The average size and size distribution range of the microspheres were plotted using a Malvern computer software package (Malvern Instruments, UK).

2.2.16 Surgical Procedure for ICV Administration.

Male Wistar rats (Charles River, UK) weighing 270-310g at time of surgery were housed in groups of 2 on a 12 hour light/dark cycle (lights on at 07:00 hours, $21 \pm 1^\circ\text{C}$ and 55% humidity). Rats were allowed free access to food pellets (standard rat diet) and water at all times. Following an acclimatisation period of two weeks the rats were surgically prepared for ICV ODN administration. Rats were anaesthetised through a mouthpiece using isoflurane (5% for induction and 2.5% for maintenance) with N_2O and O_2 (flow rate set to 1 L/min) and placed in a Kopf stereotaxic frame with the incisor bar connected to a mouthpiece delivering maintenance anaesthetic. The rats were gently wrapped in a towel and the Kopf frame ear bars inserted. Under aseptic conditions the surface of the skull was exposed, a small burr hole was made at the site of injection, followed by puncturing of the dura. A single 2µL injection was made into the left lateral ventricle at co-ordinates: 0.9mm caudal to bregma, 1.4mm lateral and 3.5mm below the surface of the dura (Paxinos and Watson, 1986). Injections were made using a 10µL Hamilton syringe (30 gauge needle) over a 2 minute period. The syringe was left in place for a further 1 minute before being slowly withdrawn. The burr hole was then sealed using bone wax and the region closed using Vetbond tissue adhesive (3M Animal Care Products, Germany). The animals were then allowed to recover from the anaesthetic in new warm padded cages before being returned to original home cages.

2.2.17 Cryostat Sectioning of Rat Brains.

Male Wistar rats (270-310g) were killed using exposure to a rising concentration of CO₂ followed by dislocation of the neck. The rats were decapitated and the skull opened to reveal the brain. Brains were carefully removed intact (over dry ice) and immediately frozen in isopentane cooled on dry ice to -40°C. The brains were then stored at -70°C until sectioning. Sections were cut on a Bright OTF cryostat (Bright Instruments Company Ltd., UK) by placing the tissue on a 2cm wide droplet of partially frozen OCT compound (BDH Laboratory Supplies, UK), on an aluminium cryostat chuck. The brain and OCT compound were kept partially frozen during manipulations with the aid of 'Cryo-Jet Freezing Spray' (BDH Laboratory Supplies, UK). Brains were sectioned either at coronal, sagittal or horizontal planes at thickness of 10-20µm, with the cryostat maintained at -22°C. Sequential cryosections were collected on gelatin coated glass microscope slides ('Superfrost Plus', 25mm x 75mm, BDH Laboratory Supplies) and stored at -20°C until used in further processes.

2.2.18 Preparation of Tissue Sections for Fluorescence Microscopy.

Tissue sections were prepared and mounted on glass microscope slides as described in section 2.2.17. Cryosections on the slides were fixed in acetone at 4°C for 30 seconds and allowed to air dry for 2-3 minutes, after which they were mounted in glycerol (50%) in PBS containing 1% v/v diazobicyclo [2,2,2] octane (DABCO) and a cover slip added. Tissue sections were examined using a Jenamed fluorescence microscope as described in section 2.2.7.3 and photographed using an Olympus camera with Jenamed adapter and Kodak colour Gold film (ISO 800).

2.2.19 Staining of Tissue Sections for Microscopy.

With reference to a stereotaxic atlas (Paxinos and Watson, 1986), structures within sequential cryosections can be identified, if the sections are suitably stained. This atlas catalogues the appearance of structural features in sequential sections of the rat brain. To allow anatomical regions of the brain to be more easily identified, and check for any neuronal toxicity, cresyl violet staining was used.

2.2.19.1 Cresyl Fast Violet Technique for Nissl Substance.

Brain cryosections were examined for histological damage, neuronal loss and glial cell proliferation using cresyl violet staining. Sections (see section 2.2.17) were initially rinsed in ddH₂O then stained with 0.5% cresyl violet for 10 minutes at room temperature. The sections were differentiated in ddH₂O before dehydration through 70%, 95% and 100% ethanol, then cleared in 100% xylene. The sections were mounted using a single drop of DABCO and a glass coverslip added, and were then allowed to air dry before being examined on the Jenamed microscope for qualitative structural changes.

2.2.19.2 Intracerebroventricular (ICV) Injection of Fluorescent Probes.

5'-FITC labelled 21-mer GRAS5 antisense ODN (Life Technologies Inc., Paisley, UK) was administered ICV to male Wistar rats (270-310g) as described in section 2.2.16 in either polymer complexed or free form in an injection volume of 2 μ L. Following administration and recovery the animals were housed for either 1 or 5 days before being killed using CO₂ exposure followed by dislocation of the neck (Schedule 1) and having their intact brains removed (section 2.2.17). The brains were processed and sectioned using a cryostat as described in section 2.2.17. Cryosections were then analysed for ODN *in vivo* CNS distribution using fluorescence microscopy (section 2.2.18).

2.2.20 Animal Post-operative Well-being Assessment.

To assess any neurotoxic effects of the treatment following surgery, rat well-being observations using a set of behavioural parameters over a specific period of time were carried out blind at determined intervals. For observations, treated rats were compared to normal untreated rats. This table of behaviour was devised by Dr. S.L. Handley (see table 2.2) and assesses the following behavioural parameters: locomotion, gait, posture, muscle tone, stereotypy, salivation, cyanosis and dyspnoea. Any difference seen in the behaviours of the test animal compared to normal untreated rats would be noted at that particular time interval. Rat well-being was assessed for a period of up to 5 days.

TABLE 2.2 Rat Behaviour Assessment Sheet.

RAT NO.	L O C O M O T I O N	G A I T	P O S T U R E	M U S C L E T O N E	S T E R E O T Y P Y	S A L I V A T I O N	C Y A N O S I S	D Y S P N O E A	O T H E R
TIME:									

LOCOMOTION:

This is the amount of animal movement (walking or running) from one place to another.

	moving a lot more
	moving more
	normal
	moving less
	moving a lot less

GAIT:

This is how the animal moves (rolling and waddling gait indicates problems with motor coordination).

	extreme 'drunken' walk
	marked rolling 'drunken' walk
	definitely waddling from side to side
	slightly rolling/waddling
	normal

POSTURE:

This is how high the animal is off the ground, when walking and when still.

	body very high when moving or when still
	body fairly high when moving or when still
	normal
	body fairly low when moving or when still
	body very low with little movement

MUSCLE TONE:

This is how floppy, firm or tense the animals body feels when picked up by the handler.

	feels extremely tense
	feels detectably more tense
	normal
	feels fairly floppy or droopy
	feels extremely floppy and droopy

STEREOTYPY:

This is a response to stimulant drugs and manifests as the animal showing vacuous chewing or vacuous licking.

	continuous
	almost continuous
	moderate intermittent
	slight intermittent
	normal

SALIVATION:

Normal animals do not salivate. Salivation occurs either when the rat is too hot or when a drug acts on the salivation mechanism.

	extreme wetness (dribbling)
	marked wetness (chin soaking)
	moderate wetness
	mild-detectable wetness
	normal

CYANOSIS:

This is a dusky grey-blue colouration of bare skin (tails and ears) which indicates deoxygenation of the blood.

	extreme
	marked
	moderate
	mild
	normal

DYSPNOEA:

You can barely see the breathing of normal rats. Therefore large breathing movements may indicate the animals are distressed.

	extreme
	marked
	moderate (heaving)
	mild (sedated)
	normal

OTHER:

Any behaviour not included above is scored in this section. Specifying nature of the change.

In addition to the well-being assessments the treated animals were also weighed daily and following the experimental endpoint had their adrenal glands removed and weighed to check for any systemic effects arising from treatment with the antisense compounds.

2.2.21 DOI Induced Rat Head-Shake Observations.

Male Wistar rats (270-310g) following ICV administration of test compounds as described in section 2.2.16 were housed in home cages in groups of 2 under control conditions (section 2.2.16). Following a period of 5 days post-surgery the animals were assigned to groups of 8 according to the day of surgery and received (0.5mL, i.p.) 1-(2,5-dimethoxy 4-iodophenyl)-2-amino propane hydrochloride (DOI) made up in sterile saline solution to give a concentration of 0.6 mg kg⁻¹. Each animal after DOI administration was isolated and placed in a separate chamber and observed for definite DOI-head-shakes for 20 minutes following i.p. administration. The DOI-head-shake observations were recorded using a SONY video recording system. The animals were then killed immediately after observations had been recorded using CO₂ exposure followed by dislocation of the neck (Schedule 1). Results of the DOI-head-shakes were then summarised in one time bin of +10-20 minutes after DOI injection. Two rats from each treatment group were tested using DOI each day and the results

from 4 days were pooled to give a final n number of 8 rats per treatment group. The DOI-head-shake counts recorded for each rat was made under 'blind' conditions to minimise any subjective variations to the result.

2.2.22 *In Vivo* ODN Stability Studies.

The stability of ICV administered 21-mer ODNs both in the polymer complexed and free form was examined at various times after administration, in rat brain homogenates. Brain tissue were homogenised with a motor driven teflon pestle (8 strokes at 120 rpm) in 10mL PBS and heated to 65°C for 30 minutes. The mixture was centrifuged at 3000 g for 30 minutes at 4°C and the pellet discarded. The resulting supernatant was desalted using Nap-10 columns (see section 2.2.4.2) and dried by vacuum centrifugation (Savant DNA Speed Vac). The dried pellet was reconstituted with 5 μ L of sterile ddH₂O and 5'-end radiolabelled and purified as described in section 2.2.3.1. The 5'-[³²P] labelled samples were analysed by 20% denaturing (7M urea) PAGE and autoradiography (see section 2.2.4) in the presence of known quantities of 5'-[³²P] labelled 21-mer PS antisense ODNs run in parallel lanes as size markers.

2.2.23 Statistics.

Unless otherwise stated, unpaired student's t-test (two-sample assuming equal variances) was used to determine whether there were significant differences between mean values of data obtained from different experimental populations. The Microsoft Excel version 5.0a package was used for this purpose (Fame Software Library, Fame Computers, USA).

Low P values indicated that experimental populations were unlikely to be sampled from populations with equal mean values. Data sets were assumed to be significantly different when P values below 0.05 were calculated. The test assumed that data were randomly sampled, that each value was obtained independent of others and that the populations were scattered according to a Gaussian distribution.

CHAPTER THREE

UPTAKE AND SUB-CELLULAR TRAFFICKING OF ANTISENSE OLIGODEOXYNUCLEOTIDES

3.1 Introduction.

Theoretically antisense ODNs have the potential to be very effective biological tools at the molecular level. However the problems of stability, cellular uptake and intracellular trafficking are some of the main issues which must be addressed before antisense ODNs become standard neuropharmacological tools.

Antisense ODNs are prone to rapid degradation by endogenous exo- and endonucleases (Leonetti *et al*, 1991; Akhtar *et al*, 1992). This problem of nuclease degradation has been largely solved by using chemically modified ODNs (Crooke, 1991). Phosphorothioate (PS) ODNs, in which an oxygen in the internucleotide linkage is substituted with a sulphur atom, are most widely used as an alternative to the unmodified phosphodiester ODNs thus extending the intracellular half-life of antisense ODNs and allowing a sufficient level of inhibition in specific gene expression. Exogenously administered ODNs reportedly enter cells by a combination of different endocytic mechanisms including fluid phase (pinocytosis), adsorptive and receptor mediated endocytosis (for reviews see Akhtar and Juliano, 1992; Reddy, 1996). Various specific oligonucleotide receptors have also been proposed, including an 80 kDa cell surface protein (Loke *et al*, 1989; Yakubov *et al*, 1989) and a 46 kDa protein (Akhtar *et al*, 1996; Hawley and Gibson, 1996). The precise mechanisms of ODN uptake however appear to be dependent upon a whole host of factors, including ODN length, chemistry, conformation, concentration and cell type as well as the cell culture conditions used (Akhtar, 1998).

In addition to delayed degradation, an advantage of phosphorothioate ODNs is that they have an increased affinity for the cell membrane compared to phosphodiester ODNs, and competitively inhibit the uptake of phosphodiester ODNs (Stein, 1997). Consequently phosphorothioate and phosphodiester ODNs are thought to at least partially share the same mechanism of entry, possibly through the same binding proteins, and enter through either receptor-mediated endocytosis or adsorptive endocytosis (Zhao *et al*, 1993). Methylphosphonates, however, which are uncharged and lipophilic, do not compete with either phosphodiester or phosphorothioate ODNs for uptake and are thought to enter cells by a distinct uptake pathway, namely fluid phase endocytosis or by adsorptive endocytosis (Shoji *et al*, 1991). As regards the effect of sequence on cellular uptake, it has been reported that purine rich ODNs demonstrate greater cellular uptake than pyrimidine-rich sequences (Zhao *et al*, 1993) and more recent research by Agrawal *et al* (1996), suggests that sequence and the resulting secondary structure influences the magnitude of cellular association, since guanine rich ODNs that form tetraplexes were shown to become cell associated in greater quantities than other ODNs, as a result of their defined secondary structure.

Delivery strategies such as the use of self-assembled cationic liposomes to produce lipoplexes, have been employed mainly *in vitro* in an attempt to enhance both cellular selectivity and uptake of antisense ODNs (Bennett *et al*, 1992). Cationic liposomes, which consist mainly of a positively charged lipid with a neutral lipid at a certain weight ratio, form stable complexes by intercalating with ODNs; the interaction involved is of an electrostatic nature involving the negatively charged deoxyribose-phosphate backbone and the cationic surface of the liposome. This lipid-ODN complex can improve delivery to cells due to enhanced cellular binding leading to greater cell membrane transfer of ODNs (Bennett *et al*, 1992). However, as entry of ODNs into the right intracellular compartments (cytoplasm and/or nucleus) is an important determinant of antisense ODN efficacy, it is important to investigate the cellular uptake and intracellular trafficking of these molecules in both cell culture and in animal models, but relatively few studies have examined this in detail for brain cells.

Lipofectamine™ is a commercial cationic liposome formulation which consists of two lipid components: positively charged multivalent (+5) 2'-(1'',2''-dioleoyloxypropyldimethylammonium bromide)-N-ethyl-6-amidospermine tetra trifluoroacetic acid (DOSPA) and neutral dioleoylphosphatidylethanolamine (DOPE) in a 3DOSPA : 1DOPE ratio. Virtually all cellular membranes have a local negative charge, from the presence of glycosylated integral membrane proteins and phospholipids, but neurons and glia in particular have an additional internal negative charge due to electrogenic Na⁺/K⁺/ATPase activity. Thus, positively charged DOSPA helps the liposome to bind to the cell membrane by charge interactions which are not tissue specific (Zhou and Huang, 1994). However, charge ratio is also a determinant of efficacy. Charge ratio is the net negative charge being exhibited by the anionic ODN phosphate backbone and the net positive charge from the liposomes cationic lipid, and has been reported to be an important determinant in the efficiency of cellular association/uptake (Bennett *et al*, 1992; Zelphati *et al*, 1996). DOPE is an inverted-cone-shaped lipid and it is included in the liposome because it is thought to facilitate cytosolic release through the fusion to and/or the disruption of the endosomal membrane (Farhood *et al*, 1992). The combined actions of these components are thought to increase the cellular association and transfer of ODNs.

Cationic liposomes appear to enhance biological activity of the encapsulated ODN by increasing the amount of ODN entering the cell, protecting nuclease sensitive ODNs from degradation and increasing sub-cellular distribution of the ODN within the cell (Bennett *et al*, 1992). How the nucleic acid is released from the cationic lipid complex is not clearly understood and is mainly of a speculative nature (Zelphati *et al*, 1996). Zelphati *et al* (1996), have shown that no localisation of ODN occurs in the nucleus at a neutral charge (equal molar ratio of 1:1) whereas at a 10:1 charge ratio approximately 70% of the ODN was localised in the nucleus thus suggesting that charge ratio is critical for optimal activity of cationic liposomal delivery of ODNs. It has also been suggested that optimal charge ratio varies with the type of cationic lipid and the type of cell line being used (Bennett *et al*, 1992).

The objectives of this chapter are to characterise the common properties of chemically modified PS ODNs, which are intended to be used throughout this thesis, in terms of cellular uptake and intracellular biodistribution in cultured rat C6 glioma cells in the presence and absence of cationic lipids. C6 glioma cells are CNS derived and express both receptors of interest (i.e. GR and 5-HT_{2A} receptors; Benda, 1968) and thus were chosen as the cell culture model for these studies. These studies involve optimising cell association/uptake of lipid-ODN complexes for charge ratio. Using a combination of electron microscopy, fluorescence microscopy and efflux studies the altered intracellular trafficking and biodistribution of lipid-ODN complexes was studied. The level of cytotoxicity to C6 glioma cells as a result of lipid-ODN exposure were also investigated using cellular viability studies. These findings have important implications in relation to developing an optimised self-assembling lipoplex delivery system for potential use of ODNs as investigative biological tools on an *in vitro* or possibly *in vivo* level.

The main purpose of the studies covered in this chapter in relation to the thesis objectives were to optimise and characterise a cationic liposomal delivery system at an *in vitro* level for phosphorothioate ODNs in order to achieve maximal cellular penetration and distribution of antisense sequences to postulated intracellular target sites (nuclear and cytoplasmic regions). This would provide the means of attaining superior levels of antisense efficacy at the cell culture level in combination with the other important element of optimal antisense sequence design.

3.2 Methods.

All relevant methods are described in chapter two, with any additional information given in the relevant results section.

Results in this chapter unless otherwise indicated were statistically compared using a one-way analysis of variance with treatment as factor. *Post hoc* comparisons were made using Dunnett's test. In all statistical analysis a value of $p < 0.05$ was considered significant.

3.3 Results.

3.3.1 Cell Association/Uptake Studies.

A 15-mer PS ODN sequence (5'-TTC TTT GGA GTC CAT-3'), designed against the first 15 bases of the rat GR cDNA nucleotide sequence (Miesfeld *et al.*, 1986), was synthesised, purified, quantified and 5'-end ^{32}P radiolabelled as described in sections 2.2.2 and 2.2.3 and used in all of the studies in this chapter. To assess how cell culture density affects cellular association/uptake, the 15-mer PS ODN was incubated at 3 different cell concentrations as described in section 2.2.5.3. As expected, cell association/uptake of PS ODN increased with increasing cell concentration (Figure 3.1), but percentage cell association per cell decreased with increasing cell concentration (Figure 3.2). This would suggest that cell association/uptake is inversely proportional to cell number.

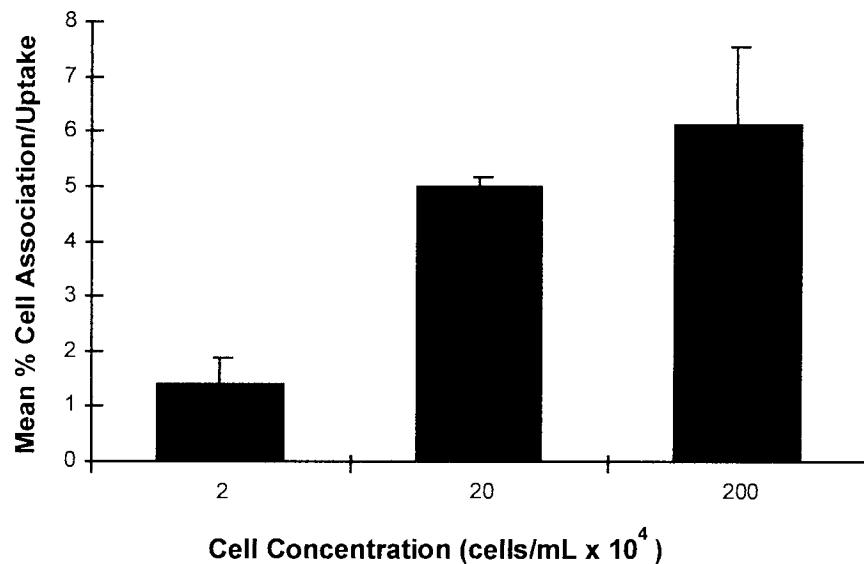


Figure 3.1 Effect of C6 glioma cell concentration on the cellular association/uptake of $1\mu\text{M}$ 15-mer PS ODN in SFM at 37°C and incubated for 1 hour at pH 7.2. Cell-associated ODN expressed as percentage of the total amount applied to the monolayer. Data are mean values \pm standard deviation, where $n=4$.

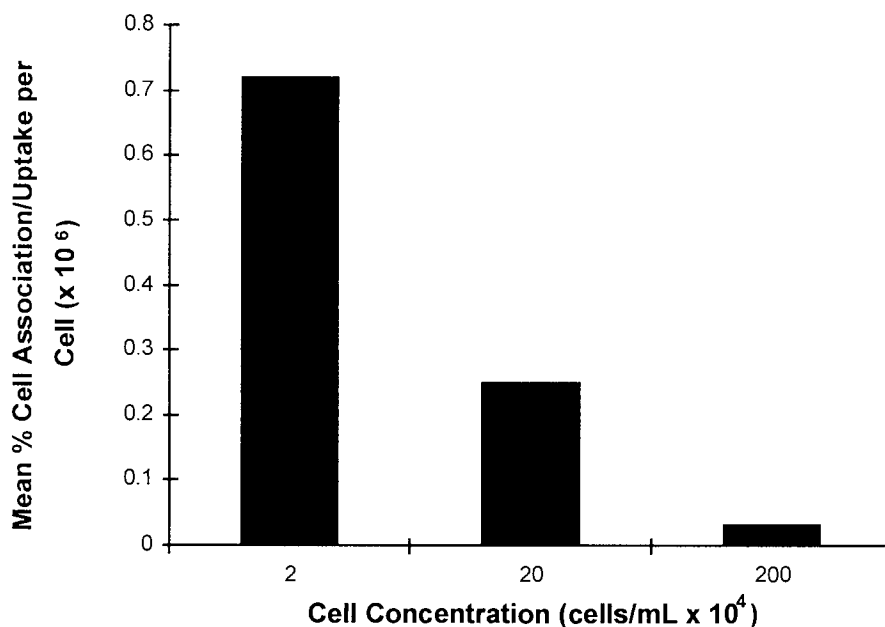


Figure 3.2 Graph showing percentage cellular association/uptake of 1 μ M 15-mer PS ODN in SFM at 37°C and incubated for 1 hour at pH 7.2 per C6 glioma cell. Data calculated using Figure 3.1.

The cellular association/uptake of PS ODNs was defined at selected time intervals and carried out as described in section 2.2.5.4. As shown in Figure 3.3 cellular association/uptake of the ODN appeared to occur via a biphasic process with an initial rapid phase of association over the first 60 minutes followed by a slower secondary phase of cellular interaction.

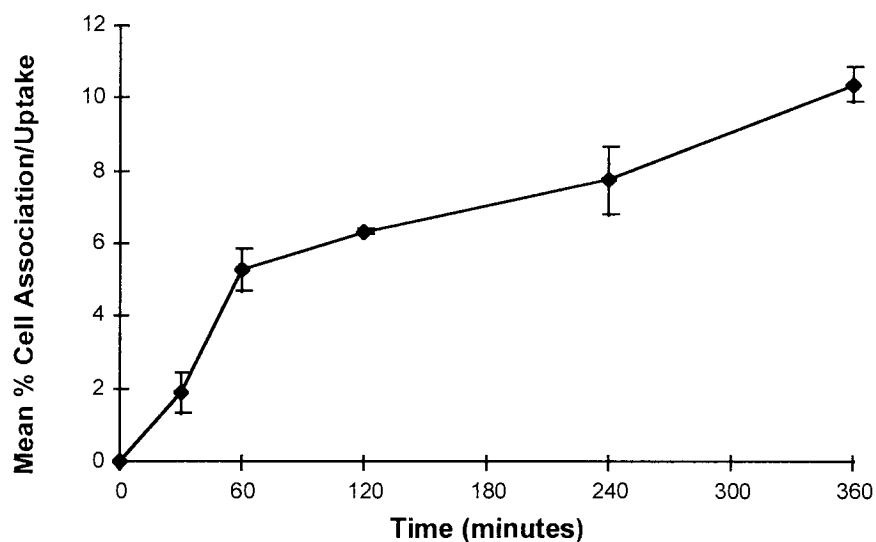


Figure 3.3 Effect of incubation times on C6 glioma cellular association/uptake of 1 μ M 15-mer PS ODN in SFM at 37°C and pH 7.2 using 2.5x10⁵ cells/mL. Cell-associated ODN expressed as percentage of the total amount applied to the monolayer. Data are mean values \pm standard deviation, where n=4.

The cellular association/uptake of PS ODNs when investigated at different pH as described in section 2.2.5.5 showed that a decrease in pH from 7 to 5 resulted in a significant 2 fold increase ($p < 0.05$) in the cellular association/uptake of the ODN, while an increase in pH from 7 to 8 caused a significant reduction ($p < 0.05$) in cellular association/uptake (Figure 3.4).

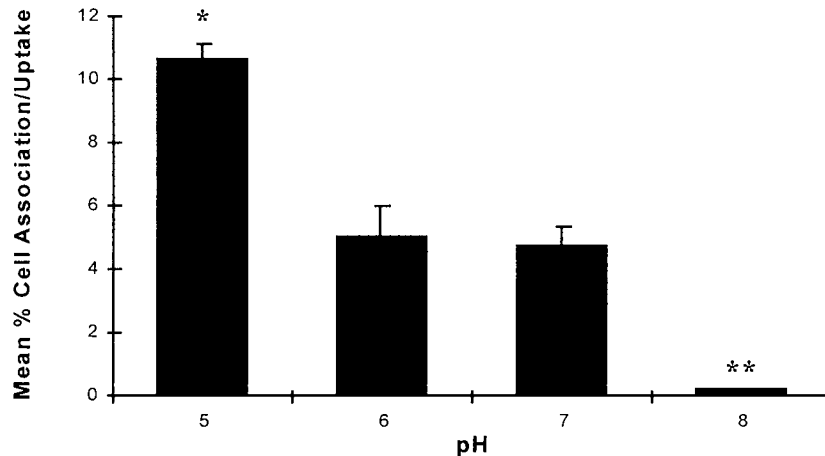


Figure 3.4 Effect of pH on C6 glioma cellular association/uptake of $1\mu\text{M}$ 15-mer PS ODN in SFM at 37°C and 1 hour incubation using 2.5×10^5 cells/mL. Cell-associated ODN expressed as percentage of the total amount applied to the monolayer. Data are mean values \pm standard deviation, where $n=4$ (Dunnett's test, * $p < 0.05$ compared to pH 7, ** $p < 0.05$ compared to pH 7).

To assess the temperature-dependence of cell association/uptake, C6 cells were incubated with phosphorothioate (PS) ODNs at two differing incubation temperatures as described in section 2.2.5.6. Figure 3.5 shows that a decrease in the incubation temperature from 37°C to 4°C resulted in a significant reduction ($p < 0.05$) in the ODN cellular association/uptake, thus indicating that PS ODN cell association/uptake is a temperature-dependent, active process.

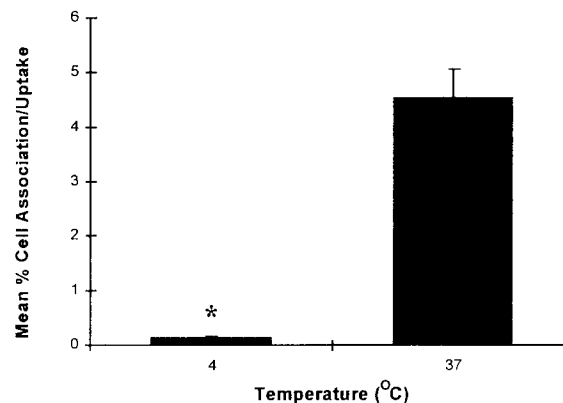


Figure 3.5 Effect of temperature on C6 glioma cellular association/uptake of $1\mu\text{M}$ 15-mer PS ODN in SFM at 37°C and 1 hour incubation using 2.5×10^5 cells/mL. Cell-associated ODN expressed as percentage of the total amount applied to the monolayer. Data are mean values \pm standard deviation, where $n=4$ (unpaired t-test, * $p < 0.05$).

3.3.2 Lipid Mediated Delivery of Oligodeoxynucleotides.

3.3.2.1 Cellular Association/Uptake of Lipid-ODN Complexes.

The effect of the lipid-ODN complex at varying charge ratios on the cellular association/uptake of the radiolabelled ODN, compared with free radiolabelled ODN, is shown in Figure 3.6. This study was performed (see section 2.2.9.3) in two ways: (i) using fixed concentration (10 μ M) of the 15-mer PS ODN and varying lipid (Lipofectamine) concentration to attain the correct charge ratio (Figure 3.6A) and (ii) using a total fixed Lipofectamine concentration (20 μ M) and varying the ODN concentration in the lipid-ODN complex (Figure 3.6B).

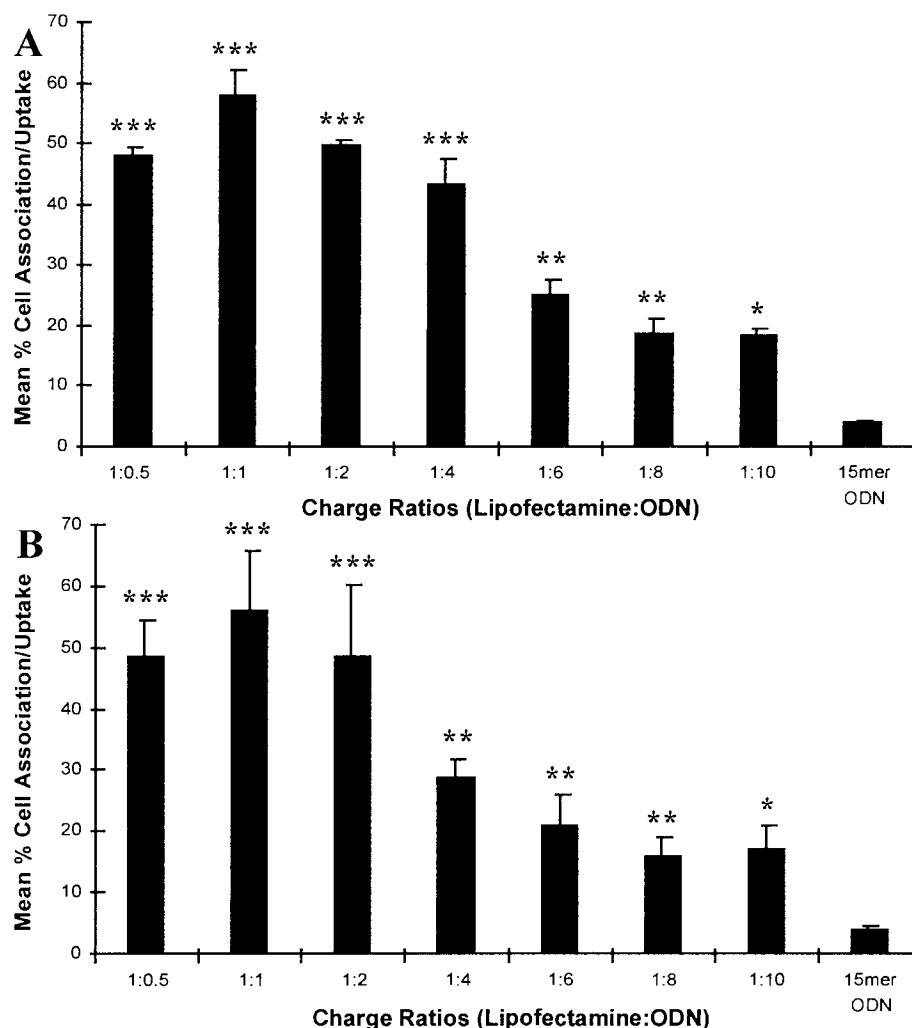


Figure 3.6 Effect of Lipofectamine:ODN charge ratio on the cellular association/uptake of ODN. C6 glioma cells at 2.5×10^5 cells/mL were incubated with: (A) standard 10 μ M 15-mer PS ODN in the Lipofectamine complex for 1 hour at 37°C and pH 7.2 in SFM, or (B) standard 20 μ M Lipofectamine in the lipid-ODN complex for 1 hour at 37°C and pH 7.2 in SFM. Cell-associated ODN expressed as percentage of the total amount applied to the monolayer. Data are mean values \pm standard deviation, where n=4 (Dunnett's test, * $p < 0.01$ compared to 15-mer ODN, ** $p < 0.01$ compared to 15-mer ODN, *** $p < 0.005$ compared to 15-mer ODN).

In both cases (see Figures 3.6A and 3.6B) cellular association/uptake of ODN significantly ($p < 0.01$) increased by approximately 3-4 fold after complexing ODNs with Lipofectamine at the poorest charge ratios (1:8 and 1:10) compared with uncomplexed ODN, while the 1:1 charge ratio significantly ($p < 0.005$) improved cellular association/uptake of ODN by approximately 10-12 fold, suggesting this to be the optimum charge ratio for ODN cellular association/uptake in the C6 glioma cell line. This lipid:ODN charge ratio of 1:1 was thus used as the optimal in subsequent studies.

3.3.2.2 Effect of Time on Lipid-ODN Complex Cellular Association and Cytotoxicity.

In order to study the effects of prolonged incubation on cellular association/uptake of optimised lipid-ODN complex, and also on cellular viability, it was necessary to conduct both cell association/uptake and cytotoxicity studies at specific time intervals (1, 2, 4, 6 and 12 hours) as described in sections 2.2.9.6 and 2.2.9.7. The effect of time on the cellular association/uptake of lipid-ODN complex at 1:1 charge ratio (Figure 3.7A) showed rapid association/uptake within the first hour with only a slight further increase by 6 hours (Figure 3.7A) similar to that seen with uncomplexed ODN (Figure 3.3). However there was a significant ($p < 0.05$) 30% reduction at 12 hours compared to the level at 1 hour (Figure 3.7A). This dramatic drop in cell association/uptake might be suggested to have arisen from toxic effects of the lipid-ODN complex after 12 hour incubation. To further substantiate this suggestion, the effect of time on cellular viability after incubation with the optimised lipid-ODN complex was examined (Figure 3.7B). This showed no statistically significant detrimental effect on cell viability for the first 6 hours of incubation, but a significant reduction ($p < 0.05$) in cell viability occurring at the 12 hour incubation time point. This reduced cell number was likely to account for the reduction in overall cell association/uptake observed at the 12 hour time point in Figure 3.7A and could be attributed to an effect of serum deprivation and/or toxicity of the complex.

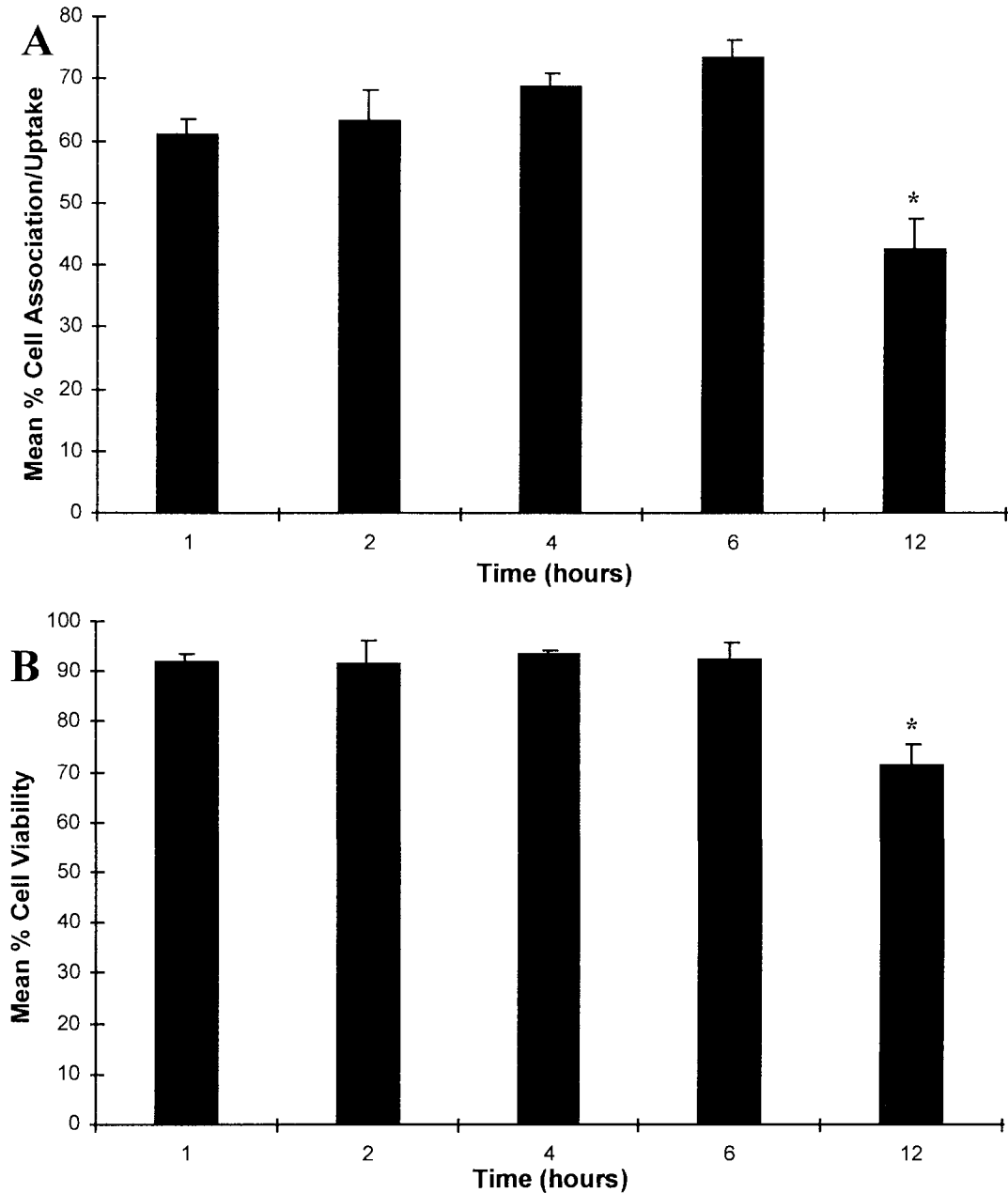


Figure 3.7 Effect of time on the cellular association/uptake (A) and viability (B) of Lipofectamine:ODN complex at 1:1 charge ratio. C6 glioma cells at 2.5×10^5 cells/mL were incubated with $10 \mu\text{M}$ 15-mer PS ODN in the lipid-ODN complex for 1, 2, 4, 6 and 12 hours at 37°C and pH 7.2 in SFM. Cell-associated ODN expressed as percentage of the total amount applied to the monolayer. Cell viability expressed as percentage of the total number of cells initially present in the monolayer. Data are mean values \pm standard deviation, where $n=4$ (Dunnett's test, $*p<0.05$ compared to 1 hour).

3.3.2.3 Effect of Different Lipid Concentrations on Cellular Viability.

During optimisation of Lipofectamine:ODN charge ratio experiments (section 3.3.2.1), concentrations of Lipofectamine from 3-57 μ M were used. To investigate whether this has any effect on cell viability, concentrations up to 500 μ M were tested for cell toxicity, as described in section 2.2.9.4. Figure 3.8 shows that Lipofectamine concentrations of 200 μ M and 500 μ M caused cellular viability to drop significantly compared to the 10 μ M Lipofectamine concentration, most likely due to cell toxicity. Hence the Lipofectamine concentrations used in the other optimisation experiments (between 3 and 57 μ M) were unlikely to cause major differences in cellular association/uptake as a direct result of cell toxicity during the 1 hour incubation.

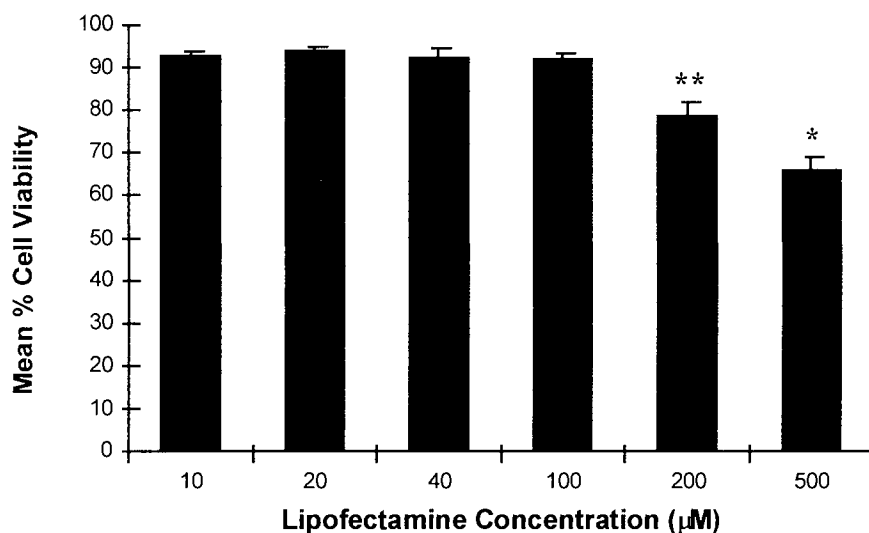


Figure 3.8 Effect of Lipofectamine concentrations on C6 glioma cellular viability in SFM at 37°C and pH 7.2 during 1 hour incubation using 2.5×10^5 cells/mL. Cell-viability expressed as percentage of the total number of cells present in the monolayer. Data are mean values \pm standard deviation, where $n=4$ (Dunnett's test, * $p < 0.05$ compared to 10 μ M, ** $p < 0.05$ compared to 10 μ M).

3.3.3.1 Effect of Different ODN Concentrations on Cellular Association/Uptake.

ODN concentration-dependence of cellular association/uptake was assessed as described in section 2.2.9.5. It was observed (Figure 3.9) that the cell association/uptake mechanisms became saturated at 10 μ M with no significant increases in cell association/uptake occurring at ODN concentrations higher than 10 μ M. This indicates that the 10 μ M ODN concentration

used in the other optimisation experiments was significantly optimised ($p < 0.05$) for cellular association/uptake during 1 hour incubation compared to the $1 \mu\text{M}$ concentration.

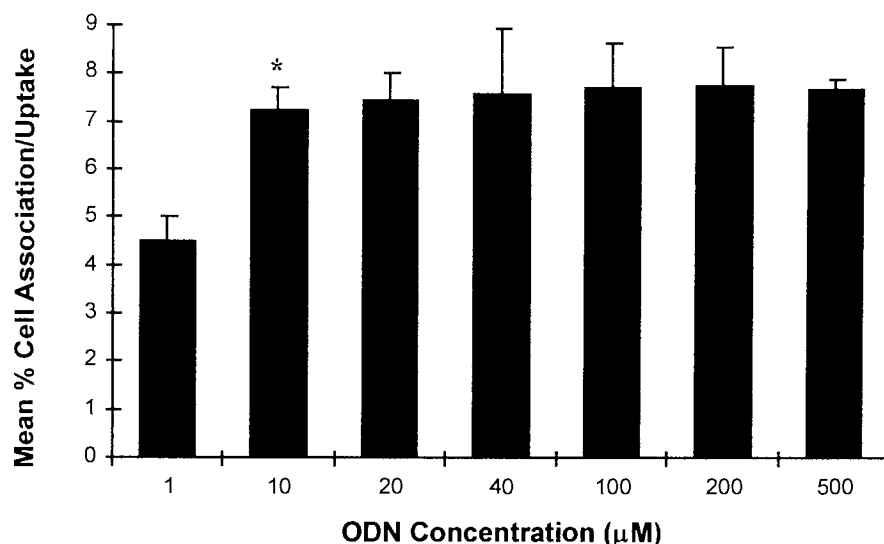


Figure 3.9 Effect of ODN concentrations on C6 glioma cellular association/uptake of 15-mer PS ODN in SFM at 37°C and pH 7.2 during 1 hour incubation using 2.5×10^5 cells/mL. Cell-associated ODN expressed as percentage of the total number of cells present in the monolayer. Data are mean values \pm standard deviation, where $n=4$ (Dunnett's test, $*p < 0.05$ compared to $1 \mu\text{M}$).

3.3.3.2 Cellular Efflux Studies.

Several reports (Loke *et al*, 1989; Stein *et al*, 1993; Tonkinson and Stein, 1994) have indicated that some proportion of ODNs which become internalised within cells are later exported to the extracellular environment, i.e. ODN efflux occurs. In an attempt to understand whether lipid-ODN complexes resulted in altered ODN trafficking from cells, the efflux properties of lipid- $[\text{}^{32}\text{P}]$ -ODN complex compared to uncomplexed $[\text{}^{32}\text{P}]$ PS ODN and the fluid phase marker D - $[\text{}^{14}\text{C}]$ mannitol, was carried out as described in section 2.2.6.

The efflux of mannitol is relatively rapid and consistent with fluid phase endocytosis/exocytosis (Fell *et al*, 1997). A representative plot of the rate of loss of these radiolabelled compounds from C6 glioma cells as a function of time is shown in Figure 3.10. Efflux appears to be biphasic, with the initial rate of efflux probably representing exocytosis from peripheral cytosolic regions (Tonkinson and Stein, 1994). At first glance it would seem that the initial rate of cellular efflux appears to increase in the order: lipid-ODN complex < PS ODN < mannitol. This therefore suggests that in the presence of an optimised lipid complex a

greater fraction of the ODN is retained within the cells with less being effluxed out of the cells which is consistent with the observed lipid-mediated change in ODN distribution (see sections 3.3.4 and 3.3.5).

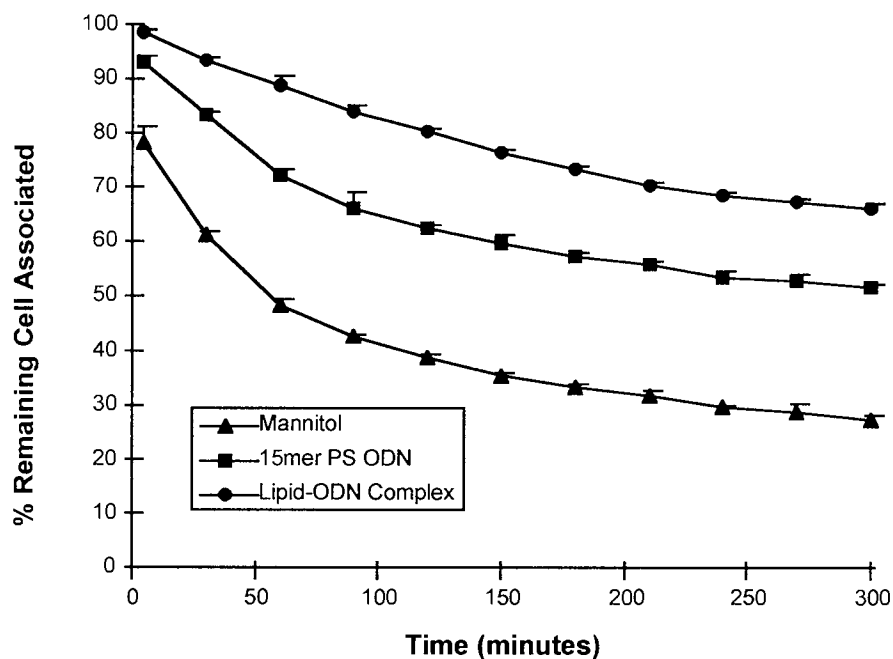


Figure 3.10 Graph demonstrating the rate of loss of radiolabelled compounds from cells over a 5 hour time period following 2 hours steady state accumulation. C6 glioma cells at 2.5×10^5 cells/mL were incubated with either $1 \mu\text{M}$ mannitol (closed triangles), $1 \mu\text{M}$ 15-mer PS ODN (closed squares), or $1 \mu\text{M}$ 15-mer PS ODN in the Lipofectamine:ODN complex at 1:1 charge ratio (closed triangles) for 2 hours at 37°C and pH 7.2 in SFM to allow steady state accumulation then washed to remove non-associated label. Cell-associated compound at each time point is expressed as a percentage of the total amount remaining in the monolayer in control samples taken at the start of the experiment. Data are mean values \pm standard deviation, where $n=4$.

3.3.4 Fluorescent Localisation Studies.

In order to trace subcellular compartmentalisation of ODNs or lipid:ODN complexes after they entered the cell, fluorescently labelled tracers were used. Unconjugated FITC, which readily enters cells due to its small molecular size, was used as a non-compartmentalised indication of uptake and cell integrity. RITC-dextran, which are known to be taken up in endocytic vesicles and lysosomes (Swanson, 1989; Yamashiro and Maxfield, 1987) was used to indicate segregation into these compartments. FITC-ODN was used to trace ODN localisation, and was given either as uncomplexed FITC-ODN, or as lipid:FITC-ODN complexes, all at $5\mu\text{M}$.

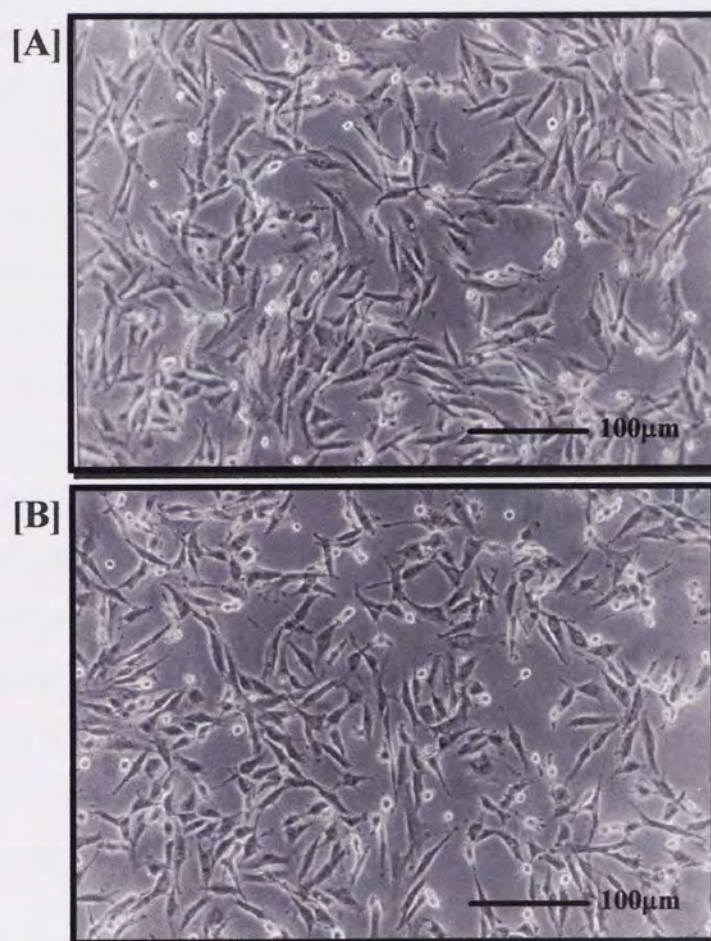


Figure 3.11 Phase contrast images of C6 glioma cells incubated for 4 hours in SFM at 37°C : [A] in the absence of any fluorescent compounds and [B] in the presence of $5\mu\text{M}$ FITC-labelled 15-mer PS ODN in the lipid-ODN complex at 1:1 charge ratio.

Using phase contrast microscopy, no morphological differences of C6 glioma cells were observed with any of the treatments (Figure 3.11), confirming the lack of toxicity seen with these ODN or lipid:ODN complex concentrations in previous studies (sections 3.3.2.2 and 3.3.2.3). Viable cell counts in these experiments also confirmed lack of toxicity (Figure 3.7B).

Using fluorescence microscopy, the cellular uptake and distribution of 5 μ M FITC labelled 15-mer PS ODN was compared with that of both free FITC and RITC-dextran at the same concentration (5 μ M) incubated for 4 hours as described in 2.2.7.2. Unconjugated FITC and RITC-dextran were used as negative and positive controls respectively. Incubation with free FITC label produced an intense fluorescence within C6 glioma cells, indicating cellular uptake. Fluorescence was widely distributed throughout the cells (Figure 3.12) indicating lack of segregation to different subcellular compartments.

C6 glioma cells following incubation with RITC-dextran as described in section 2.2.7.2 produced fluorescence exhibiting a punctate pattern of intracellular localisation with a majority of the fluorescence being localised at the cell periphery close to the cell membrane (Figure 3.13). This is similar to that observed for FITC labelled ODN treated cells (Figure 3.14). The cellular distribution of FITC labelled ODN was distinctly different from that of free FITC distribution (Figure 3.14) since the majority of fluorescence was localised at the periphery of cells close to the cell membrane. In addition the punctate pattern of distribution observed would be consistent with a predominantly endosomal localisation of the FITC labelled ODN. This would suggest that PS ODN, like RITC-dextran, were mainly sequestered into endosomal vesicles following cell entry while the uptake mechanism being mediated by an endocytic process with molecules entering cells by either fluid phase endocytosis, adsorptive endocytosis, or receptor mediated endocytosis (Akhtar and Juliano, 1992).

The clear differences observed in cellular localisation patterns of the FITC labelled ODN and free FITC label indicate that the FITC tag attached to the ODN can be used as a specific label for fluorescence localisation studies in intracellular environments for at least 4 hours.

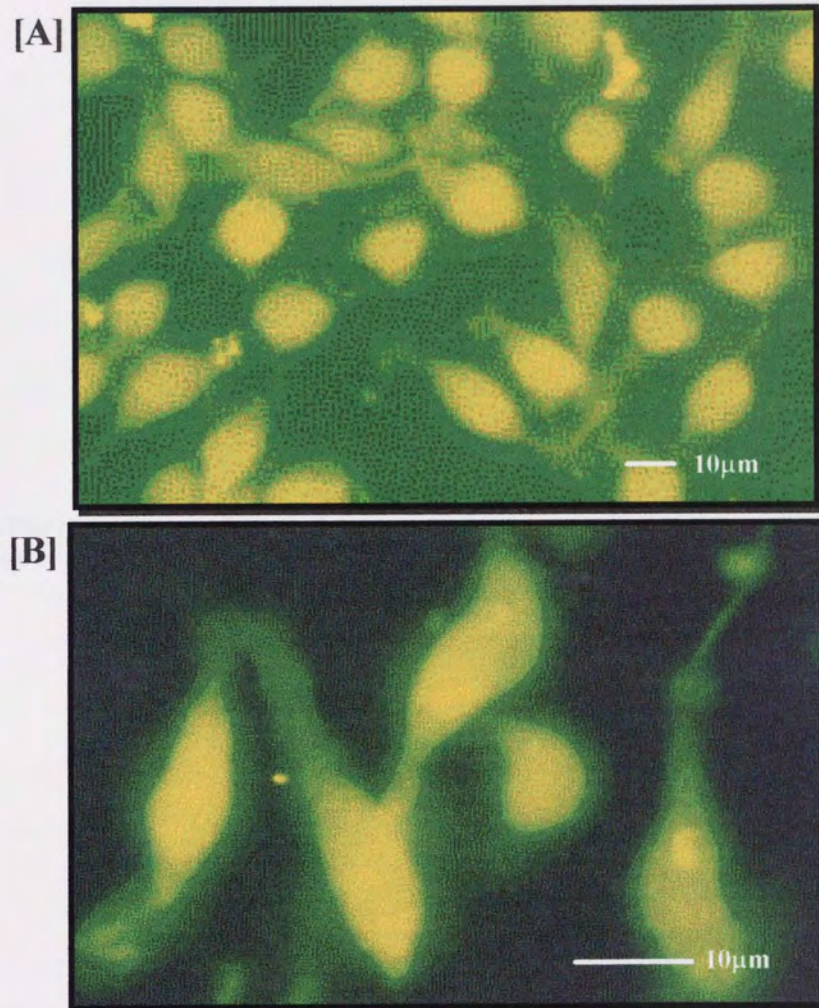


Figure 3.12 Fluorescence detection of 5µM free FITC label associated with C6 glioma cells during 4 hours incubation at 37°C in SFM (see section 2.2.7.2): at [A] low and [B] high magnification.

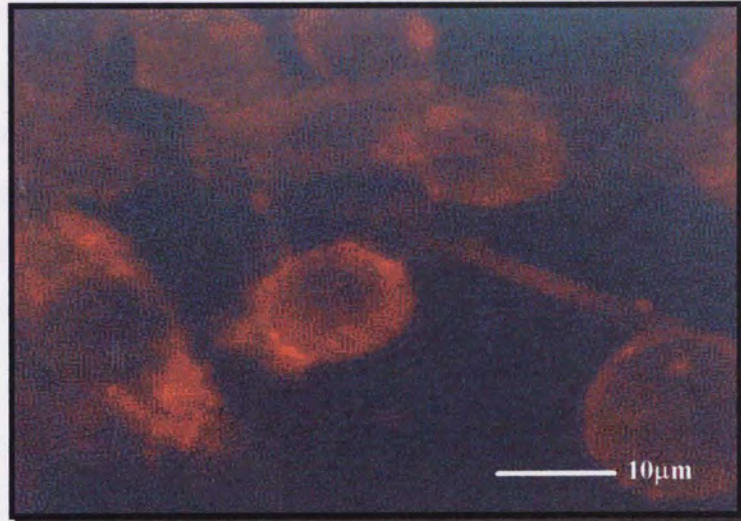


Figure 3.13 Fluorescence detection of 5µM RITC-dextran associated with C6 glioma cells during 4 hours incubation at 37°C in SFM (see section 2.2.7.2).

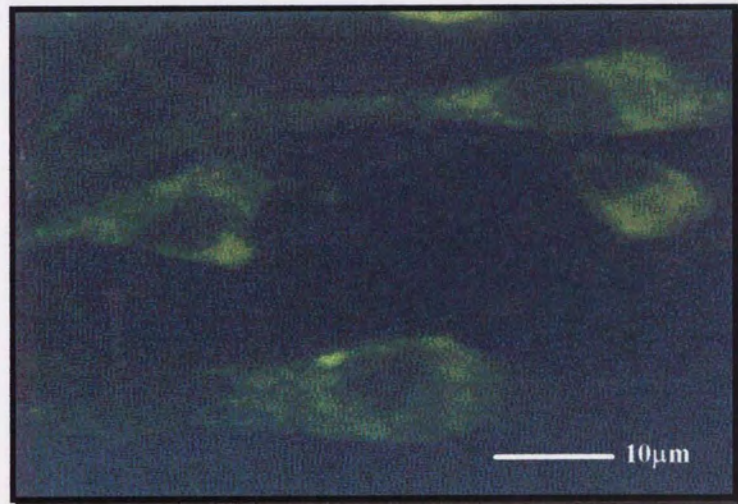


Figure 3.14 Fluorescence detection of 5µM FITC-labelled 15-mer PS ODN associated with C6 glioma cells during 4 hours incubation at 37°C in SFM (see section 2.2.7.2).

3.3.4.1 Time-dependent Subcellular Trafficking of Fluorescein-labelled Lipid-ODN Complexes.

To visualise the subcellular trafficking of FITC-labelled ODN-lipid complex, C6 glioma cells were incubated with the lipid:ODN complex for 15 or 60 minutes as described in section 2.2.7.2. Studies using the FITC-labelled lipid-ODN complex after 15 minutes incubation showed there to be intense fluorescence associated with the C6 glioma cells mainly located at the periphery of the cells in a distinct punctate pattern (Figure 3.15). This labelling was more intense than that seen with uncomplexed FITC-ODN (Figure 3.14) showing the enhanced ODN uptake produced by lipid:ODN complexes.

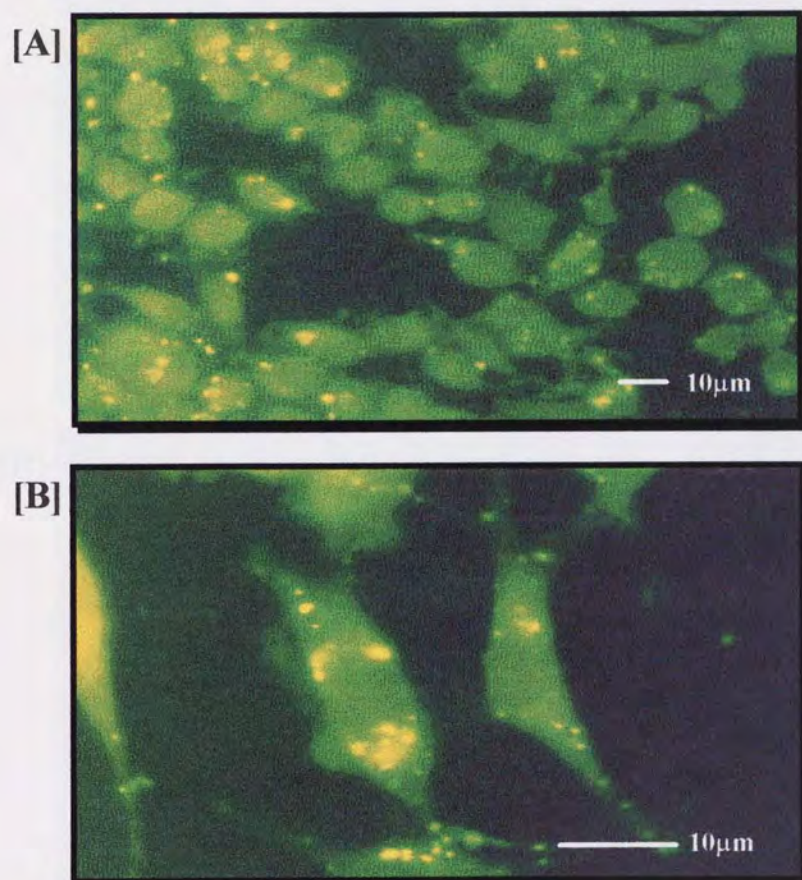


Figure 3.15 Fluorescence detection of 5µM FITC-labelled 15-mer PS ODN in the lipid-ODN complex at 1:1 charge ratio after 15 minutes incubation at 37°C in SFM (see section 2.2.7.2): at [A] low and [B] high magnification.

After 60 minutes incubation with the FITC-labelled ODN-lipid complex, a more diffuse pattern of fluorescence was associated with the C6 glioma cells (Figure 3.16). This distribution was quite different to the punctate labelling seen with uncomplexed FITC-ODN after 60 minutes (Figure 3.13). This therefore suggests that complexing of PS ODNs with cationic liposomes clearly alters their intracellular distribution following entry into the cells. The entry of ODNs into the cells itself may occur more efficiently in the presence of cationic liposomes due to the intense fluorescence seen associated with these cells and also the rapid onset in distribution of this fluorescence, seen within the entire cell.

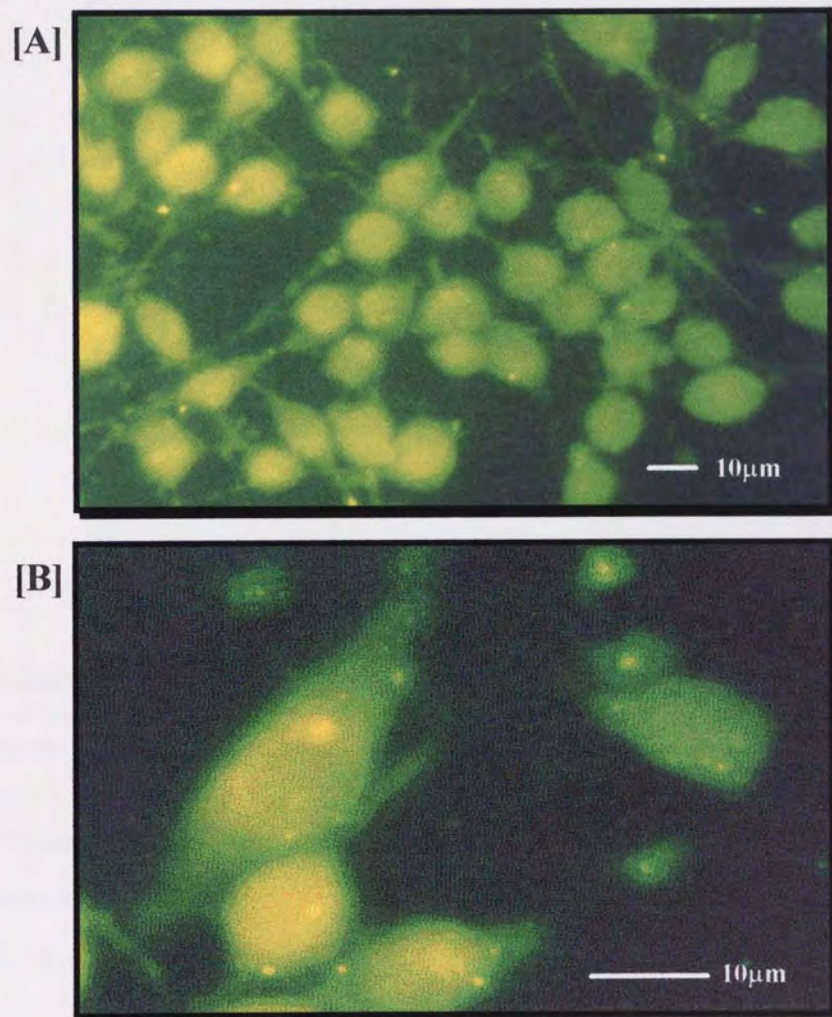


Figure 3.16 Fluorescence detection of 5µM FITC-labelled 15-mer PS ODN in the lipid-ODN complex at 1:1 charge ratio after 60 minutes incubation at 37°C in SFM (see section 2.2.7.2): at [A] low and [B] high magnification.

3.3.5 Ultrastructural Trafficking of Biotin-Labelled Lipid-ODN Complexes.

Detailed analysis of the uptake and sub-cellular trafficking of PS ODNs in the presence and absence of an optimised Lipofectamine complex was carried out using transmitted electron microscopy (TEM) as described in section 2.2.8. Initially untreated C6 glioma cells were glutaraldehyde fixed, sectioned and stained to view general cellular ultrastructure (Figure 3.17).

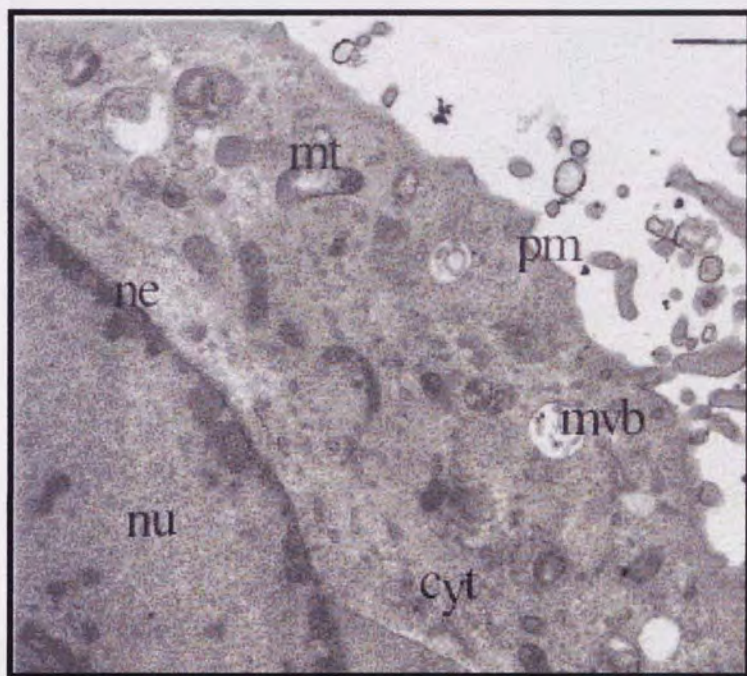


Figure 3.17 Transmission electron micrographs visualising ultrastructural features of C6 glioma cells in the proximity of the cell nucleus (nu). Mitochondria (mt), multi-vesicular bodies (mvb), nuclear envelope (ne), cytoplasm (cyt), plasma membrane (pm) have been labelled. Bar = 500nm.

A milder fixation protocol ('205 fixative') was developed for biotin-ODN treated cells to preserve the biotin antigenicity for subsequent immunogold labelling. However, this somewhat compromised ultrastructural integrity.

In cells treated with uncomplexed biotin-ODN, it was possible to visualise directly the ODN localised within or at the periphery of two types of vesicular bodies. These included the electron dense, lysosome-like structures (Figure 3.18A) and clear, endosome-like structures (Figure 3.18B) which were also previously visualised by Beltinger *et al*, (1995) and Tarrason *et al*, (1995).

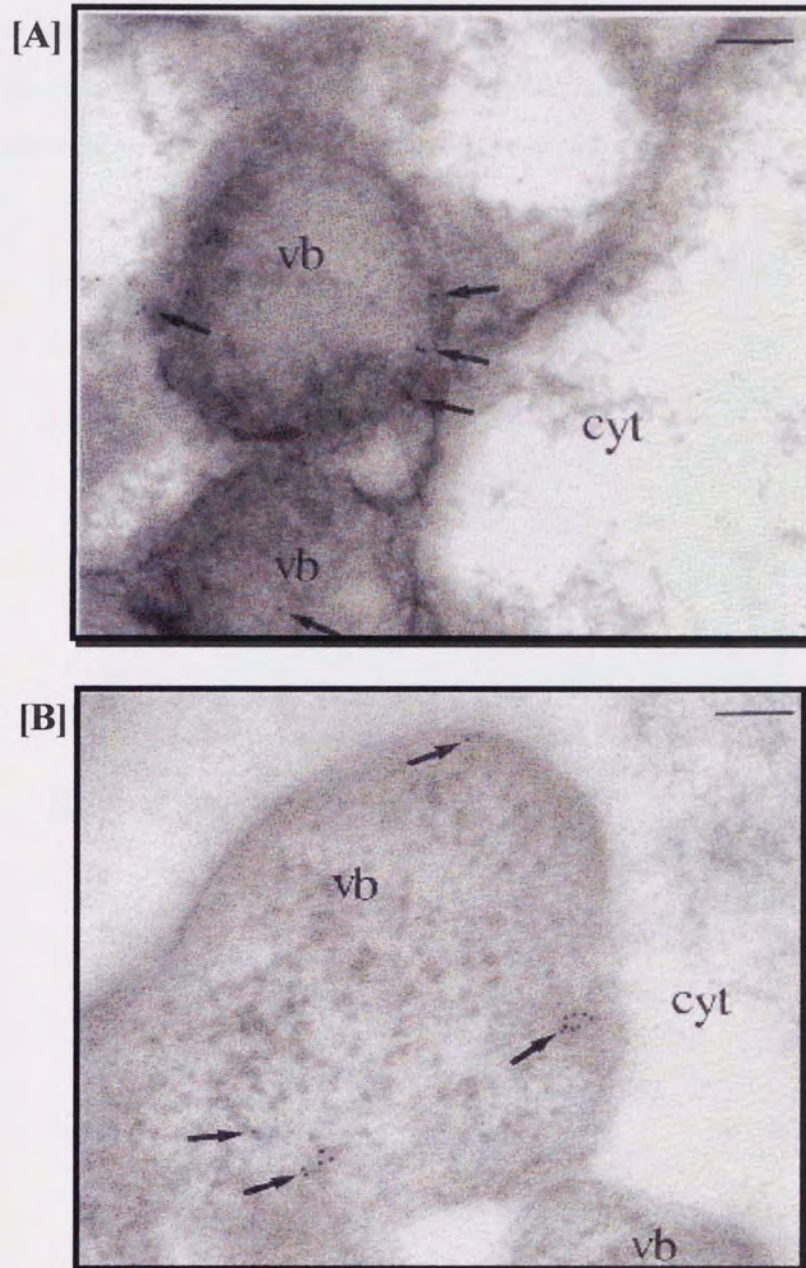


Figure 3.18 Transmission electron micrographs visualising the uptake and subcellular trafficking of biotinylated PS ODNs in C6 glioma cells. (A) Localisation of ODN inside lysosome-like vesicular bodies (vb). Bar = 100nm. (B) Localisation of ODN inside endosome-like vesicular bodies (vb). Bar = 100nm.

In other sections, ODNs were visualised both within the cytoplasm and within the nucleus itself (Figure 3.19A). For sections treated with the optimised lipid:biotin-ODN complex at 1:1 charge ratio, immunolabelled PS ODNs were again visualised intracellularly. However, there were obvious differences in the subcellular trafficking of these liposome complexed ODNs compared to that for the free uncomplexed ODNs. The main differences were the more than 4 fold increase in intracellular gold particle density (Table 3.1), particularly in the cytosol and nuclear regions and significantly reduced density in vesicular bodies (Figure 3.19B). This again confirms that the presence of Lipofectamine increases cellular uptake of PS ODNs, and allows release from vesicular bodies into cytosol, to enhance access into the nucleus.

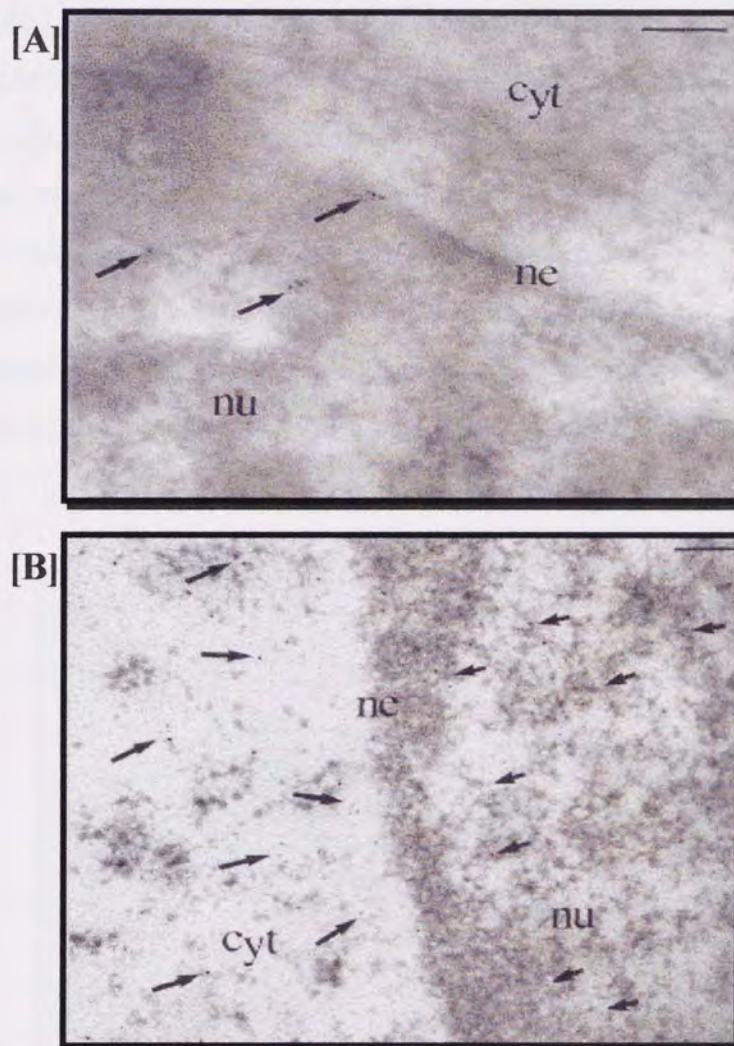


Figure 3.19 Transmission electron micrographs visualising the uptake and sub-cellular trafficking of biotinylated PS ODNs in C6 glioma cells. (A) Localisation of ODN within the cell nucleus (nu) and with the nuclear envelope (ne). [Bar = 100nm]. (B) Increased penetration of ODN in the Lipofectamine:ODN complex (1:1 charge ratio) within the cell cytoplasm (cyt) and nucleus (nu). Bar = 100nm.

Table 3.1 Mean number of gold particles visualised in different fields of TEM micrographs illustrating the distribution of biotinylated PS ODNs (10 μ M) within C6 glioma cells in the presence and absence of an optimised Lipid-ODN complex. Data are mean values \pm standard deviation, where n = 3 (unpaired t-test, *p<0.05, **p<0.01).

Intracellular Compartment	Gold Particles Conjugated to 15-mer PS ODN	Gold Particles Conjugated to Lipid-ODN Complex
Vesicular	15.6 \pm 2.5	7.7 \pm 1.5*
Nuclear/Cytosolic	13.3 \pm 4.2	53.7 \pm 9.5**

Control sections processed by Beltinger *et al*, (1995) which were incubated with free biotin label showed little or no gold particles within cells, suggesting free biotin within cells was not significantly labelled by avidin-gold particles. Although this control was not carried out in C6 glioma cells, it is unlikely that free biotin contributed significantly to the immunogold labelling observed here. Although the exact mechanism of endosomal release was not investigated in these studies, the release of ODNs into the cytoplasm from a clear vesicular body through disruption of the vesicular body membrane was occasionally visualised in sections treated with the optimised lipid-ODN complex (Figure 3.20) but not with uncomplexed ODN. This seems to confirm the supposition that DOPE enhances uptake by disrupting endosomal membranes, and may be specific only to cationic liposomal delivery of ODNs, thus allowing enhanced nuclear entry.

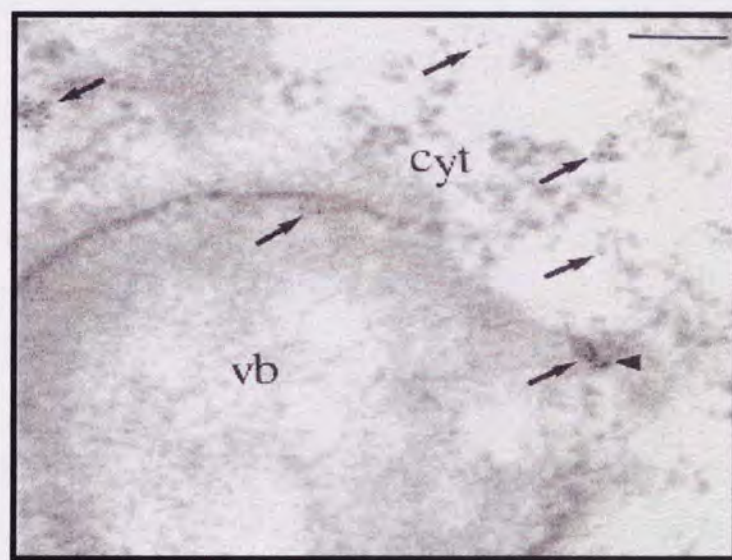


Figure 3.20 Transmission electron micrographs visualising release of biotinylated PS ODN from a disrupted (arrow head) endosomal vesicular body (vb) in C6 glioma cells. Bar = 100nm.

3.4 Discussion.

Cell association/uptake studies were used to optimise delivery of antisense PS ODNs to C6 glioma cells *in vitro*. Figure 3.1 shows that the cell association/uptake of PS ODN increased with an increase in cell concentration while Figure 3.2 shows that cell association/uptake per cell decreased with increasing cell concentration. This effect could be due to the PS-ODN concentration applied being limited at the higher cell concentrations therefore effectively lowering the available ODN concentration per cell. This is generally what is expected as indicated by a study carried out by Akhtar *et al*, (1996).

The cellular association/uptake of PS ODNs with C6 glioma cells appeared to be biphasic, with a rapid initial loading/accumulation that was complete within 60 minutes, followed by a slower sustained incorporation indicative of surface-endosomal membrane cycling (Figure 3.3), but ODN internalisation occurs within 15 minutes with Lipofectamine (Figure 3.15). Thus, the 60 minute time point used in most of the experiments is sufficient to allow significant levels of cellular association/uptake to occur before the cells were processed. When compared to other studies carried out (Hawley and Gibson, 1996; Beck *et al*, 1996) it seems that cellular binding is cell type dependent due to the varying amounts of oligonucleotide binding proteins present with each cell type (Hawley and Gibson, 1996).

In C6 glioma cells the cellular association/uptake of uncomplexed PS ODNs was pH dependent (Figure 3.4) with increased cellular association/uptake occurring at low pH. It is suggested (Beck *et al*, 1996) that the increase in cell association/uptake at lower pH is due to the fact that a decrease in pH would either protonate the cell-surface proteins making them more attractive to the negatively charged oligonucleotides by causing a reduction in repulsion to the oligonucleotides leading to increased cellular binding and therefore cellular association and uptake.

Figure 3.5 shows that the cellular association/uptake of PS ODNs was temperature dependent in this cell line. This implicates the process of ODN binding and internalisation is an active, energy dependent mechanism (Loke *et al*, 1989).

Relatively few studies (Zelphati *et al*, 1996; Bennett *et al*, 1992) have examined in detail the distribution and ultrastructural trafficking and efflux of ODNs in cultured brain cells when delivered with cationic liposomes. In this chapter, we have in detail examined the cellular uptake, intracellular trafficking and efflux of PS ODNs when delivered as a complex with Lipofectamine in C6 glioma cells.

Optimal charge ratio, the net negative charge being exhibited by the anionic ODN phosphate backbone and the net positive charge from the liposomes cationic lipid, has been suggested to vary with the type of cationic lipid and the type of cell line used (Bennett *et al*, 1992). Hence optimisation experiments using the cationic liposome Lipofectamine with the overall objective of enhancing the cell association/uptake and therefore delivery of PS ODNs in C6 glioma cells were carried out. It was observed (Figure 3.6) that the lipid-ODN complex at a 1:1 charge ratio caused the greatest increase in cellular association/uptake while at a charge ratio of 1:8 and 1:10 the complex produced the poorest cell association/uptake, although this was significantly greater than the cell association/uptake of free PS ODNs. It is thought that this liposomal enhancement of PS ODN cell association/uptake could be attributed to the fact that these lipids both increase ODN cell transfer and decrease ODN degradation (Zabner, 1997). Other groups have shown that cationic lipids enhance oligonucleotide cell transfer *in vitro* with efficient oligonucleotide nuclear accumulation (Guy-Caffey *et al*, 1995; Chin *et al*, 1990) while cationic lipids appear to be effective in decreasing oligonucleotide degradation both intracellularly and in human serum (Quattrone *et al*, 1994; Puyal *et al*, 1995). The fact that the lipid-ODN complex at a charge ratio of 1:1 produced the greatest cell association/uptake probably results from this charge ratio yielding the most stable and homogenous form(s) of the complex, culminating in the effective transfer of ODN to glioma cells (Zabner, 1997) rather than preventing ODN degradation. Most of the optimised lipid-ODN complex at 1:1 charge ratio was associated with C6 glioma cells over the first hour of incubation (Figure 3.7A). However there was a significant drop in cellular association at the 12 hour time interval. It was shown that this decline in cell association was due to cellular toxicity for there was also a significant drop in cell viability at this time point (Figure 3.7B). Since some disruption of endosomal vesicles was observed with 1 hour Lipofectamine:ODN treatment, it seems likely that prolonged Lipofectamine exposure may cause further detrimental endosomal and lysosomal breakdown leading to cell death. Therefore it can be assumed that the other

experiments carried out using Lipofectamine over 15 minutes to 6 hours incubation would be unaffected by any Lipofectamine induced cellular toxicity.

Fluorescence microscopy was used to reveal the distribution of PS ODNs in C6 glioma cells. FITC labelled PS ODNs exhibited punctate patterns of distribution confined to vesicular structures with only diffuse cytoplasmic fluorescence (Figure 3.13) similar to those observed with RITC labelled dextran (Figure 3.14). As dextran, following cell entry, is known to reside in endocytic vesicles and lysosomes (Swanson, 1989; Yamashiro and Maxfield, 1987) it can be concluded that PS ODNs are also sequestered in vesicular structures such as endosomes or lysosomes following cell entry. This is supported by the work of Tomkinson and Stein (1994) who found in addition that fluorescein-labelled PS ODNs were detected at higher intensities compared with PO ODNs in HL60 cells. The fluorescence pattern observed for FITC labelled PS ODN is unlikely to result from the redistribution of free FITC cleaved from the ODN, since quite a different pattern of distribution was observed when the cells were incubated with free FITC (Figure 3.12).

FITC labelled PS ODN in the lipid-ODN complex, after a short incubation interval of 15 minutes produced intense fluorescence associated with the C6 glioma cells, exhibiting the characteristic punctate pattern of distribution (Figure 3.15). This suggests an initial enhanced endocytic mechanism of cellular entry for these liposomal complexes. In contrast, incubation for 60 minutes results in an altered distribution for these lipid-ODN complexes, with a more diffuse pattern of fluorescence observed within the cells (Figure 3.16) which suggests subsequent release of ODN from endosomes, followed by cytosolic and nuclear penetration. This would infer that ODN release from endosomes for these lipid-ODN complexes is mediated by the DOSPA/DOPE components of the complex involving certain mechanisms. Such mechanisms of cytosolic entry of liposome complexed ODN include endosomal membrane fusion or direct diffusion and has been discussed by several authors (Yaroslavov *et al*, 1994; Wrobel and Collins, 1995; Zelphati and Szoka, 1996).

With the use of TEM, we confirmed the presence of uncomplexed PS ODN within vesicular bodies thought to be either endosome or lysosome like structures (Beltinger *et al*, 1995; Tarrason *et al*, 1995). In addition, as previously reported (Bennett *et al*, 1992; Wagner, 1994; Guy-Caffey *et al*, 1995) cationic liposome:ODN complexes not only increased the amount of PS ODN that enters the cell, but more importantly, also enhanced release from the endosome compartment into the cytoplasm and nucleus.

In the main TEM studies have shown a distinct alteration of intracellular distribution and trafficking of ODNs when delivered by cationic liposomes. These findings are further supported by efflux studies which revealed a slower rate of ODN loss in the presence of Lipofectamine compared to free ODN and mannitol.

In conclusion, we have demonstrated that optimised cationic liposomes improve both ODN cell association/uptake and intracellular release from endosomal vesicles, leading to a more favourable distribution of ODNs into cytosolic and nuclear regions. In addition a reduced efflux of ODNs from cells when treated with Lipofectamine, will tend to extend the duration in which ODNs are present in the cytosol/nucleus. These two effects combined are likely to lead to an enhanced antisense effect in down-regulation of the glucocorticoid receptor *in vitro* and also lead to the development of cationic liposomes as suitable delivery systems for ODNs compared to delivery of uncomplexed ODNs alone.

CHAPTER FOUR

DESIGN AND SELECTION OF ANTISENSE OLIGODEOXYNUCLEOTIDES

4.1 Introduction.

The development of antisense ODNs as biological agents for protein receptor function elucidation, i.e. for blocking or reducing target mRNA and/or protein expression, relies on the ability of ODNs to bind to the target mRNA by Watson-Crick base pairing, thereby preventing translation into protein. Thus ODNs targeted to sequences only a few bases apart on the mRNA can have quite different efficacy. The interaction between target sequence and antisense ODN is determined in part by mRNA secondary and tertiary structures, which are difficult to predict (Lima *et al*, 1992). The search for accessible sites on mRNA may be further complicated by the presence of RNA-binding proteins that may further prevent ODN hybridisation to otherwise single-stranded accessible sites within the target mRNA (Akhtar, 1998).

Computational approaches have been developed to help predict antisense ODN efficacy by determining folding of target mRNA. But these programmes have proved to be inadequate in appropriate target selection (Stull *et al*, 1992). Recently, two highly elegant strategies based on combinatorial chemistry have been employed in an attempt to select and design effective antisense ODNs. These are (a) Hybridisation of target mRNA to scanning antisense arrays and (b) RNase H accessibility mapping of target mRNA with random ODN libraries (Akhtar, 1998; Southern, 1996; Milner *et al*, 1997).

Scanning combinatorial oligonucleotide arrays is the most recent of the developments in the field of antisense oligonucleotide design (for review see Southern, 1996) and involves a series of overlapping oligonucleotides, of defined or variable length, sequentially targeting every conceivable site within chosen segments of the target mRNA being synthesised by standard phosphoramidite chemistry on a modified polymer membrane or glass surface (Southern, 1996). Hybridisation of these to a radiolabelled target mRNA transcript, immobilised antisense oligonucleotides *in vitro* can be used to identify ODNs accessible sites on the mRNA to which ODN can bind with accuracy at the level of a single nucleotide (Southern *et al*, 1994). This approach can potentially allow comprehensive ‘walking’ of the full-length mRNA sequence to identify accessible sites for optimal antisense effect. However, only short specified regions of the mRNA are normally targeted for combinatorial array design. This strategy has been effectively used to select potent antisense ODNs targeted against bacterial genes (Saizieu *et al*, 1998) and rabbit β -globulin (Milner *et al*, 1997).

Another effective procedure in identifying optimal antisense sequences is the RNase H accessibility mapping technique which relies on the ability of the enzyme RNase H to recognise and selectively cleave the mRNA at sites within the hybridised RNA-DNA duplex. This cleavage reaction is initiated by combining the mRNA transcript of interest with a random, or semi-random, library of chemically synthesised ODNs, which will hybridise to their complementary sequences in the mRNA only if they are accessible. The resulting mRNA cleavage fragments produced thus determine the location of accessible sites for random ODN hybridisation. Such sites can then be used to focus design of optimally acting antisense ODNs to known sequences spanning the cleavage site. This strategy has been effectively used to select potent antisense ODNs targeted to the human multiple drug resistance gene (Ho *et al*, 1996) and to the RNA of hepatitis C virus (Lima *et al*, 1997).

For this thesis RNase H accessibility mapping was adopted as the ideal technique to isolate optimally acting antisense sequences due to the free availability and ease in adopting this technique as opposed to scanning combinatorial oligonucleotide arrays.

The aim of this chapter was to use RNase H mapping to identify accessible regions on a GR RNA transcript, generated by combining reverse transcriptase polymerase chain reaction (RT-PCR) to generate a cDNA construct incorporating the T7 promoter, followed by *in vitro* transcription. Following RNase H cleavage initiated by random ODNs a readily available accessible site would be used to design a series of PS antisense ODNs. The designed antisense sequences would then be optimised for GR RNA cleavage efficiency (a marker for the level of ODN-mRNA hybridisation) and the optimal sequence selected for use as the antisense ODN for downregulating the GR expression both *in vitro* and *in vivo*.

4.2 Methods.

All relevant methods are described in chapter two, with any additional information given in the relevant results section.

4.3 Results.

4.3.1 Synthesis of GR cDNA Template.

To generate a linear GR DNA template containing a T7 promoter region, which allows the recognition of the DNA sequence by a viral T7 RNA polymerase to catalyse the *in vitro* transcription reaction, total RNA was isolated from C6 glioma cells as described in section 2.2.13.1. The integrity and purity of this RNA extract was analysed by 1% agarose gel electrophoresis (2.2.13.2). Figure 4.1 shows the presence of two clear bands representing 28s and 12s ribosomal RNA without any contamination or degradation indicating the integrity of the RNA within the total extract. This total RNA extract was used to generate a 509 base pair GR cDNA transcript corresponding to bases 911-1420 of the full length rat GR, with a 23 base pair T7 promoter site at the 5' end, as described in section 2.2.14.2. RT-PCR cDNA products were analysed by 2.5% agarose gel electrophoresis (2.2.13.2), revealing a single band of approximately 532 base pairs (Figure 4.2).



Figure 4.1 Representative gel electrophoresis of total RNA (1 μ g per lane) isolated from C6 glioma cells as described in section 2.2.13.1 illustrating the 28s and 12s ribosomal RNA sub-units.

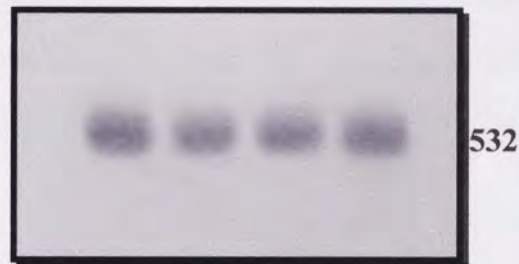


Figure 4.2 Representative gel electrophoresis of T7-GR RT-PCR products (12 μ g of cDNA per lane) obtained as described in section 2.2.14.2, illustrating a product band size of approximately 532 base pairs.

```

911  AGATACAATC TTATCAAGTC CCAGCAGTGT GGCCTACCC CAAGTGAAAA
961  CAGAAAAAGA TGATTTTCATT GAACTTTGCA CCCCCGGGGT AATTAAGCAA
1011 GAGAAACTGG GCCCAGTTTA TTGTCAGGCA AGCTTTTCTG GGACAAATAT
1061 AATTGGTAAT AAAATGTCTG CCATTTCTGT TCATGGTGTG AGTACCTCTG
1111 GAGGACAGAT GTACCACTAT GACATGAATA CAGCATCCCT TTCTCAGCAG
1161 CAGGATCAGA AGCCTGTTTT TAATGTCATT CCACCAATTC CTGTTGGTTC
1211 TGAAAACTGG AATAGGTGCC AAGGCTCCGG AGAGGACAGC CTGACTTCCT
1261 TGGGGGCTCT GAACTTCCCA GGCCGGTCAG TGTTTTCTAA TGGGTAICTA
1311 AGCCCTGGAA TGAGACCAGA TGTAAGCTCT CCTCCATCCA GCTCGTCAGC
1361 AGCCACGGGA CCACCTCCCA AGCTCTGCCT GGTGTGCTCC GATGAAGCTT
1411 CAGGATGTCA

```

Figure 4.3 The nucleotide sequence of the generated GR cDNA fragment as verified by single stranded sequencing.

4.3.2 PCR Product Verification Using Single Strand Sequencing.

The sequence of the T7-GR RT-PCR product was determined out of house (GATC GmbH, Konstanz, Germany) using an ABI 377 automated sequencer. The sequence obtained was identical to the rat GR mRNA sequence (Accession Number: M14053) for bases 911-1420 (Figure 4.3), but with the additional T7 promoter sequence (TTC TAA TAC GAC TCA CTA TAG GG) at the 5' end.

4.3.3 Synthesis of 5'-Radiolabelled GR RNA Transcript.

A 515 base pair GR RNA transcript [³²P]-radiolabelled at the 5'-end was *in vitro* transcribed and purified as described in section 2.2.14.3. The resulting product was subjected to 6% denaturing PAGE (section 2.2.4.1). Figure 4.4 shows the integrity of the synthesised RNA transcript.



Figure 4.4 Autoradiogram of *in vitro* transcribed GR RNA fragment (0.1 μmole per lane) subjected to 6% denaturing PAGE at 25 watts for 2.5 hours as described in section 2.2.4.1.

4.3.4 Identification of RNase H Accessible Sites.

The 5'-radiolabelled 515 base pair RNA transcript from section 4.3.3 encompassing bases 911-1420 of the GR mRNA sequence was probed using a random 12-mer phosphodiester ODN library as described in section 2.2.14.4. Reaction of the 5'-radiolabelled GR RNA transcript with library and RNase H enzyme (lanes 2-4, Figure 4.5) produced specific and discrete cleavage bands, representing accessible sites A-D as compared to the control reactions which produced no cleavage products (Figure 4.5). Densitometric analysis of the cleavage bands using Scion NIH image analysis software, relative to the intensity of the intact GR mRNA transcript (section 2.2.13.5), confirmed the band corresponding to accessible site

D to be the most intense (Figure 4.5) therefore suggesting it to be the site most accessible to antisense ODN hybridisation. Site D was thus chosen to be the optimal site for designing antisense ODNs.

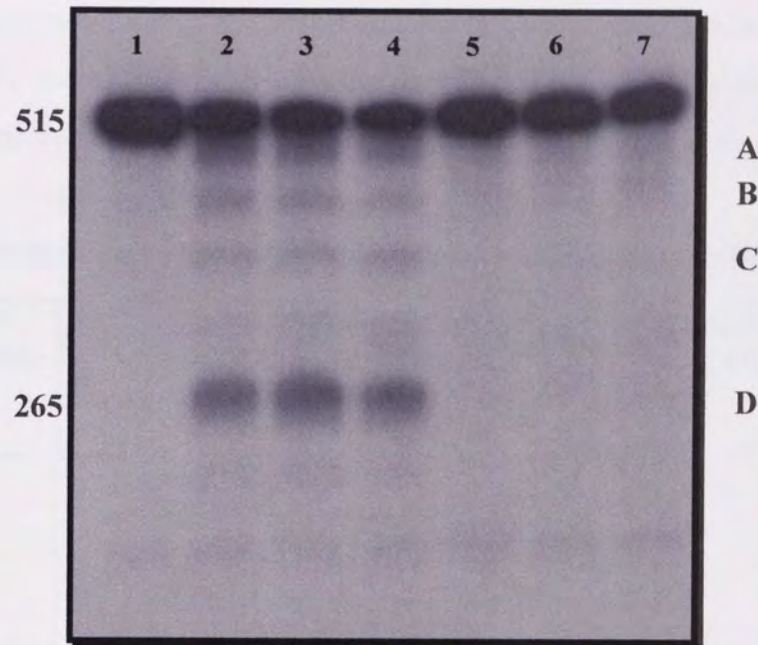


Figure 4.5 Autoradiogram of GR RNA fragments showing RNase H mediated cleavage at accessible sites A-D due to ODN:RNA hybridisation as described in section 2.2.14.4. Lane 1: 5'-radiolabelled GR mRNA transcript. Lanes 2-4: transcript with random ODN library at concentrations of 0.5nM (2), 1nM (3) and 2nM (4) with RNase H enzyme. Lane 5: transcript with 0.5nM random ODN library only. Lane 6: transcript with RNase H enzyme only. Lane 7: transcript with reaction buffer only.

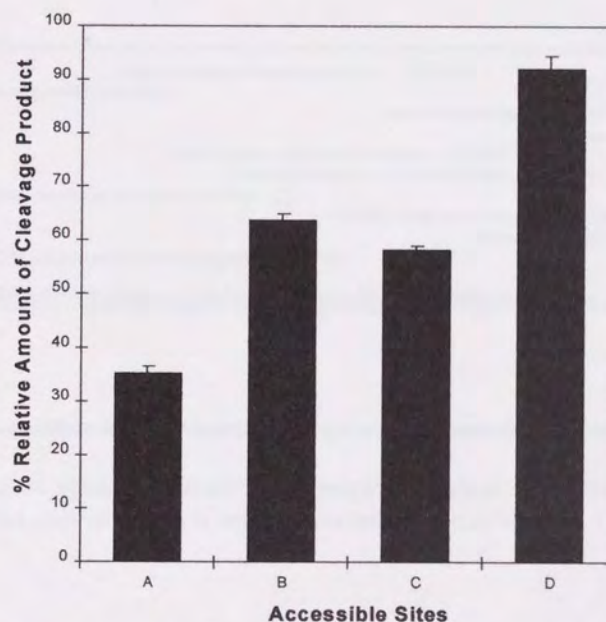


Figure 4.6 Densitometric analysis of cleavage bands, relative to intact GR mRNA transcript, corresponding to accessible sites A-D as shown in figure 4.5. Data shown are mean values (of replicate readings from same electrophoresis gel) \pm standard deviation, where $n=3$.

4.3.5 Design and *In Vitro* Screening of Antisense ODNs.

RNase H cleavage of the T7-GR fragment at approximately 265 base pairs corresponds to cleavage at base 1170 of the full length rat GR mRNA. The DNA sequence around this site, was used to design ten 21-mer PS antisense ODNs (Table 4.1). These antisense ODNs, termed GRAS1-10, were designed against the rat GR mRNA sequence scanning 30-40 base pairs up-and downstream of the predicted cleavage site, as shown in Figure 4.7.

Table 4.1 Antisense oligodeoxynucleotide sequences designed using optimal accessible site D.

ANTISENSE ODN DESIGNS	21-mer PS DESIGN SEQUENCES (REVERSE STRAND) (5' to 3')	SENSE STRAND COMPLEMENT BASES
GRAS1	AACAGGCTTCTGATCCTGCTG	1158-1178
GRAS2	GCTGCTGAGAAAGGGATGCTG	1141-1161
GRAS3	AATTGGTGGAAATGACATTAA	1179-1199
GRAS4	GAACCAACAGGAATTGGTGG	1190-1210
GRAS5	TAAAAACAGGCTTCTGATCCT	1162-1182
GRAS6	GACATTAAAAACAGGCTTCTG	1167-1187
GRAS7	GATCCTGCTGCTGAGAAAGGG	1147-1167
GRAS8	GGAATGACATTAAAAACAGGC	1172-1192
GRAS9	CCAACAGGAATTGGTGGAAATG	1187-1207
GRAS10	GGCTTCTGATCCTGCTGCTGA	1154-1174

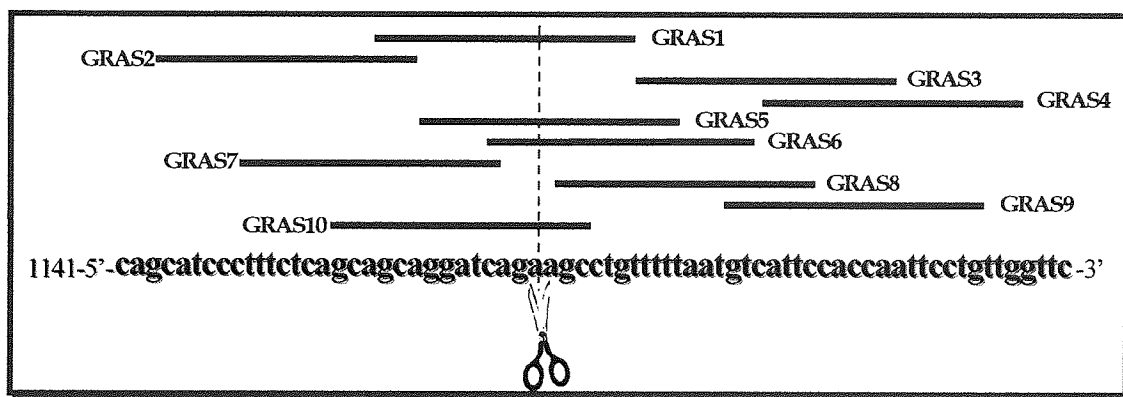


Figure 4.7 Antisense ODN designs GRAS1-10 designed against the GR mRNA sequences around accessible site D. Predicted cleavage site is approximated to occur at base 1170 and is indicated by the scissors.

These 21-mer antisense ODNs were then screened individually against 5'-radiolabelled GR mRNA transcript *in vitro*, using RNase H accessibility mapping as described in section 2.2.14.4. This was carried out to assess the RNase H enzyme mediated RNA cleavage potency of the individual antisense designs. Figure 4.8 shows cleavage of an approximately 265 base pair fragment using antisense ODNs GRAS 1,5,6, and 10. The fragment size produced by GRAS 2 and 7 were somewhat shorter (~250 base pair), while those produced by GRAS 3,4,8, and 9 were somewhat longer (~300 base pair). Since GRAS 1,5,6, and 10 align across the predicted cleavage site, these appear to be mediating cleavage as expected. However, the shorter bands produced by GRAS 2 and 7 binding more 5' appear to indicate cleavage at a secondary, more 5' site, while the longer fragments produced by GRAS 3,4,8 and 9, by binding more 3', indicate another 3' cleavage site. Densitometric analysis of cleavage band intensities (Figure 4.9) shows GR antisense design number 5 (GRAS5) to be maximal (Figure 4.9).



Figure 4.8 Autoradiogram of GR RNA fragments showing cleavage potency by the GRAS designs shown in figure 4.7 as described in section 2.2.14.4. Lane a: 515 base pair 5'-radiolabelled GR mRNA transcript. Lanes 1-10: transcript with corresponding 21-mer PS antisense ODN GRAS designs 1-10 and RNase H enzyme.

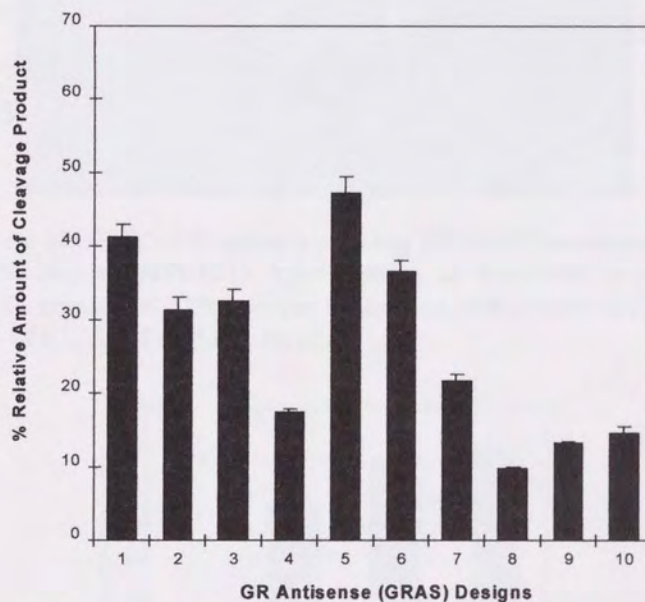


Figure 4.9 Densitometric analysis of cleavage bands, relative to intact GR mRNA transcript, illustrating RNA cleavage potency by 21-mer PS ODN GR antisense (GRAS) designs as shown in figure 4.8. Data shown are mean values (of replicate readings from same electrophoresis gel) \pm standard deviation, where $n=3$.

4.3.6 Assessment of Mapping and *In Vitro* RNase H Experimental Conditions.

The effect of RNase H concentrations ranging from 0.1-5.0 units per reaction on ODN:RNA duplex cleavage efficiency was investigated using mapping reactions as described in section 2.2.14.4. Figure 4.10 shows the generation of cleavage bands of differing intensities associated with each mapping reaction using a particular RNase H enzyme concentration. Densitometric analysis of cleavage efficiency shows cleavage band intensity to increase with increasing RNase H concentration with saturation of this enzyme dependent reaction occurring at 5 units of RNase H enzyme (Figure 4.11). This supports the use of RNase H enzyme at the optimal concentration of 1 unit in further mapping reaction experiments.

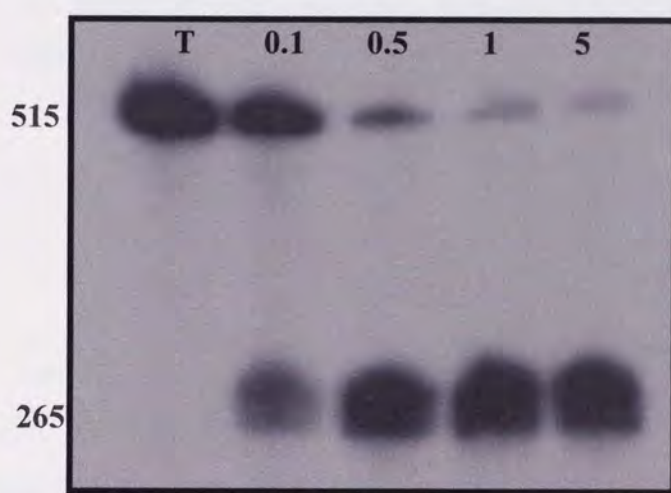


Figure 4.10 Autoradiogram of GR RNA fragments showing RNase H concentration dependent cleavage in the presence of GRAS5 due to ODN:RNA hybridisation as described in section 2.2.14.4. Lane T: 5'-radiolabelled GR mRNA transcript. Other lanes: transcript with 21-mer GRAS5 ODN and RNase H enzyme at concentrations of 0.1, 0.5, 1 and 5 units/ μ L.

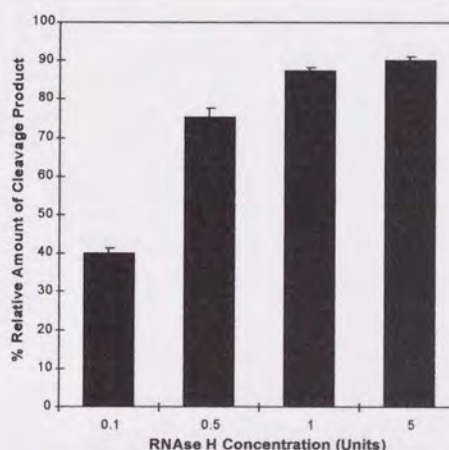


Figure 4.11 Densitometric analysis of cleavage bands, relative to intact GR mRNA transcript, illustrating effect of RNase H concentration on cleavage efficiency as shown in figure 4.10. Data shown are mean values (of replicate readings from same electrophoresis gel) \pm standard deviation, where $n=3$.

The effect of RNase H enzyme concentration on RNA cleavage efficiency was further investigated by using the random ODN library, in the mapping reactions as described in section 2.2.14.4. Figure 4.12 shows the generation of cleavage bands of differing intensities associated with each mapping reaction using a particular RNase H enzyme concentration. Densitometric analysis (Figure 4.13) shows cleavage band intensity to increase with increasing RNase H concentration up to 1 unit/reaction. However the RNase H mediated reaction became saturated at 5 units of RNase H, thus again suggesting 1 unit of RNase H enzyme to be an optimal concentration for further mapping reaction experiments.

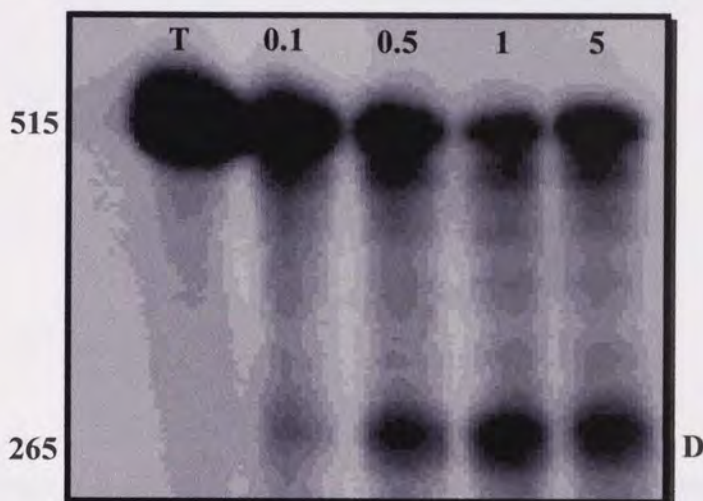


Figure 4.12 Autoradiogram of GR RNA fragments showing RNase H concentration dependent cleavage at accessible site D due to ODN:RNA hybridisation as described in section 2.2.14.4. Lane T: 5'-radiolabelled GR mRNA transcript. Other lanes: transcript with random ODN library and RNase H enzyme at concentrations of 0.1, 0.5, 1 and 5 units/ μ L.

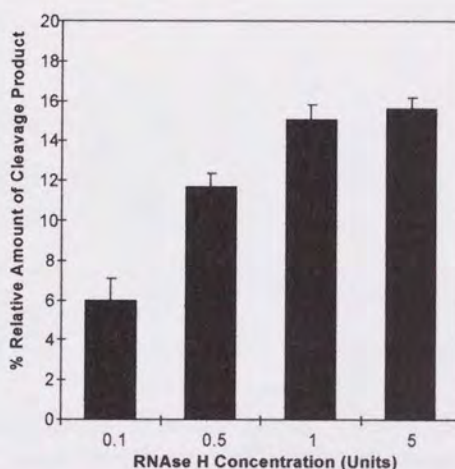


Figure 4.13 Densitometric analysis of cleavage bands, relative to intact GR mRNA transcript, illustrating effect of RNase H concentration on cleavage efficiency as shown in figure 4.12. Data shown are mean values (of replicate readings from same electrophoresis gel) \pm standard deviation, where $n=3$.

The effect of incubation times on ODN:RNA duplex cleavage efficiency was assessed using mapping reactions as described in section 2.2.14.4 using the optimal 21-mer antisense ODN GRAS5. Figure 4.14 illustrates the cleavage bands generated in the mapping reactions for each of the incubation times (1-60 minutes). Densitometric analysis of cleavage efficiency (section 2.2.13.5), shows a exponential decay profile of RNA cleavage efficiency over the 60 minutes incubation time (Figure 4.15). This time dependant profile shows that at 30 minutes incubation, a near-maximal level of cleavage of the RNA has occurred. Thus further mapping experiments can be terminated after 30 minutes.

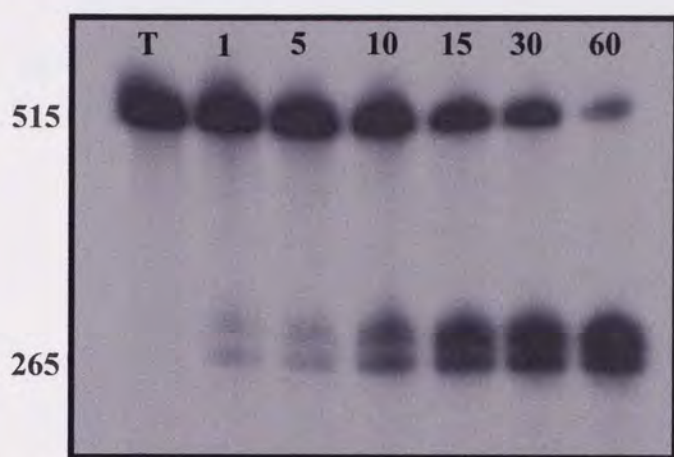


Figure 4.14 Autoradiogram of GR RNA fragments showing incubation time dependent cleavage in the presence of GRAS5 due to ODN:RNA hybridisation as described in section 2.2.14.4. Lane T: 5'-radiolabelled GR mRNA transcript. Other lanes: transcript with 21-mer GRAS5 ODN and RNase H enzyme incubated for 1, 5, 10, 15, 30 and 60 minutes.

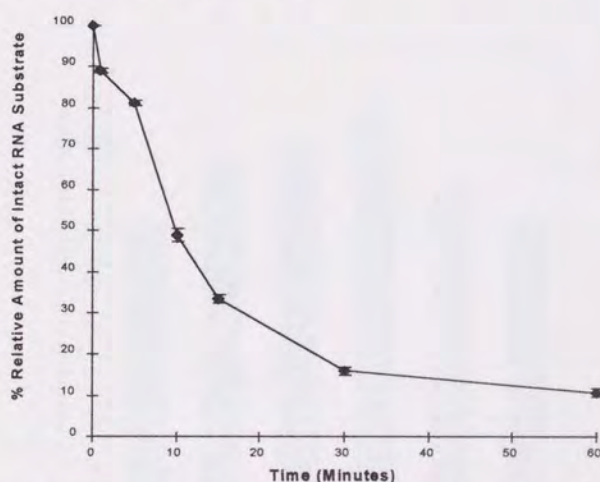


Figure 4.15 Densitometric analysis of cleavage bands, relative to intact GR mRNA transcript, illustrating effect of incubation times on cleavage efficiency as shown in figure 4.14. Data shown are mean values (of replicate readings from same electrophoresis gel) \pm standard deviation, where $n=3$.

The effect of concentration of the optimal 21-mer antisense ODN GRAS5 on ODN:RNA duplex cleavage efficiency was investigated using mapping reactions as described in section 2.2.14.4. Figure 4.16 illustrates the degree of cleavage at different GRAS5 concentrations (0.05-2nM) in the presence of RNase H (1 unit) for 30 minutes. Densitometric analysis of cleavage efficiency (Figure 4.17) shows that a maximum level of cleavage product is produced by 0.5nM GRAS5, suggesting this to be the optimal concentration for carrying out further mapping reaction experiments.

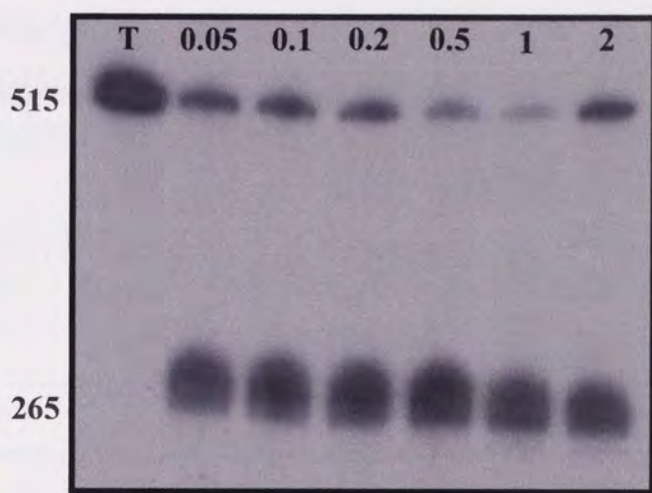


Figure 4.16 Autoradiogram of GR RNA fragments showing GRAS5 concentration dependent cleavage due to ODN:RNA hybridisation as described in section 2.2.14.4. Lane T: 5'-radiolabelled GR mRNA transcript. Other lanes: transcript with RNase H enzyme and 21-mer GRAS5 ODN at concentrations of 0.05, 0.1, 0.2, 0.5, 1 and 2nM.

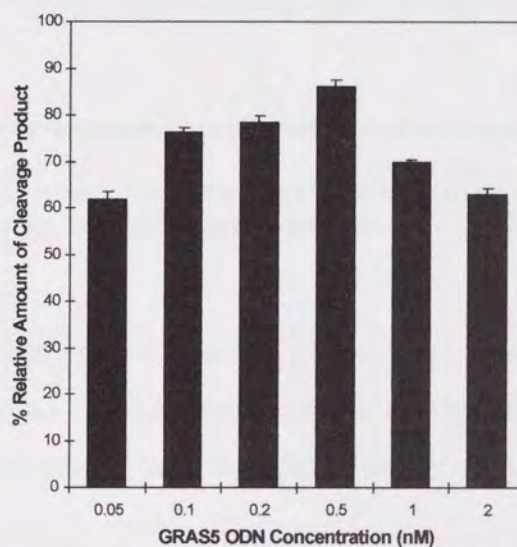


Figure 4.17 Densitometric analysis of cleavage bands, relative to intact GR mRNA transcript, illustrating effect of GRAS5 concentration on cleavage efficiency as shown in figure 4.16. Data shown are mean values (of replicate readings from same electrophoresis gel) \pm standard deviation, where $n=3$.

4.3.7 Optimisation of Antisense ODN Length in Mapping and *In Vitro* RNase H Reactions.

Mapping reactions as described in section 2.2.14.4 were used to investigate the effect of antisense ODN length on RNase H mediated cleavage efficiency of the target RNA transcript, comparing the GRAS5 sequence with an extended 30-mer sequence (GRAS11) and a truncated 10-mer sequence (GRAS12) as shown in Table 4.2 and Figure 4.18.

Table 4.2 Antisense oligodeoxynucleotide sequences of varying lengths designed using accessible site D.

ANTISENSE PS ODN DESIGNS	ACCESSIBLE SITE D DESIGN SEQUENCES (5' to 3')
GRAS5 (21-mer) GRAS11 (30-mer) GRAS12 (10-mer)	TAAAAACAGGCTTCTGATCCT GACATTA AAAACAGGCTTCTGATCCTGCTG ACAGGCTTCT

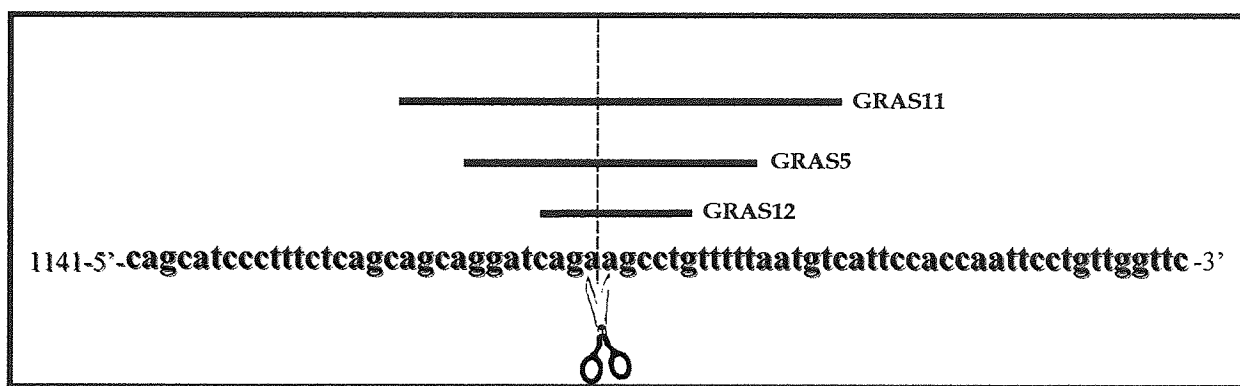


Figure 4.18 Antisense ODNs of varying lengths designed against the GR cDNA sequences corresponding to accessible site D. Predicted cleavage site is approximated to occur at base 1170 and is indicated by the scissors.

Figure 4.19 shows the intensity of the cleavage products generated for GRAS 5, 11 and 12. Densitometric analysis of these cleavage product bands revealed the GRAS5 band to be most intense, therefore GRAS5 appears to have the optimal sequence length.

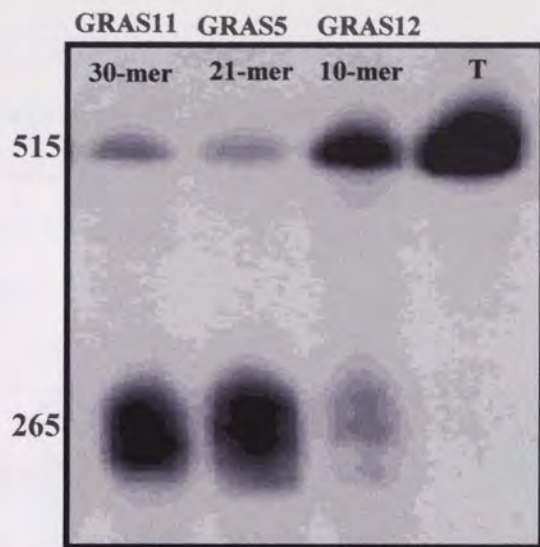


Figure 4.19 Autoradiogram of GR RNA fragments showing sequence length dependent cleavage due to ODN:RNA hybridisation as described in section 2.2.14.4. Lane T: 5'-radiolabelled GR mRNA transcript. Other lanes: transcript with RNase H enzyme and antisense ODN designs: GRAS11 (30-mer), GRAS5 (21-mer) and GRAS12 (10-mer).

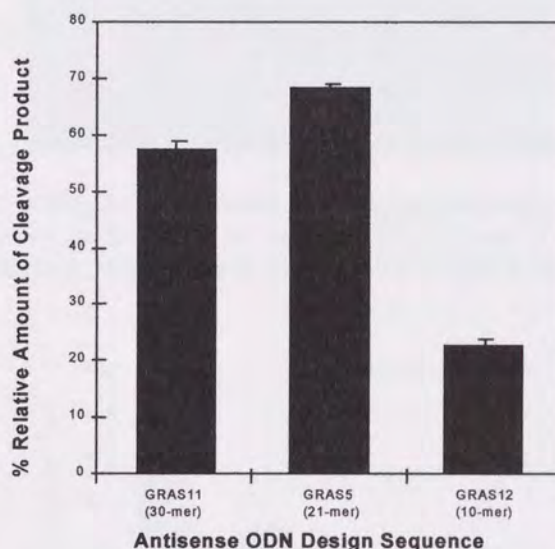


Figure 4.20 Densitometric analysis of cleavage bands, relative to intact GR mRNA transcript, illustrating effect of antisense sequence length on cleavage efficiency as shown in figure 4.19. Data shown are mean values (of replicate readings from same electrophoresis gel) \pm standard deviation, where $n=3$.

4.3.8 Assessment of the Activity of Selected GR Antisense Designs.

Using RNase H enzyme directed mapping reactions as described in section 2.2.14.4 a varied selection of the GR antisense design sequences were reviewed and direct comparisons made of their activity in terms of cleavage potency. These designs included GRAS5, GRAS1, GRAS6 and GRAS8 (see Table 4.1). Individual mapping reactions using the particular antisense ODN designs and their corresponding reaction cleavage products signifying cleavage efficiency is

illustrated in Figure 4.21. Densitometric analysis of these cleavage product band intensities to measure RNA cleavage efficiency shows cleavage potency for the GRAS designs to increase in the order, GRAS8<GRAS6<GRAS1<GRAS5 (Figure 4.22). This further supports the findings shown in Figures 4.9 and 4.10 which suggests GRAS5 to be the optimally effective antisense design sequence.

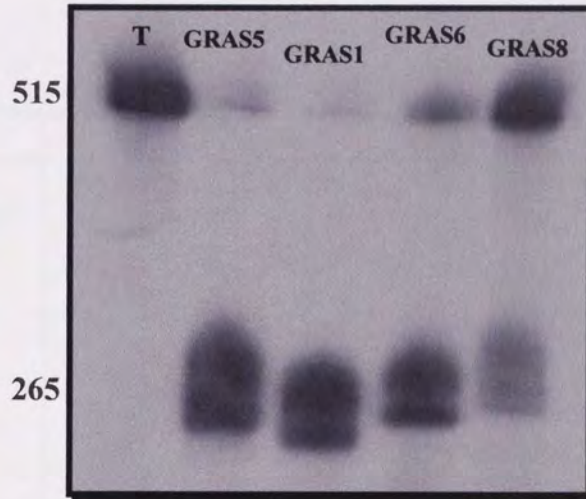


Figure 4.21 Autoradiogram of GR RNA fragments showing GRAS design sequence dependent cleavage due to ODN:RNA hybridisation as described in section 2.2.14.4. Lane T: 5'-radiolabelled GR mRNA transcript. Other lanes: transcript with RNase H enzyme and antisense ODN designs: GRAS5, GRAS1, GRAS6 and GRAS8.

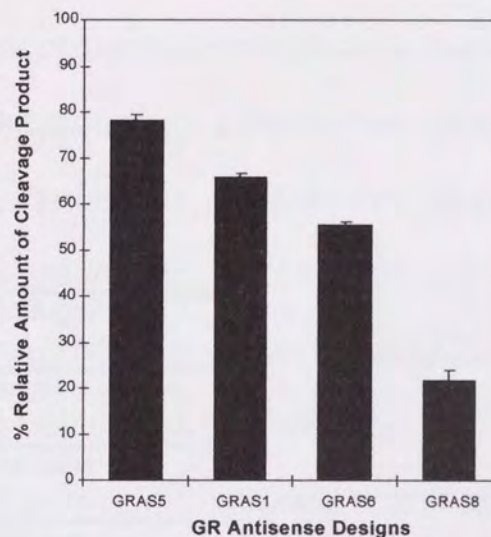


Figure 4.22 Densitometric analysis of cleavage bands, relative to intact GR mRNA transcript, illustrating effect of antisense design sequence on cleavage efficiency as shown in figure 4.21. Data shown are mean values (of replicate readings from same electrophoresis gel) \pm standard deviation, where $n=3$.

4.3.9 Assessment of Alternative GR mRNA Accessible Sites.

Although accessible site D was cleaved by RNase H at greatest frequency, antisense ODN probes were designed to span accessible sites A-C to compare cleavage efficiency at the different sites, compared with that at site D mediated by GRAS5. The designs of these antisense ODNs is given in Table 4.3 with their alignment to the rat GR mRNA shown in Figure 4.23.

Table 4.3 Antisense oligodeoxynucleotide sequences designed against accessible sites A, B, C and D.

ANTISENSE 21-mer PS ODN DESIGNS	ACCESSIBLE SITES	ACCESSIBLE SITE DESIGN SEQUENCES (5' to 3')
AGRAS1	A	ACACCAGGCAGAGCTTGGGAG
BGRAS2	B	TCTGGTCTCATTCCAGGGCTT
CGRAS3	C	CTGGGAAGTTCAGAGCCCCCA
GRAS5	D	TAAAAACAGGCTTCTGATCCT

911	AGATACAATC	TTATCAAGTC	CCAGCAGTGT	GGCACTACCC	CAAGTGAAAA
961	CAGAAAAAGA	TGATTTTCATT	GAACCTTGCA	CCCCCGGGGT	AATTAAGCAA
1011	GAGAAACTGG	GCCCAGTTTA	TTGTCAGGCA	AGCTTTTCTG	GGACAAATAT
1061	AATTGGTAAT	AAAATGTCTG	CCATTTCTGT	TCATGGTGTG	AGTACCTCTG
1111	GAGGACAGAT	GTACCACTAT	GACATGAATA	CAGCATCCCT	TTCTCAGCAG
1161	<u>CAGGATCAGA</u>	<u>AGCCTGTTTT</u>	<u>TAATGTCATT</u>	CCACCAATTC	CTGTTGGTTC
	GRAS5-SITE D				
1211	<u>TGAAACTGG</u>	<u>AATAGGTGCC</u>	<u>AAGGCTCCGG</u>	AGAGGACAGC	CTGACTTCCT
	NAGRAS4-CONTROL				
1261	<u>TGGGGGCTCT</u>	<u>GAACTTCCCA</u>	<u>GGCCGGTCAG</u>	TGTTTTCTAA	TGGGTACTCA
	CGRAS3-SITE C				
1311	<u>AGCCCTGGAA</u>	<u>TGAGACCAGA</u>	TGTAAGCTCT	CCTCCATCCA	GCTCGTCAGC
	BGRAS2-SITE B				
1361	AGCCACGGGA	CCACCTCCCA	<u>AGCTCTGCCT</u>	GGTGTGCTCC	GATGAAGCTT
	AGRAS1-SITE A				
1411	CAGGATGTCA				

Figure 4.23 Alignment of antisense sequences listed in tables 4.3 and 4.4 on the predicted nucleotide sequence of the rat GR mRNA/cDNA.

Figure 4.24 shows the cleavage product bands produced by RNase H using GRAS5 compared with the antisense sequences directed against accessible sites A-C. Densitometric analysis of these cleavage product bands revealed GRAS5 produced the greatest amount of cleavage products compared to the other designs (Figure 4.25). Therefore, the observation that accessible site D is most readily cleaved using random 12-mer sequences, has been confirmed using 21-mer antisense ODNs designed to span each of the 4 sites.

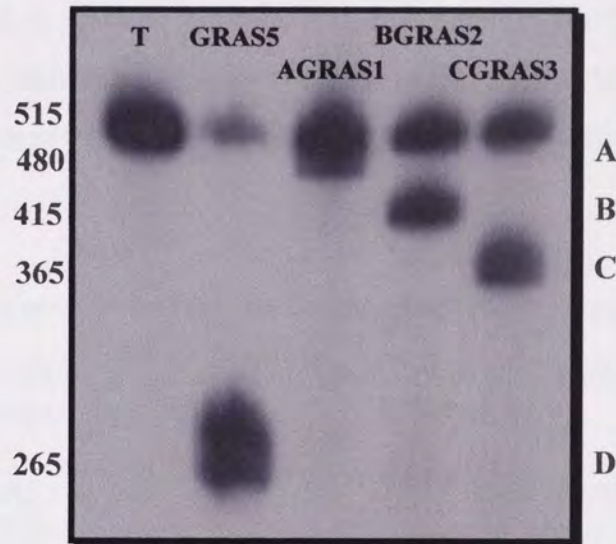


Figure 4.24 Autoradiogram of GR RNA fragments showing GRAS design sequence dependent cleavage due to ODN:RNA hybridisation as described in section 2.2.14.4. Lane T: 5'-radiolabelled GR mRNA transcript. Other lanes: transcript with RNase H enzyme and antisense ODN designs: GRAS5, AGRAS1, BGRAS2 and CGRAS3 directed against accessible sites A-D as shown in table 4.3.

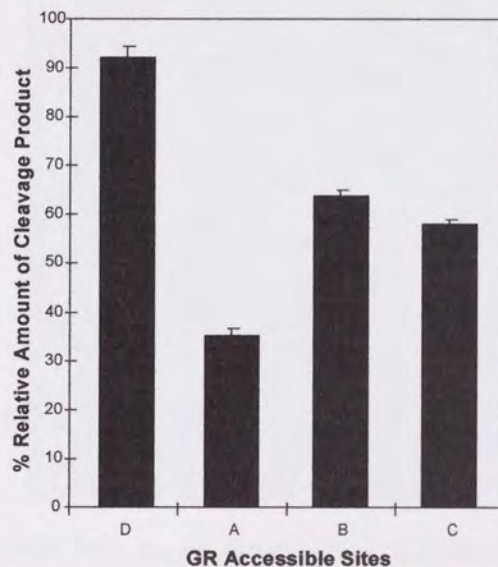


Figure 4.25 Densitometric analysis of cleavage bands, relative to intact GR mRNA transcript, illustrating effect of antisense design sequence on cleavage efficiency as shown in figure 4.24. Data shown are mean values (of replicate readings from same electrophoresis gel) \pm standard deviation, where $n=3$.

4.3.10 Design and Assessment of Control Antisense ODN Sequences Using Mapping and *In Vitro* RNase H Reactions.

To ensure that RNase H enzyme cleavage of the RNA component of the ODN:RNA duplex is brought about by specific sequence recognition of accessible regions along mRNA transcripts, control sequences based on GRAS5 or to regions of the T7-GR transcript in between the accessible sites, were designed and their RNA cleavage potency evaluated using mapping reactions as described in section 2.2.14.4. Sequences based on GRAS5 include a sense (GRSS5) and a 50% mismatch sequence (GRMM5) along with the other control sequence NAGRAS4 designed as shown in Figure 4.23, to a non-accessible site on the T7-GR fragment transcript.

Table 4.4 Control 21-mer phosphorothioate oligodeoxynucleotide design sequences.

ANTISENSE PS ODN DESIGNS	DESIGNED CONTROL SEQUENCES (5' to 3')
GRAS5 GRSS5 GRMM5 NAGRAS4	TAAAAACAGGCTTCTGATCCT ATTTTGTCCGAAGACTAGGA CGGAAAAGTGCTCACGATAAC TGGCACCTATTCCAGTTTTCA

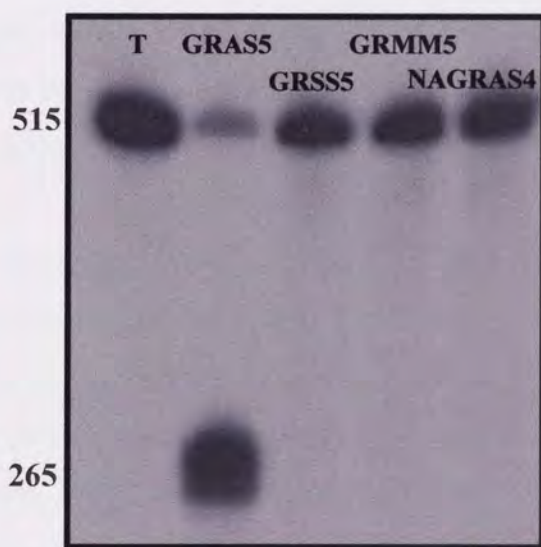


Figure 4.26 Autoradiogram of GR RNA fragments showing GRAS design sequence dependent cleavage due to ODN:RNA hybridisation as described in section 2.2.14.4. Lane T: 5'-radiolabelled GR mRNA transcript. Other lanes: transcript with RNase H enzyme and antisense ODN designs: GRAS5, GRSS5, GRMM5 and NAGRAS4 as shown in table 4.4.

Figure 4.26 illustrates the effect of the control antisense sequences on their ability to cleave the RNA transcript in the presence of RNase H compared to the GRAS5 sequence. It was observed that only the GRAS5 sequence, generated any cleavage product. This confirms that RNase H mediated cleavage is dependent upon both complementary sequence specificity and access to appropriate regions on the RNA transcript to form the required ODN:RNA duplex.

4.3.11 Comparison of Actual and *mfold* Computer mRNA folding Algorithms on Accessible Sites in the T7-GR mRNA Transcript.

To predict the accessibility of target sites within the *in vitro* transcribed *GR* mRNA transcript, 500 bases of the mRNA sequence were folded using the RNA *mfold* program, which is part of the Wisconsin EGCG package (Washington University School of Medicine, USA). The Unix system at the Daresbury Laboratory allowed RNA sequences of 500 bases to be analysed using the *mfold* program. Sequences were folded into the lowest energy structure and two energetically sub-optimal structures using the *mfold* program (version 3.0). Graphic representations of folded structures were obtained as 'squiggle' plots using Ghost-View for Windows[®] (courtesy of Dr. Peter Lambert, Aston University). Target sites within the folded structures were then identified and examined for their apparent accessibility to ODN binding. Target sites at or near single stranded regions (within loop regions), and/or sites containing distorted double-stranded regions which were free of complex secondary structure, were considered to be the most favourable theoretical targets for ODN:RNA duplex formation and subsequent cleavage by RNase H enzyme.

The most energetically favourable predicted secondary structure of the *GR* mRNA transcript (Figure 4.27) shows the location of target sites (accessible regions) by the loops of hairpin regions as denoted by *a-i* on Figure 4.27. When comparing the accessible sites as determined by RNase H cleavage with these *mfold* predicted target sites, it was evident that there is not a good consensus. Accessible sites A and C appear to coincide with single stranded loops which may be accessible to RNase H cleavage, however, these sites only produced weak cleavage product bands *in vitro*.

Furthermore, there is no predicted secondary structure theoretically accessible to RNase H at site B, though this region is cleaved *in vitro*. However, the predicted structure around accessible site D does have some small single stranded regions that may theoretically be accessible to RNase H, but this would not tend to support the practical observation that this is the predominant cleavage site.

Furthermore, NAGRAS4, designed as a control antisense ODN to a region (site X) between accessible sites D and C, and shown not to mediate RNase H cleavage *in vitro*, would appear to correspond to a region on the *mfold* predicted RNA transcript at least as accessible as that complementary to GRAS5. Thus, of four identified regions of the T7-GR transcript fragment known to be accessible to RNase H, only one is accurately predicted by *mfold* (site C), one is equivocal (site D), one is omitted (site A), and two are positively contradicted (accessible site B, and non accessible site X). Therefore these mapping reaction data, together with the inability of RNA folding algorithms to predict tertiary structure, suggest that such programs at their current level of sophistication have limited use for the selection of active antisense sequences against a particular mRNA target.

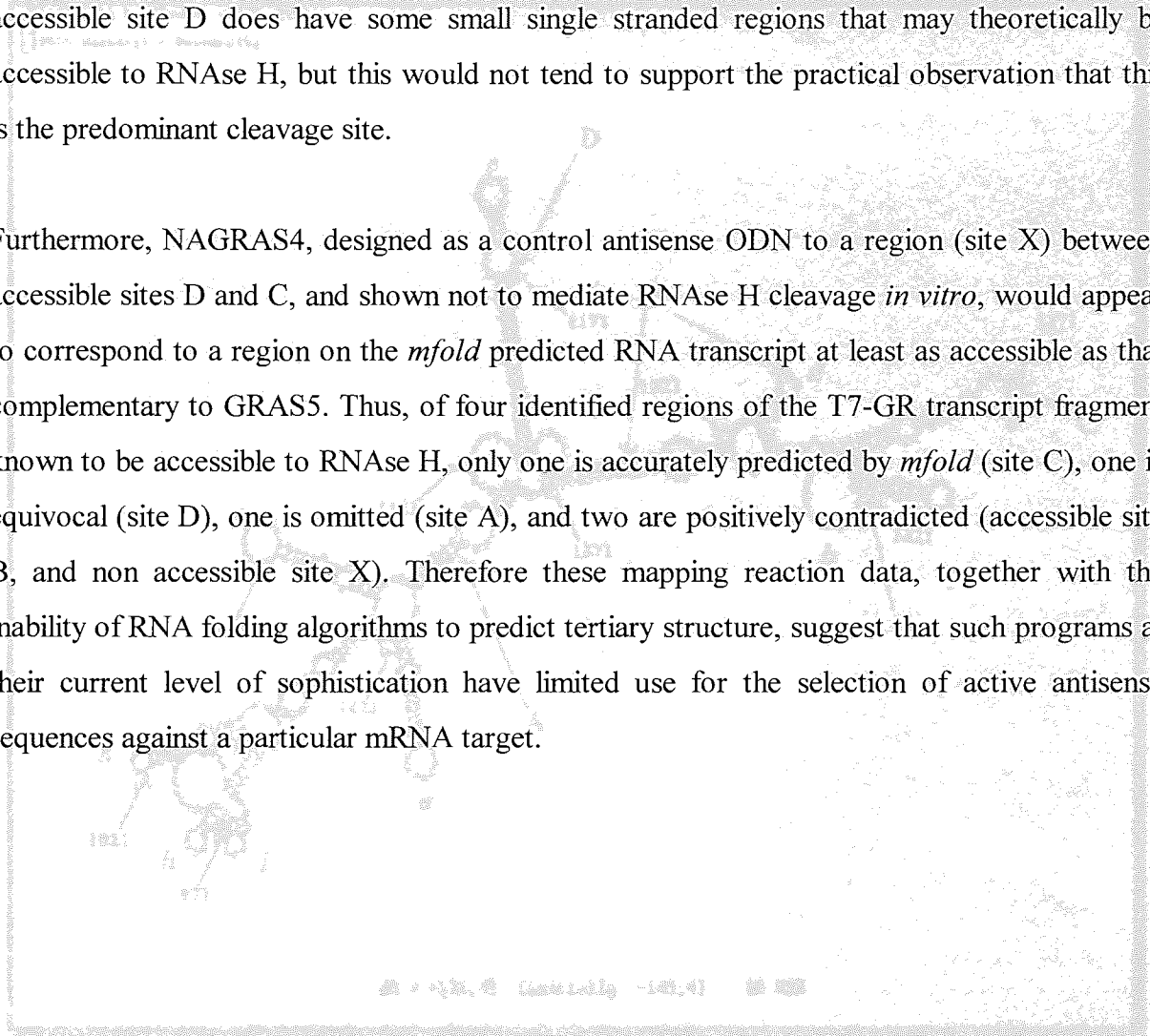


Figure 4.7 Synoptic plot showing the secondary structure of the T7 *in vitro* transcribed 488 nucleotide mRNA transcript (bases 921-1421), folded using the RNA *mfold* algorithm. The positions of numbered bases along the mRNA sequence are indicated. Theoretical RNase H accessible sites (hairpin loop regions) as predicted by the RNA *mfold* algorithm are represented by the characters a-d. A-D are experimentally determined RNase H cleavage sites. X is the region complementary to the control antisense ODN, NAGRAS4, designed to a site where no cleavage occurs and shown experimentally not to mediate RNase H cleavage.

4.3.12 Analysis of Antisense Design Sequences.

Before using selected antisense sequences in both *in vitro* and *in vivo* experiments, it was important to confirm that these sequences were complementary to the rodent GR mRNA sequence and not to any other rodent gene/mRNA sequences. Consequently, a BLAST sequence alignment search against the Genbank DNA sequence data base (version 4.6, Incyte Pharmaceuticals) was carried out for all antisense and control ODN sequences (Table 4.5). The best match alignment search result for sequence is shown in Table 4.5 (Altschul *et al*, 1997).

Table 4.5 BLAST search alignment results for empirically determined design and control sequences.

ANTISENSE DESIGN ID	SEQUENCE (5' to 3')	SIGNIFICANT BLAST SEARCH RESULT
GRAS1	AACAGGCTTCTGATCCTGCTG	Rat and mouse GR mRNA
GRAS2	GCTGCTGAGAAAGGGATGCTG	Rat and mouse GR mRNA
GRAS3	AATTGGTGGAAATGACATTAAA	Rat and mouse GR mRNA
GRAS4	GAACCAACAGGAATTGGTGGA	Rat and mouse GR mRNA
GRAS5	TAAAAACAGGCTTCTGATCCT	Rat and mouse GR mRNA
GRAS6	GACATTAAAAACAGGCTTCTG	Rat and mouse GR mRNA
GRAS7	GATCCTGCTGCTGAGAAAGGG	Rat and mouse GR mRNA
GRAS8	GGAATGACATTAAAAACAGGC	Rat and mouse GR mRNA
GRAS9	CCAACAGGAATTGGTGGAAATG	Rat and mouse GR mRNA
GRAS10	GGCTTCTGATCCTGCTGCTGA	Rat and mouse GR mRNA
GRSS5	ATTTTTGTCCGAAGACTAGGA	Rat megalin mRNA
GRMM5	CGGAAAAGTGCTCACGATAAC	No BLAST matches
AGRAS1	ACACCAGGCAGAGCTTGGGAG	Rat and mouse GR mRNA
BGRAS2	TCTGGTCTCATTCCAGGGCTT	Rat and mouse GR mRNA
CGRAS3	CTGGGAAGTTCAGAGCCCCCA	Rat GR mRNA
NAGRAS4	TGGCACCTATTCCAGTTTCA	Rat and mouse GR mRNA

All antisense sequences designed against the rat GR mRNA transcript (Table 4.5) produced a significant alignment to the rat and/or mouse GR mRNA. Only the control sequences GRSS5 (sense) and GRMM5 (mismatch) failed to align to the rat and/or mouse GR mRNA. This suggests that these designed antisense ODN sequences possess a very high level of specificity for the rodent GR mRNA.

4.4 Discussion.

The objective of this chapter was to develop and optimise appropriate antisense and control sequences against the target GR mRNA using RNase H accessibility mapping. To do this the reaction substrate, a 5' [³²P]-radiolabelled GR RNA transcript (Figure 4.4) was generated *in vitro* from a T7 promoter-rat GR PCR fragment construct.

The RNase H mapping method reliably identified accessible regions on the GR RNA transcript which, were used to develop effective antisense ODNs. By equating RNA cleavage efficiency using cleavage product band intensity profiles as a marker for the degree of ODN:RNA hybridisation, it was found that a particular accessible region (accessible site D) was optimal for ODN:RNA duplex formation and consequent cleavage by the RNase H enzyme (Figure 4.6). Using this optimal region, and from the length of the cleavage fragment, estimating that cleavage occurs at base pair number 1170, a series of PS antisense ODNs spanning this region were designed and synthesised to determine the best antisense sequence to mediate cleavage at this site. Following a series of mapping reactions it was found that GR antisense design 5 (GRAS5) was optimal for GR RNA cleavage efficiency and potency (Figures 4.8-4.9 and 4.21-4.22).

Further mapping reactions were carried out to investigate and optimise *in vitro* RNase H mapping experimental conditions. Factors such as RNase H concentration, reaction incubation time, ODN concentration and ODN length were investigated. It was found that a RNase H concentration of 1 unit/ μ L (Figures 4.10-4.11 and 4.12-4.13), an incubation time of 30 minutes (Figures 4.14 and 4.15), an ODN concentration of 0.5nM (Figures 4.16 and 4.17) and a 21-mer sequence length (Figures 4.19 and 4.20) produced the best level of GR RNA cleavage. These parameters were thus adopted in subsequent mapping reactions.

To fully characterise the accessibility of sites A-D, discovered and to corroborate further the suitability of site D for antisense sequence design, mapping reactions were performed using GR antisense designs specifically targeted around this site. Of these designs GRAS5 caused greatest RNase H mediated cleavage of the GR RNA transcript and further suggests this region to be the most accessible on this RNA transcript.

In addition to the specific antisense designs which were intended to cause sequence specific cleavage of the RNA transcript, control sequences designed to produce no such RNase H mediated cleavage were assessed. Sense (GRSS5), mismatch (GRMM5) and non-accessible site-directed (NAGRAS4) ODNs produced no cleavage product bands. This therefore supports the rational design strategy used in these experiments of following RNase H accessibility mapping, and clearly identified both accessible and inaccessible regions along the RNA transcript.

The value of using the RNA folding programs, *mfold*, to design theoretically optimal antisense ODNs against the GR mRNA target was compared with the empirically identified RNase H accessible sites *in vitro*. This showed that the predictive value of *mfold* in accurately identifying accessible target sites is limited extremely. Thus, use of empirical techniques, such as RNase H accessibility mapping in antisense ODN design studies is much preferred. Such similar conclusions have been made by several other reports (Ho *et al*, 1996 and 1998; Lima *et al*, 1997; Birikh *et al*, 1997).

To verify the GR specificity of the sequences designed using RNase H mapping, a BLAST search of the Genbank database showed significant alignment to the rodent GR mRNA sequence for all sequences except the sense strand and mismatch control sequences. This confirms the specificity of the antisense sequence designs to the rat GR mRNA.

In conclusion, we have rationally isolated and screened *in vitro* a series of antisense and control sequences against a T7-rat GR fragment using the RNA mapping method. This has been proved to be a consistent and reliable method of identifying antisense sequences (Ho *et al*, 1996 and 1998; Lima *et al*, 1997; Birikh *et al*, 1997), able to mediate RNase H cleavage *in vitro*. The selected antisense and control sequences can now be evaluated for their efficacy to downregulate GR mRNA and protein expression in a cell based system *in vitro*.

CHAPTER FIVE

IN VITRO EFFECTS OF ANTISENSE OLIGODEOXYNUCLEOTIDES TARGETING THE GLUCOCORTICOID RECEPTOR

5.1 Introduction.

Cell cultures provide a convenient system to investigate the knockdown of receptor proteins and the optimisation of experimental conditions prior to investigations performed *in vivo*. Cell cultures have been commonly employed in antisense optimisation experiments and have been used with varying degrees of success (Chapter 1, section 1.9). However, since the intention is to use the antisense ODN to knockdown GR expression in the rat, following ICV administration, an appropriate cell line was required. The rat C6 glioma cell line, is known to express both GR and 5-HT_{2A} receptors (Benda, 1968), and was therefore selected for the current studies as the appropriate CNS-derived cell culture model.

Rat C6 glioma cells were treated with PS ODNs in the presence of Lipofectamine™ at the optimal lipid:ODN complex as described in chapter three. This cationic liposomal delivery system was shown (Chapter three, section 3.3.2) to provide an efficient means of delivery of ODNs to the C6 glioma cell line and would thus help attain maximal levels of antisense directed efficacy in terms of GR downregulation and any possible related functional effects expressed as changes to 5-HT_{2A} receptor expression. This level of downregulation was to be assessed at both the level of the receptor mRNA and the functional protein.

Quantitative competitive RT-PCR was developed to measure both GR and 5-HT_{2A} receptor mRNA expression in C6 glioma cells. This is a highly sensitive and specific method for detecting the expression of a particular mRNA sequence and relies on the use of two DNA primers specific to the target sequence to initiate a polymerisation reaction producing cDNA products of interest which can be quantified (O'Driscoll *et al*, 1993). For this study the RT-PCR method was modified as described in section 2.2.13 to make it a competitive assay allowing quantitative analysis.

The established technique of radioligand binding was used to measure GR and 5-HT_{2A} receptor protein levels in C6 glioma cells. This technique determines the ability of a substance to act as an agonist/antagonist by direct binding to a receptor or the ability to alter the binding of a known agonist/antagonist (Cooper and Stewart, 1998). GR binding was measured with the radioligand [1,2,4,6,7-³H]-dexamethasone in the presence and absence of the GR antagonist mifepristone (RU 486) using a competition binding assay protocol (O'Donnell *et al*, 1995) and has been subsequently adapted by others (Turner, 1986; Meaney *et al*, 1988; Barden, 1996). 5-HT_{2A} receptor binding was determined with the radioligand [³H]-ketanserin and methysergide for non-specific binding using a saturation binding assay protocol (Scatton *et al*, 1983).

The antisense sequences used in the present *in vitro* investigation (Table 5.1) were developed as described in chapter four and were administered to the C6 glioma cells as fully modified phosphorothioate (PS) ODN sequences. All the ODN sequence probes used were 21 bases in length which would ensure such sequences were sufficiently specific to the mRNA of interest, but also small enough to cross the cellular membrane leading to intracellular effects (Brysch and Schlingensiepen, 1994; Wahlestedt, 1994).

The time course of the treatment of the C6 glioma cell line with the PS ODN sequences prior to measurement of GR and 5-HT_{2A} receptor expression is dependent on the turnover of the antisense targeted protein receptor (GR) and the receptor reserve in this particular cell type. There is no direct evidence for the turnover of GR in neuronal cells in culture or in rat brains, however it is predicted that most intracellular hormone receptors have a half-life of about 2-3 days (Herz *et al*, 1997). Thus a 5 day treatment period representing approximately 2 half-life intervals was chosen for the experiments conducted with the C6 glioma cell line.

Table 5.1 Phosphorothioate oligodeoxynucleotide sequences used in rat C6 glioma cell cultures.

ANTISENSE DESIGN ID	SEQUENCE (5' to 3')	SEQUENCE TYPE (sense strand complement bases)
AGRAS1	ACACCAGGCAGAGCTTGGGAG	Antisense to site A (1375-1395)
BGRAS2	TCTGGTCTCATTCAGGGCTT	Antisense to site B (1310-1330)
CGRAS3	CTGGGAAGTTCAGAGCCCCCA	Antisense to site C (1261-1281)
NAGRAS4	TGGCACCTATTCCAGTTTTCA	Non-accessible site control (1211-1231)
GRAS1	AACAGGCTTCTGATCCTGCTG	Antisense to site D (1158-1178)
GRAS5	TAAAAACAGGCTTCTGATCCT	Antisense to site D (1162-1182)
GRAS6	GACATTAAAAACAGGCTTCTG	Antisense to site D (1167-1187)
GRAS8	GGAATGACATTAAAAACAGGC	Antisense to site D (1172-1192)
GRSS5	ATTTTTGTCCGAAGACTAGGA	Sense control
GRMM5	CGGAAAAGTGCTCACGATAAC	Mismatch control

The objectives of this chapter were to investigate the biological effects of the ODN sequences listed in Table 5.1, using the C6 glioma cell line as the *in vitro* model. These effects were assessed in terms of GR downregulation at both the mRNA and receptor protein level using the standard molecular biological techniques mentioned above. In parallel studies, any related functional consequences of alterations in GR expression as a result of the ODN treatment on 5-HT_{2A} receptor expression, were also determined at both the mRNA and receptor protein level. This would therefore provide a first insight to the activity of these developed ODN sequences and a measure of the level of their antisense mediated effects *in vitro*. Thus allowing suitable antisense and control sequences to be evaluated *in vivo*.

5.2 Methods.

All relevant methods are described in chapter two, with any additional information given in the relevant results section.

Results in this chapter unless otherwise indicated were statistically compared using a one-way analysis of variance with treatment as factor. *Post hoc* comparisons were made using lowest significant difference (LSD) multiple range test. In all statistical analysis a value of $p < 0.05$ was considered significant.

5.3 Results.

5.3.1 *In Vitro* Stability of PS Oligodeoxynucleotides.

Cellular stability studies were performed to monitor degradation of ^{32}P -radiolabelled ODN caused by nuclease action to establish an *in vitro* treatment regimen that would ensure adequate antisense ODN exposure. Electrophoresis and autoradiography (section 2.2.4) were used to assess 5'-end labelled ODN, taken up by cells in culture, in comparison to a control labelled ODN of the same length which had not been exposed to cells. Apical medium (that the cells are bathed in) containing labelled ODN was collected after the stated incubation period/condition, taking care not to remove cells. Media samples were electrophoresed on a 20% acrylamide/7M urea gel for 1.5 hours at 10-20 watts to size separate ODNs. Autoradiography was used to visualise the ^{32}P -labelled fragments. Degradation would result in ODN fragmentation with autoradiography detecting labelled fragments of different lengths and free ^{32}P -ATP. The degradation pattern was compared with the intact control ODN and stability studies were performed parallel to an uptake experiment as described in section 2.2.5.



Figure 5.1 Autoradiogram of 5'-end ^{32}P -labelled ODNs showing stability of 21-mer PS GRAS5 ODN ($1\mu\text{M}$) incubated with C6 glioma cells over 24 hours at 37°C . Lane number corresponds to incubation time in hours. Lane A: free ^{32}P -ATP. Lane B and C: intact 21-mer PS GRAS5 ODN.

Figure 5.1 shows the stability profile for the 21-mer PS ODN GRAS5 (1 μ M) in the C6 glioma cell line over a period of 1-24 hours. Although some degradation was apparent from 12-24 hours (reduction in GRAS5 band density and appearance of degradation product bands), more than 50% of the ODN remained intact during this period. Therefore, it was assumed that intact GRAS5 ODN was available to the C6 glioma cells for up to 24 hours at 37°C, but that ODN replenishment (by media changing) would be required every 24 hours during the 5 day treatment period to sustain antisense ODN exposure.

5.3.2 Effect of Different GRAS5 ODN Concentrations on Cellular Viability.

The effect of GRAS5 ODN concentration delivered using Lipofectamine as an optimal lipid:ODN complex (section 3.3.2) at a 1:1 charge ratio on C6 glioma cell viability was investigated as described in section 2.2.9.4. Figure 5.2 shows that an ODN concentration at 50 μ M begins to induce cell toxicity while at 100 μ M cellular viability fell significantly ($p < 0.05$). Thus ODN concentrations to be used in the following experiments were restricted to less than 10 μ M, to avoid any effect of cell toxicity on receptor expression during the 5 day treatment period.

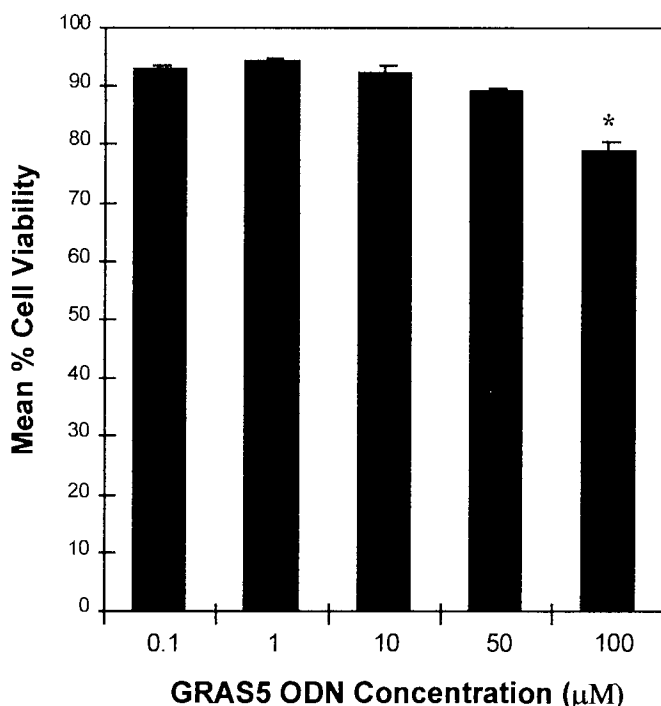


Figure 5.2 Effect of GRAS5 ODN concentrations on C6 glioma cell viability during the 5 day treatment period as described in section 2.2.14.5. Cell viability is expressed as the percentage of the number of cells present in untreated, control cultures. Data shown are mean values \pm standard deviation, where $n=3$ (Dunnett's test, * $p < 0.05$ compared to other groups).

5.3.3 *In Vitro* Assessment of ODN Treatment on GR mRNA Expression Using Quantitative RT-PCR.

C6 glioma cells were treated at an ODN concentration range of 0.01-1 μ M as described in section 2.2.14.5 and measurement of both GR and 5-HT_{2A} receptor mRNA expression in treated samples as a comparison to untreated control samples was made using quantitative RT-PCR as described in sections 2.2.13.4 and 2.2.13.5. The ODN concentration range used was selected from previously published *in vitro* studies (Wahlestedt *et al*, 1993; Owens *et al*, 1995).

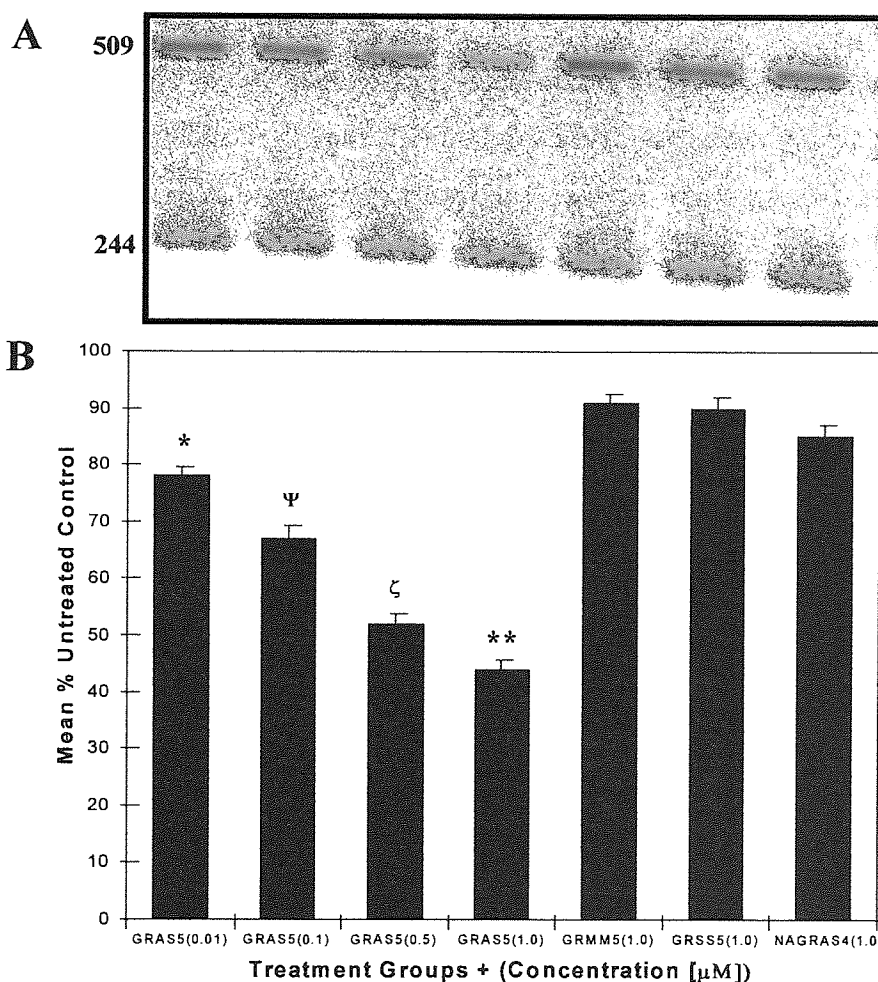


Figure 5.3 (A) Representative gel electrophoresis of RT-PCR products obtained as described in sections 2.2.13.4 and 2.2.13.5. Lanes illustrating GR (509 nucleotides) and control β -actin (244 nucleotides) cDNA product bands corresponding to the respective treatment groups shown on the x-axis of the graph below with ODN concentrations in μ M given in parentheses. (B) Densitometric analysis of GR bands standardised to the mean β -actin band density, illustrating the effect of ODN sequence and dose on the expression of GR mRNA in C6 glioma cells. Data shown are mean values \pm standard deviation, where $n=3$ (LSD test, $^{*\psi\zeta}p<0.05$ compared to GRMM5, GRSS5 and NAGRAS4; $^{**}p<0.05$ compared to other groups).

Treatment with the optimally effective GRAS5 antisense ODN produced a dose-dependent reduction in GR mRNA expression in C6 glioma cells after 5 days of treatment (Figure 5.3), resulting in a significant ($p < 0.05$) 56% decrease in GR mRNA expression at the $1\mu\text{M}$ concentration (Figure 5.3B). Lower GRAS5 concentrations were less effective, but a significant ($p < 0.05$) 22% decrease in GR mRNA expression was still achieved at $0.01\mu\text{M}$, compared to the 9 to 15% decrease seen with the mismatch (GRMM5), sense (GRSS5) and non-accessible site (section 4.3.10) antisense sequences (NAGRAS4) all at $1\mu\text{M}$ (Figure 5.3B). This confirms that the antisense ODN GRAS5, produces a very marked inhibition of the GR mRNA expression *in vitro*.

To assess further the efficacy of the GRAS5 sequence, its effects on GR mRNA expression was compared to other antisense designs shown to be less effective at cleaving the GR mRNA fragment using the RNase H accessibility mapping technique (see Table 5.1 and Figure 5.4). At $1\mu\text{M}$ (Figure 5.4B) GRAS5 produced the greatest GR mRNA reduction compared to the other 3 antisense designs targeting accessible sites, A-C, and to the other antisense designs to site D (Chapter 4). Interestingly GRAS1 and GRAS6, which in the RNase H accessibility mapping experiments (section 4.3.5) were very effective at cleaving GR mRNA, also proved to be effective at GR mRNA inhibition in cells, causing 42% and 32% reduction in GR mRNA expression respectively (Figure 5.4B). Other designs targeted at accessible site D, such as GRAS8, which performed poorly in the RNase H accessibility mapping experiments, also caused marginal reduction (13%) in the levels of GR mRNA. However antisense designs AGRAS1, BGRAS2 and CGRAS3 (see Table 5.1 and Figure 5.4B) targeting accessible sites A-C did not produce much greater levels of reduction when compared to the poorer GRAS8 design targeting the optimal accessible site D. This would suggest that the design optimisation carried out by RNase H mapping reactions in a cell-free system in terms of determining optimal accessible site and antisense sequence, can be used to directly correlate efficacy in a cell-based system.

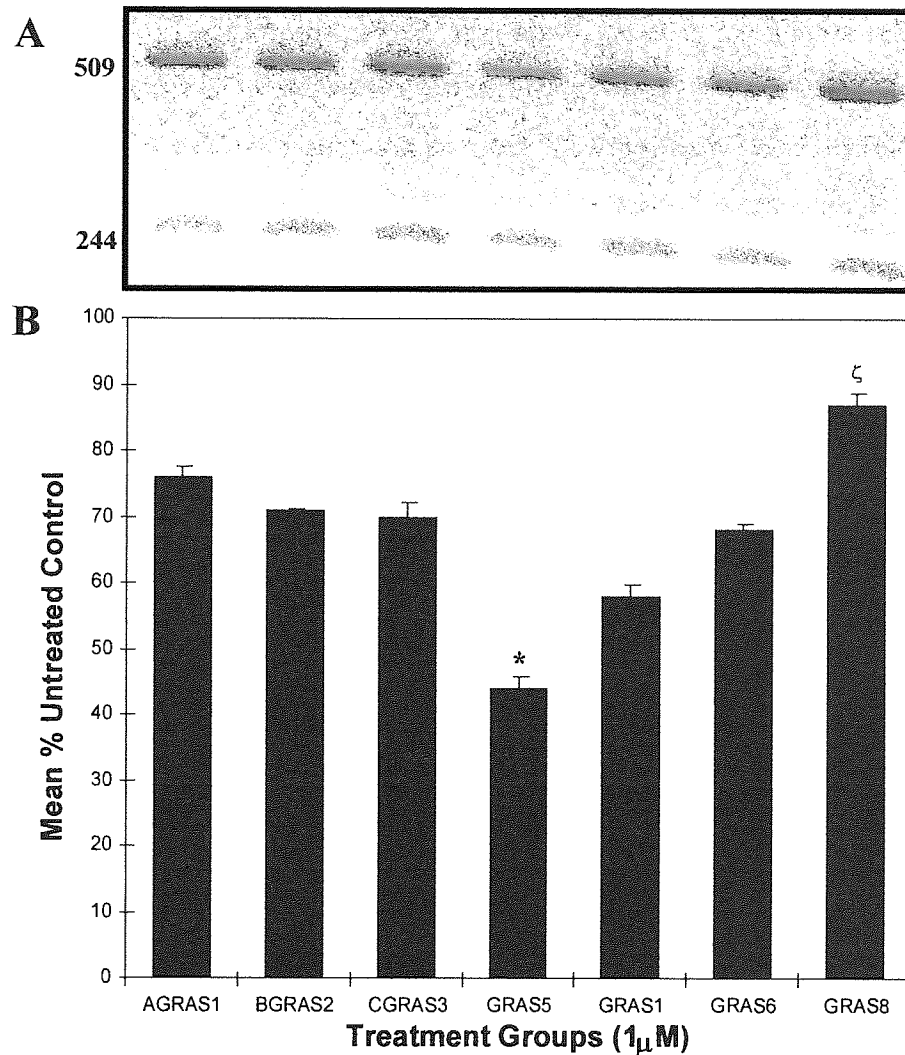


Figure 5.4 (A) Representative gel electrophoresis of RT-PCR products obtained as described in sections 2.2.13.4 and 2.2.13.5. Lanes illustrating GR (509 nucleotides) and control β -actin (244 nucleotides) cDNA product bands corresponding to the respective treatment groups shown on the x-axis of the graph below. (B) Densitometric analysis of GR bands standardised to mean β -actin band density, illustrating the effect of ODN sequence on the expression of GR mRNA in C6 glioma cells. Data shown are mean values \pm standard deviation, where $n=3$ (LSD test, * $p<0.05$ compared to other groups; $\zeta p<0.05$ compared to AGRAS1, BGRAS2, and CGRAS3).

5.3.4 *In Vitro* Assessment of ODN Treatment on 5-HT_{2A} Receptor mRNA Expression Using Quantitative RT-PCR.

The expression of 5-HT_{2A} receptor mRNA was investigated in C6 glioma cells treated with the antisense and control ODN sequences (Table 5.1) to determine the functional consequence of downregulating GR mRNA expression *in vitro*. The optimally effective GRAS5 antisense sequence produced a dose-dependent increase in 5-HT_{2A} mRNA expression in C6 glioma cells after 5 days of treatment (Figure 5.5). A significant ($p < 0.05$) 29% increase in 5-HT_{2A} receptor mRNA expression occurred at 1 μ M (Figure 5.5B), but not at lower concentrations. No significant changes in 5-HT_{2A} mRNA were seen with the mismatch (GRSS5), sense (GRMM5) or non-accessible site (NAGRAS4) sequences. This increase in 5-HT_{2A} mRNA expression in parallel with the marked reduction in GR mRNA expression seen with GRAS5 antisense suggests negative regulation of 5-HT_{2A} expression by the GR in C6 glioma cells.

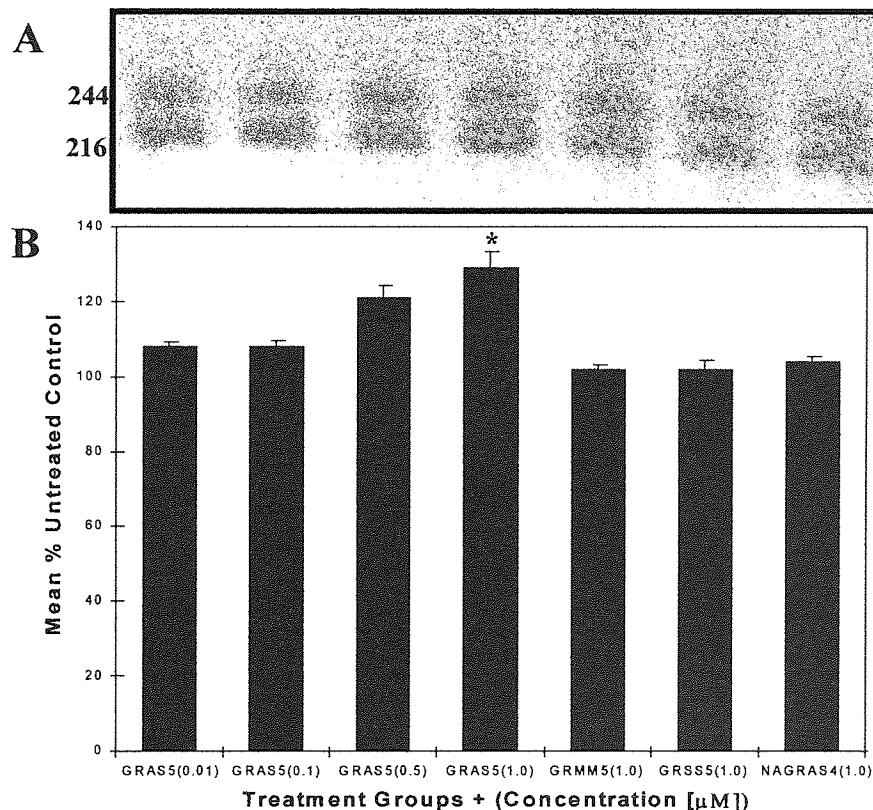


Figure 5.5 (A) Representative gel electrophoresis of RT-PCR products obtained as described in sections 2.2.13.4 and 2.2.13.5. Lanes illustrating 5-HT_{2A} receptor (216 nucleotides) and control β -actin (244 nucleotides) cDNA product bands corresponding to the respective individual treatment groups shown on the x-axis of the graph below with ODN concentrations in μ M given in parentheses. (B) Densitometric analysis of 5-HT_{2A} receptor bands standardised to mean β -actin band density, illustrating the effect of ODN sequence and concentration on the expression of GR mRNA in C6 glioma cells. Data shown are mean values \pm standard deviation, where $n=3$ (LSD test, * $p < 0.05$ compared to GRMM5, GRSS5 and NAGRAS4).

5.3.5 *In Vitro* Assessment of ODN Treatment on GR Protein Expression Using Radioligand Binding Assays.

C6 glioma cells were treated at an ODN concentration range of 0.01-1 μ M as described in section 2.2.14.5 and measurement of GR protein expression in treated samples compared to untreated control samples, was made using a single concentration displacement competition radioligand binding assay, as described in section 2.2.10.2. Values derived indicate total number of binding sites labelled by a maximal concentration of the GR ligand [3 H]-dexamethasone. Maximal binding sites (B_{max}) of 115 fmol/mg protein and dissociation constant (K_d) of 1.2nM for GR in untreated groups were derived from saturation experiments.

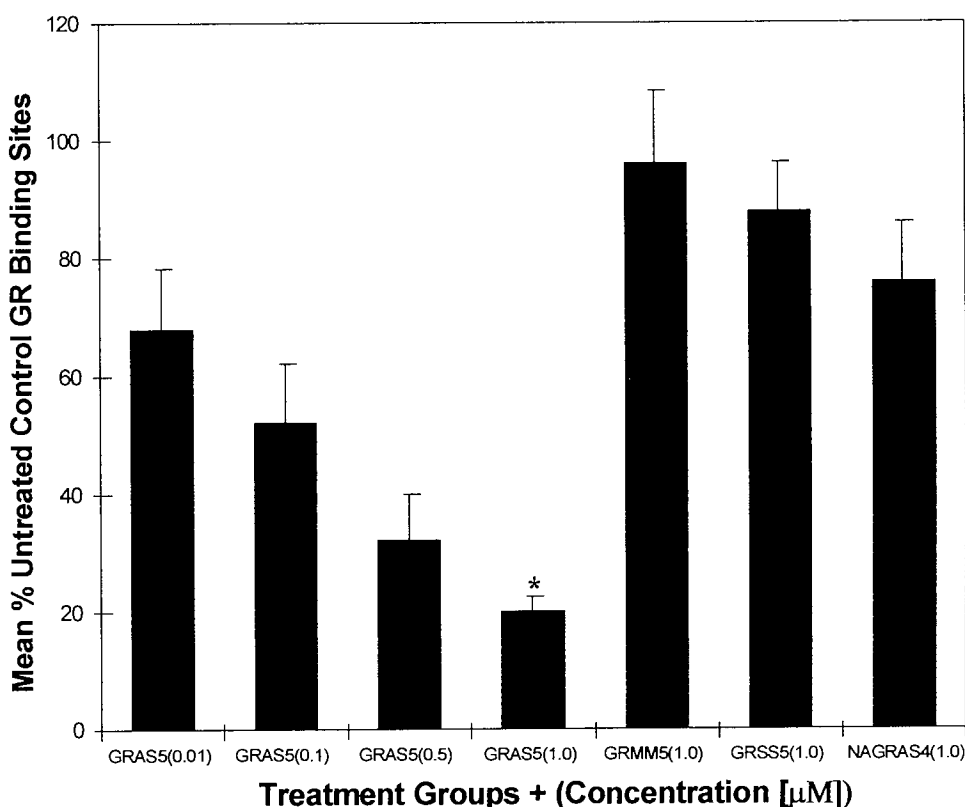


Figure 5.6 GR binding sites in C6 glioma cells as described in section 2.2.10.2 following treatment with various ODN sequences. Data are expressed as a percentage of specific binding for control untreated cells. Data shown are mean values \pm standard deviation, where $n=3$ (LSD test, * $p<0.05$ compared to GRMM5, GRSS5 and NAGRAS4).

GR binding was reduced dose-dependently following treatment with GRAS5, resulting in a significant 80% decrease in GR binding sites at 1 μ M (Figure 5.6), compared to the 4%, 12% and 24% decreases seen in the mismatch (GRMM5), sense (GRSS5) and non-accessible site (NAGRAS4) treatment groups, respectively. This confirms the efficacy of the GRAS5 antisense sequence for inhibition of GR mRNA and protein expression *in vitro*.

Comparison of the efficacy of GRAS5 with antisense designs GRAS1 and GRAS6 also targeting the optimal accessible site D (Figure 5.7) and which had good GR mRNA cleavage efficacy as determined by the RNase H accessibility (section 4.3.5) and mRNA downregulation (section 5.3.3) similarly reduced GR binding with GRAS5 producing the greatest reduction (80%). The site D directed antisense sequences were significantly more effective than the site A-C directed antisense sequences (AGRAS1, BGRAS2, and CGRAS3) at reducing GR binding while the GRAS8 antisense design, targeting the accessible site D but having poor GR mRNA cleavage efficacy (section 4.3.5) produced the smallest decrease in GR binding (28%).

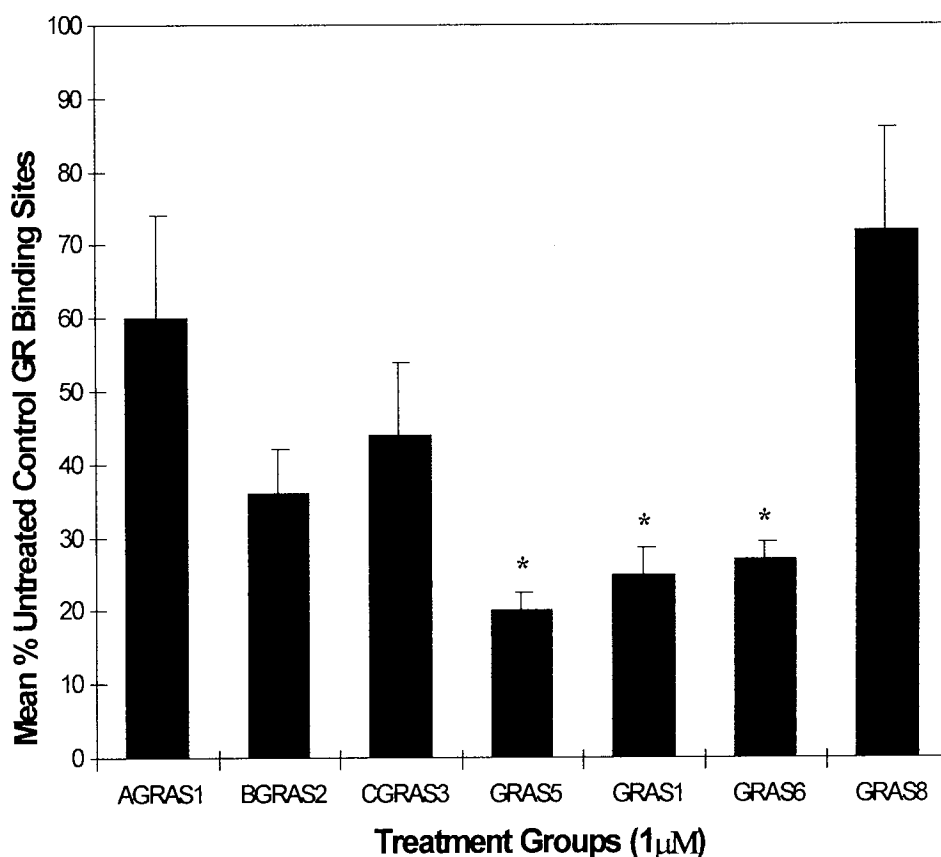


Figure 5.7 GR binding sites in C6 glioma cells as described in section 2.2.10.2 following treatment with various ODN sequences. Data expressed as a percentage of specific binding for control untreated cells. Data shown are mean values \pm standard deviation, where $n=3$ (LSD test, $*p<0.05$ compared to AGRAS1, BGRAS2, CGRAS3 and GRAS8).

These results showing differential antisense efficacy at reducing GR binding sites closely mirror the results obtained using quantitative RT-PCR to assess GR mRNA expression in C6 cells (section 5.3.3) and therefore further supports the use of rational antisense design and antisense sequences most likely to be effective both in cells *in vitro*, and potentially *in vivo*.

5.3.6 *In Vitro* Assessment of ODN Treatment on 5-HT_{2A} Receptor Protein Expression Using Radioligand Binding Assays.

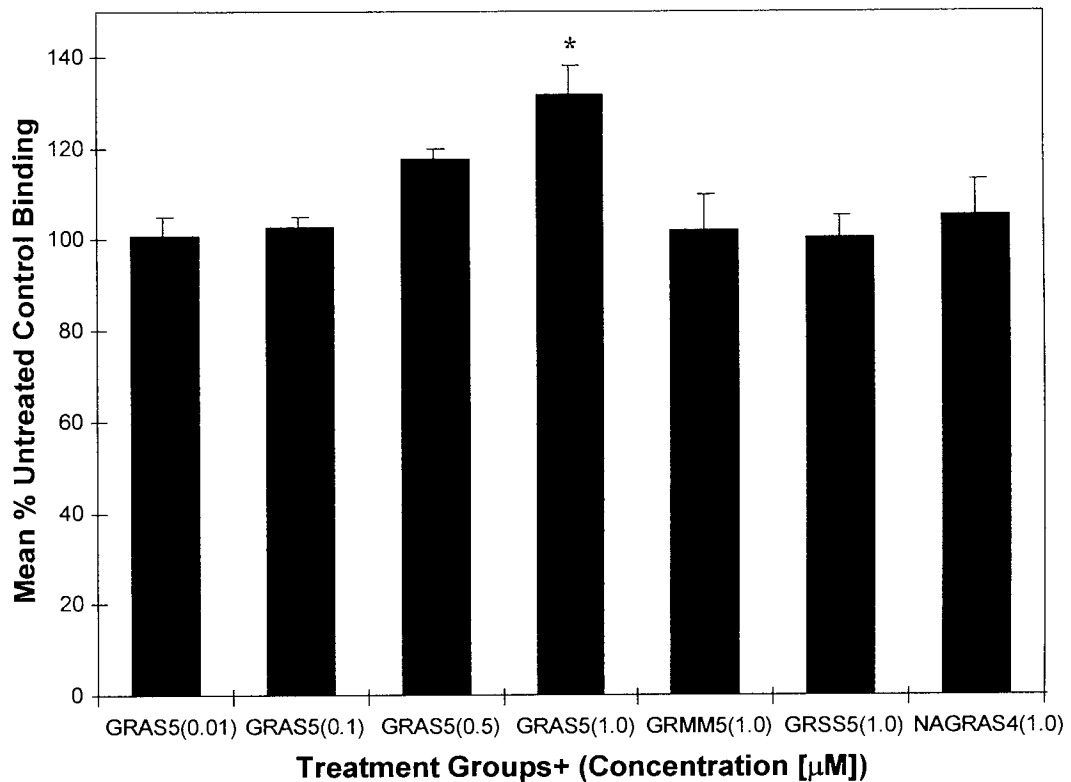


Figure 5.8 5-HT_{2A} receptor binding in C6 glioma cells as described in section 2.2.10.5 following treatment with various ODN sequences. Data expressed as a percentage of B_{max} for control untreated cells. Data shown are mean values ± standard deviation, where n=3 (LSD test, *p<0.05 compared to GRMM5, GRSS5 and NAGRAS4).

The expression of 5-HT_{2A} receptor protein in C6 glioma cells treated with the antisense and control ODN sequences listed in Table 5.1 was measured using saturation binding experiments with a range of 8 concentrations (0.5-50nM) of the 5-HT_{2A} receptor radioligand [³H]-ketanserin to determine the K_d (dissociation constant) and B_{max} (maximum number of binding sites) for [³H]-ketanserin and thus determine the possible functional consequence of downregulating GR expression using antisense ODNs *in vitro* (sections 2.2.10.4 and 2.2.10.5). Maximal binding sites (B_{max}) of 250 fmol/mg protein and dissociation constant (K_d) of 0.5nM for 5-HT_{2A} receptor in untreated groups were derived from saturation experiments.

Treatment with the optimally effective GRAS5 antisense ODN after 5 days produced a dose-dependent increase in 5-HT_{2A} receptor expression in C6 glioma cells (Figure 5.8), resulting in a significant ($p < 0.05$) 32% increase in 5-HT_{2A} receptor binding at 1 μ M. No significant changes in 5-HT_{2A} receptor binding were seen with the mismatch (GRMM5), sense (GRSS5) or non-accessible site (NAGRAS4) sequences.

This further supports the finding of the quantitative RT-PCR experiments (sections 5.3.3 and 5.3.4) that 5-HT_{2A} receptor expression is negatively regulated by GR. The pattern of this relationship between GR and 5-HT_{2A} receptor expression is illustrated in Table 5.2.

Table 5.2 The effect on 5-HT_{2A} receptor expression in C6 glioma cells following optimal GRAS5 antisense ODN treatment targeting the GR as determined using quantitative RT-PCR and radioligand binding assay. Increase (\uparrow) Decrease (\downarrow).

	PROTEIN	mRNA
Glucocorticoid Receptor	\downarrow	\downarrow
5-HT _{2A} Receptor	\uparrow	\uparrow

5.4 Discussion.

The aims of the experiments described in this chapter were to explore the efficacy of the antisense ODN sequences in Table 5.1 in a cell-based system, and to reveal modulation of 5-HT_{2A} receptor expression by the GR in C6 glioma cells. These experiments would also justify the use of RNase H accessibility mapping to design and characterise the efficacy of these sequences. In these studies cell-based effects were assessed by measuring antisense targeted receptor (GR) downregulation and any related changes in 5-HT_{2A} receptor expression at both mRNA and functional receptor protein using quantitative RT-PCR and radioligand binding analysis respectively.

Generally PS ODNs are reported to have considerably extended half lives relative to phosphodiester (PO) sequences when challenged with a number of purified nucleases (Hoke *et al*, 1991), or injected into *Xenopus* oocytes, (Woolf *et al*, 1990), although they were still degraded within 30 minutes in *Xenopus* embryos (Woolf *et al*, 1990). The half life of PS ODNs in HeLa cell nuclear extracts was reported to be 60 minutes (Furdon *et al*, 1989). Others found little or no degradation after 60 minutes in HeLa nuclear or cytoplasmic extract (Akhtar *et al*, 1991), although complete degradation by the same extract was reported to occur after 24-48 hours (Hoke *et al*, 1991). It has been shown here that the GRAS5 21-mer PS ODN remained intact for up to 24 hours in the presence of C6 glioma cells at 37°C. This infers that the intact 21-mer ODN is available to the C6 glioma cell line for the duration of the 24 hour intervals between media/antisense ODN replenishments, throughout the 5 day treatment period.

Phosphorothioate (PS) ODNs have been widely used *in vitro* but few studies using cultures of CNS-derived cells have been published. Concentrations of 1-3µM appear to be well tolerated by cells *in vitro* but PS ODNs at 30µM have been shown to be toxic (Wahlestedt *et al*, 1993; Owens *et al*, 1995) and similar toxicity at 50µM and above has been seen here. Consequently, antisense knockdown experiments in this chapter were conducted at a concentration range of 0.01-1µM, and no apparent neurotoxicity was observed.

Quantitative RT-PCR revealed a concentration-dependent downregulation of GR mRNA in C6 glioma cells after 5 daily treatments with the optimally effective GRAS5 ODN sequence. This achieved a 56% reduction in GR mRNA expression at 1 μ M. In the same cells, quantitative RT-PCR also revealed a concentration-dependent upregulation in 5-HT_{2A} receptor mRNA, producing a parallel 29% increase at 1 μ M. This shows that the GRAS5 antisense sequence significantly reduces GR mRNA expression *in vitro* with a consequential increase in 5-HT_{2A} receptor mRNA expression, highlighting the negative regulatory effect exerted by the GR on 5-HT_{2A} receptor expression. Similar effects were observed using radioligand binding assays to measure protein receptor expression following GRAS5 treatment: concentration-dependant GR downregulation by 80% and 5-HT_{2A} receptor upregulation by 32%. The GR regulatory effect of the GR on 5-HT_{2A} expression has been reported previously, using mainly glucocorticoid-mediated GR activation *in vitro* (Kuroda *et al*, 1992; Garlow and Ciaranello, 1995). In our study, knockdown of GR expression in C6 glioma cells using antisense ODNs resulted in an increase in 5-HT_{2A} receptor expression (Table 5.2) which is analogous to the observations made by Garlow and Ciaranello (1995) in non-CNS derived cells, in which GR activation using dexamethasone resulted in inhibition of a rat 5-HT_{2A} promoter-luciferase reporter construct. However in CNS derived Neuro-2a cells the opposite effect was seen: dexamethasone stimulated reporter expression from the 5-HT_{2A} promoter (Garlow and Ciaranello, 1995). This reversal of the regulatory effect of the GR on 5-HT_{2A} reporter expression may be a cell-type specific effect (glioma vs. neuroblastoma), rather than a species difference (rat C6 vs. mouse Neuro2a) since the use of a rat 5-HT_{2A} promoter-luciferase reporter eliminates species differences at the DNA level. However, Garlow and Ciaranello (1995) also point out that there is not a complete glucocorticoid response element (GRE) consensus in the rat 5-HT_{2A} promoter (only 11/15 bases match the consensus), and deletion of this sequence does not affect glucocorticoid stimulation of the reporter gene expression, therefore it would appear that glucocorticoids regulate 5-HT_{2A} expression by an indirect mechanism allowing both cell-type and species-specific differences in gene regulation.

In our studies it is interesting that GR knockdown caused an increase in 5-HT_{2A} expression. This indicates that there was tonic repression of 5-HT_{2A} expression in the C6 cells used for these experiments. In the absence of exogenous corticosteroid/dexamethasone, it is not clear why the GR should be activated to repress 5-HT_{2A} expression. It appears therefore, either that there is some degree of constitutive GR activation leading to 5-HT_{2A} repression or that some corticosterone is present in the culture medium, in the foetal calf serum. The latter has been confirmed. The foetal calf serum was shown by the supplier (Life Technologies, UK): to contain cortisol (0.1-2.24 µg/L), as well as the gonadal steroids estradiol (8.78-36 µg/mL), progesterone (0.03-0.18 ng/mL) and testosterone (0.01-0.18 ng/mL). Therefore the culture medium would have contained approximately 5nM of cortisol which is in the concentration range to allow binding to the GR ($K_d = 2-5\text{nM}$).

To assess the level of potency of the GRAS5 sequence, and thereby to justify the optimisation of the antisense designs using RNase H accessibility mapping (Chapter 4), GR downregulation at the level of both mRNA and receptor protein using GRAS5 was compared to the other antisense ODN designs listed in Table 5.1. It was evident that the antisense designs: GRAS1, GRAS5 and GRAS6 effective at RNase H cleavage of accessible site D (section 4.3.4) produced the greatest downregulation of GR mRNA and protein expression compared to mismatch (GRMM5), sense (GRSS5) or non-accessible site (NAGRAS4) control sequences. This site was found to be the most accessible to RNase H cleavage, in a cell-free system, and appears equally accessible in cells. The antisense sequences against the less accessible sites A-C (AGRAS1, BGRAS2 and CGRAS3) also reduced GR mRNA and protein expression in cells, but to a lesser extent, reflecting the lower accessibility of these sites to RNase H in the cell free system. Yet further validation of RNase H accessibility of *in vitro* T7-transcribed mRNA translating to identical accessibility in cells comes from the observation that GRAS8, a sequence mapping adjacent to accessible site D and causing poor cleavage *in vitro*, similarly had little effect on GR mRNA or protein expression in C6 glioma cells. Furthermore, the antisense effects are sequence specific, because mismatch (GRMM5) and sense (GRSS5) sequences, as well as a non-accessible site sequence (NAGRAS4) produced little inhibition of GR expression.

In conclusion, several antisense and control ODN sequences have been evaluated in a cell culture system with GRAS5 antisense ODN being the most effective at inhibiting GR mRNA and protein expression in C6 glioma cells. The significant effects of the GRAS5 sequence on both GR mRNA and protein levels but not mismatch or sense sequences confirms the involvement of an antisense-mediated knockdown mechanism. The integrity of the GR transcriptional regulation mechanism has also been confirmed, in that a consequential change in the expression of 5-HT_{2A} receptors in these cells also occurred. This effect is consistent with negative regulation of 5-HT_{2A} expression by the GR. Also, since GRAS5 downregulated GR expression, but upregulated 5-HT_{2A} receptor expression, this suggests the GRAS5 ODN effect is not non-specific. Furthermore the use of RNase H mapping reactions in selecting optimal antisense sequences has been justified in terms of the level of *in vitro* efficacy seen with such optimally designed antisense ODN sequences, especially the GRAS5 design. We can therefore investigate the use of this GRAS5 antisense sequence, with appropriate controls, *in vivo* to determine its efficacy at GR knockdown and reveal any causal effects on 5-HT_{2A} receptor expression.

CHAPTER SIX

IN VIVO EFFECTS OF ANTISENSE OLIGODEOXYNUCLEOTIDES TARGETING THE GLUCOCORTICOID RECEPTOR

6.1 Introduction.

This chapter investigates the effects of the selected antisense and control sequences targeting the GR using male Wistar rats as the *in vivo* model. In the present study the effect of GRAS5 antisense ODN treatment on expression of GR in the rat CNS has been determined, using quantitative RT-PCR, radioligand binding techniques and western blot analysis. In the relevant tissue samples analysis of 5-HT_{2A} receptor expression was determined using quantitative RT-PCR and radioligand binding techniques to assess GR modulation of 5-HT_{2A} receptor expression *in vivo* (Chaouloff, 1995; Kuroda *et al*, 1993; Lopez *et al*, 1997). The functional consequences of GR knockdown using GRAS5 was also investigated indirectly by measuring 5-HT_{2A} receptor specific head-and body shakes in rats following DOI administration (Kennett and Curzon, 1991). Before these main objectives were tackled several important factors which influence the use of antisense ODNs *in vivo* such as: delivery and route of GRAS5 administration, the time course of target receptor protein turnover governing duration of GRAS5 treatment, the antisense sequence/chemistry, controlling for potential toxicity and, *in vivo* stability and CNS distribution of GRAS5 (Schlingensiepen and Heilig, 1997; LeCorre *et al*, 1997), were addressed first.

Several techniques have been developed for the administration of ODNs to the rat CNS, including repeated bolus ICV injections, continuous infusions using devices such as osmotic minipumps, and repeated direct injections to specific brain regions (Wahlestedt, 1994). As stress increases glucocorticoid release, which in turn regulates the level of GR expression via the HPA axis (section 1.7.3), repeated ICV injection procedures which increase overall stress

to the animals would not be an ideal means of ODN administration. Also devices such as minipumps, which are normally surgically implanted in the fold of skin at the nape of the neck near the animals' head would cause problems in the measurement of the functional consequences of GR inhibition when using behavioural tests such as DOI-induced head-shake observations. In the case of site-specific injections, some localised tissue damage can be expected and therefore this route of CNS administration is not deemed suitable.

To overcome this problem of ODN administration to rat CNS a slow-release polymer microsphere delivery system was used. This involved producing microscopic spherical matrices of biodegradable polymer which had ODNs dispersed within the polymer matrix to be released in a slow, sustained manner into the exogenous medium. Unlike cationic liposomes, microspheres can provide ODN delivery across the cell membrane without the cellular toxicity associated with cationic liposomes (Lewis *et al*, 1995; Cleek *et al*, 1997). Microspheres also provide ODNs with protection from nuclease degradation (Lewis *et al*, 1995) and can be manufactured to provide ODN release over a predetermined period of time, therefore enabling lower concentrations of ODN to be used, and only necessitating a single ICV injection. Such use of biodegradable polymer microspheres in delivering antisense ODNs has been carried out previously both *in vitro* and *in vivo* (section 1.9), but not directly to the brain, thus making the use of this delivery system in this study a novel approach.

The turnover of GR *in vivo* is not known, but is predicted to have a half-life of about 2-3 days, as is the case for most intracellular hormone receptors (Herz *et al*, 1997). Thus a 5 day sustained period of ODN treatment, equivalent to 2 half-lives, was chosen, and therefore ODNs were formulated in polymer microspheres which were developed to give complete degradation and dissolution of the polymer matrix within approximately 5-7 days (Lewis *et al*, 1995). A majority of *in vivo* experiments using antisense ODNs (Wahlestedt *et al*, 1993; Zhang and Creese, 1993; Whitesell *et al*, 1993; Weiss *et al*, 1997) have used nuclease resistant PS ODNs rather than phosphodiester ODNs, and continuous infusion rather than repeated ICV injections. This method of administration has been shown to give superior brain distribution and concentrations, and reduce any potential toxicity (Whitesell *et al*, 1993). Therefore PS ODN sequences formulated within sustained-release polymer microspheres were

used with the aim of achieving this superior brain distribution at non-toxic concentrations of PS ODNs.

Assessment of systemic toxicity and any histological damage as a result of treatment was made by carrying out animal well-being assessments (section 2.2.20) and cresyl fast violet staining (section 2.2.19.1) respectively. Post-operative well-being assessments assessed any behavioural toxicity of the treatment following surgery using a set of well defined behavioural parameters over a specific period of time and was scored in terms of the degree of the particular behaviour which was different in treated animals compared to normal untreated animals (section 2.2.20). Cresyl fast violet staining examined histological damage as a result of neuronal loss and glial cell proliferation. In addition, animals were also weighed daily and, following the experimental endpoint, adrenal glands were removed and weighed to check for any systemic HPA-axis related effects arising from the treatments.

The uptake of antisense ODNs *in vivo* has previously been investigated by a number of groups using a number of different methods, which include fluorescent labelling of oligonucleotides, immunocytochemical assays and the use of radiolabelled oligonucleotides. But there is still limited information regarding the anatomical distribution of the antisense ODN following administration into the rat brain (Whitesell *et al*, 1993; Yee *et al*, 1994; Yaida and Nowak, 1995; Szklarczyk and Kaczmarek, 1995; Schlingensiepen and Heilig, 1997). ICV application in the rat of biotinylated ODNs was previously found to penetrate brain tissue and neurones, giving rise to specific cellular staining, and appeared to be randomly distributed within many types of cells (Wahlestedt, 1994). To establish for this study the pattern of distribution and penetration in the rat CNS of the administered ODNs, FITC-labelled ODNs were injected ICV in either polymer-complexed or free form and the animals killed after 1 or 5 days. The rat brains were paraformaldehyde-fixed and sectioned using a cryostat and analysed for ODN distribution with fluorescence microscopy (section 2.2.19.2). The fluorescent-labelled ODN is more convenient to use than a radiolabelled probe as it is commercially synthesised and is easier to handle for *in vivo* experiments giving comparable levels in obtained results.

Time course studies into the uptake and the stability of PS oligonucleotides *in vivo* suggest that the free PS oligonucleotide is stable in the brain for approximately 24 hours (Zhang *et al*,

1996; Weiss *et al.*, 1997). *In vivo* stability studies (section 2.2.22) were conducted to establish the period of survival of the intact 21-mer PS ODN GRAS5 antisense design sequence both in the polymer complexed and free form at various times following ICV administration.

Table 6.1 Developed oligodeoxynucleotide sequences used in male Wistar rats as polymer formulations.

ANTISENSE DESIGN ID	SEQUENCE (5' to 3')	SEQUENCE TYPE
GRAS5 GRMM5	TAAAAACAGGCTTCTGATCCT <u>CGGAAAAGTGCTCACGATAAC</u>	Antisense to site D Mismatch control

The aim of this chapter was to investigate the potential of the optimally effective GRAS5 antisense sequence in its role as a biological tool, with the presence of appropriate control sequences (Table 6.1) and treatment groups, for the knockdown of CNS GR expression *in vivo* and also determine the existence and level of any modulation of the 5-HT_{2A} receptor system as seen in the *in vitro* studies (Chapter 5). This was to be assessed in terms of GR and 5-HT_{2A} receptor expression at both the mRNA and receptor protein level in corresponding rat brain regions which include the hypothalamus, hippocampus and frontal cortex. The functional consequences of any change in 5-HT_{2A} receptor expression as a result of possible GRAS5 specific downregulation of GR was assessed using the behavioural experiment of DOI-induced head-shake frequency.

6.2 Methods.

All relevant methods are found in chapter two, with any additional information given in the relevant results section.

Results in this chapter, unless otherwise indicated, were statistically compared using a one-way analysis of variance with treatment as factor. *Post hoc* comparisons were then made using Tukey-HSD test, with alpha set at $p < 0.05$. In all statistical analysis a value of $p < 0.05$ was considered significant.

6.3 Results.

6.3.1 Oligonucleotide Synthesis and Preparation of Microspheres.

Both the antisense 21-mer PS GRAS5 and control 21-mer PS GRMM5 ODN sequences (Table 6.1) were custom synthesised and cartridge purified commercially (Gibco BRL, Life Technologies, UK). ODN loaded microspheres were prepared as described in section 2.2.15.1 at a concentration of 20 $\mu\text{g}/\mu\text{L}$ of ODN for every 0.2mg of polymer, which when considering a microsphere entrapment efficiency of 50%, polymer solubility of 1mg/5 μL in ddH₂O and complete polymer matrix degradation and dissolution occurring within 5-7 days (Lewis *et al*, 1995), provided an approximate dose of 2 $\mu\text{g}/\mu\text{L}$ of ODN per day over a treatment period of 5 days. This ODN concentration was selected from assessing previously published *in vivo* studies (Zon, 1995; Nicot and Pfaff, 1997; Szklarczyk and Kaczmarek, 1999) and based on the findings from the *in vitro* studies (Chapter 5). For control blank polymer microspheres saline was used to replace the ODN aqueous solution in the microsphere preparation protocol (section 2.2.15.1). Surface morphology of the prepared microspheres was examined using scanning electron microscopy (SEM) as described in section 2.2.15.2 and is shown in Figure 6.1.

The polymer microsphere particle size distribution range was also characterised as described in section 2.2.15.3 and is shown in Figure 6.2. Examination by SEM showed that all batches of microspheres had formed with the expected spherical morphology and possessed a smooth external surface immediately after the preparation (Figure 6.1). There were no ODN crystals observed on the surface of the microspheres, probably due to the washing procedure during the preparation of microspheres.

Microsphere particle size analysis showed that all batches of polymer microspheres used in the *in vivo* studies had a size distribution ranging from 0.1-100 μm (Figure 6.2) which was consistent to achieve the expected 50% loading efficiency (Lewis *et al*, 1995). This achieved size distribution range would also provide a continued release profile of entrapped ODN as a result of different particle sizes and therefore exposed surface areas presented by these microspheres in a particular batch. This is because these microspheres would have varying

degradation rates in a particular batch due to differences in their surface area and thus provide sustained degradation of polymer matrix, continually releasing ODN over a specific time period (Lewis *et al*, 1995).

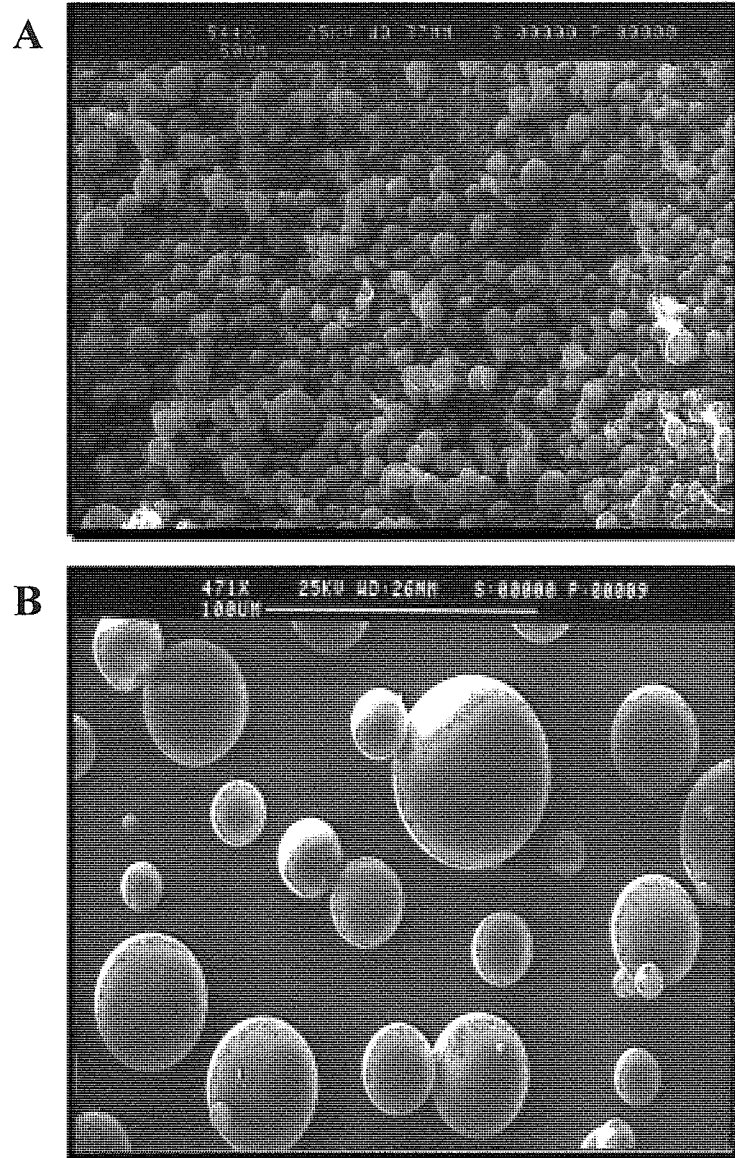


Figure 6.1 Representative scanning electron micrographs of poly D,L-lactide co-glycolide (PL-GA) polymer microspheres containing GRAS5 ODN at different viewing fields: (A) low power magnification, (B) high power magnification.

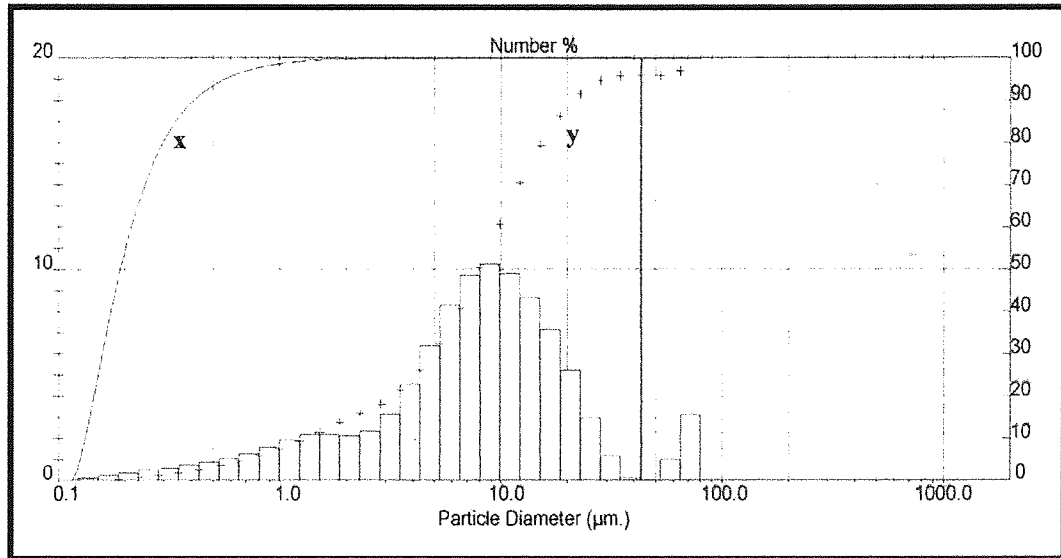


Figure 6.2 Representative particle size distribution range for ODN loaded microspheres as measured using a Malvern Mastersizer (see section 2.2.15.3). Curve x: distribution expressed as the mean number of particles. Curve y: distribution expressed as the mean volume of particles.

6.3.2 Preliminary Assessment of GRAS5 ODN Treatment.

Pilot studies were performed in order to meet with Home Office regulations concerning ethical issues and to determine the safety and suitability of the optimally effective antisense GRAS5 sequence *in vivo*. These studies determined the safety of GRAS5 ODN treatment, administered as both the polymer microsphere loaded (AS) and free uncomplexed (FAS) form, using animal well-being assessments (section 2.2.20) and CNS histological examination (section 2.2.17). The extent and duration of GRAS5 treatment achieved using the polymer microsphere delivery system was investigated by performing stability studies of recovered GRAS5 following *in vivo* treatment (section 2.2.22). Further preliminary studies were also conducted to examine the nature of GRAS5 distribution within the brain after single ICV administration of this novel GRAS5-polymer microsphere delivery system using fluorescent localisation of microsphere entrapped FITC labelled GRAS5 ODN (section 2.2.18).

6.3.2.1 Preliminary Well-being Assessments.

Initial well-being assessments as described in section 2.2.20, carried out on animals (n=2) following ICV administration of either AS or FAS treatment (section 2.2.16) using an estimated total dose of 10µg/µL of ODN for each, produced no noticeable differences in behaviour after 5 days compared to untreated animals. This shows that GRAS5 treatment resulted in no behavioural toxicity *in vivo* after 5 days of treatment. A more extensive well-being assessment study is presented in section 6.3.3.2.

6.3.2.2 Histological Examination.

Rat brain cryosections, prepared as described in section 2.2.17, were examined 5 days following ICV administration of either AS (at 2µg/µL of ODN per day, n=3) or FAS (10µg/µL of ODN, n=3) for histological damage using cresyl fast violet staining as described in section 2.2.19 and by making comparisons to cresyl fast violet stained cryosections from untreated animals. Figure 6.3 highlights the accuracy in directing the injection needle to the intended target of the left lateral ventricle (Figure 6.3B) using the stereotaxic co-ordinates (section 2.2.16) by the observations of needle tract projections to the left lateral ventricle (Figure 6.3C). The anatomical brain regions investigated using histological examination is illustrated in Figure 6.3A. Cresyl violet staining revealed no observed neurological damage, neuronal loss or evidence of glial cell proliferation in any of the two treatment groups as highlighted by the tissue morphology seen in the following brain regions: frontal cortex, hippocampus, hypothalamus, cerebellum, striatum and corpus callosum (Figures 6.4 to 6.9) of treated animals compared to untreated animals. This shows there is no apparent toxicity associated with AS or FAS treatments following single ICV administration.

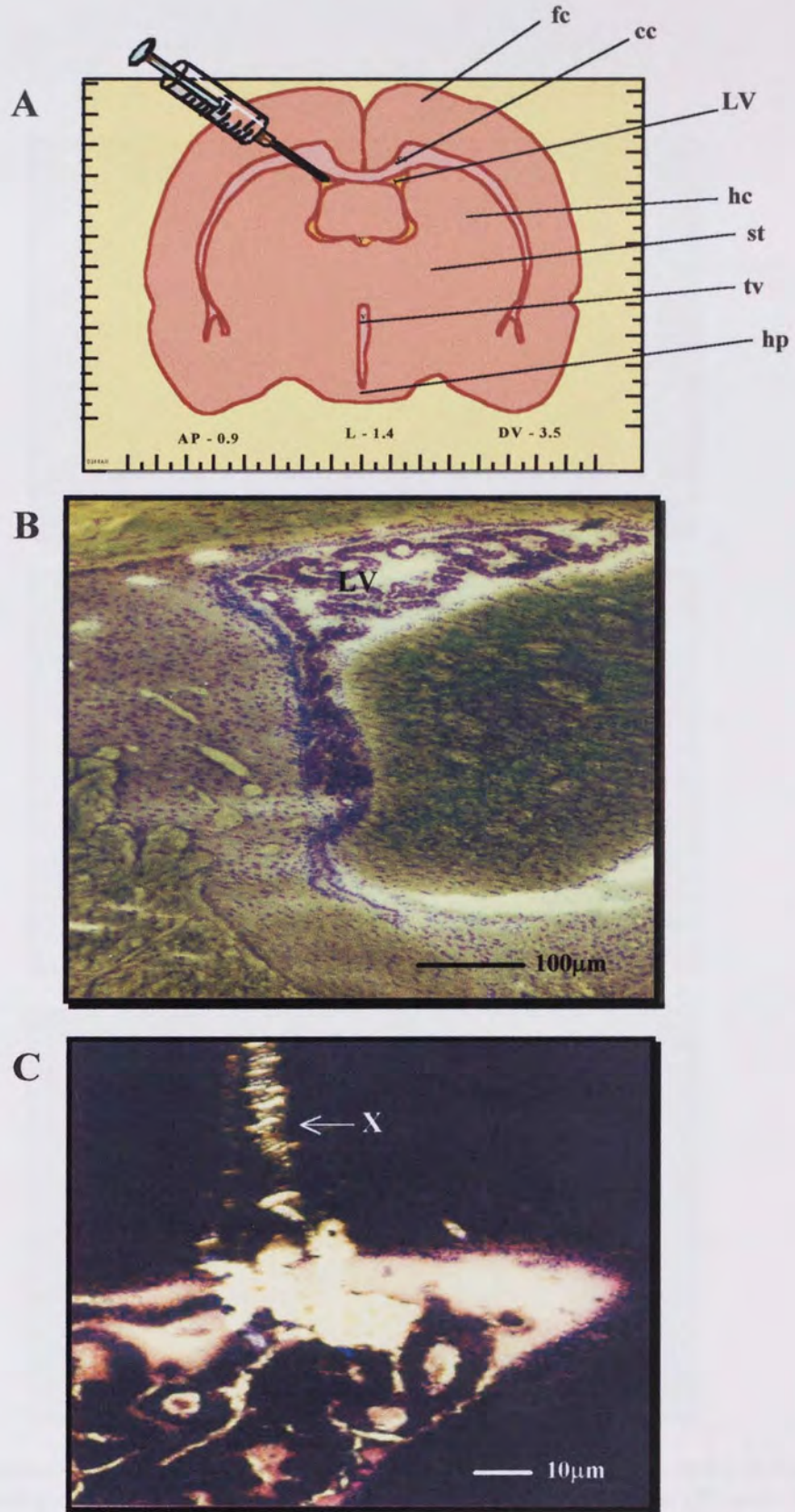


Figure 6.3 (A) Illustration of ICV administration (syringe) to left lateral ventricle using coronal section of rat brain highlighting common anatomical regions: frontal cortex (fc), corpus callosum (cc), lateral ventricle (LV), hippocampus (hc), striatum (st), third ventricle (tv), hypothalamus (hp). Light microscope photograph of coronal section of rat brain showing: (B) the left lateral ventricle (LV) using cresyl violet staining and (C) needle tract (X) made by ICV administration of AS treatment using stereotaxic co-ordinates entering the left lateral ventricle as described by the procedure in section 2.2.16.

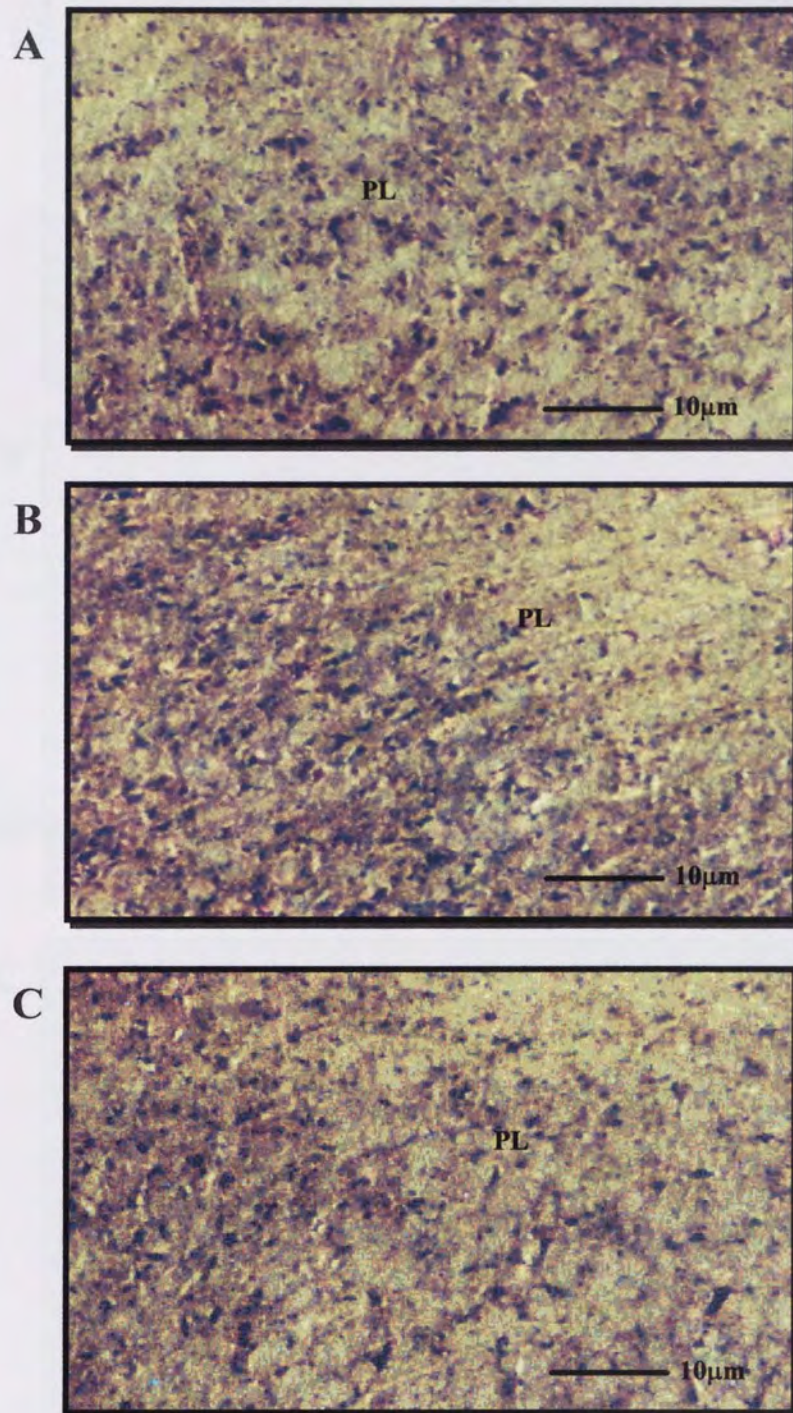


Figure 6.4 Representative light microscope photographs of coronal sections of rat brain showing an area of frontal cortex using cresyl violet staining in: (A) untreated male Wistar rats, (B) male Wistar rats following AS treatment and (C) male Wistar rats following FAS treatment as described in section 6.3.2.2. Abbreviation: PL, pyramidal layer.

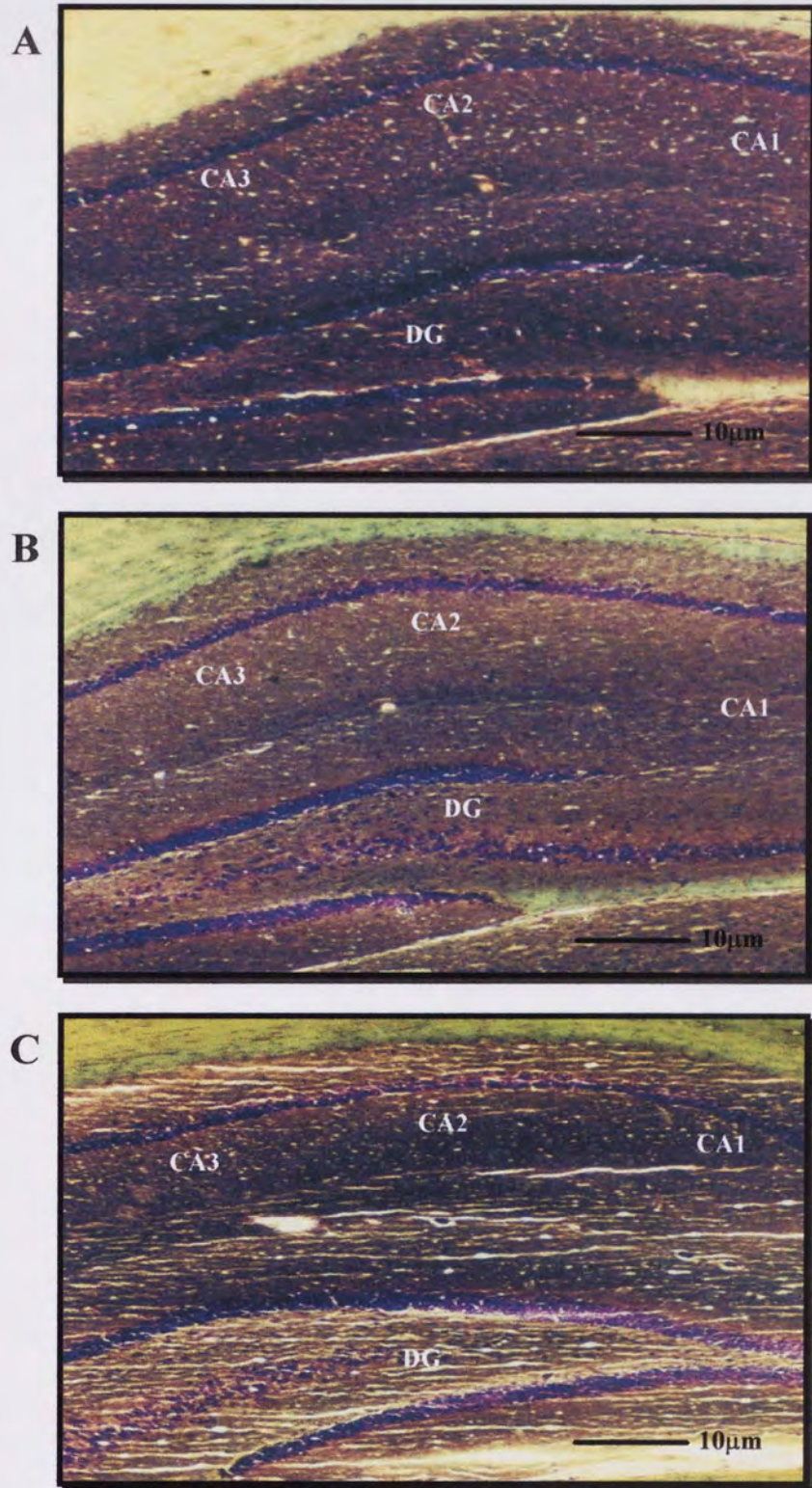


Figure 6.5 Representative light microscope photographs of coronal sections of rat brain showing an area of hippocampus using cresyl violet staining in: (A) untreated male Wistar rats, (B) male Wistar rats following AS treatment and (C) male Wistar rats following FAS treatment as described in section 6.3.2.2. Abbreviations: DG, dentate gyrus; hippocampal longitudinal zones CA1, CA2 and CA3.

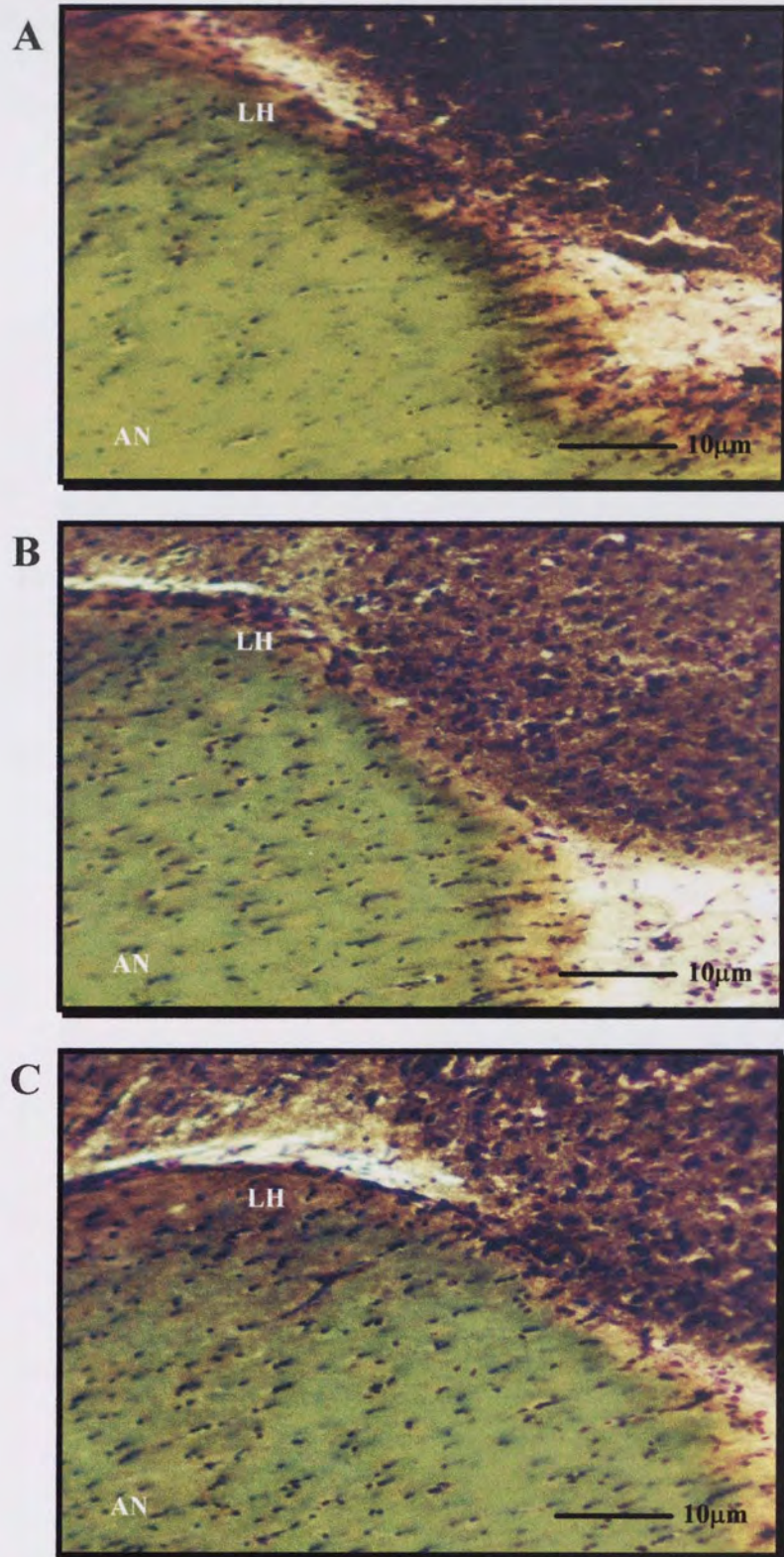


Figure 6.6 Representative light microscope photographs of coronal sections of rat brain showing an area of hypothalamus using cresyl violet staining in: (A) untreated male Wistar rats, (B) male Wistar rats following AS treatment and (C) male Wistar rats following FAS treatment as described in section 6.3.2.2. Abbreviations: AN, arcuate nucleus; LH, lateral hypothalamus.

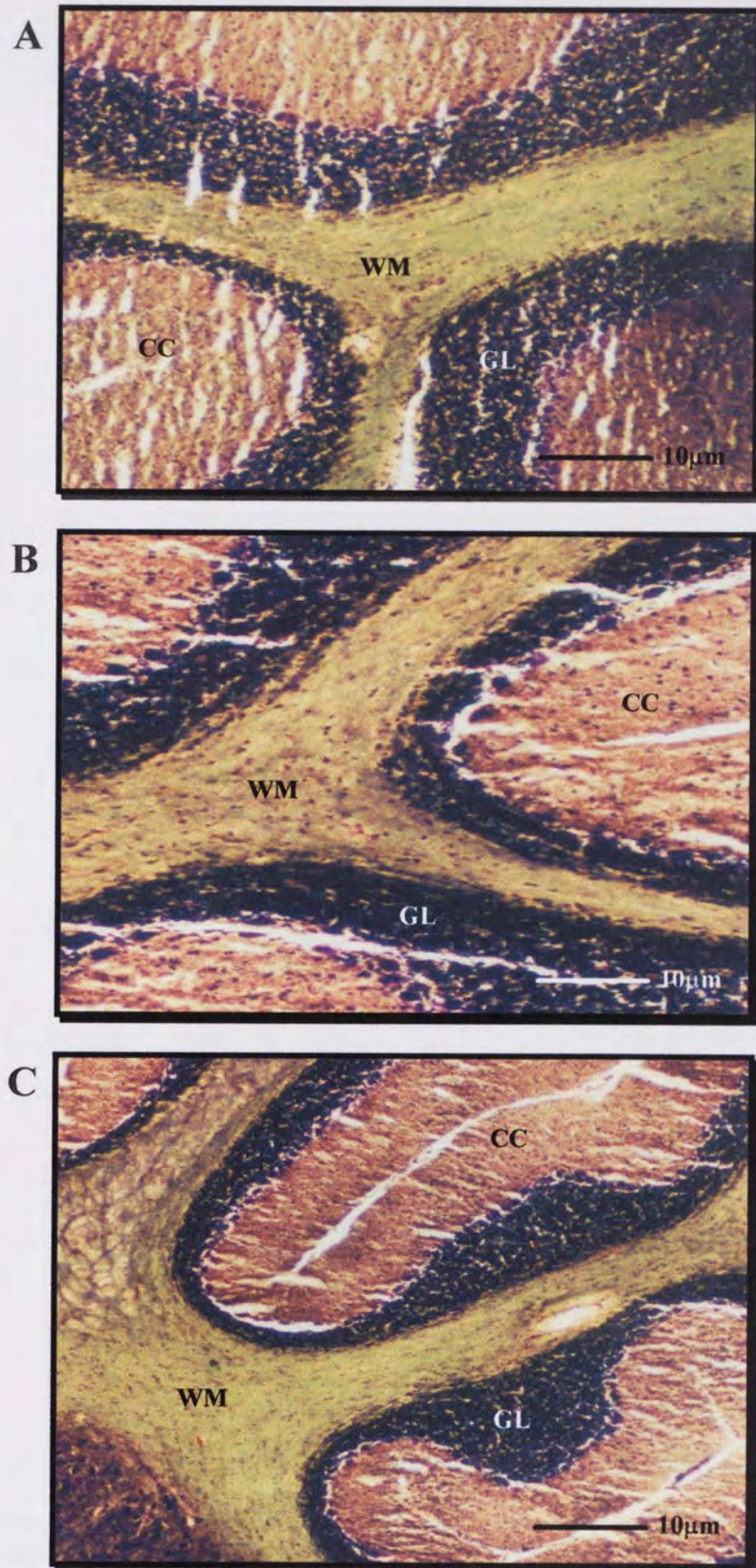


Figure 6.7 Representative light microscope photographs of coronal sections of rat brain showing an area of cerebellum using cresyl violet staining in: (A) untreated male Wistar rats, (B) male Wistar rats following AS treatment and (C) male Wistar rats following FAS treatment as described in section 6.3.2.2. Abbreviations: WM, white matter; GL, granular layer; CC, cerebellar cortex.

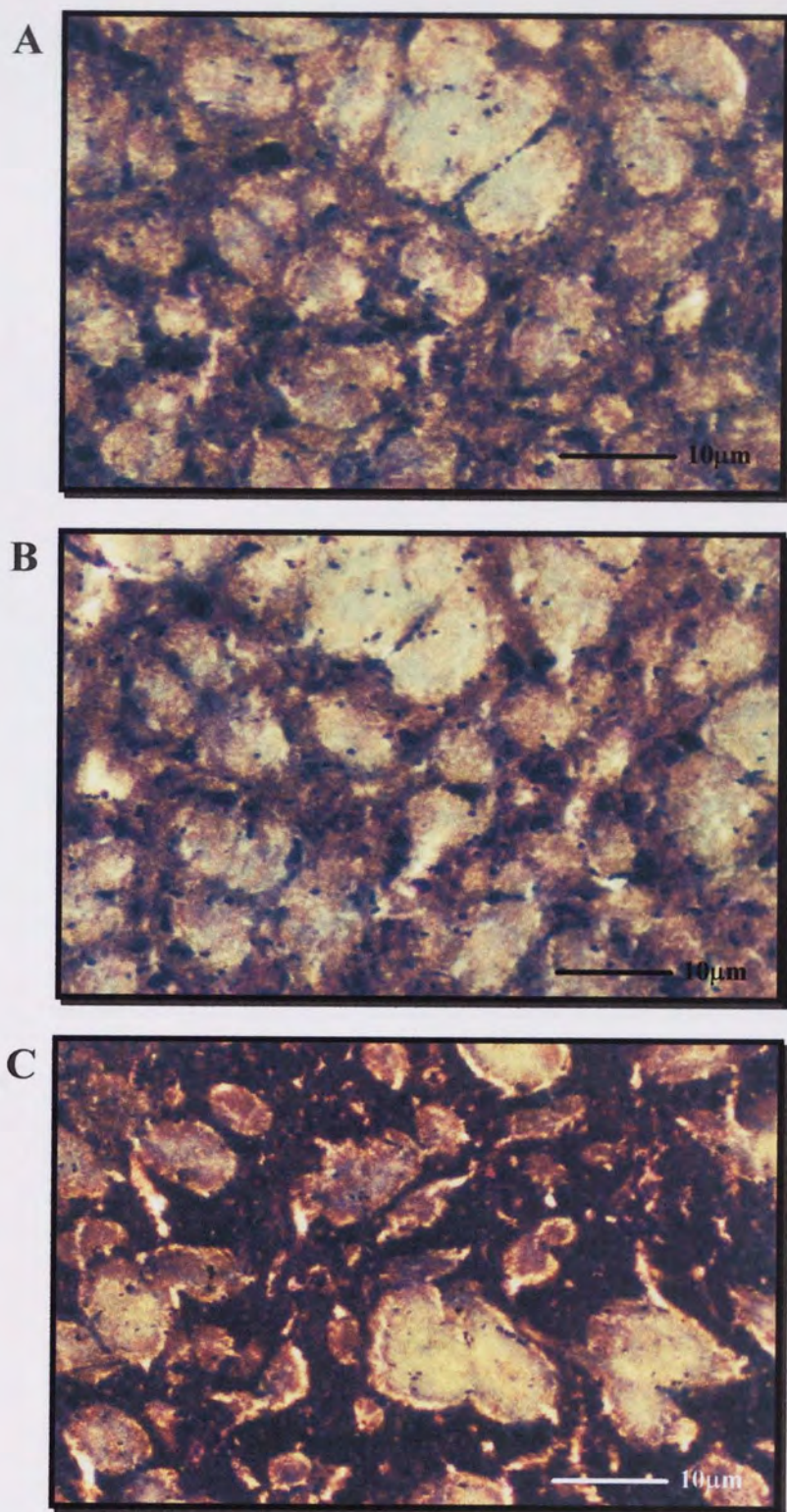


Figure 6.8 Representative light microscope photographs of coronal sections of rat brain showing an area of striatum using cresyl violet staining in: (A) untreated male Wistar rats, (B) male Wistar rats following AS treatment and (C) male Wistar rats following FAS treatment as described in section 6.3.2.2.

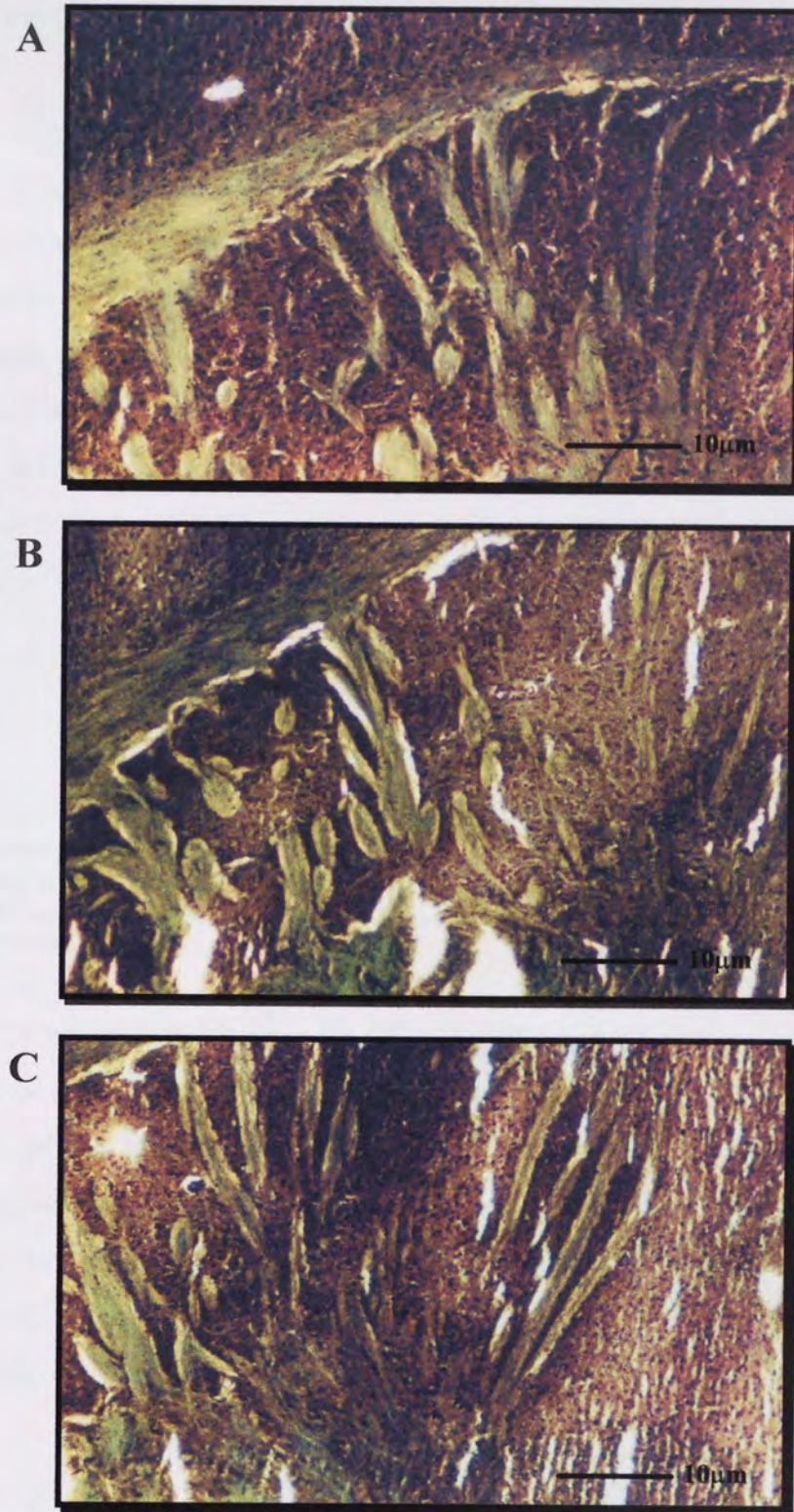


Figure 6.9. Representative light microscope photographs of coronal sections of rat brain showing an area of corpus callosum using cresyl violet staining in: (A) untreated male Wistar rats, (B) male Wistar rats following AS treatment and (C) male Wistar rats following FAS treatment as described in section 6.3.2.2.

6.3.2.3 *In Vivo* Oligonucleotide Stability.

The stability of ICV administered 21-mer PS GRAS5 ODN in the polymer-complexed form in the rat CNS was examined at 24 hours and at 5 days after administration as described in section 2.2.22 (n=3), to assess the presence of intact GRAS5 ODN within the rat brain following treatment. Figure 6.10 shows the ODN remains intact in the rat CNS after 24 hours (Lanes 1-3) and 5 days (Lanes 4-6) following ICV administration. Therefore the intact full length 21-mer GRAS5 ODN was available for up to 5 days in the rat CNS using the polymer microsphere delivery system. Partial degradation of the ODN was shown by the lower intensity bands obtained for the two time points compared to bands illustrating the intact 21-mer GRAS5 ODN as represented by lane A.

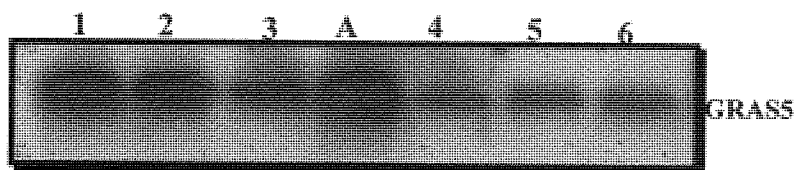


Figure 6.10 Autoradiogram of 5'-end ^{32}P -labelled ODNs electrophoresed by 20% denaturing PAGE showing stability of 21-mer PS GRAS5 ODN administered ICV in the polymer-complexed form to male Wistar rats and retrieved 24 hours (Lanes 1-3) or 5 days (Lanes 4-6) following administration. Lane A: intact 21-mer PS GRAS5 ODN.

Stability of ICV administered 21-mer PS GRAS5 ODN in the free form in the rat CNS was also assessed 24 hours after administration as described in section 2.2.22 (n=3) to compare with GRAS5 stability in the polymer-complexed form. Figure 6.11 shows the ODN to be extensively degraded in the rat CNS 24 hours following ICV administration as represented by the detection of faint bands (Lanes 1-3). However, due to the presence of bands of appropriate size, corresponding to the intact 21-mer GRAS5 ODN, some of the full length 21-mer ODN remained intact for up to 24 hours.

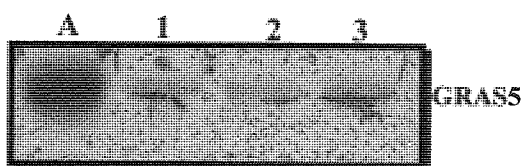


Figure 6.11 Autoradiogram of 5'-end ^{32}P -labelled ODNs electrophoresed by 20% denaturing PAGE showing stability of 21-mer PS GRAS5 ODN administered ICV in the free form to male Wistar rats and retrieved 24 hours (Lanes 1-3) following administration. Lane A: intact 21-mer PS GRAS5 ODN.

6.3.2.4 *In Vivo* Fluorescent Localisation Studies.

5'-FITC labelled GRAS5 ODN in either polymer complexed form (at 2 μ g/ μ L of ODN per day, n=3) or in the free form (10 μ g/ μ L of ODN, n=3) were administered to male Wistar rats ICV as described in section 2.2.19.2. Rat brains were processed and sectioned using a cryostat (section 2.2.17) and analysed for ODN distribution using fluorescence microscopy (section 2.2.18) 1 and 5 days following ICV administration of either free ODN or polymer complexed ODN. Representative pictures from a selection of brain areas are shown in Figures 6.12 to 6.19 which illustrate the distribution of ODNs within the CNS in either the free or polymer complexed form.

It was evident that 5 days following single ICV administration of free ODN the fluorescent signal within the brain tissue was very poor, suggesting clearance of the ODN from the CNS after 5 days (Figure 6.12) and as a result distribution of free ODN was investigated up to 1 day after ICV administration (Figures 6.14 to 6.16). The fluorescent signal detected 1 day following single ICV administration of polymer-complexed ODN revealed distribution to the right lateral ventricle and surrounding areas (Figure 6.13A), highlighting the diffuse spread of ODNs from the site of injection (left lateral ventricle). Under higher magnification the polymer microspheres can be seen in the choroid plexus of the left lateral ventricle (Figure 6.13B).

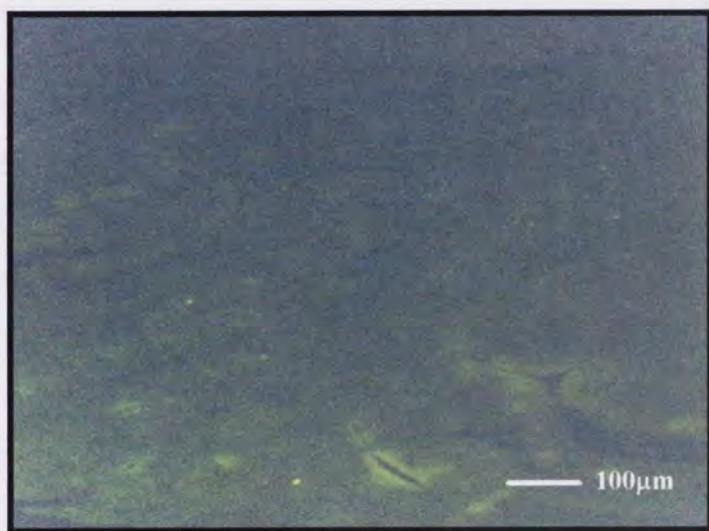


Figure 6.12 Fluorescent photomicrograph of a coronal section of rat brain (left hemisphere) 5 days after ICV administration of FITC-labelled GRAS5 ODN as described in section 2.2.19.2.

A high intensity of fluorescence was frequently observed within the choroid plexus, situated within the lateral ventricles. The choroid plexus is the term used to describe capillaries within the ventricles of the brain and certain types of glia, such as astrocytes, are frequently associated with the choroid plexus (Nauta and Feirtag, 1986). A high fluorescence signal intensity, associated with the choroid plexus alone, would not indicate that FITC labelled ODNs were able to depart these structures and reach other areas of the brain. However, further examination of other brain areas revealed the presence of high fluorescent signal intensities (Figures 6.17 to 6.19).

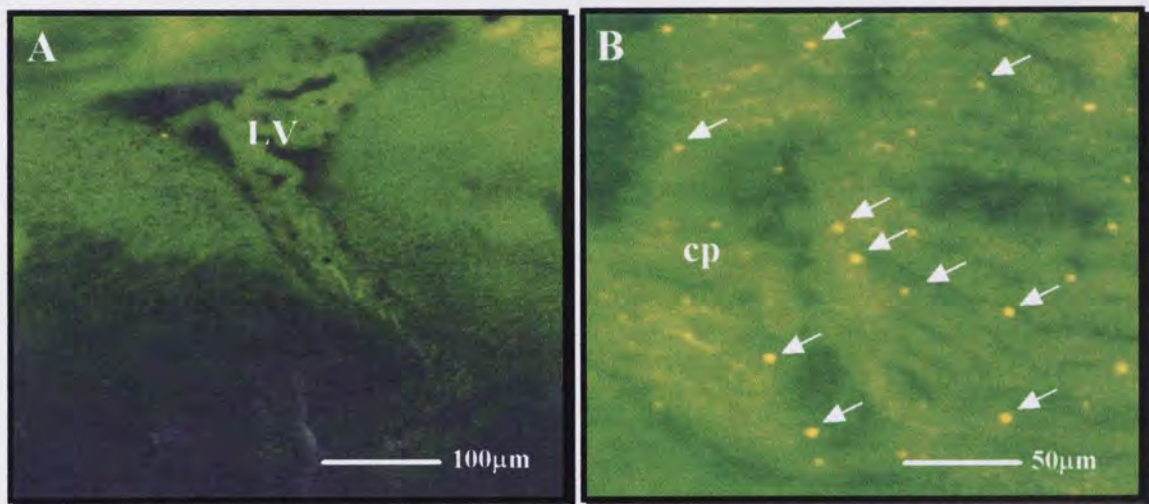


Figure 6.13 Fluorescence photomicrographs of coronal sections of rat brain 1 day after ICV administration of FITC-labelled GRAS5 ODN in polymer complexed form as described in section 2.2.19.2 showing: (A) fluorescent signal detected in the right lateral ventricle (LV) and (B) fluorescent polymer microsphere particles (arrows) within the choroid plexus (cp) of the left lateral ventricle.

When comparing the fluorescent signal obtained for the FITC labelled ODN following ICV administration, either as the free or polymer complexed form, it was apparent that the fluorescence was diffusely spread, being detected in both hemispheres of the brain. However the fluorescent signal intensities and regional distribution obtained for the free ODN 1 day after ICV administration was much lower than that for the polymer complexed ODN 5 days after ICV administration. This was observed in regions such as the frontal cortex, cerebellum and striatum (Figures 6.14 to 6.16).

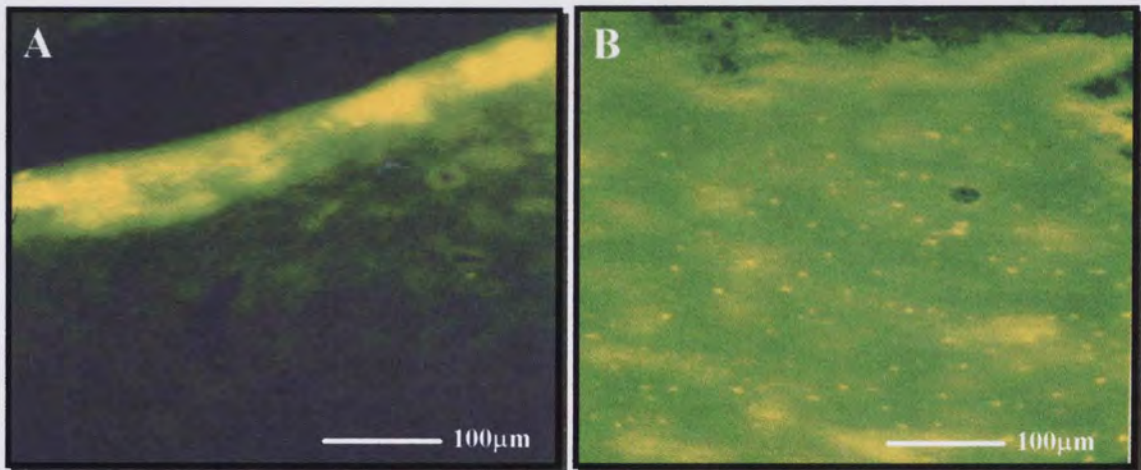


Figure 6.14 Fluorescence photomicrographs of coronal sections of rat brain showing fluorescence signal detected in an area of frontal cortex: (A) 1 day after ICV administration of free FITC-labelled GRAS5 ODN and (B) 5 days after ICV administration of FITC-labelled GRAS5 ODN in polymer-complexed form.

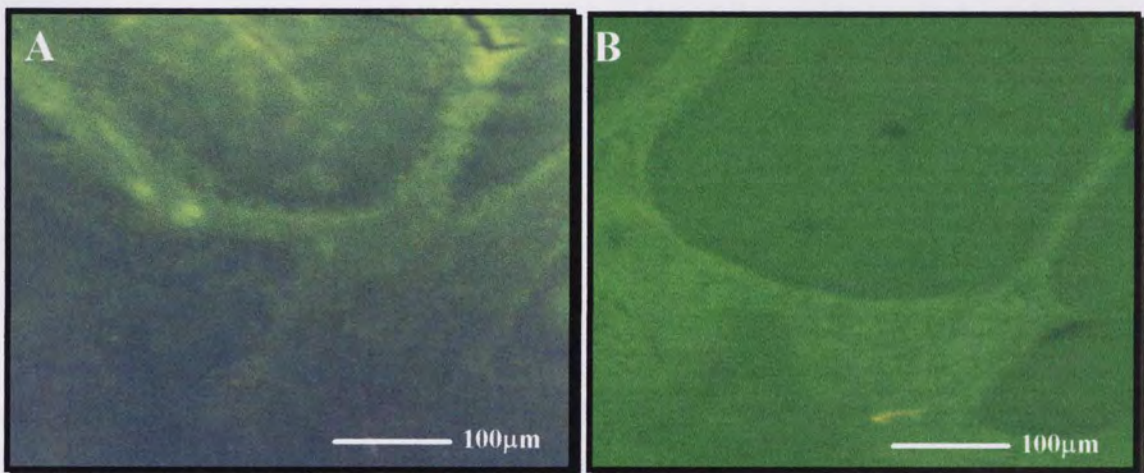


Figure 6.15 Fluorescence photomicrographs of coronal sections of rat brain showing fluorescence signal detected in an area of cerebellum: (A) 1 day after ICV administration of free FITC-labelled GRAS5 ODN and (B) 5 days after ICV administration of FITC-labelled GRAS5 ODN in polymer-complexed form.

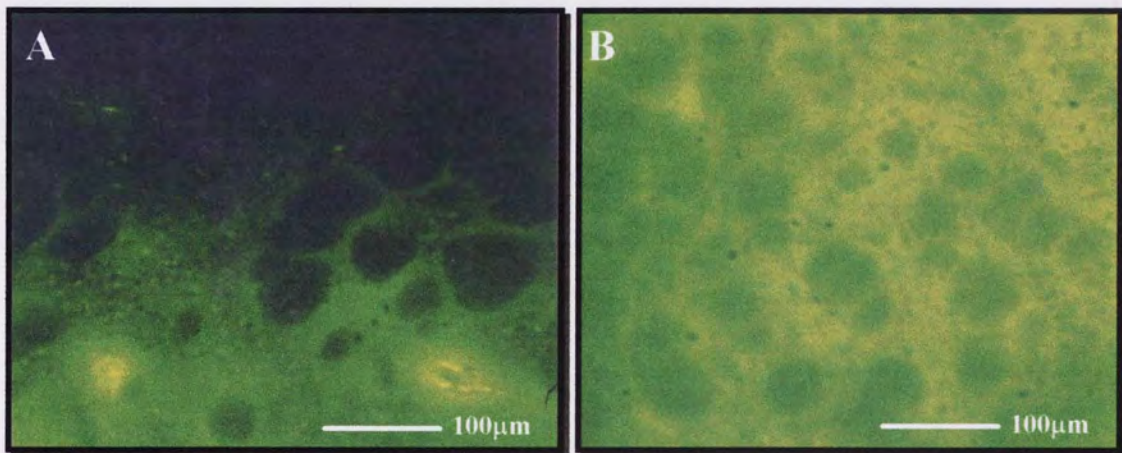


Figure 6.16 Fluorescence photomicrographs of coronal sections of rat brain showing fluorescence signal detected in an area of striatum: (A) 1 day after ICV administration of free FITC-labelled GRAS5 ODN and (B) 5 days after ICV administration of FITC-labelled GRAS5 ODN in polymer-complexed form.

The fluorescent signal of the ODN in the polymer-complexed form 5 days following ICV administration was detected mainly around areas of the lateral ventricle (Figure 6.13), the frontal cortex (Figure 6.17), the hippocampus (Figure 6.18) and the hypothalamus (Figure 6.19). These regions showed a strong fluorescent signal which appeared to be within the cells of these brain regions when viewed under high magnification (Figures 6.17C, 6.18C and 6.19C).

The outer surface of the cerebral hemispheres demonstrated a stronger fluorescent signal than the rest of the cerebral cortex (Figure 6.17A). This probably represented FITC labelled ODNs which had flowed around the brain in the subarachnoid space. The subarachnoid space is continuous with the ventricles and contains cerebro-spinal fluid (CSF), which coats the outer surface of the brain (Sherwood, 1989). The surface of the brain beneath the subarachnoid space is encapsulated by a continuous limiting membrane consisting of glial cells and is termed the pial-glial membrane (Nauta and Feirtag, 1986). Therefore it may be this pial-glial membrane which is favourably associated with the FITC labelled ODNs circulating the outer surface of the brain.

The pattern of the strong fluorescent signal in the hippocampus showed evidence of differential uptake within the different hippocampal cell layers (Figures 6.18A and B), while the even fluorescence observed in the hypothalamic area of the brain (Figures 6.19A and B), which was stronger in signal intensity compared to surrounding areas, again indicates differential cellular uptake of fluorescent ODNs.

Therefore it is apparent that ODNs are almost certainly able to access a wide range of brain areas following ICV administration using a polymer matrix delivery system which enables sustained controlled release of ODNs over the required 5 day treatment period.

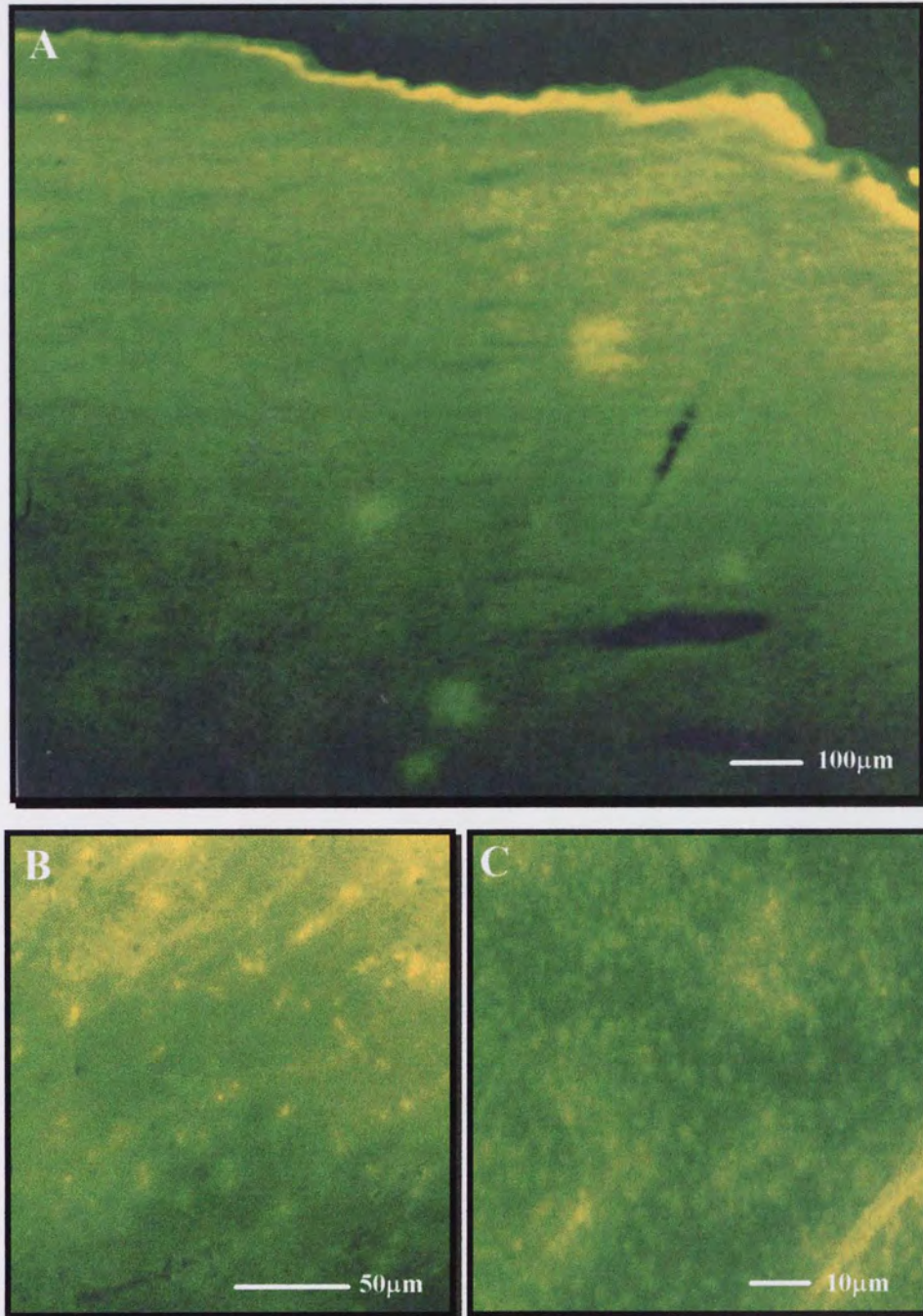


Figure 6.17 Fluorescence photomicrographs of coronal sections of rat brain showing fluorescence signal detected in an area of frontal cortex 5 days after ICV administration of FITC-labelled GRAS5 ODN in polymer complexed form as described in section 2.2.19.2 using a series of increasing level of magnification (A-C).

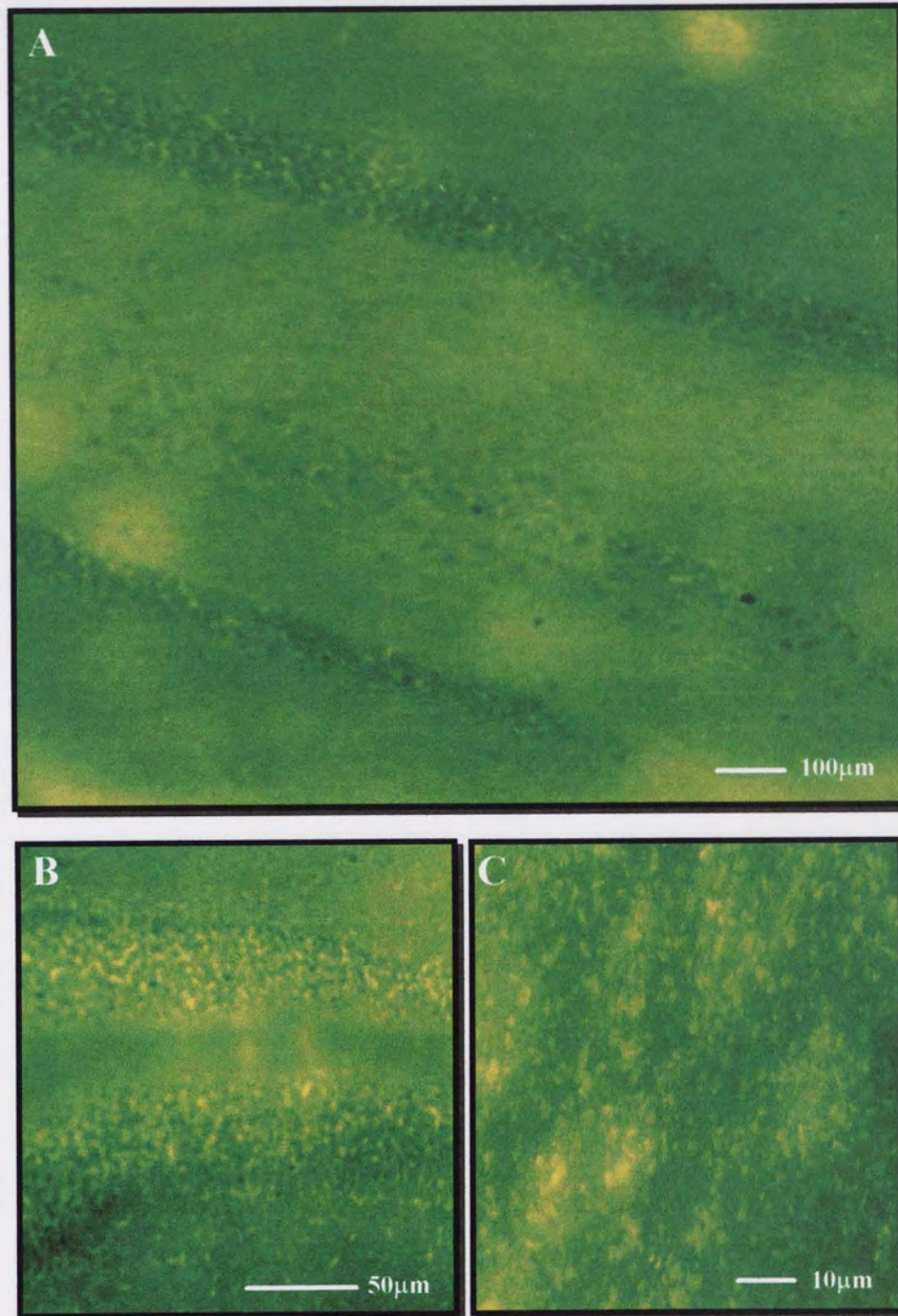


Figure 6.18 Fluorescence photomicrographs of coronal sections of rat brain showing fluorescence signal detected in an area of hippocampus 5 days after ICV administration of FITC-labelled GRAS5 ODN in polymer complexed form as described in section 2.2.19.2 using a series of increasing level of magnification (A-C).

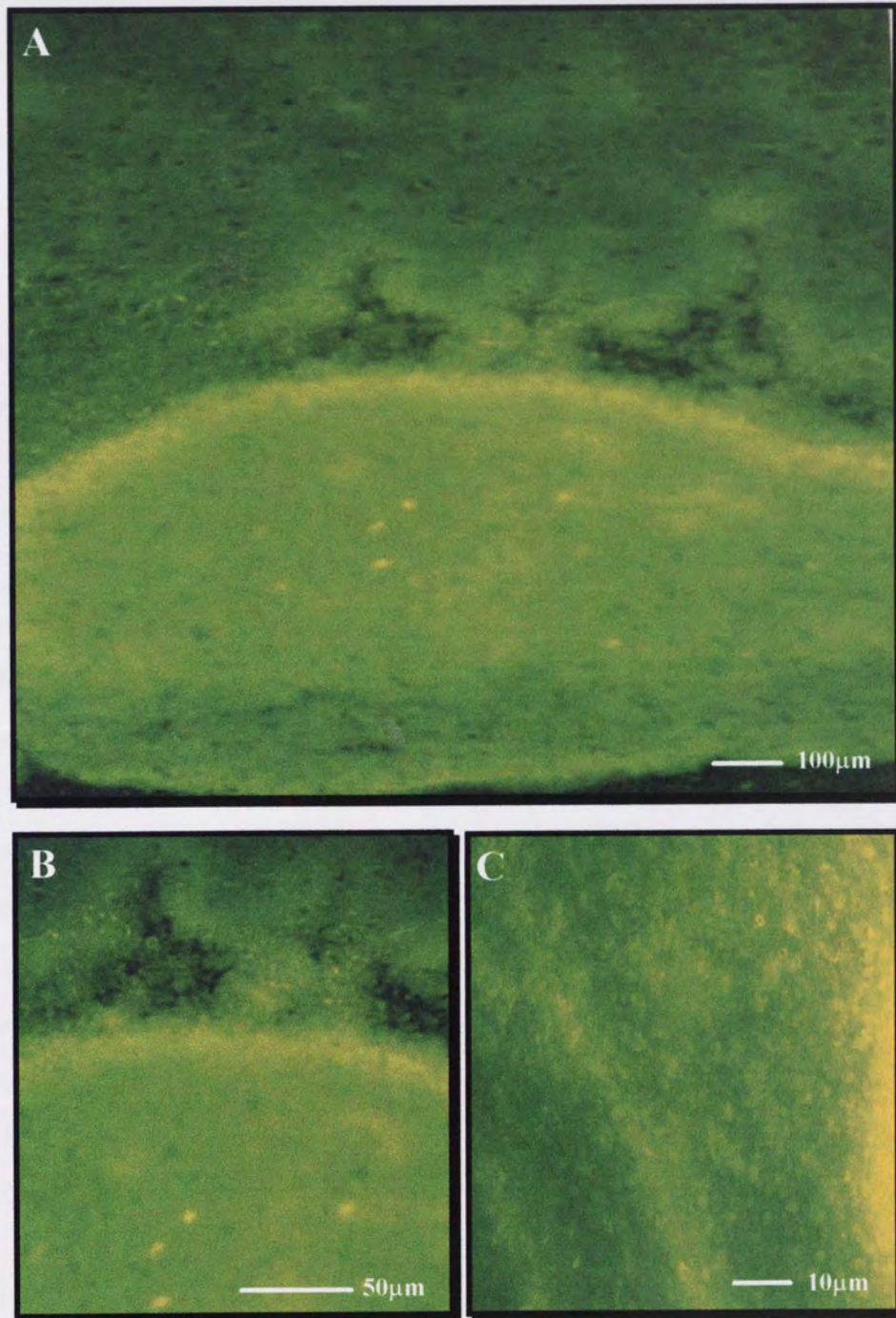


Figure 6.19 Fluorescence photomicrographs of coronal sections of rat brain showing fluorescence signal detected in an area of hypothalamus 5 days after ICV administration of FITC-labelled GRAS5 ODN in polymer complexed form as described in section 2.2.19.2 using a series of increasing level of magnification (A-C).

6.3.3 *In Vivo* Assessment of GRAS5 ODN Treatment.

Following the preliminary studies shown in section 6.3.2, experiments were conducted to study the effects of GRAS5 treatment on GR expression with possible modulation of 5-HT_{2A} expression in selected brain regions and to replicate the *in vitro* findings (Chapter 5) *in vivo*, using treatment groups following an alternating block design in administration. Animal well-being assessments as described in section 2.2.20 were also carried out throughout these experiments to detect possible toxicity of treatment groups and to confirm the findings of the pilot studies (section 6.3.2.1).

6.3.3.1 *In Vivo* Treatment Design and Groups.

In the first set of experiments, rats received a single 2 μ L injection of one of two treatments using an alternating block design: GRAS5 antisense ODN-loaded polymer microspheres (AS) at an estimated dose of 2 μ g/ μ L of ODN per day (0.2mg/ μ L of polymer) or free GRAS5 antisense ODN (FAS) at a single dose of 10 μ g/ μ L. 8 animals per treatment group were used over a 2 day period according to the treatment regime shown in Table 6.2. In the second set of experiments four treatments were used in a 2 μ L injection volume: sham injection (SH), 0.2mg/ μ L of saline-loaded polymer microspheres (PL), 0.2mg/ μ L of GRAS5 antisense ODN-loaded polymer microspheres (AS) or 0.2mg/ μ L of mismatch ODN-loaded polymer microspheres (MM) each at an estimated dose of 2 μ g/ μ L of ODN per day (0.2mg/ μ L of polymer). 8 animals per group were treated over a 4 day period with 8 animals being treated per day according to the treatment regime shown in Table 6.3.

Table 6.2 Two day block design treatment schedule for optimal GRAS5 antisense ODN-loaded polymer microspheres (AS) and free GRAS5 antisense ODN (FAS) administered using single ICV injections as described in section 6.3.3.1. Each animal is only given one treatment with new animals being used on subsequent days.

RAT	1	2	3	4	5	6	7	8
DAY 1	AS	FAS	AS	FAS	AS	FAS	AS	FAS
DAY 2	FAS	AS	FAS	AS	FAS	AS	FAS	AS

Table 6.3 Four day block design treatment schedule for sham injection (SH), saline-loaded polymer microspheres (PL), optimal GRAS5 antisense ODN-loaded polymer microspheres (AS) and mismatch ODN-loaded polymer microspheres (MM) administered using single ICV injections as described in section 6.3.3.1. Each animal is only given one treatment with new animals being used on subsequent days.

RAT	1	2	3	4	5	6	7	8
DAY 1	AS	MM	SH	PL	AS	MM	SH	PL
DAY 2	MM	SH	PL	AS	MM	SH	PL	AS
DAY 3	SH	PL	AS	MM	SH	PL	AS	MM
DAY 4	PL	AS	MM	SH	PL	AS	MM	SH

6.3.3.2 Animal Post-operative Well-being Assessment.

Well-being assessments carried out as described in section 2.2.20 and using a rat behaviour assessment sheet (Table 2.2) showed no differences in the treated animals' behaviour using the following behavioural parameters: locomotion, gait, posture, muscle tone, stereotypy, salivation, cyanosis, and dyspnoea, when compared to normal untreated animals over the treatment period of 5 days, with assessments made at 24 hour intervals. Overall, no animals lost weight over the treatment period and no significant changes were seen in mean daily weights of animals in FAS group compared to AS treatment group in the first set of experiments (Figure 6.20), and in PL, AS and MM groups compared to SH treatment group during the second set of experiments (Figure 6.21). When assessing adrenal gland weights, no significant changes were seen in the FAS treated group compared to AS treatment group (Figure 6.22), while PL, AS and MM treatments produced no significant changes compared to SH treatment 5 days after treatment (Figure 6.23). This suggests that none of the treatment groups produced any noticeable neurotoxic and/or related systemic effects affecting either rat behaviour or HPA axis homeostasis.

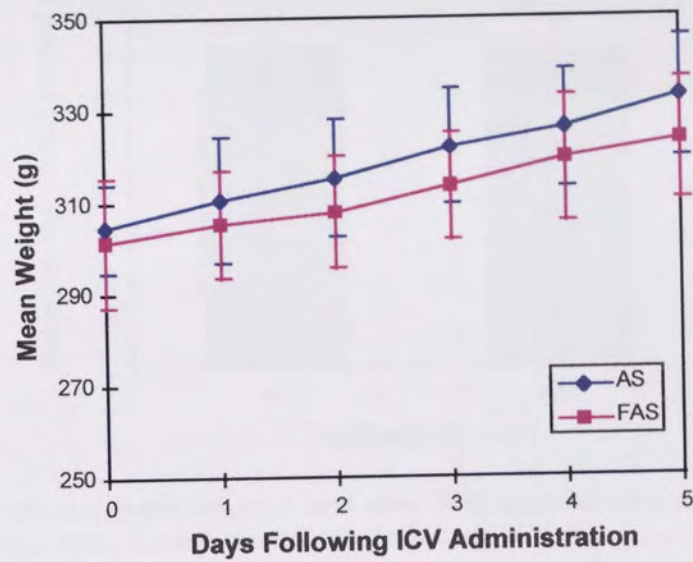


Figure 6.20 Mean body weight measured daily over a 5 day period following ICV administration of AS and FAS treatment groups. Data shown are mean values \pm standard deviation, where $n=8$.

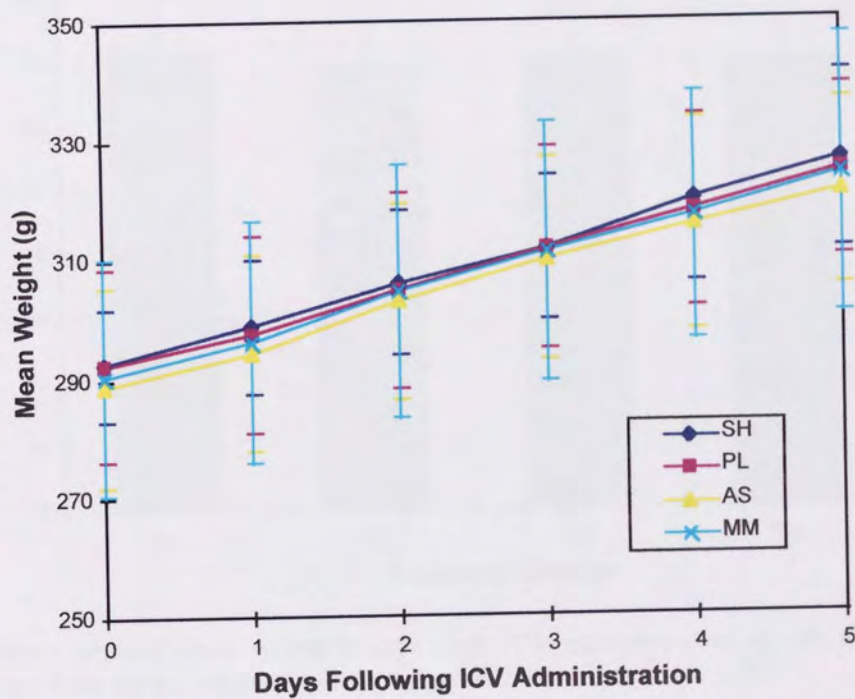


Figure 6.21 Mean body weight measured daily over a 5 day period following ICV administration of SH, PL, AS and MM treatment groups. Data shown are mean values \pm standard deviation, where $n=8$.

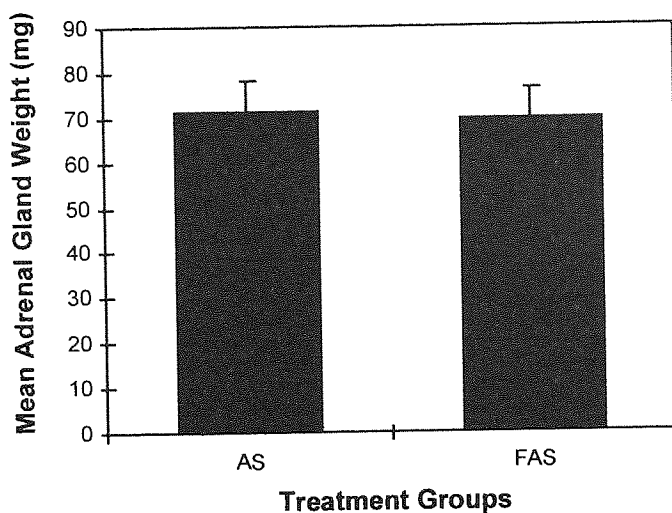


Figure 6.22 Mean adrenal gland weight 5 days after ICV administration of AS and FAS treatment groups. Data shown are mean values \pm standard deviation, where n=8.

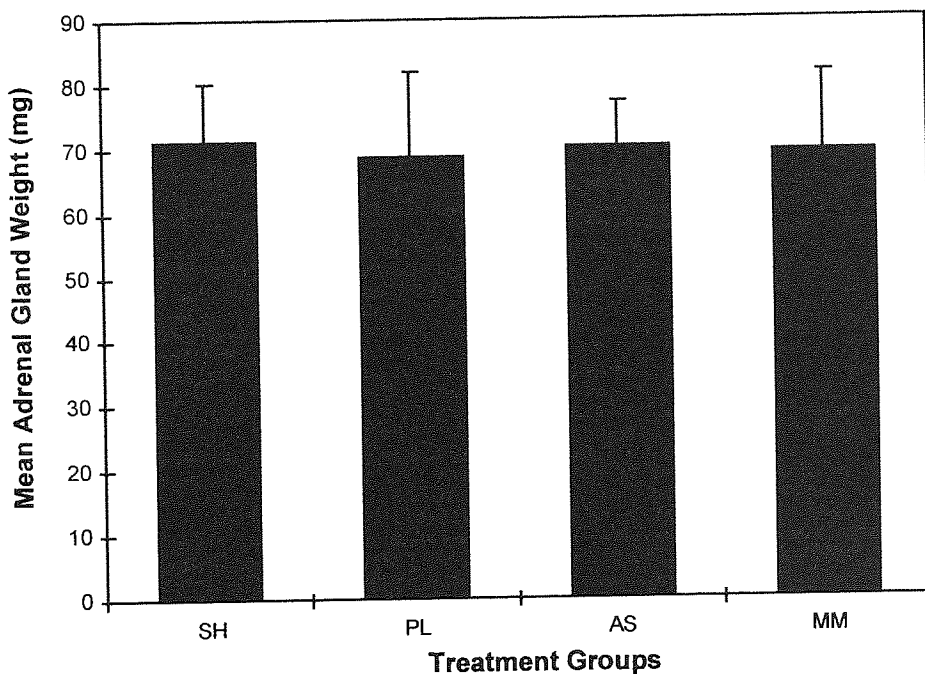


Figure 6.23 Mean adrenal gland weight 5 days after ICV administration of SH, PL, AS and MM treatment groups. Data shown are mean values \pm standard deviation, where n=8.

6.3.3.3 *In Vivo* Assessment of GRAS5 Treatment Using Quantitative RT-PCR.

Male Wistar rats 5 days following ICV administration of treatment groups SH, PL, AS, MM and FAS as described in section 6.3.3.1 had measurement of both GR and 5-HT_{2A} receptor mRNA expression carried out using quantitative RT-PCR as described in sections 2.2.13.4 and 2.2.13.5. GRAS5 treatment administered in the polymer complexed form (AS) significantly ($p < 0.05$) reduced GR mRNA expression by 40% compared to GRAS5 administered in the free form (FAS) in rat hypothalamus (Figure 6.24). Conversely, in the same animals 5-HT_{2A} receptor mRNA expression in rat hypothalamus following AS treatment significantly ($p < 0.05$) increased by 12% compared to FAS treatment (Figure 6.24). This would suggest the efficacy of the GRAS5 antisense ODN in suppressing GR mRNA expression and causing related changes in 5-HT_{2A} receptor mRNA expression was enhanced by ICV administration of GRAS5 using a polymer microsphere delivery system in rat hypothalamus over 5 days *in vivo*.

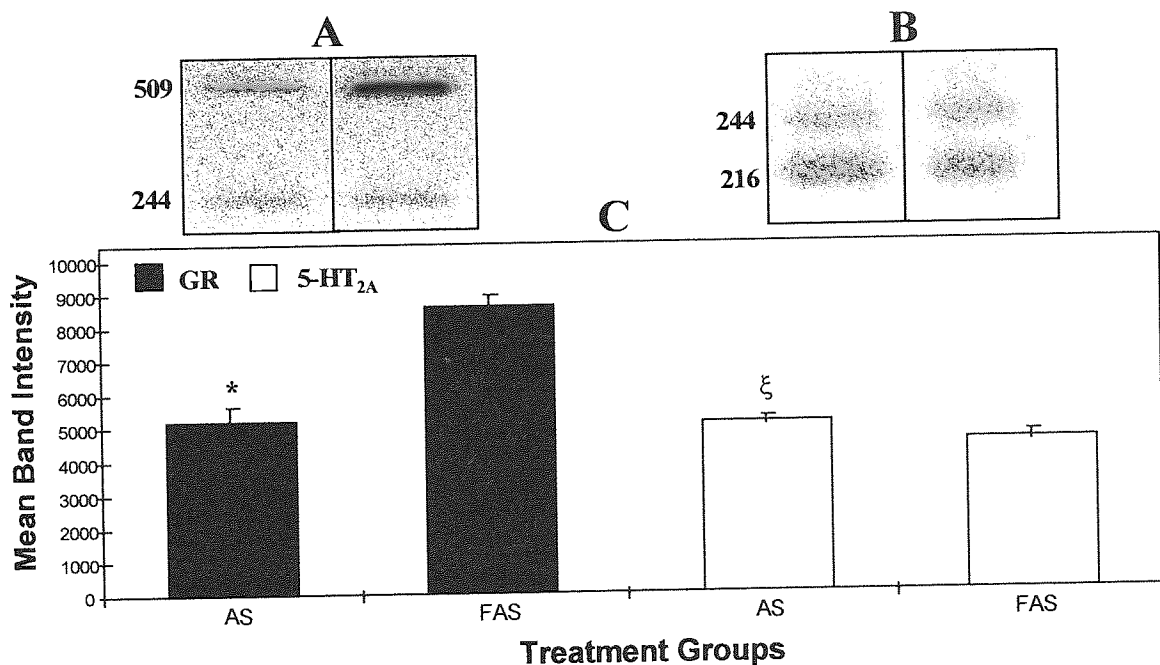


Figure 6.24 Representative gel electrophoresis of RT-PCR products obtained as described in sections 2.2.13.4 and 2.2.13.5. (A) Lanes illustrating GR (509 nucleotides) and control β -actin (244 nucleotides) cDNA product bands corresponding to the respective treatment groups shown on the x-axis of the graph below. (B) Lanes illustrating 5-HT_{2A} receptor (216 nucleotides) and control β -actin (244 nucleotides) cDNA product bands corresponding to the respective treatment groups shown on the x-axis of the graph below. (C) Densitometric analysis of GR and 5-HT_{2A} receptor bands standardised to the mean β -actin band density illustrating the effect of treatment group on the expression of GR (black bars) and 5-HT_{2A} receptor (white bars) mRNA in the hypothalamic region of male Wistar rats. Data shown are mean values \pm standard deviation, where $n=8$ (unpaired t-test, $*p < 0.05$ and $^{\xi}p < 0.05$).

Figures 6.25-6.27 showed the AS treatment group produced significant ($p < 0.05$) reductions in GR mRNA expression in the following rat brain regions: frontal cortex ($F_{3,28} = 45.02$), hippocampus ($F_{3,28} = 69.93$) and hypothalamus ($F_{3,28} = 69.36$) by 26, 35 and 39% respectively compared to sham (SH). Whereas polymer (PL) and mismatch (MM) treatments had negligible effects on GR mRNA expression compared to sham (not significant). In these animals quantitative RT-PCR also showed the AS treatment group to significantly ($p < 0.05$) increase 5-HT_{2A} receptor mRNA density in the rat brain regions of frontal cortex ($F_{3,28} = 28.15$), hippocampus ($F_{3,28} = 16.99$) and hypothalamus ($F_{3,28} = 14.81$) by 13, 7 and 5% respectively compared to sham (Figures 6.25-6.27). Polymer and mismatch treatments had no significant effect compared to sham. This shows GRAS5 antisense ODN when administered ICV using polymer microspheres, suppressed GR mRNA expression in the rat brain regions of frontal cortex, hippocampus and hypothalamus over 5 days *in vivo*. The concomitant increase in 5-HT_{2A} receptor mRNA density in these animals in the same brain regions suggests its expression to be under tonic inhibitory control by GR *in vivo*.

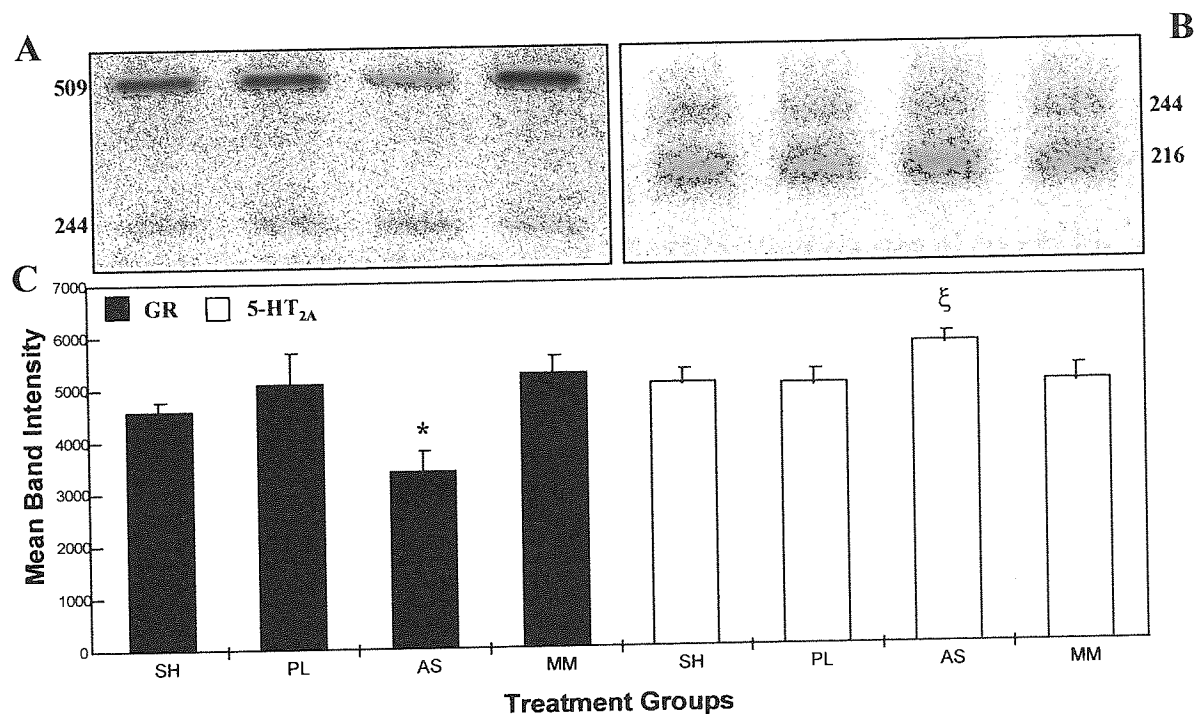


Figure 6.25 Representative gel electrophoresis of RT-PCR products obtained as described in sections 2.2.13.4 and 2.2.13.5. (A) Lanes illustrating GR (509 nucleotides) and control β -actin (244 nucleotides) cDNA product bands corresponding to the respective treatment groups shown on the x-axis of the graph below. (B) Lanes illustrating 5-HT_{2A} receptor (216 nucleotides) and control β -actin (244 nucleotides) cDNA product bands corresponding to the respective treatment groups shown on the x-axis of the graph below. (C) Densitometric analysis of GR and 5-HT_{2A} receptor bands standardised to the mean β -actin band density illustrating the effect of treatment group on the expression of GR (black bars) and 5-HT_{2A} receptor (white bars) mRNA in the frontal cortex region of male Wistar rats. Data shown are mean values \pm standard deviation, where $n=8$ (Tukey-HSD test, $*p < 0.05$ and $^{\xi}p < 0.05$ compared to other groups).

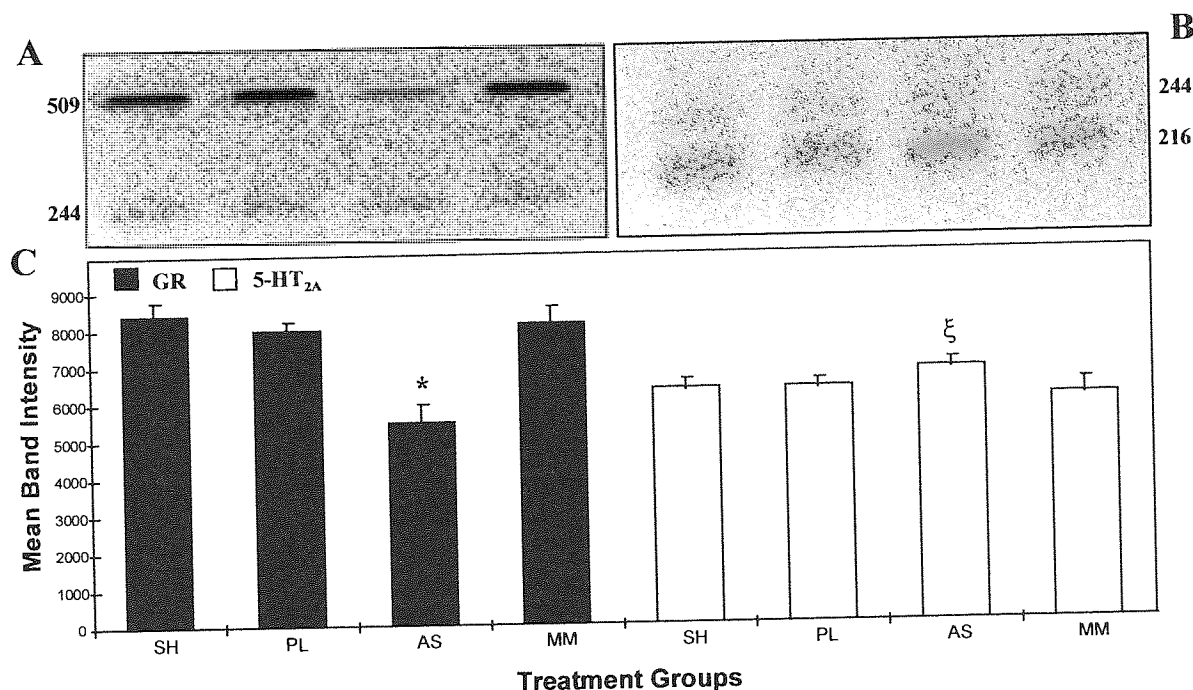


Figure 6.26 Representative gel electrophoresis of RT-PCR products obtained as described in sections 2.2.13.4 and 2.2.13.5. (A) Lanes illustrating GR (509 nucleotides) and control β -actin (244 nucleotides) cDNA product bands corresponding to the respective treatment groups shown on the x-axis of the graph below. (B) Lanes illustrating 5-HT_{2A} receptor (216 nucleotides) and control β -actin (244 nucleotides) cDNA product bands corresponding to the respective treatment groups shown on the x-axis of the graph below. (C) Densitometric analysis of GR and 5-HT_{2A} receptor bands standardised to the mean β -actin band density illustrating the effect of treatment group on the expression of GR (black bars) and 5-HT_{2A} receptor (white bars) mRNA in the hippocampal region of male Wistar rats. Data shown are mean values \pm standard deviation, where n=8 (Tukey-HSD test, *p<0.05 and ^ξp<0.05 compared to other groups).

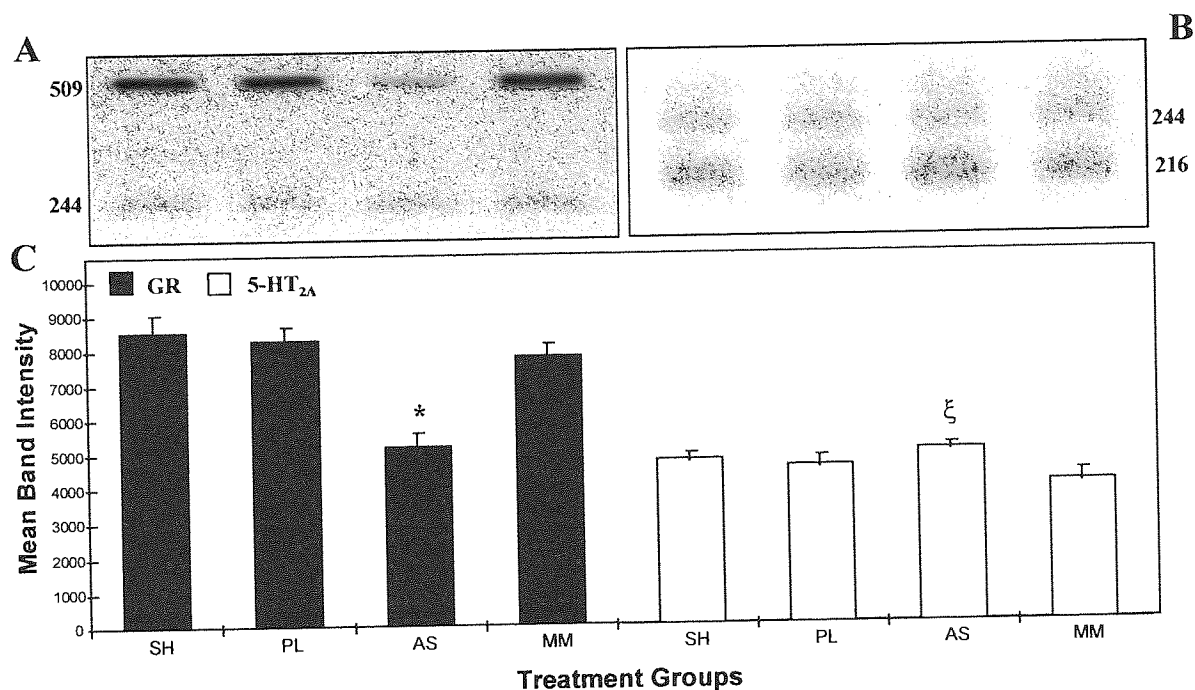


Figure 6.27 Representative gel electrophoresis of RT-PCR products obtained as described in sections 2.2.13.4 and 2.2.13.5. (A) Lanes illustrating GR (509 nucleotides) and control β -actin (244 nucleotides) cDNA product bands corresponding to the respective treatment groups shown on the x-axis of the graph below. (B) Lanes illustrating 5-HT_{2A} receptor (216 nucleotides) and control β -actin (244 nucleotides) cDNA product bands corresponding to the respective treatment groups shown on the x-axis of the graph below. (C) Densitometric analysis of GR and 5-HT_{2A} receptor bands standardised to the mean β -actin band density illustrating the effect of treatment group on the expression of GR (black bars) and 5-HT_{2A} receptor (white bars) mRNA in the hypothalamic region of male Wistar rats. Data shown are mean values \pm standard deviation, where $n=8$ (Tukey-HSD test, * $p<0.05$ and $\xi p<0.05$ compared to other groups).

6.3.3.4 *In Vivo* Assessment of GRAS5 Treatment Using Radioligand Binding Assays.

Male Wistar rats 5 days following ICV administration of either AS or FAS were tested for GR protein expression using a radioligand binding assay as described in sections 2.2.10.2, 2.2.10.4 and 2.2.10.5. GR binding was significantly ($p < 0.05$) reduced by 76% following GRAS5 treatment administered in the polymer complexed form (AS) compared to GRAS5 administered in the free form (FAS) in rat hypothalamus (Figure 6.28). This further confirms the efficacy of the GRAS5 antisense ODN in suppressing GR expression was enhanced by ICV administration of GRAS5 using a polymer microsphere delivery system. No measurements of 5-HT_{2A} receptor binding was possible in the hypothalamus of these animals due to the amount of tissue required to determine the 5-HT_{2A} Bmax.

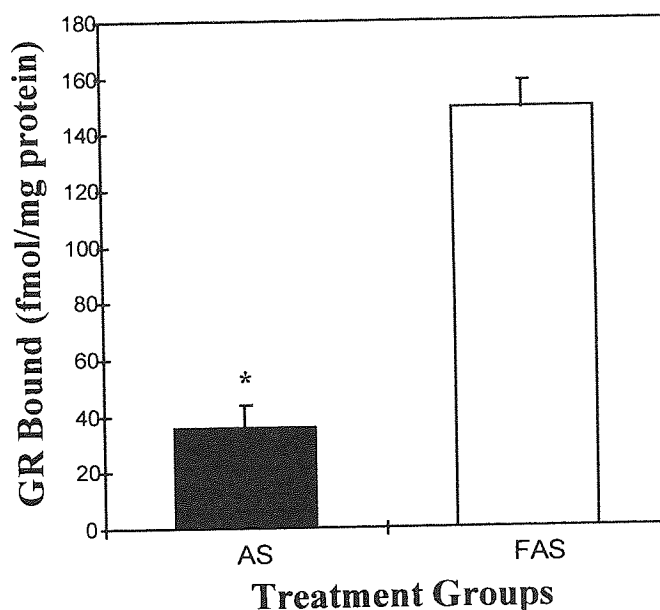


Figure 6.28 GR binding in hypothalamic region of male Wistar rats 5 days after ICV administration of AS (black bars) and FAS (white bars) treatment groups. Data shown are mean values \pm standard deviation, where $n=8$ (unpaired t-test, $*p < 0.05$).

In the second experiment, male Wistar rats after 5 days treatment with SH, PL, AS or MM, had both GR and 5-HT_{2A} receptor protein expression in frontal cortex and hippocampus determined by radioligand binding, with effects on expression of GR alone determined in the hypothalamus. AS treatment significantly ($F_{3,28}=97.55$, $p < 0.05$) reduced GR binding in rat frontal cortex by 67% compared to sham (Figure 6.29), whereas polymer and mismatch treatments had no significant effect. In the same animals, 5-HT_{2A} receptor density significantly ($F_{3,28}=14.39$, $p < 0.05$) increased by 21% compared with sham (Figure 6.29). Polymer and

mismatch treatments again produced no significant effects compared to sham. This showed the GRAS5 antisense sequence to significantly inhibit GR expression in rat frontal cortex over 5 days *in vivo* and also indicates the existence of tonic inhibitory control of 5-HT_{2A} receptors by GR *in vivo* due to the increase in 5-HT_{2A} receptor density seen with GRAS5 treatment.

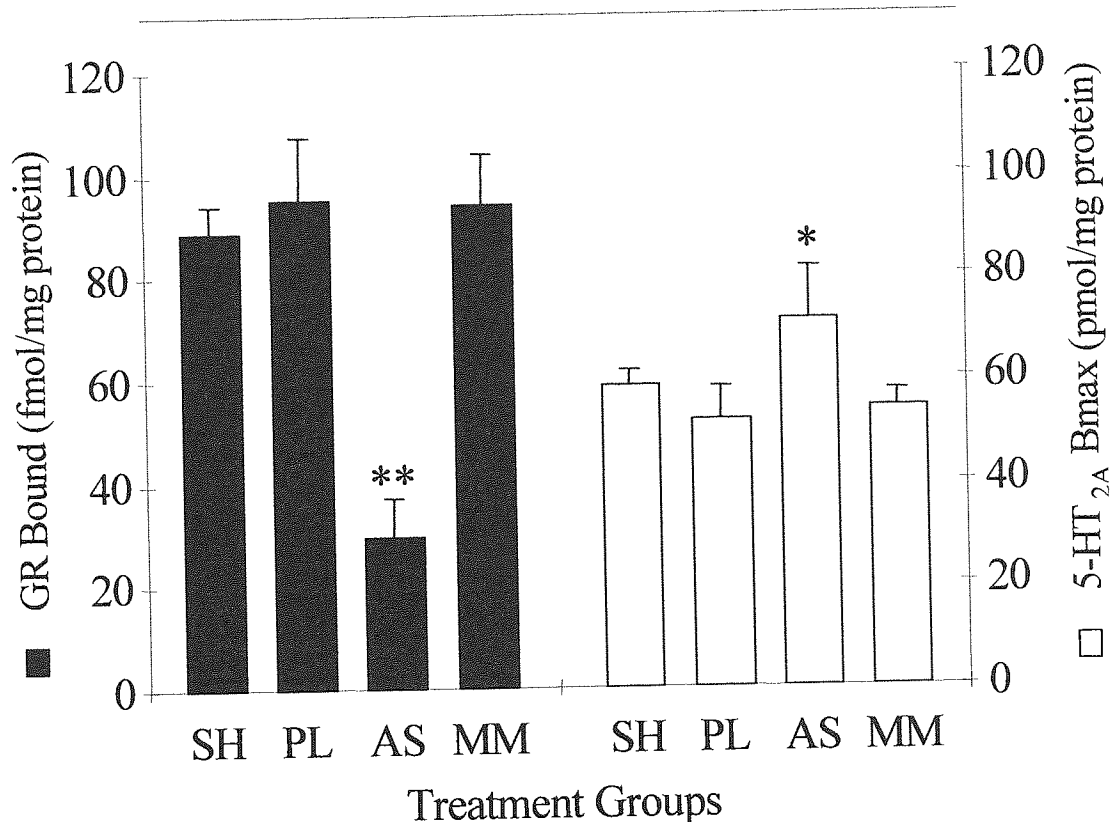


Figure 6.29 GR (black bars) and 5-HT_{2A} receptor (white bars) binding in frontal cortex of male Wistar rats as described in section 2.2.10.2 and 2.2.10.5 respectively, 5 days following ICV administration of SH, PL, AS or MM treatment groups. Data shown are mean values \pm standard deviation, where $n=8$ (Tukey-HSD test, * $p<0.05$ and ** $p<0.05$ compared to other groups).

In the hippocampus (Figure 6.30) AS treatment produced a significant ($F_{3,28}=398.45$, $p<0.05$) 69% reduction in GR binding compared to sham while a significant ($F_{3,28}=407.72$, $p<0.05$) 75% reduction in GR binding compared to sham is shown in the hypothalamus (Figure 6.31). No significant increase in 5-HT_{2A} receptor density was shown in the hippocampus (Figure 6.30) following AS treatment compared to sham, although this would be due to the fact that in this experiment the n number was halved ($n=4$) as a result of pooling tissue samples together to carry out the binding analysis. Polymer and mismatch treatments in these animals produced no significant effects compared to sham (Figures 6.30 and 6.31). As before, no measurements in 5-HT_{2A} receptor binding was made for the hypothalamic region due to the unavailability of sufficient amounts of appropriate tissue samples for the binding procedure.

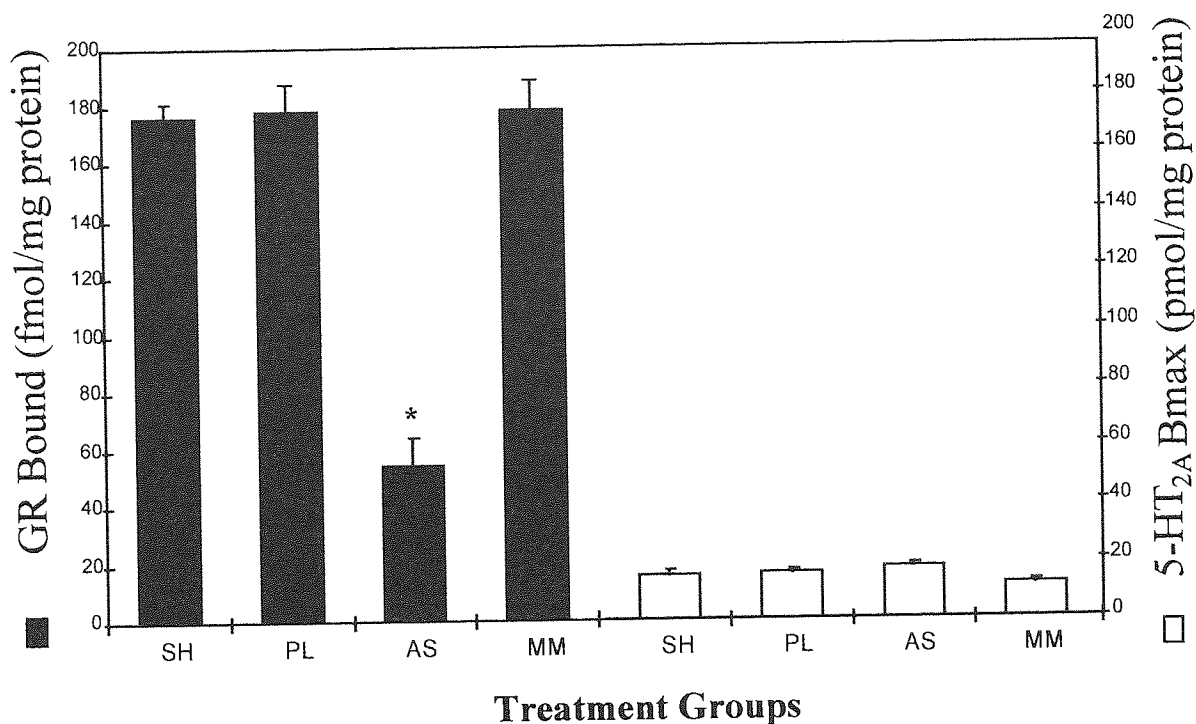


Figure 6.30 GR (black bars) and 5-HT_{2A} receptor (white bars) binding in hippocampi of male Wistar rats as described in section 2.2.10.2 and 2.2.10.5 respectively 5 days following ICV administration of SH, PL, AS or MM treatment groups. Data shown are mean values \pm standard deviation for GR binding, where $n=8$ and data shown are mean values \pm standard deviation for 5-HT_{2A} receptor binding, where $n=4$ (Tukey-HSD test, $*p<0.05$ compared to other groups).

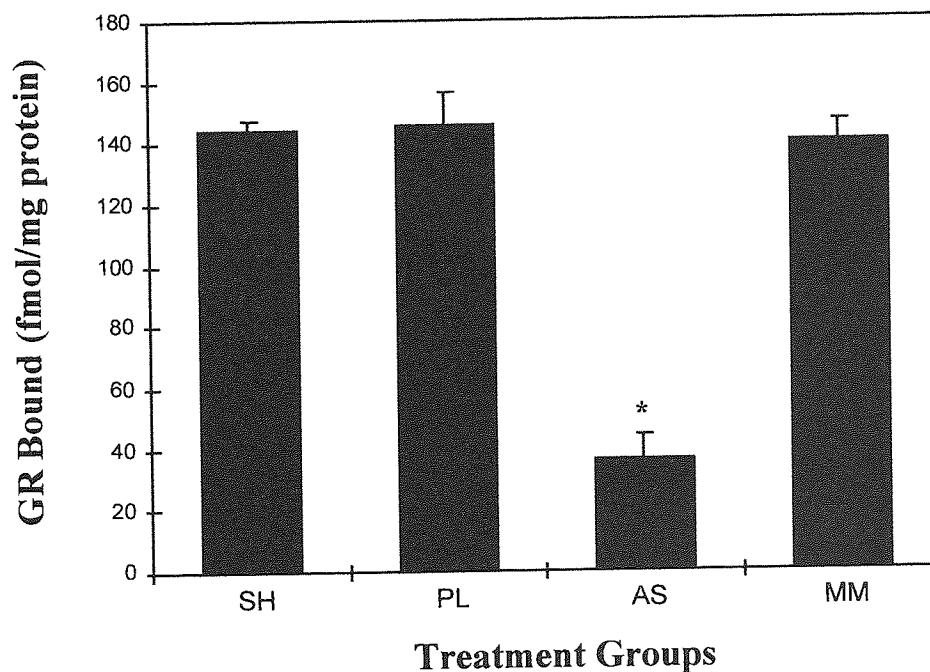


Figure 6.31 GR binding in the hypothalami of male Wistar rats as described in section 2.2.10.2 5 days following ICV administration of SH, PL, AS or MM treatment groups. Data shown are mean values \pm standard deviation, where $n=8$ (Tukey-HSD test, $*p<0.05$ compared to other groups).

6.3.4. Functional Consequences of GRAS5 ODN Treatment Assessed by Behavioural Observations.

The findings in section 6.3.3 have shown that GRAS5 is a suitable biological tool to knockdown GR expression in the CNS bringing about parallel GR-modulated upregulation in 5-HT_{2A} receptor expression. To establish the functional significance of this GR-mediated modulatory action upon 5-HT_{2A} expression, behavioural observations were made following administration of the 5-HT_{2A/2C} receptor specific agonist DOI (Glennon *et al*, 1986) to ODN-treated animals as described in section 2.2.21. Head-shakes and wet-dog shakes occur in rodents following administration of agents which increase 5-HT activity, and have been shown to be due to activation of 5-HT_{2A} receptors (Kennett and Curzon, 1991). The head-shake response in rats using DOI is a well-recognised behavioural response to 5-HT_{2A} receptor specific stimulation (Lucki *et al*, 1984), and in this present study was used to make direct functional correlation to any changes in the density of 5-HT_{2A} receptor expression brought about by GRAS5 treatment.

To make this functional analysis of GRAS5 treatment a third set of *in vivo* experiments were carried out using the treatment groups: SH, PL, AS and MM and following the experimental treatment design as described in section 6.3.3.1 and illustrated in Table 6.3, with appropriate well-being assessments also made (section 2.2.20). Due to the limited availability of brain tissue obtained from the first two sets of *in vivo* experiments, tissue samples from this experiment following DOI treatment were used to carry out the radioligand binding assay for analysis of GR in the hypothalamus (Figure 6.31) and Western blot analysis of GRAS5 treatment both in the hippocampus (Figure 6.35) and hypothalamus (Figure 6.36). This was done to provide further confirmation of the ability of GRAS5 to knockdown GR expression *in vivo* and also provide a means of comparing data obtained on GR expression using tissue samples from animals which were and were not subjected to DOI treatment. As DOI is a direct 5-HT_{2A/2C} receptor agonist (Glennon *et al*, 1986) and due to its short exposure to the animals (section 2.2.21), it is highly unlikely that DOI treatment would interfere with assays analysing GR expression, though the presence of DOI does interfere with 5-HT_{2A} binding (Kettle *et al*, 1999).

6.3.4.1 Animal Post-operative Well-being Assessment.

Well-being assessments carried out as described in section 2.2.20 for the animals in the third set of *in vivo* experiments again showed no deviation in the treated animals behaviour compared to normal untreated animals over the treatment period of 5 days. No significant changes were seen to daily weights of animals in PL, AS and MM groups compared to SH treatment group (Figure 6.32). Also no significant changes were seen in adrenal gland weights of PL, AS and MM treatments compared to SH treatment group (Figure 6.33). This further confirmed the findings presented in section 6.3.3.2 and suggested that no neurotoxic and/or related systemic effects affecting both rat behaviour and HPA axis homeostasis were present as a result of treatment with PL, AS and MM treatment groups in this study.

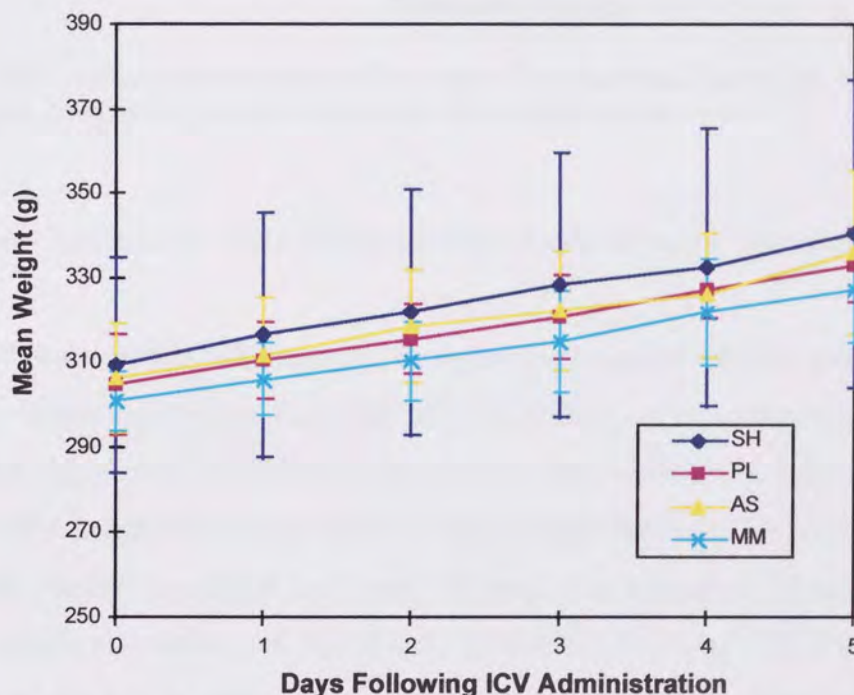


Figure 6.32 Mean body weight measured daily over a 5 day period following ICV administration of SH, PL, AS and MM treatment groups. Data shown are mean values \pm standard deviation, where $n=8$.

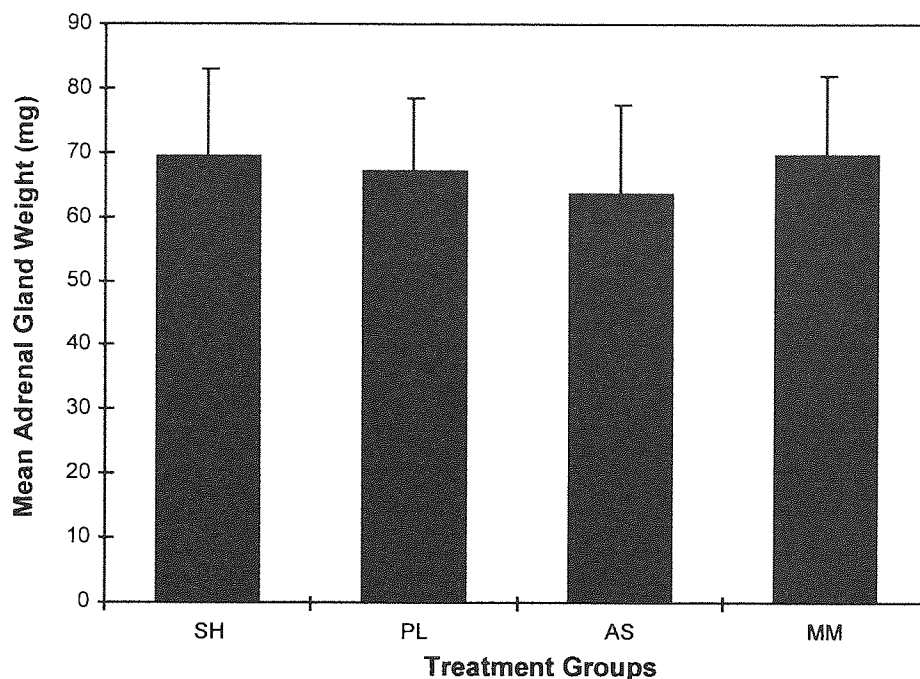


Figure 6.33 Mean adrenal gland weight 5 days after ICV administration of SH, PL, AS and MM treatment groups. Data shown are mean values \pm standard deviation, where $n=8$.

6.3.4.2 *In Vivo* Assessment of GRAS5 Treatment Using Western Blot Analysis.

To assess further the level of inhibition of GR expression using the GRAS5 antisense sequence *in vivo*, male Wistar rats 5 days following ICV administration of treatment groups AS and FAS in the first experiment, and 5 days following ICV administration of treatment groups SH, PL, AS, and MM in the second experiment as described in section 6.3.3.1, had measurement of GR protein expression carried out using Western blot analysis as described in section 2.2.11. GR protein expression was significantly ($p<0.05$) reduced by 77% following GRAS5 treatment administered in the polymer complexed form (AS) compared to GRAS5 administered in the free form (FAS) in rat hypothalamus (Figure 6.34). This again confirms the enhancement of GRAS5 inhibition of GR protein expression in rat hypothalamus over 5 days *in vivo* when administered as a polymer microsphere formulation as opposed to GRAS5 administration in the free form as was demonstrated previously by both quantitative RT-PCR (Figure 6.24) and radioligand binding assay (Figure 6.28).

AS treatment produced a significant ($F_{3,28}=909.88$, $p<0.05$) 76% reduction in GR protein expression compared to sham whereas no significant changes were seen with polymer and mismatch treatments compared to sham in rat hippocampus over 5 days (Figure 6.35). Likewise AS treatment produced a significant ($F_{3,28}=913.08$, $p<0.05$) 80% reduction in GR protein expression compared to sham in rat hypothalamus over 5 days (Figure 6.36). Polymer and mismatch treatments produced no significant effect on GR protein expression compared to sham. This provides further evidence in the ability of the GRAS5 antisense sequence to suppress GR expression over 5 days *in vivo* and is supported by the data obtained using both quantitative RT-PCR (section 6.3.3.3) and radioligand binding assay (section 6.3.3.4).

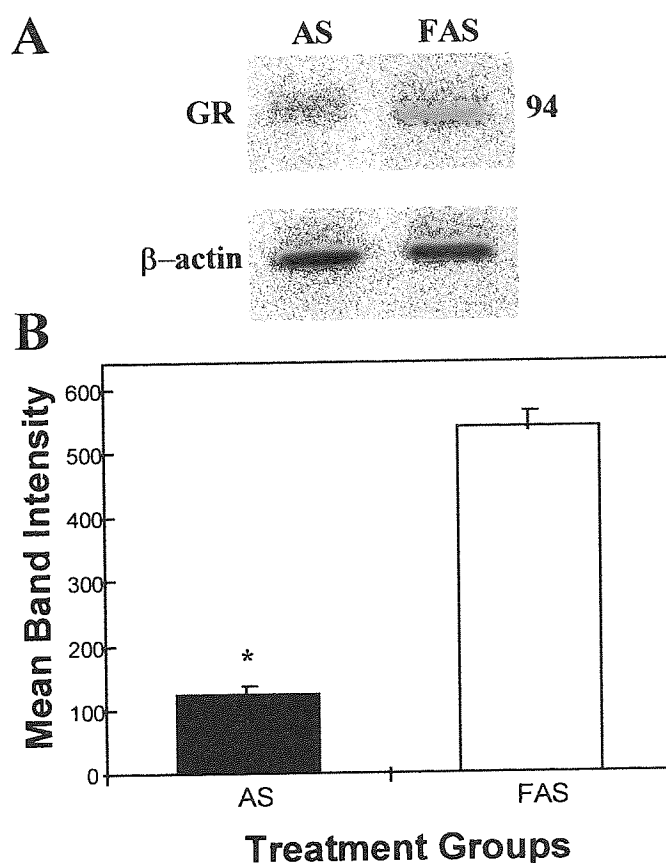


Figure 6.34 Effects of treatment groups on GR protein expression measured by Western blot analysis as described in section 2.2.11 in hypothalamic region of male Wistar rats. (A) Representative Western blot illustrating GR (94 kDa) and control β -actin protein levels in AS and FAS treatment group animals 5 days following ICV administration. (B) Densitometric analysis of GR bands standardised to the mean β -actin band density illustrating the effect of treatment group on the expression of GR protein. Data shown are mean values \pm standard deviation, where $n=8$ (unpaired t-test, $*p<0.05$).

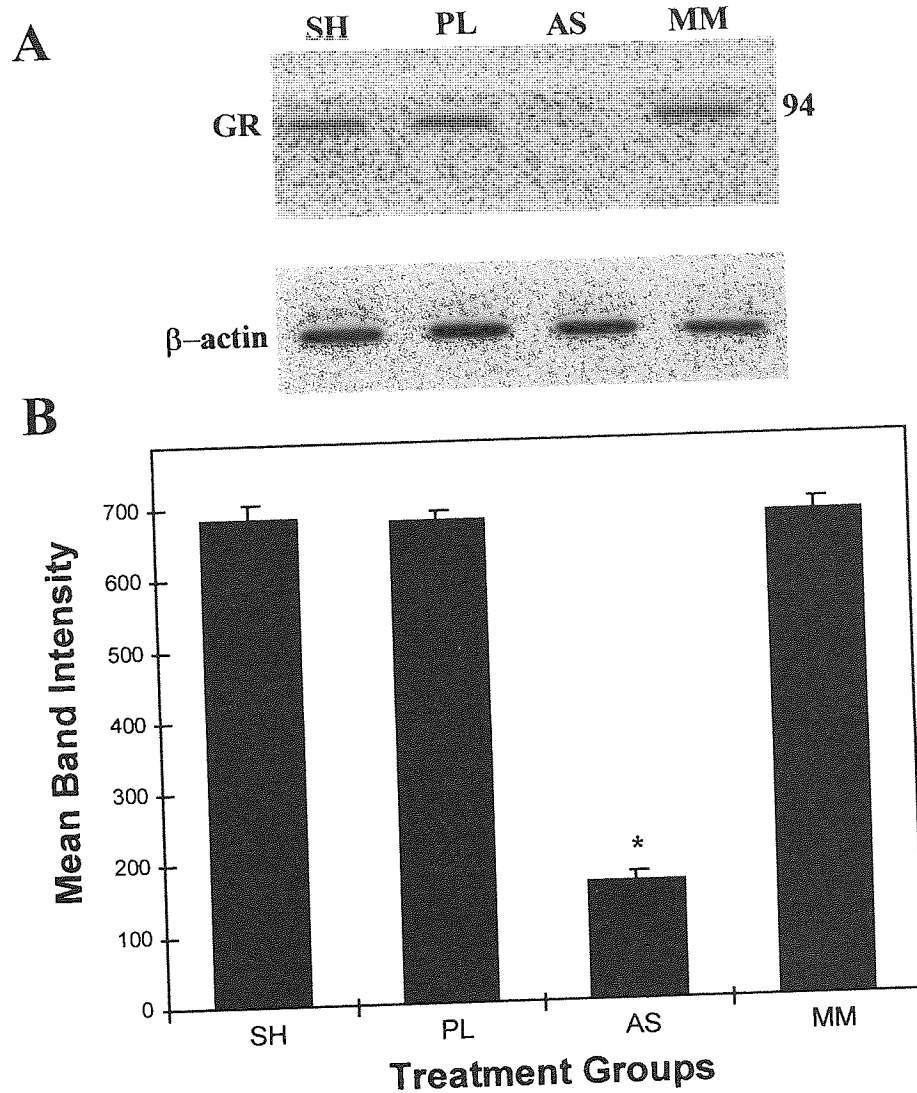


Figure 6.35 Effects of treatment groups on GR protein expression measured by Western blot analysis as described in section 2.2.11 in hippocampal region of male Wistar rats. (A) Representative Western blot illustrating GR (94 kDa) and control β -actin protein levels in SH, PL, AS and MM treatment group animals 5 days following ICV administration. (B) Densitometric analysis of GR bands standardised to the mean β -actin band density illustrating the effect of treatment group on the expression of GR protein. Data shown are mean values \pm standard deviation, where $n=8$ (Tukey-HSD test, $*p<0.05$ compared to other groups).

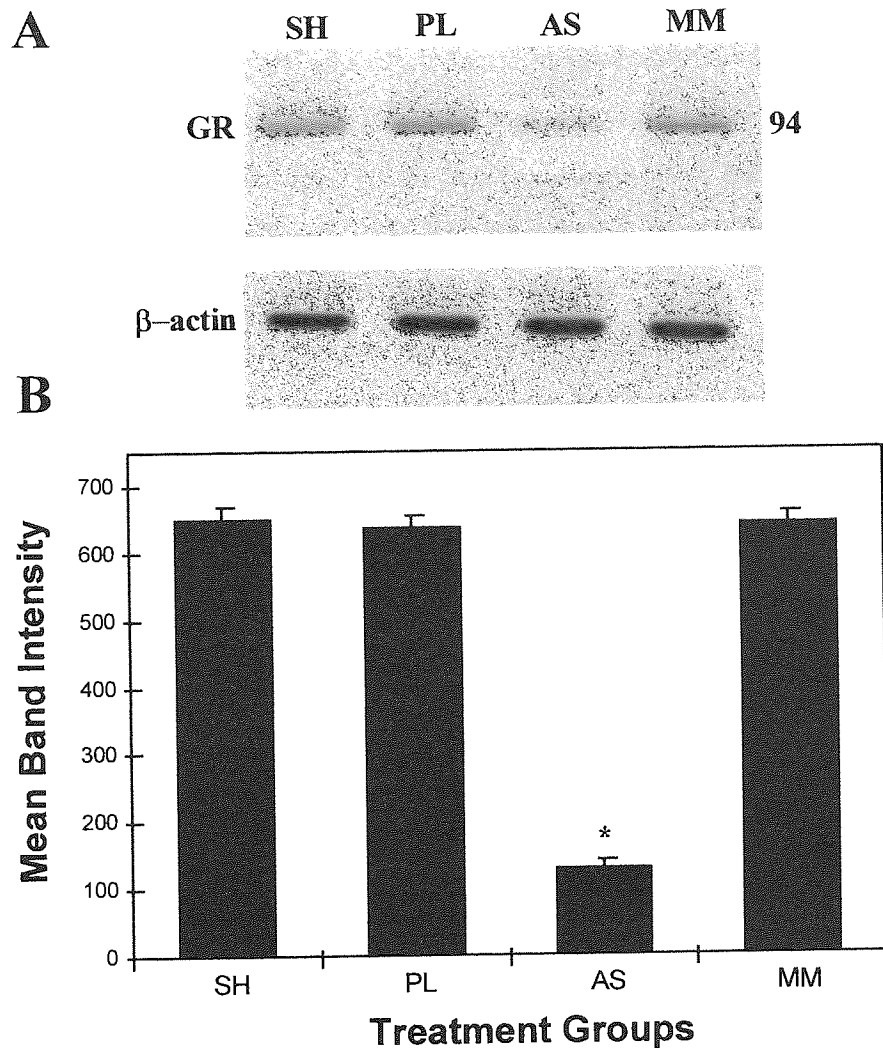


Figure 6.36 Effects of treatment groups on GR protein expression measured by Western blot analysis as described in section 2.2.11 in hypothalamic region of male Wistar rats. (A) Representative Western blot illustrating GR (94 kDa) and control β -actin protein levels in SH, PL, AS and MM treatment group animals 5 days following ICV administration. (B) Densitometric analysis of GR bands standardised to the mean β -actin band density illustrating the effect of treatment group on the expression of GR protein. Data shown are mean values \pm standard deviation, where $n=8$ (Tukey-HSD test, $*p<0.05$ compared to other groups).

6.3.4.3 DOI Induced Rat Head-Shake Observations.

Since GRAS5 treatment ICV increases 5-HT_{2A} expression, the expectation is that it will also increase the frequency of DOI induced head-shakes. Therefore, preliminary studies were conducted in order to optimise the dose of DOI and to select an appropriate time interval which gave a sub-maximal number of DOI induced head-shakes suitable for making head-shake measurements in treated animals. This involved administering DOI at a dose range of 0.3 to 3mg/Kg to male Wistar rats (n=3 per treatment) and making DOI-head-shake observations as described in section 2.2.21 over 60 minutes using 5 minute time-bins. The results showed that a DOI dose of 0.6mg/kg at time-bin +10-20 minutes following DOI administration produced the most suitable non-saturated plateau of head-shakes appropriate for analysing the behavioural response to GRAS5 treatment (Figure 6.37).

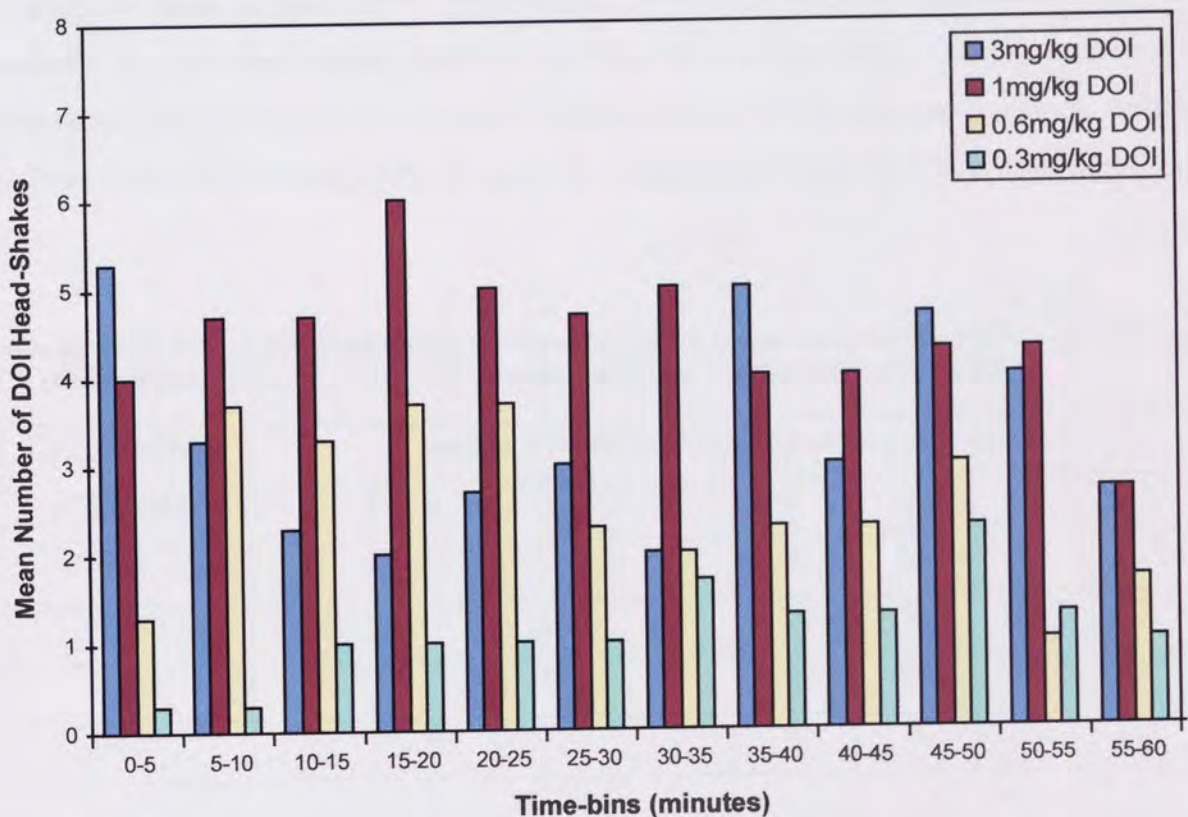


Figure 6.37 Effect of DOI at varying dose (0.3-3mg/kg) on the number of DOI-head-shakes measured at 5 minute intervals over a total 60 minute post-treatment period. Data shown are mean values, where n=3.

Following preliminary head-shake studies, male Wistar rats 5 days after ICV administration of treatment groups SH, PL, AS and MM as described in section 6.3.3.1, were treated with DOI (0.6mg/kg in 0.5mL, ip) before head-shake observations were conducted as described in section 2.2.21. DOI-head-shake data (Table 6.4) were analysed using the non-parametric Kruskal-Wallis ANOVA test ($p < 0.02$) which is valid for this data since it is a distribution-free test. However, no significant difference was seen in any of the treatment groups compared to the sham (SH) group (Figure 6.38). On further analysis of the raw data (Table 6.4) it was apparent that one of the animals in the AS group showing no headshakes, and a similar animal in the PL group, could be excluded on the behavioural evidence that DOI had failed to elicit headshakes, most likely due to a misplaced ip injection. On exclusion of these values, the data showed AS treatment significantly ($p < 0.01$) increased head-shakes by 55.3% compared to sham, whereas polymer (PL) and mismatch (MM) treatments produced no significant effects compared to sham (Figure 6.39). This increase in 5-HT_{2A} receptor functional activity, as measured by DOI-head-shakes, together with the increase in 5-HT_{2A} receptor expression shown previously (sections 6.3.3.3 and 6.3.3.4) following GRAS5 antisense treatment, further confirms CNS 5-HT_{2A} receptors to be under tonic inhibitory control by GR *in vivo* as well as *in vitro*.

Table 6.4 Raw data of DOI-head-shakes measured at +10-20 minute time-bin (section 2.2.21) following ICV administration of SH, PL, AS and MM treatment groups as described in section 6.3.3.1.

TREATMENT GROUPS	Number of DOI-Head-Shakes/10 minutes per Animal							
	a	b	c	d	e	f	g	h
SH	14	14	2	10	8	11	11	12
PL	10	17	11	0	15	2	13	8
AS	17	17	15	15	18	12	0	18
MM	13	10	13	2	4	6	18	5

Table 6.5 summarises the findings of the *in vivo* antisense studies in terms of the three main experiments carried out as described in sections 6.3.3.1 and 6.3.4.

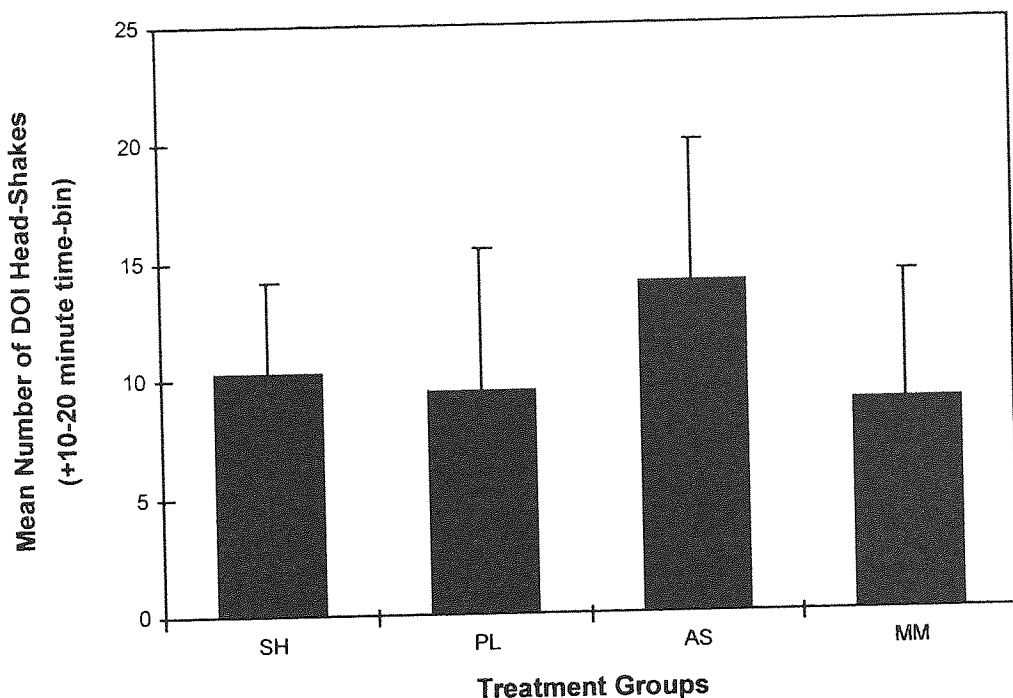


Figure 6.38 Effect of SH, PL, AS and MM treatment groups on DOI-induced head-shake frequency measured at +10-20 minute time bin as described in section 2.2.21. Data shown are mean values \pm standard deviation, where $n=8$, with all data included.

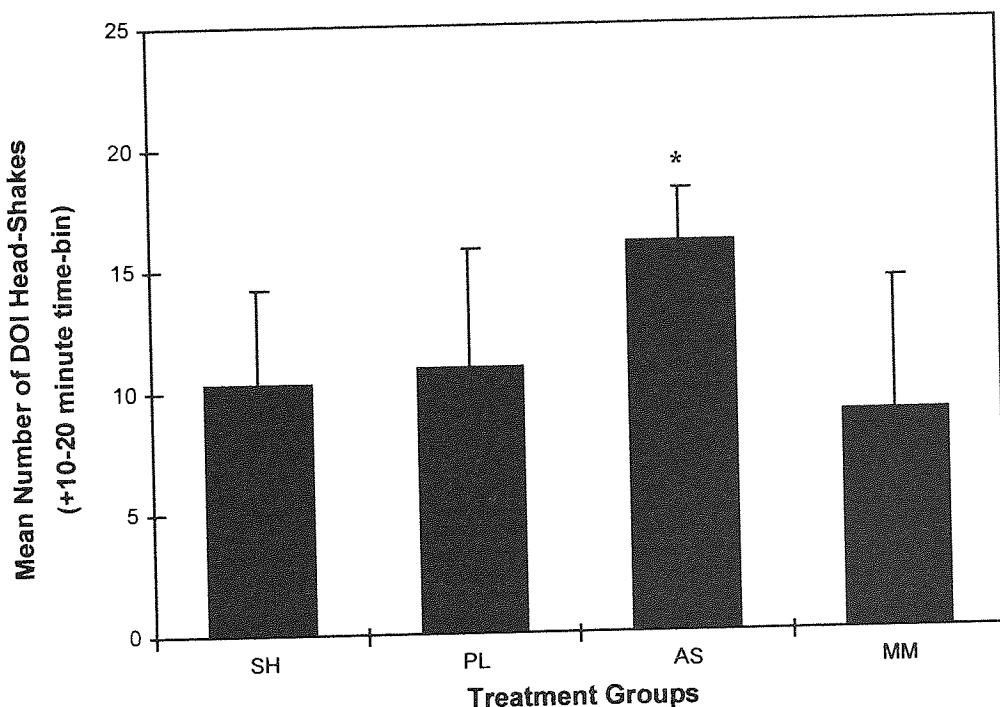


Figure 6.39 Effect of SH, PL, AS and MM treatment groups on DOI-induced head-shake frequency measured at +10-20 minute time bin as described in section 2.2.21. Data shown are mean values \pm standard deviation, omitting the apparently mis-dosed animals, where $n=8$ for SH and MM, and $n=7$ for AS and PL (Kruskal-Wallis ANOVA, $*p<0.05$ compared to other groups).

Table 6.5 Summary of the *in vivo* antisense experiments and the parameters determined in each experiment. Abbreviations: AS, GRAS5 antisense ODN in polymer microspheres; FAS, free GRAS5 antisense (without polymer microspheres); SH, sham injection; PL, saline-loaded polymer microspheres; MM, GRAS5 mismatch ODN in polymer microspheres; FC, frontal cortex; Hipp, hippocampus; Hypo, hypothalamus; NS, no significant effect; n.d., not determined. For all experiments, n=8 unless otherwise noted. All animals in Experiment 3 were treated with DOI (0.6mg/kg i.p.) and headshakes counted 10-20 minutes after treatment; animals were then killed and tissues collected within 60 minutes of DOI treatment. Thus, DOI was present in the tissues when collected for analysis, but was not expected to interfere with GR binding or western blot analysis.

Expt.	Group	GR mRNA (PCR band intensity)	5-HT _{2A} mRNA (PCR band intensity)	GR protein (Binding, % GR bound)	5-HT _{2A} protein (Binding, Bmax)
1	AS FAS	AS ↓40%* vs FAS in Hypo	AS ↑12%* vs FAS in Hypo	AS ↓76%* vs FAS in Hypo	
2	SH PL AS MM	AS ↓26%* vs SH in FC AS ↓35%* vs SH in Hipp AS ↓39%* vs SH in Hypo All other groups: NS	AS ↑13%* vs SH in FC AS ↑7%* vs SH in Hipp AS ↑5%* vs SH in Hypo All other groups: NS	AS ↓67%* vs SH in FC AS ↓69%* vs SH in Hipp All other groups: NS	AS ↑21%* vs SH in FC AS ≈ SH in Hipp (n=4) All other groups: NS
3	SH PL AS MM			AS ↓75%* vs SH in Hypo All other groups: NS	5-HT _{2A} binding in Hypo: n.d.

Table 6.5 continued.

Expt.	Group	GR protein (western band intensity)	5-HT _{2A} function (DOI headshakes)
1	AS FAS	AS ↓77%* vs FAS in Hypo	
2	SH PL AS MM		
3	SH PL AS MM	AS ↓76%* vs SH in Hipp AS ↓80%* vs SH in Hypo All other groups: NS	No significant effect (all data included) AS ↑55%* vs SH (omitting zeros: AS, PL n=7)

6.4 Discussion.

The objectives of the experiments described in this chapter were to investigate the efficacy of the optimally effective GRAS5 antisense ODN sequence *in vivo*, and to explore the possible modulation of 5-HT_{2A} receptor expression and function by GR *in vivo*. The present study would in addition provide justification to the use of a novel polymer microsphere delivery system for delivering antisense ODNs over a sustained period to the rat CNS following a single ICV administration. Measurement of GR antisense-targeted receptor downregulation, and any related changes in 5-HT_{2A} receptor expression, was carried out at both the mRNA and functional receptor protein levels using quantitative RT-PCR, radioligand binding assay and Western blot analysis accordingly.

Both the antisense GRAS5 and mismatch GRMM5 ODN sequences (Table 6.1) were loaded into polymer microspheres and administered ICV using an alternating block design treatment plan as described in section 6.3.3.1 in order to reduce both day to day, operator and time of day variations making the data obtained more realistic and giving genuine statistical validity. Following treatment of the animals, well-being assessments (Table 2.2), daily animal body and final adrenal gland weight measurements produced no noticeable neurotoxic and/or related systemic effects affecting rat behaviour and HPA axis homeostasis. This indicated that treatment groups PL, MM, AS and FAS had no apparent behavioural and physiological toxic side effects compared to SH. Previous studies have reported repeated infusions of phosphorothioate ODNs cause non-specific toxicity, including sickness-like behaviour, fever, weight loss, suppressed food and water intake (Schobitz *et al*, 1997) and non-specific behavioural effects such as ataxia, decreased muscular tone, arched back and passive eye-closures (Bourson *et al*, 1995). This would suggest that the present phosphorothioate antisense and mismatch sequences lacked such reported toxicity (Bourson *et al*, 1995; Schobitz *et al*, 1997), possibly due to the use of lower ODN concentrations and masking of such properties as a result of being formulated within the polymer matrix of microspheres, thus imparting greater ODN stability and limiting the overall exposure of the brain to the phosphorothioate toxic chemistry (Lewis *et al*, 1995; Cleek *et al*, 1997).

In addition histological examination of frontal cortex, hippocampus, hypothalamus, cerebellum, striatum and corpus callosum using cresyl fast violet staining in AS and FAS treatment groups following 5 days treatment revealed no observed neurological damage, neuronal loss or evidence of glial cell proliferation, thus further supporting the protective role of the polymer microsphere delivery system in minimising phosphorothioate ODN toxicity *in vivo*. This is in contrast to the detrimental effects on cellular morphology of brain tissue produced following repeated injections of high concentrations of free phosphorothioate ODNs reported by several authors (Chiasson *et al*, 1994; Widnell *et al*, 1996; Wojcik *et al*, 1996; Le Corre *et al*, 1997).

The major route of ODN elimination *in vivo* appears to be via their enzymatic degradation (Szkłarczyk and Kaczmarek, 1999). The stability of phosphorothioate ODNs in the cerebrospinal fluid (CSF) after delivery into the rat brain ventricular system has been studied and is reported to be present in the intact full length form for up to 22 hours after a single infusion within nervous tissue (Liu *et al*, 1994; Yee *et al*, 1994). The present study analysed the time course of tissue retention of the GRAS5 sequence in the polymer-complexed (AS) and free form (FAS) after single ICV administration. The AS treatment revealed the presence of the intact GRAS5 ODN sequence at both 24 hours and 5 days following ICV administration, although the sequence had been degraded to some extent after 5 days. In contrast, the FAS treatment revealed very little intact GRAS5 ODN 24 hours following ICV administration. This clearly identifies the ability of polymer microspheres to impart greater stability to ODNs when they are formulated within these delivery agents and also confirms the availability of the intact antisense GRAS5 and mismatch GRMM5 sequences to male Wistar rat brains 5 days following ICV administration of the AS and MM treatment groups.

ODNs do not easily pass an intact blood-brain barrier (Agrawal *et al*, 1991; Gillardon *et al*, 1997), and their systemic application to the CNS requires vector-mediated delivery systems (Pardridge *et al*, 1995). Therefore studies reporting the delivery and distribution of ODNs in the brain have mainly used simple and low-cost delivery of ODN, which was mainly achieved by means of ICV infusion or intracerebral (IC) injection (for a review see Szkłarczyk and Kaczmarek, 1999). When injected ICV, ODNs can in theory be distributed in the volume of the whole rat brain (~1.5mL), but this does not readily occur due to poor ODN penetration

and distribution throughout brain tissue. Even more limited is the distribution of ODN following IC delivery (Haque and Isacson, 1997). However by optimising the dose of injected ODNs it has been shown that CNS administered ODNs can spread and concentrate in regions of the rat brain such as the hippocampus, striatum, hypothalamus and amygdala (Szklarczyk and Kaczmarek, 1995; Guzowski and McGaugh, 1997; Hooper *et al*, 1994; Guo *et al*, 1996).

Following single ICV administration of FITC-labelled GRAS5 ODN in the free form to the rat brain, a fluorescent signal could be detected in diverse areas of the brain after 24 hours, although this signal severely diminished during 5 day treatment period, indicating the rapid clearance of the ODN in the free form within the CNS. The most intense fluorescent signals were detected at the choroid plexus within the lateral ventricles (site of administration). Detailed examination revealed fluorescent signals within areas of brain tissue in the frontal cortex, cerebellum and striatum. In comparison, single ICV administration of FITC-labelled GRAS5 ODN in the polymer complexed form produced a fluorescent signal which was also detected in diverse areas of the brain and revealed a signal intensity which remained 5 days following administration. This fluorescent intensity of microsphere delivered GRAS5 ODN after 5 days was visually greater in both intensity and distribution compared to GRAS5 ODN 24 hours after ICV administration without the aid of microsphere delivery, in brain regions such as the frontal cortex, cerebellum and striatum. This effect is probably due to the enhanced stability imposed on the GRAS5 ODN within the polymer matrix which can limit the exposure of the ODN to CNS nucleases and thus allow greater penetration of brain regions from the site of ODN administration. Moreover, under closer examination a highly diffuse pattern of fluorescence distribution was observed within the frontal cortex, hippocampus and hypothalamus, which appeared to represent cellular localisation of polymer microsphere delivered FITC-labelled GRAS5 ODN within these tissues. However, the exact identity of the cell types to which ODNs became localised was uncertain and requires a more detailed examination. Therefore it would appear that the GRAS5 antisense ODN delivered using the polymer microsphere system was capable of penetrating brain regions where the expression and density of both GR (hippocampus and hypothalamus) and 5-HT_{2A} receptors (frontal cortex) are reported to be predominant (Meijer and de Kloet, 1998; Chaouloff, 1995).

It was clearly identified using quantitative RT-PCR, radioligand binding assay and Western blot analysis that GRAS5 administered ICV in the polymer complexed form (AS) produced far greater reduction in GR expression in rat hypothalamus compared to GRAS5 administered in the free uncomplexed form (FAS), as a 40, 76 and 77% downregulation in hypothalamic GR expression was achieved 5 days following AS treatment compared to FAS treatment with the respective analysis techniques. This would suggest the ability of polymer microsphere entrapped ODN being distributed to the hypothalamus and remaining intact to achieve significant levels in GR knockdown over the 5 day treatment period, whereas single ICV injections of free ODN are degraded and cleared from the CNS within 24 hours of administration (Szklarczyk and Kaczmarek, 1999). This view was supported by the *in vivo* stability and distribution data discussed previously.

As determined by quantitative RT-PCR, GR mRNA expression was significantly reduced by 26, 35 and 39% in the brain regions of frontal cortex, hippocampus and hypothalamus respectively following AS treatment compared to sham (SH). Consequently quantitative RT-PCR also revealed a significant 13, 7 and 5% increase in 5-HT_{2A} receptor mRNA density in the frontal cortex, hippocampus and hypothalamus respectively of the same animals. Radioligand binding revealed AS treatment to cause a significant 67% reduction in frontal cortical GR binding with a 21% increase in 5-HT_{2A} receptor density. GR binding in both the hippocampal and hypothalamic region of the rat brain also showed a significant decrease by 69 and 75% respectively 5 days following AS treatment compared to sham. Although no significant changes in 5-HT_{2A} receptor density was observed in the hippocampus of these animals, possibly as a result of using a low 'n' number (n=4) due to the pooling of tissue samples in order to carry out the binding procedure. No 5-HT_{2A} receptor binding assays were performed in the hypothalamic region of the rat brain due to the availability of insufficient amounts of appropriately treated tissue samples. The effect on GR in terms of magnitude and direction of the changes to its protein expression in rat brains following AS treatment was further confirmed by Western blot analysis. It was shown that a significant 76 and 80% reduction in GR protein expression occurred in the hippocampus and hypothalamus respectively compared to sham. The mismatch (MM) and polymer (PL) control treatment groups as defined in section 6.3.3.1 showed no significant differences to the expression of GR

and 5-HT_{2A} receptor compared to sham in any of the quantitative RT-PCR, radioligand binding assay or Western blot analysis experiments described above. This demonstrated the effect seen with the GRAS5 ODN *in vivo* in terms of GR gene inhibition to be one involving ODN sequence-specific mechanisms as described for antisense ODN technology (Zamecnik and Stephenson, 1978; Crooke, 1992; Weiss *et al*, 1997).

The magnitude of GR receptor knockdown at both the mRNA and receptor protein observed in the present study in the brain regions of frontal cortex, hippocampus and hypothalamus demonstrated both the efficient nature of polymer microspheres in their distribution of the GRAS5 ODN sequence to these CNS regions of interest following ICV administration and also the superior potency of GRAS5 ODN in its ability to downregulate GR expression *in vivo* as determined by RNase H accessibility mapping. The majority of studies investigating receptor knockdown of target neurotransmitter receptors in specific brain areas have claimed modest levels of downregulation ranging from 20-30% compared to controls (Zhang and Creese, 1993; Le Corre *et al*, 1997; Schobitz *et al*, 1997; Weiss *et al*, 1997). This is also seen in antisense *in vivo* studies targeting the GR specifically (Korte *et al*, 1996; Engelmann *et al*, 1998). This reduced inhibition of target receptor can be partly due to the absence of any optimisation protocol for antisense sequence selection in these studies. What seems apparent is the ability of such levels of downregulation to bring about inhibition of receptor-mediated function and thus contradicts the conventional receptor reserve theory which would require the majority of the receptor population to be inhibited before a decrease in function was observed. To explain this discrepancy between receptor expression and function Qin *et al*, (1995) have suggested that there may be more than one pool of receptors and only a proportion of these receptors make up the functionally active pool and therefore antisense ODNs specifically inhibit receptor-mediated function by affecting this functionally active pool of receptors due to this pool being rapidly turned over compared to the remainder of the receptor population (Weiss *et al*, 1997). In any case the levels of inhibition in GR expression achieved in this study should in theory contribute to some GR-mediated functional change. This was confirmed by the significant 55.3% increase in 5-HT_{2A}-mediated DOI-head-shakes following AS treatment compared to sham, suggesting a concomitant increase in both 5-HT_{2A} receptor density and functional activity as a result of GR knockdown.

The level of inhibition in GR expression shown following GRAS5 treatment in male Wistar rats produced an opposite change in the density of both 5-HT_{2A} receptor mRNA and protein mainly in the frontal cortex where this receptor is highly expressed (Chaouloff, 1995). This was shown by GR knockdown in the brain regions of frontal cortex, hippocampus and hypothalamus which caused an increase in 5-HT_{2A} receptor expression *in vivo*. This, along with the findings of the DOI-head-shake observations, indicated a negative regulatory effect exerted by the GR on 5-HT_{2A} receptor expression seen *in vivo* and *in vitro* in C6 glioma cells (Chapter 5) and thus highlights tonic repression of 5-HT_{2A} receptor expression by activated GR under circadian levels of circulating corticosterone in the rat. At basal circadian levels of circulating corticosterone, the GR is approximately 10% occupied (Reul and de Kloet, 1985), which illustrates the importance of this relationship between the GR and 5-HT_{2A} and their regulatory functions during circadian peaks and stress conditions when the GR becomes extensively occupied by corticosterone (Reul and de Kloet, 1985). The modulatory impact of glucocorticoids (GR mediated) on 5-HT_{2A} receptor expression and function has not been extensively studied *in vivo*, but studies carried out using rats artificially exposed to chronic stress or prolonged treatment with dexamethasone have all shown increases in 5-HT_{2A} receptor binding in the brain, suggesting this to be an effect mediated by the GR following its downregulation and involving HPA axis inactivation (Kuroda *et al*, 1992; Kuroda *et al*, 1993; McKittrick *et al*, 1995). Other evidence of GR-mediated modulation of the 5-HT_{2A} system exist following reports of stimulation or inhibition of 5-HT_{2A} receptors causing a respective increase or decrease in hippocampal GR density (Meaney *et al*, 1994; Mitchell *et al*, 1990).

In summary, the optimally effective GRAS5 antisense ODN sequence targeting the GR has been successfully shown specifically to knockdown GR expression in the rat brain 5 days following single ICV administration within a novel polymer microsphere delivery system. This inhibition of GR in specific brain areas has occurred with no obvious neurological or behavioural toxicity and within this delivery system the ODN proved to be both stable and well distributed throughout the brain 5 days after ICV injection. Consequently, an associated upregulation in the 5-HT_{2A} receptor expression in these animals confirmed GR modulation of this receptor system *in vivo* by a negative regulatory mechanism as shown previously in C6 glioma cells (Chapter 5). The involvement of ODN sequence specific mechanisms in inhibiting

target GR gene expression has been determined following the inability of the control GRMM5 mismatch ODN sequence to significantly alter GR expression. Therefore, with both the magnitude and specificity shown in the level of GR downregulation with GRAS5 treatment, the use of RNase H accessibility mapping to select optimally effective antisense sequences for assessment of *in vivo* efficacy has been justified. The functional consequence of this increase in 5-HT_{2A} receptor density *in vivo* has also been determined using behavioural observations of 5-HT_{2A} receptor mediated DOI-induced head-shakes in rats and the significance of this is discussed in the general discussion (Chapter 7).

CHAPTER SEVEN

GENERAL DISCUSSION

Antisense Oligodeoxynucleotides (ODNs) have important applications as both molecular tools in the study of gene expression and as therapeutic inhibitors of disease causing genes (Wahlestedt, 1994; Weiss *et al*, 1997). It is the first of these applications in the role of studying receptor function which has been adopted/investigated extensively and has become an important aim of these studies. As a consequence of the applications of antisense ODNs, CNS glucocorticoid receptors (GR) and their possible relationship with the serotonergic system via 5-HT_{2A} receptors has been investigated using antisense ODNs specifically developed against the GR and such studies therefore form an integral part of the principal aims of this thesis, especially in light of their being a lack of highly-specific ligands with which to characterise the GR. This possible role of GR modulating 5-HT_{2A} receptors in the CNS is of particular pharmacological interest as both receptors and their functional expression have been associated in chronic stress conditions (Chaouloff, 1995; Lopez *et al*, 1997) and any discovery of potential mechanisms by which GR may control 5-HT_{2A} receptor expression/function under such conditions may offer the possibility of therapeutic interventions in the regulation of mood states such as depression and anxiety.

The use of antisense ODNs in the CNS has recently become widespread, and successful gene inhibition has been reported for such diverse targets as those encoding neurotransmitter receptors, neuropeptides, trophic factors, transcription factors, cytokines, transporters, and ion channels (for review see Szklarczyk and Kaczmarek, 1999). This antisense technique is also favoured over the use of other gene-based manipulations such as transgenic 'knockout' animal models because the effects of the antisense approach are reversible and do not induce developmental changes to animals in the absence of a particular receptor which may incur compensatory mechanisms leading to false characterisation of effects of the receptor in question (Weiss *et al*, 1997). However the use of antisense technology is not as 'clear cut' as once thought (Zamecnik and Stephenson, 1978) since issues relating to antisense ODN

stability, cellular delivery and target sequence selection (finding optimally acting antisense ODNs) are important factors that need to be fully addressed in order to achieve successful antisense-mediated knockdown of receptor gene expression (Akhtar, 1995) and therefore allow investigation of target receptor properties to be carried out. These studies (Chapters 3 and 4) uniquely address these concerns in detail and are discussed later in this chapter.

The rat C6 glioma cell line was selected as an appropriate CNS-derived cell culture model for the *in vitro* studies as they expressed both receptors of interest. More importantly their characteristics in terms of cellular regulation and functions, in particular those relating to glucocorticoid regulation of 5-HT_{2A} receptor gene expression, as a result of their glial derivation, would be expected to be similar to those of the tissues investigated using the *in vivo* model (brain of male Wistar rats). This is supported by the studies of Garlow and Ciaranello (1995) which show factors regulating the expression of the 5-HT_{2A} receptor gene *in vitro* to be both cell-type dependent and species-specific, and have postulated that this pattern of regulation may also occur *in vivo*. Neuronal cell cultures would have been an even more appropriate CNS-derived cell culture model for the *in vitro* studies performed due to their characteristics being more closely associated to that of the tissues used in the *in vivo* studies, compared to glial cell cultures. However no neuronal cell line expressing both GR and 5-HT_{2A} receptors were available.

Cellular association/uptake studies (Chapter 3) were carried out using phosphorothioate (PS) ODNs which have been chemically modified from their natural phosphodiester (PO) form to impart biological stability by increasing the resistance of the ODN to nuclease degradation (Uhlmann *et al.*, 1990). These studies identified PS ODN cellular binding and internalisation to be an active energy dependent process, which was sensitive to changes in pH. But, this was comparatively an inefficient process yielding poor transfer of PS ODNs across the cell membrane (about 5% becoming cell associated after 1 hour). This is primarily due to the polar nature and large molecular size of PS ODNs (Akhtar and Juliano, 1992) causing low affinity of PS ODNs for cell-surface binding proteins which bring about cellular association and therefore uptake (Hawley and Gibson, 1996). These modest levels of ODN cellular internalisation can therefore lead to a reduced antisense-mediated effect in terms of receptor protein downregulation. Thus, to improve the delivery of ODNs by targeting cellular regions

such as the cytoplasm or nucleus (Akhtar, 1998) the cationic lipid Lipofectamine was successfully used as a delivery agent to increase levels of ODN cellular internalisation in order to bring about the 'favoured' sub-cellular sorting/trafficking of ODNs thereby resulting in an enhanced antisense effect. This liposomal enhancement of PS ODN cell association/uptake could be attributed to the fact that cationic lipids both increase ODN cell transfer and decrease ODN degradation (Zabner, 1997). Such cellular delivery strategies using cationic lipids have been commonly employed to obtain biological effects with antisense ODNs *in vitro* (Bennett, 1995; Felgner *et al*, 1995; Zelphati and Szoka, 1996; Wyman *et al*, 1997; Coulson and Akhtar, 1997), although very few studies exist detailing intracellular trafficking of ODNs and application of cationic liposomes to enhance antisense effects in brain cells of primary cultures and/or cell lines. This, along with the fact that the effectiveness of cationic lipids is dependent on variables including cell type, ODN chemistry and charge ratio (Coulson and Akhtar, 1997) places greater emphasis on the importance of carrying out optimisation studies for antisense ODN cellular delivery in C6 glioma cells.

The use of cationic liposomes such as Lipofectamine is undesirable for the *in vivo* delivery of ODNs due to proven cytotoxicity problems and general ineffectiveness in the presence of serum proteins (Litzinger *et al*, 1996; Coulson and Akhtar, 1997; Akhtar, 1998). Most antisense studies in the CNS have relied on the use of direct administration of ODNs into the brain using localised or intracerebroventricular (ICV) injections, producing modest levels of target receptor downregulation (Szklarczyk and Kaczmarek, 1999). In light of this, a novel *in vivo* delivery method using biodegradable polylactide-co-glycolide (PLGA) polymer microspheres was adopted to provide ODNs with protection from nuclease degradation and allowing sustained release of ODNs within the CNS over the required treatment period. This is the first known use of such a delivery system for ODNs in the CNS and its application achieves greater levels of ODNs within the CNS, leading to enhanced antisense-mediated effects *in vivo* (Lewis *et al*, 1995; Cleek *et al*, 1997). Furthermore, using biodegradable polymer microsphere delivery (Chapter 6) achieved other important benefits, which included minimising total ODN concentration administered due to microsphere formulations imparting greater stability to the entrapped ODNs and therefore reducing overall PS-induced toxicity (Agrawal and Zhao, 1998). The use of single ICV injections which necessitated the need of less complicated forms of stereotaxic surgery, lowered the levels of overall stress experienced

by the animals and was also only possible due to polymer microsphere delivery of ODNs. As these studies examined the level of GR expression within the HPA axis, which is sensitive to the presence of increased levels of glucocorticoids as found in stress conditions and mediated via negative feedback mechanisms regulating the HPA axis (Fink, 1997), it was very important that experimental animals were subjected to procedures which minimised their overall exposure to stress, therefore reducing non-treatment based changes to GR expression.

An important factor in the design and selection of antisense ODNs is the physical accessibility of the ODN to target sites within the mRNA sequence. The use of RNA folding analyses have been used, without much success, to predict relative activities of ODNs directed to short, synthetic substrates *in vitro* (Stull *et al*, 1992). But, some studies have shown *mfold* to be unreliable in identifying accessible sites within some large RNA molecules (Dropulic and Jeang, 1994; Birikh *et al*, 1997). Here, studies (Chapter 4) confirm this inadequacy of the RNA folding algorithm *mfold* to accurately identify accessible target sites, and promote the use of empirical techniques (Lieber and Strauss, 1995; Birikh *et al*, 1997) such as RNase H accessibility mapping to be more reliable in identifying accessible target sites. This inadequacy of RNA folding algorithms in appropriate target site selection is considered to be due to an inability of such computer programs at their present level of sophistication to assess RNA folding accurately due to RNA molecules exhibiting a high degree of secondary and tertiary structure and the presence of RNA-binding proteins within cells (Akhtar, 1998). Indeed, folding pathways of large RNAs are poorly understood (Sohail *et al*, 1999) and by the use of oligonucleotide arrays technology it has been shown that altering RNA fragment size by 5' and 3' truncations, does and does not change accessible sites respectively, therefore suggesting that RNA folding creates local stable states that are trapped early in the transcription or folding process (Sohail *et al*, 1999).

The RNase H accessibility mapping experiments (Chapter 4) in these studies resulted in the identification of four accessible sites termed A-D on a 515 base pair *in vitro* transcribed T7-promoter-rat GR PCR fragment construct, of which site D was shown to be optimal for ODN:RNA hybridisation and consequent cleavage by RNase H. This accessible site was further characterised and an optimally effective antisense sequence (GRAS5) was selected on the basis of GR RNA cleavage efficiency and potency. The specificity of GRAS5 to the rodent

GR mRNA was confirmed using a BLAST search (Genbank database) which showed significant alignment to the rat GR mRNA but no other gene. Furthermore, control sequences: sense (GRSS5), mismatch (GRMM5), and non-accessible site-directed (NAGRAS4) ODNs, designed to produce no RNase H mediated cleavage, produced no such cleavage product bands thus highlighting the rational design strategy of RNase H accessibility mapping experiments. One main concern in carrying out these antisense design studies was the use of the 515 base pair GR mRNA fragment encompassing bases 911-1420, instead of the full length GR mRNA sequence, to act as the RNase H mapping reaction substrate. This was because there was no way of guaranteeing that the shorter GR RNA fragment would have the same structural conformation exhibited by the full length GR mRNA sequence. Any differences in RNA structural conformation would therefore result in the identification of inappropriate accessible sites and thus antisense ODN sequence designs which may not be suitable for *in vivo* studies with the aims of downregulating GR expression. However the *in vitro* studies (Chapter 5) were conducted partly with this reservation in mind and would have highlighted such problems and the need to address this particular concern in more detail before proceeding to *in vivo* studies. Fortunately this was not the case and the reason for not using the full length GR mRNA sequence in the first place was due to not being able to obtain a suitable GR plasmid in time for the antisense design studies. This thesis is the first to report such use of a rational approach in designing antisense ODNs against the GR, although RNase H accessibility mapping reactions have been previously successfully employed against other mRNA targets (Lima *et al*, 1997; Birikh *et al*, 1997; Ho *et al*, 1996 and 1998). Recent antisense studies investigating the GR have not presented much detail as regards to the selection of their antisense sequences, although it is likely that a computer-based algorithm method was adopted, which may account for their modest levels (<30%) of downregulation in GR expression *in vivo* (Korte *et al*, 1996; Engelmann *et al*, 1998). This is in marked contrast to the transgenic mouse created by Barden (1999) in which the GR is dramatically downregulated by a complete antisense mRNA construct.

The *in vitro* experiments (Chapter 5) were set-up using cultured rat C6 glioma cells to provide a system for determining the efficacy of RNase H accessibility mapping optimised antisense ODN sequences targeting the GR prior to *in vivo* administration. The results from these experiments produced an antisense-mediated reduction in GR expression, since control

sequences GRMM5, GRSS5 and NAGRAS4 produced little or no inhibition of GR expression. Both quantitative RT-PCR and radioligand binding assays revealed the GRAS5 sequence to be optimally effective at reducing GR mRNA expression, by 56%, and GR protein expression by 80%, respectively. These experimental techniques also revealed an associated upregulation in the expression of 5-HT_{2A} receptor mRNA by 29% and 5-HT_{2A} receptor protein by 32% in the same GRAS5 treated cells. This revealed an important relationship of the GR exerting negative regulatory control on 5-HT_{2A} receptor expression *in vitro* and also reported the highest level of antisense mediated knockdown of GR expression *in vitro* to date.

Garlow and Ciaranello (1995), investigated whether the GR could influence the transcription of the rat 5-HT_{2A} receptor gene using three different cell lines, CCL-39 line (Chinese hamster lung fibroblasts), Neuro-2a line (mouse neuroblastoma), and RS-1 line (rat adrenal PC-12 cells). Dexamethasone treatment activating GR produced 5-HT_{2A} receptor reporter gene inhibition in the RS-1 and CCL-39 cells, while no such 5-HT_{2A} receptor reporter gene inhibition was obtained with Neuro-2a cells. This suggested that the 5-HT_{2A} receptor promoter is subject to cell-type specific regulation in response to the activated GR, and that the positive (transactivation) and negative (transrepression) responses may be mediated through different promoter elements with possible influence from additional transcription factors.

Since GR regulation of 5-HT_{2A} receptor expression occurs at both mRNA and receptor protein (Chapters 5 and 6) it can be suggested that GR modulates 5-HT_{2A} expression at the DNA/transcription level. In the absence of the ligand (glucocorticoids), GR are trapped in an inactive cytosolic complex together with heat shock proteins. Upon ligand binding, this complex dissociates and the receptor translocates into the nucleus where the transcriptional activity of target genes is modulated via different mechanisms (McDonnell *et al*, 1993). In the nucleus the GR normally forms homodimers and binds to specific DNA sequences known as glucocorticoid receptor-responsive elements (GREs) ie. AGAACAXXXTGTCT, to bring about transcriptional modulation of responsive genes (Weigel, 1996). This DNA binding-dependent mechanism is thought to activate gene transcription following interaction of the dimerised receptor complex with the basal transcriptional machinery (Beato *et al*, 1995). Other mechanisms involving protein-protein interactions with the GR and certain transcription

factors can control gene expression by preventing transactivation, resulting in repression of gene transcription (Jonat *et al*, 1990). One such example is MR-GR heterodimerisation which prevents GR-GR homodimers promoting stabilisation and transcription by blockade of cellular transcriptional activity following MR-GR heterodimer interaction with the GRE (Ou *et al*, 2000). As the *in vitro* antisense studies showed GR to have a negative regulatory effect on 5-HT_{2A} expression then GR regulatory mechanisms repressing 5-HT_{2A} gene transcription are likely to be dominant in C6 glioma cells. The rat 5-HT_{2A} gene possesses functional response elements for a variety of transcription factors including AP-1, AP-2, Egr-1, NF-1, and SP-1 as well as having GREs (Garlow and Ciaranello, 1995). Since direct interaction of the GR with GREs would primarily cause activation of 5-HT_{2A} gene transcription (Beato *et al*, 1995) and as the 5-HT_{2A} receptor DNA sequence is known to possess response elements for several other transcription factors apart from GREs, then it can be suggested that activated GR complexes must interact with specific transcription factors in order to inhibit 5-HT_{2A} receptor expression in this cell line. It has been shown that GR interactions with AP-1 and NF-κB transcription factors produce repression of target gene transcription (Reichardt and Schutz, 1998) and therefore AP-1 and its complex interactions with GR may be responsible for the regulation of 5-HT_{2A} receptors in C6 glioma cells. This would tend to support the observation of Garlow and Ciaranello (1995), that the deletion of the region of the rat 5-HT_{2A} promoter containing the GRE did not abrogate the negative effect of dexamethasone on the reporter gene expression. Clearly, the regulation of GR function is a complex phenomenon involving many factors and many steps and other mechanisms have been proposed for repressing target gene transcription (Weigel, 1996). These include the binding of GR to negative glucocorticoid receptor-responsive elements (nGRE) (Meijer and de Kloet, 1998) and non-ligand GR phosphorylation (Bodwell *et al*, 1991). However, such mechanisms are yet to be studied in detail as regards to GR modulation of 5-HT_{2A} receptors and their future characterisation may offer alternative pathways for explaining GR regulation of the 5-HT_{2A} receptor gene.

The primary *in vivo* studies (Chapter 6) showed biodegradable polymer microsphere delivered GRAS5 antisense ODN to be taken up from the lateral ventricle and be distributed to both surrounding and diverse brain areas, namely, the striatum, cerebellum, hippocampus, hypothalamus and frontal cortex. This level of distribution was observed at the end of the treatment period without the presence of apparent histological or behavioural toxicity.

Furthermore, stability studies confirmed the availability of intact 21-mer GRAS5 to the rat CNS for the 5 day treatment period. Such positive distribution and non-toxic bioavailability of ODN in the rat brain was attributed to the novel polymer microsphere delivery system used and to the unique properties it possessed for maintaining ODN stability and sustaining release (Lewis *et al.*, 1995; Cleek *et al.*, 1997). This would give rise to great potential for the future use of this delivery system in antisense *in vivo* studies targeting the CNS. The present ODN distribution studies could have been further improved by assessing the localisation of polymer microsphere delivered FITC-labelled ODNs with molecules capable of selectively tagging either neuron or glial cells using neurofilaments and glial fibrillary acidic protein respectively. This could confirm the detailed localisation of ODNs in specific brain cell types. Nevertheless, the penetration of the brain tissue by GRAS5 and the apparent cellular localisation following ICV administration *in vivo*, demonstrates their potential to exert biological effects within the brain and is confirmed by the *in vivo* efficacy experiments.

The *in vivo* characterisation of the optimally-effective GRAS5 antisense sequence to the GR in rat brain was assessed using radioligand binding, quantitative RT-PCR and Western blot analysis (Chapter 6). These studies, like the *in vitro* studies, showed antisense ODN specific reductions in GR expression at both mRNA and receptor protein level in brain areas of frontal cortex, hippocampus and hypothalamus. It was observed that GRAS5 treatment significantly downregulated GR mRNA expression by 26, 35 and 39% in frontal cortex, hippocampus and hypothalamus respectively. In addition GR protein expression were also significantly downregulated at the protein level by 67, 69 and 75% in frontal cortex, hippocampus and hypothalamus respectively, by radioligand binding analysis. Further confirmation of GRAS5 mediated GR protein knockdown was shown by 76 and 80% downregulation of its expression in hippocampus and hypothalamus respectively using Western blot analysis. Furthermore, changes in 5-HT_{2A} receptor expression in the rat brain were evident following GRAS5 treatment. There was a significant upregulation of 5-HT_{2A} receptor mRNA in frontal cortex, hippocampus and hypothalamus by 13, 7 and 5% respectively. Using radioligand binding, a significant 21% upregulation of 5-HT_{2A} receptor protein was observed in frontal cortex, where 5-HT_{2A} receptor density is known to be highest (Chaouloff, 1995). 5-HT_{2A} receptor density was not fully determined in other brain regions owing to the unavailability of appropriate amounts of tissue required to perform binding studies determining 5-HT_{2A} B_{max}. The

significance of these important *in vivo* findings can be summarised in four ways. Firstly, they highlight the greatly enhanced ability of GRAS5 to downregulate GR expression in the CNS compared to other similar antisense studies using GR antisense ODNs (Korte *et al*, 1996; Engelmann *et al*, 1998). This enhancement can be explained by the unique incorporation of detailed design and delivery strategies (Akhtar, 1995) in these studies as discussed previously. Secondly, the specificity of the GRAS5 sequence to downregulate selectively GR expression is supported by the inability of the mismatch sequence (GRMM5) to significantly alter GR and 5-HT_{2A} expression, and by the fact that an upregulation is seen in 5-HT_{2A} expression following GRAS5 treatment, since non-specific antisense effects might be expected to result in the downregulation of receptors other than GR. Possible future studies to confirming antisense targeted gene specificity might be to assess in parallel the expression of other receptors related to the receptor of interest. Suitable candidates for these studies would include other nuclear hormone receptors such as the mineralocorticoid receptor (MR) and the evaluation of its expression is something which would have definitely strengthened the findings of this thesis. However it would have been very difficult to separate findings relating to non-specific effects of GRAS5 treatment on MR expression, from any specific effects of GR knockdown on the regulation of MR expression. Thirdly, as found in the *in vitro* studies, GRAS5 treatment showed GR to have a negative regulatory effect on 5-HT_{2A} receptor expression *in vivo* and due to this regulation being shown at both mRNA and receptor protein, it is possible that such GR modulation of the 5-HT_{2A} gene occurs at the DNA level by GR preventing transactivation of 5-HT_{2A} via those mechanisms (protein-protein interactions), as previously discussed for C6 glioma cells, resulting in a repressive effect on 5-HT_{2A} gene transcription. Fourthly, the findings relating to GR regulation of 5-HT_{2A} receptor expression and function would suggest HPA axis modulation of 5-HT_{2A} receptors and thus further involve 5-HT_{2A} in HPA-axis linked mood/neuropsychiatric disorders such as stress, depression, anxiety and schizophrenia (Chaouloff, 1995; Barnes and Sharp, 1999). To evaluate this fully it would have been appropriate to measure also CRF, ACTH and corticosterone levels in the animals of the *in vivo* studies. But as a result of limited time and to an extent resources this was not possible, although it can be suggested for future studies.

The studies using DOI-head-shake observations (Chapter 6) further confirmed GR regulation of 5-HT_{2A} receptors at a functional level. This was shown by a 55% increase in 5-HT_{2A} mediated DOI headshakes following GRAS5 treatment, therefore suggesting an increase in 5-HT_{2A} receptor activity caused by antisense ODN knockdown of GR. Thus CNS 5-HT_{2A} receptors are most likely to be under tonic inhibitory control by GR *in vivo*. GRAS5 treatment, when assessed in terms of the HPA axis, which is controlled by a negative feedback mechanism via the GR and MR (Fink, 1997) would result in obvious downregulation of GR which would produce decreased GR-ligand occupancy and thus initiate feedback signals stimulating the central drive of the HPA axis (hippocampus and amygdala). This would be expected to lead to increased synthesis and release of corticotropin-releasing factor (CRF) and arginine vasopressin (AVP) from the hypothalamus, which then would result in the generation of an increased adrenocorticotropic hormone (ACTH) signal from the pituitary gland. This would cause increased synthesis and secretion of glucocorticoids from the adrenal cortex. As a result GRAS5 treatment would be expected to increase the total mass of the adrenal gland by imposing artificially 'allostatic load' on the animals and overcompensating stress responsiveness due to GRAS5 treatment-mediated continued synthesis and secretion of glucocorticoids (McEwen, 1998). This was not the case in these studies and could be explained by the fact that GRAS5 treatment was not continued for a long enough period to initiate such changes to adrenal gland mass and HPA axis homeostasis to affect stress responsiveness and body weight.

Another interesting finding of the *in vivo* studies is the differential effect of GRAS5 treatment on 5-HT_{2A} expression at both the molecular and functional level ie. 5-13% mRNA upregulation, 21% protein receptor binding upregulation, and 55% functional DOI-head-shake upregulation. This may be accounted for by the fact that not all copies of mRNA expressed translate directly to protein on an equal ratio. Likewise not all receptor protein within a given receptor pool are directly involved in producing functional activity and therefore result in this magnitude discrepancy between receptor expression and function (Qin *et al*, 1995). Other explanations such as individual factors governing mRNA and protein turnover, and differences in the individual sensitivities of each assay used to measure the components of mRNA, protein, and function may account for these observations made on 5-HT_{2A} expression and function.

In vivo studies incorporating antisense and non-antisense methods of investigation have looked at the relationship between the HPA axis and 5-HT_{2A} receptors and support the findings of this thesis as regards GR-dependent modulation of 5-HT_{2A} receptors (Pertouka and Snyder, 1980; McKittrick *et al*, 1995; Kuroda *et al*, 1992 and 1993; Barden, 1999). Other studies also report this relationship, but unlike our findings suggest GR to have a positive regulatory effect on 5-HT_{2A} receptor expression, as shown by increased hippocampal GR density following 5-HT_{2A} receptor stimulation (Meaney *et al*, 1994; Mitchell *et al*, 1990). Such conflicting findings may be explained by the mediation of other HPA-axis related effects which have not been fully investigated and by brain regional variations which are indicative of cell-type specific effects. One such HPA-axis related variable is the expression and function of the MR. The study and characterisation of this receptor has somewhat been ignored with regards to its role in stress responsiveness of the HPA axis and its possible regulation of the CNS serotonergic system. One recent study investigated the role of MR in the regulation of neuroendocrine and behavioural responses during stress, by applying antisense ODN knockdown to enhance responsiveness of ACTH to stressful situations, which was accompanied by reduced sensitivity of the adrenal gland to ACTH thus producing lowered circulating corticosteroid concentrations (Reul *et al*, 1997). Such studies investigating the role of the MR within the HPA axis are essential for the detailed understanding of the mechanisms controlling the neuroendocrine and behavioural response to stress. Other variables such as the circulating levels of corticosteroid and serotonin may have specific effects due to their direct interactions, as yet unknown, which can co-ordinate GR regulation of 5-HT_{2A} receptors *in vivo* under circadian and stress conditions (Lopez *et al*, 1997).

In summary, the experiments described in this thesis have shown the application and characterisation of an antisense ODN sequence targeting the GR in the rat. The antisense sequence (GRAS5) has been shown to inhibit specifically GR expression in appropriate brain areas following novel CNS delivery using biodegradable polymer microspheres. This antisense directed inhibition has resulted in consequent upregulation of CNS 5-HT_{2A} receptors in terms of both expression and function, confirming GR modulation of 5-HT_{2A} receptors. Since elevated levels of 5-HT_{2A} receptors, measured in blood platelets and in frontal cortex, have been implicated in the pathophysiology of psychiatric disorders including depression and

schizophrenia (Hrdina *et al*, 1993; Pandey *et al*, 1990; Stanley and Mann, 1983; Yates *et al*, 1990), it would seem that treatments producing specific increases in CNS GR density or antisense-based strategies inhibiting 5-HT_{2A} receptor expression may provide a novel approach to treat these conditions. This is analogous to current pharmaceutical approaches with 5-HT_{2A/2C} antagonists for treating anxiety and depression.

Several interesting lines of investigation are suggested by the findings obtained during the course of these studies. These include further experiments to assessing MR expression during GRAS5 knockdown of GR expression, in order to confirm both antisense specificity and also to determine any possible GR-mediated effect on MR expression. MR knockdown using antisense ODNs and assessment of 5-HT_{2A} receptors would also characterise the role of MR in the regulation of the serotonergic system and possibly suggest further mechanisms which may be involved in cellular regulation of 5-HT_{2A} receptor transactivation. Another antisense-based approach would be to knockdown 5-HT_{2A} receptor expression in rat brain and evaluate both GR and MR expression to further study the relationship between the HPA axis and the serotonergic system. Further investigation into the neurochemical effects of antisense to the 5-HT_{2A} receptor, and comparison with 5-HT_{2A} receptor antagonists and antidepressant drugs using an animal model of depression, will provide a better understanding of the role of 5-HT_{2A} receptor downregulation in depression and related conditions. Furthermore, to fully evaluate GRAS5 treatment in terms of stress related behavioural responses it would be beneficial to subject such animals to behavioural testing using models such as the elevated plus maze test (Handley and Mithani, 1984).

APPENDIX I

Publications

Agarwal, S. (1996). Antisense Oligonucleotides: Towards Clinical Trials. *Trends in Biotechnology*, 14: 376-387.

Papers

Agarwal, S., Ghoshal, S., Ghosh, S., and Akhtar, S. (1998). Oligonucleotide-mediated

Islam, A., Handley, S.L., Thompson, K.S.J., and Akhtar, S. (2000). Studies on uptake, sub-cellular trafficking and efflux of antisense oligodeoxynucleotides in glioma cells using self-assembling cationic lipoplexes as delivery systems. *Journal of Drug Targeting*, 7: 373-382.

Agarwal, S., Bhatnagar, P.L., Tewari, S., Ghosh, S., and Akhtar, S. (1998). Effect of antisense oligonucleotides on the synthesis, purification, hybridization, cell uptake and cytotoxicity of oligonucleotides. *Bioorganic and Medicinal Chemistry Letters*, 9: 225-228.

Abstracts

Islam, A., Thompson, K.S.J., Akhtar, S., and Handley, S.L. (2000). Antisense oligodeoxynucleotide to rat glucocorticoid receptor given ICV in polymer microspheres, reduces glucocorticoid- and increases 5-HT_{2A}-receptor binding. *British Journal of Pharmacology*, 129: 244P (January Supplement).

Agarwal, S. and Akhtar, S. (1996). In vivo studies on antisense oligonucleotide mediated oligonucleotide-induced toxicity in vivo. *Antisense and Nucleic Acid Drug Development*, 4: 133-139.

Akhtar, S. (1995). Delivery strategies for antisense oligonucleotide therapeutics. In: (Ed) CRC Press Inc, London, UK.

Akhtar, S. (1998). Antisense technology: selection and delivery of optimally acting antisense oligonucleotides. *Journal of Drug Targeting*, 6: 229-234.

Akhtar, S., and Agarwal, S. (1997). In vivo studies with antisense oligonucleotides. *Trends in the Pharmaceutical Sciences*, 18: 15-19.

Akhtar, S., and Ghosh, S. (1998). Cellular uptake and intracellular site of action of oligonucleotides. *Trends in Cell Biology*, 8: 139-143.

Akhtar, S., and Leach, K.J. (1997). Antisense oligodeoxynucleotide delivery to cultured macrophages is improved by lipopolyplexes and sustained release biodegradable polymer microspheres. *International Journal of Pharmaceutics*, 151: 57-67.

Akhtar, S., Rowlands, A., Prasad, R., and Godwin, J.M. (1999). Synthesis of mono- and dimannoside phosphoramidite derivatives for solid-phase conjugation to oligonucleotides. *Tetrahedron Letters*, 40: 7323-7326.

REFERENCES

- Agrawal, S. (1996). Antisense Oligonucleotides: Towards clinical trials. *Trends in Biotechnology*. **14**: 376-387.
- Agrawal, S., Goodchild, J., Civeira, M.P., Thornton, A.H., Sarin, P.S., and Zamecnik, P.C. (1988). Oligodeoxynucleoside phosphoramidites and phosphorothioate as inhibitors of human immunodeficiency virus. *The Proceedings of the National Academy of Sciences USA*. **85**: 7079-7083.
- Agrawal, S., Iadarola, P.L., Tamsamani, J., Zhao, Q.Y., and Shaw, D.R. (1996). Effect of G-rich sequences on the synthesis, purification, hybridisation, cell uptake and haemolytic activity of oligonucleotides. *Biorganic and Medicinal Chemistry Letters*. **6**: 2219-2224.
- Agrawal, S., Tamsamani, J., and Tang, J.Y. (1991). Pharmacokinetic, biodistribution and stability of oligodeoxynucleotide phosphorothioates in mice. *The Proceedings of the National Academy of Sciences USA*. **88**: 7595-7599.
- Agrawal, S., and Zhao, Q. (1998). Mixed backbone oligonucleotides: Improvement in oligonucleotide-induced toxicity *in vivo*. *Antisense and Nucleic Acid Drug Development*. **8**: 135-139.
- Akhtar, S. (1995). Delivery strategies for antisense oligonucleotide therapeutics. Akhtar, S. (Ed). CRC Press Inc, London, UK.
- Akhtar, S. (1998). Antisense technology: selection and delivery of optimally acting antisense oligonucleotides. *Journal of Drug Targeting*. **5**: 225-234.
- Akhtar, S., and Agrawal, S. (1997). *In vivo* studies with antisense oligonucleotides. *Trends in the Pharmaceutical Sciences*. **18**: 12-18.
- Akhtar, S., and Juliano, R.L. (1992). Cellular uptake and intracellular fate of antisense oligonucleotides. *Trends in Cell Biology*. **2**: 139-143.
- Akhtar, S., and Lewis, K.J. (1997). Antisense oligodeoxynucleotide delivery to cultured macrophages is improved by incorporation into sustained release biodegradable polymer microspheres. *International Journal of Pharmaceutics*. **151**: 57-67.
- Akhtar, S., Routledge, A., Patel, R., and Gardiner, J.M. (1995). Synthesis of mono- and dimannoside phosphoramidite derivatives for solid-phase conjugation to oligonucleotides. *Tetrahedron Letters*. **36**: 7333-7336.

- Akhtar, S., Shoji, Y., and Juliano, R.L. (1992). Pharmaceutical aspects of the biological stability and membrane transport characteristics of antisense oligonucleotides. In: *Gene Regulation. Biology of Antisense RNA and DNA*. Erickson, R.P., and Izant, J.G. (Eds). Raven Press Ltd, New York, USA.
- Alahari, S.K., Dean, N.M., Fisher, M., Delong, R., Manoharan, M., Tivel, K.L., and Juliano, R.L. (1996). Inhibition of expression of the multidrug resistance-associated P-glycoprotein by phosphorothioate and 5'-cholesterol-conjugated phosphorothioate antisense oligonucleotides. *Molecular Pharmacology*. **50**: 808-819.
- Alberts, B., Bray, D., Lewis, J., Raff, M., Roberts, K., Watson, J.D. (1989). Intracellular sorting and the maintenance of cellular compartments. In: *The Molecular Biology of the Cell*. Garland Publishing, New York, USA.
- Altschul, S.F., Madden, T.L., Schaffer, A.A., Zhang, J., Zhang, Z., Miller, W., and Lipman, D.J. (1997). Gapped BLAST and PSI-BLAST: a new generation of protein database search programs. *Nucleic Acids Research*. **25**: 3389-3402.
- Amano, F., Hashida, R., and Mizuno, D. (1981). Lysosomal fusion in endocytosis and exocytosis-1-Demonstration and characterisation of 2 fusion reactions proceeding simultaneously in non-phagocytosing guinea pig polymorphonuclear leukocytes. *Experimental Cell Research*. **136**: 15-26.
- Aoki, M., Morishita, R., Higaki, J., Moriguchi, A., Kida, I., Hayashi, S., Matsushita, H., Kaneda, Y., and Ogihara, T. (1997). *In vivo* transfer efficiency of antisense oligonucleotides into the myocardium using HVJ-liposome method. *Biochemical and Biophysical Research Communication*. **231**: 540-545.
- Arango, V., Underwood, M.D., and Mann, J.J. (1992). Alterations in monoamine receptors in the brain of suicide victims. *Journal of Clinical Psychopharmacology*. **12**: 8S-12S (Supplement).
- Armbruster, B.L., Carlemalm, E., Chiovetti, R., Garavito, R.M., Hobot, J.A., Kellenberger, E., and Villiger, W. (1982). Specimen preparations for electron-microscopy using low-temperature embedding resins. *Journal of Microscopy-Oxford*. **126**: 77-85.
- Aynie, I., Vauthier, C., Chacun, H., Fattal, E., and Couvreur, P. (1999). Spongelike alginate nanoparticles as a new potential system for the delivery of antisense oligonucleotides. *Antisense and Nucleic Acid Drug Development*. **9**: 301-312.
- Azmitia, E.C., Algeri, S., and Costa, E. (1970). *In vivo* conversion of ³H-L-tryptophan into ³H-serotonin in brain areas of adrenalectomised rats. *Science*. **169**: 201-203.
- Azmitia, E.C., Liao, B., and Chen, Y.S. (1993). Increase of tryptophan hydroxylase enzyme protein by dexamethasone in adrenalectomised rat midbrain. *Journal of Neuroscience*. **13**: 5041.

- Bannai, M., Ichikawa, M., Nishimura, F., Nishimura, M., and Takahashi, M. (1998). Water-absorbent polymer as a carrier for a discrete deposit of antisense oligodeoxynucleotides in the central nervous system. *Brain Research Protocols*. **3**: 83-87.
- Barden, N. (1996). Modulation of glucocorticoid receptor gene expression by antidepressant drugs. *Pharmacopsychiatry*. **26**: 12-22.
- Barden, N. (1999). Regulation of corticosteroid receptor gene expression in depression and antidepressant action. *Journal of Psychiatry and Neuroscience*. **24**: 25-39.
- Barnes, N.M., and Sharp, T. (1999). A review of central 5-HT receptors and their function. *Neuropharmacology*. **38**: 1083-1152.
- Beato, M., Chalepakis, G., Schauer, M., and Slater, E.P. (1989). DNA regulatory elements for steroid hormones. *Journal of Steroid Biochemistry*. **32**: 737-747.
- Beato, M., Herrlich, P., and Schutz, G. (1995). Steroid hormone receptors: many actors in search of a plot. *Cell*. **83**: 851-857.
- Beck, G.F., Irwin, W.J., Nicklin, P.L., and Akhtar, S. (1996). Interactions of phosphodiester and phosphorothioate oligonucleotides with intestinal epithelial Caco-2 cells. *Pharmaceutical Research*. **13**: 1028-1037.
- Beltinger, C., Saragovi, H.U., Smith, R.M., Lesauteur, L., Shah, N., Dedionisio, L., Christensen, L., Raible, A., Jarett, L., and Gewirtz, A.M. (1995). Binding, uptake, and intracellular trafficking of phosphorothioate modified oligodeoxynucleotides. *Journal of Clinical Investigation*. **95**: 1814-1823.
- Benda, P., Lightbody, J., Sato, G., Levine, L., and Sweet, W. (1968). Differential rat glial cell strain in tissue culture. *Science*. **161**: 370.
- Bennett, C.F. (1995). Intracellular delivery of oligonucleotides with cationic liposomes. In: Akhtar, S. (Ed). *Delivery strategies for antisense oligonucleotide therapeutics*. CRC Press Inc, London, UK.
- Bennett, C.F., Chiang, M.Y., Chan, H., Shoemaker, J.E.E., and Mirabelli, C.K. (1992). Cationic lipids enhance cellular uptake and activity of phosphorothioate antisense oligonucleotides. *Molecular Pharmacology*. **41**: 1023-1033.
- Bergan, R., Connell, Y., Fahmy, B., and Neckers, L. (1993). Electroporation enhances c-myc antisense oligonucleotide efficacy. *Nucleic Acids Research*. **21**: 3567.
- Bergan, R., Kyle, E., Connell, Y., and Neckers, L. (1995). Inhibition of protein-tyrosine kinase activity in intact cells by the aptameric action of oligodeoxynucleotides. *Antisense Research and Development*. **5**: 33-38.

- Bielinska, A., Kukowska-Latallo, J.F., Johnson, J., Tomalia, D.A., and Baker, J.R. (1994). Regulation of *in vitro* gene expression using antisense oligonucleotides or antisense expression plasmids transfected using starburst PAMAM dendrimers. *Nucleic Acids Research*. **24**: 2176-2182.
- Birikh, K.R., Berlin, Y.A., Soreq, H., and Eckstein, F. (1997). Probing accessible sites for ribozymes on human acetylcholinesterase RNA. *RNA*. **3**: 429-437.
- Bodwell, J.E., Orti, E., Coull, J.M., Pappin, D.J., Swift, F., and Smith, L.I. (1991). Identification of phosphorylated sites in the mouse glucocorticoid receptor. *Journal of Biological Chemistry*. **266**: 7549-7555.
- Bouille, C., and Bayle, J.D. (1973). Effects of limbic stimulation or lesions on basal and stress-induced hypothalamic-pituitary-adrenocortical activity in the pigeon. *Neuroendocrinology*. **13**: 264.
- Bourson, A., Borroni, E., Austin, R.H., Monsma, J. Jnr., and Sleight, A.J. (1995). Determination of the role of the 5-HT₆ receptor in the rat brain: a study using antisense oligonucleotides. *Journal of Pharmacology and Experimental Therapy*. **274**: 173-180.
- Bradbury, M., and Dallman, M.F. (1989). Effects of hippocampal type 1 and type 2 glucocorticoid antagonists on ACTH levels in the PM. *Program of the 19th Annual Meeting of the Society for Neuroscience*. Phoenix, Arizona, USA, pp 716 (Abstract).
- Bradford, M.M. (1976). A rapid sensitive method for the quantification of protein using the principle of protein dye binding. *Analytical Biochemistry*. **72**: 248-252.
- Bradley, M.O., Chrisey, L.A. and Hawkins, J.W. (1992). Antisense therapeutics. In: *Gene Regulation. Biology of Antisense RNA and DNA*. Erickson, R.P. and Izant, J.G. (Eds) Raven Press Ltd, New York USA.
- Brooke, S.M., de Haas-Johnson, A.M., Kaplan, J.R., Manuck, S.B., and Sapolsky, R.M. (1994). Dexamethasone resistance associated with a selective decrease of glucocorticoid receptors in the hippocampus and a history of social instability. *Neuroendocrinology*. **60**: 134-140.
- Brown, T., and Brown, D.J.S. (1991). Modern machine-aided methods of oligodeoxyribonucleotide synthesis. In: *Oligonucleotides and Analogues: A Practical Approach*. Eckstein, F. (Ed). Oxford University Press, Oxford, UK, pp 1-24.
- Brysch, W., and Schlingensiepen, K-H. (1994). Design and application of antisense oligonucleotides in cell culture, *in vivo* and as therapeutic agents. *Cellular and Molecular Neurobiology*. **14**: 555-567.
- Chalmers, D.T., Lopez, J.F., Akil, H., and Watson, S.J. (1993). Molecular aspects of the stress axis and serotonergic function in depression. *Clinical Neuroscience*. **1**: 122-128.

- Chalmers, D.T., Lopez, J.F., Vasquez, D.M., Akil, H., and Watson, S.J. (1994). Regulation of hippocampal 5-HT_{1A} receptor gene expression by dexamethasone. *Neuropsychopharmacology*. **10**: 215-222.
- Chalmers, D.T., and Watson, S.J. (1991). Comparative anatomical distribution of 5-HT_{1A} receptor mRNA and 5-HT_{1A} binding in rat brain—a combined *in situ* hybridisation/*in vitro* receptor autoradiographic study. *Brain Research*. **561**: 51-60.
- Chaouloff, F. (1993). Physiopharmacological interactions between stress hormones and central serotonergic systems. *Brain Research Reviews*. **18**: 1-32.
- Chaouloff, F. (1995). Regulation of 5-HT receptors by corticosteroids: where do we stand? *Fundamental Clinical Pharmacology*. **9**: 219-233.
- Checkley, S. (1996). The neuroendocrinology of depression and chronic stress. *British Medical Bulletin*. **52**: 597-617.
- Chiasson, B.J., Armstrong, J.N., Hooper, M.L., Murphy, P.R., and Robertson, H.A. (1994). The application of antisense oligonucleotide technology to the brain: some pitfalls. *Cellular and Molecular Neurobiology*. **14**: 507-521.
- Chin, D.J., Green, G.A., Zon, G., Szoka, F.C., and Straubinger, R.M. (1990). Rapid nuclear accumulation of injected oligonucleotides. *The New Biologist*. **2**: 1091-1100.
- Chiou, H.C., Tangco, M.V., Levine, S.M., Robertson, G., Kormis, K., Wu, C.H., and Wu, G.Y. (1994). Enhanced resistance to nuclease degradation of nucleic acids complexed to asialoglycoprotein-polylysine carriers. *Nucleic Acids Research*. **22**: 5439-5446.
- Citro, G., Perrotti, D., Cucco, C., D'Agnano, I., Sacchi, A., Zupi, G., and Calabretta, B. (1992). Inhibition of leukemia cell proliferation by receptor-mediated uptake of c-myc antisense oligodeoxynucleotides. *The Proceedings of the National Academy of Sciences USA*. **89**: 7031-7035.
- Cleek, R.L., Rege, A.A., Denner, L.A., Eskin, S.G., Mikos, A.G. (1997). Inhibition of smooth muscle cell growth *in vitro* by an antisense oligonucleotide released from poly(DL-lactic-co-glycolic acid) microparticles. *Journal of Biomedical Materials Research*. **35**: 525-530.
- Cook, E.H. (1990). Autism: review of neurochemical investigation. *Synapse*. **6**: 292-308.
- Cooper, J.R., Bloom, F.E., and Roth, R.H. (1996). Serotonin (5-hydroxytryptamine) and histamine. In: *The Biochemical Basis of Neuropharmacology*. Cooper, J.R., Bloom, F.E., and Roth, R.H. (Eds). Oxford University Press, New York, USA. 7th Edition.
- Cooper, M., and Stewart, P.M. (1998). The syndrome of apparent mineralocorticoid excess. *QJM-Monthly Journal of the Association of Physicians*. **91**: 453-455.
- Coulson, J.M., and Akhtar, S. (1997). A c-myc phosphorothioate oligonucleotide protects U87-MG cells from toxicity at high concentrations of lipofectin and streptolysin O. *Pharmaceutical Science*, in press.

- Coulson, J.M., Poyner, D.R., Chantry, A., Irwin, W.J., and Akhtar, S. (1996). A non-antisense sequence-selective effect of a phosphorothioate oligonucleotide targeted to EGFR in A431 cells. *Molecular Pharmacology*. **50**: 314-325.
- Crooke, S.T. (1992). Therapeutic applications of oligonucleotides. *Annual Review of Pharmacology*. **32**: 329-379.
- Csernansky, J.G., Poscher, M., and Faull, K.F. (1992). Serotonin (5-HT) in schizophrenia. In: *Serotonin in Major Psychiatric Disorders*. Coccaro, E.F., and Murphy, D.L. (Eds). American Psychiatric Press, Washington D.C., USA.
- Dahlstrom, A., and Fuxe, K. (1965). Evidence for the existence of monoamine containing neurone in the central nervous system. Demonstration of monoamine in the cell bodies of brain stem neurons. *Acta Physiology Scandinavia*. **232**: 1-55.
- Dallman, M.F., Akana, S.F., Cascio, C.S., Darlington, D.N., Jacobson, L., and Levin, N. (1987). Regulation of ACTH secretion: variations on a theme of B. *Recent Progress in Hormone Research*. **43**: 113.
- De Kloet, E.R. (1991). Brain corticosteroid receptor balance and homeostatic control. *Frontiers in Neuroendocrinology*. **12**: 95-164.
- De Kloet, E.R., de Kock, S., Schild, V., and Veldhuis, H.D. (1988). Antigluocorticoid RU38486 attenuates retention of a behaviour and disinhibits the hypothalamic-pituitary adrenal axis at different brain sites. *Neuroendocrinology*. **47**: 109.
- De Kloet, E.R., and Reul, J.M.H.M. (1987). Tonic influence and feedback action of corticosteroids: a concept arising from heterogeneity of brain corticosteroid receptor systems. *Psychoneuroendocrinology*. **12**: 83.
- De Kloet, E.R., Sybesma, H., and Reul, J.M.H.M. (1986). Selective control by corticosterone of serotonin-1 receptor capacity in raphe-hippocampal system. *Neuroendocrinology*. **42**: 513-521.
- De Montigny, C., and Blier, P. (1992). Electrophysiological evidence for the distinct properties of presynaptic and postsynaptic 5-HT_{1A} receptors: possible clinical relevance. In: *Serotonin Receptor Subtypes: Pharmacological Significance and Clinical Implications*. Langer, S.Z., Brunello, N., Racagni, G., Mendlewicz, G. (Eds). *International Journal of Academic Biomedical Drug Research*. Karger, Basel, Switzerland.
- Dolnick, B.J. (1991). Antisense agents in cancer research and therapeutics. *Cancer Investigation*. **9**: 185-194.
- Dropulic, B., and Jeang, K.T. (1994). Intracellular susceptibility to ribozymes in a tethered substrate-ribozyme pro-virus model is not predicted by secondary structures of human immunodeficiency virus type I RNAs *in vitro*. *Antisense Research and Development*. **4**: 217-221.

- Eckstein, F. (1985). Nucleoside phosphorothioates. *Annual Review of Biochemistry*. **54**: 367-402.
- Engelmann, M., Landgraf, R., Lorscher, P., Conzelmann, C., Probst, J.C., Holsboer, F., and Reul, J.M.H.M. (1998). Downregulation of brain mineralocorticoid and glucocorticoid receptor by antisense oligodeoxynucleotide treatment fails to alter spatial navigation in rats. *European Journal of Pharmacology*. **361**: 17-26.
- Englehard, H., Narang, C., Homer, R., and Duncan, H. (1996). Urokinase antisense oligodeoxynucleotides as a novel therapeutic agent for malignant glioma-*in vitro* and *in vivo* studies of uptake, effects and toxicity. *Biochemical and Biophysical Research Communication*. **227**: 400-405.
- Evans, R.M. (1988). The steroid and thyroid hormone receptor superfamily. *Science*. **240**: 889.
- Farhood, H., Bottega, R., Epanand, R.M., and Huang, L. (1992). Effect of cationic cholesterol derivatives on gene transfer and protein kinase C activity. *Biochimica et Biophysica Acta*. **1111**: 239-246.
- Fattal, E., Vauthier, C., Aynie, I., Nakada, Y., Lambert, G., Malvy, C., and Couvreur, P. (1998). Biodegradable polyalkylcyanoacrylate nanoparticles for the delivery of oligonucleotides. *Journal of Controlled Release*. **53**: 137-143.
- Felgner, P.L., Zaugg, R.H., and Norman, J.A. (1995). Synthetic recombinant DNA delivery for cancer therapeutics. *Cancer Gene Therapy*. **1**: 61-65.
- Fell, P.L., Hudson, A.J., Reynolds, M.A., and Akhtar, S. (1997). Cellular uptake properties of a 2'-amino/2'-o-methyl-modified chimeric hammerhead ribozyme targeted to the epidermal growth factor receptor mRNA. *Antisense and Nucleic Acid Drug Development*. **7**: 319-326.
- Fink, G. (1997). Mechanism of negative and positive feedback of steroids in the hypothalamic-pituitary system. In: *Principles of Medical Biology*. Bittar, E.E., Bittar, N. (Eds). JAI Press, pp 29-100.
- Fischette, C.T., Komisaruk, B.R., Edinger, H.M., Feder, H.H., and Siegel, A. (1980). Differential fornix ablations and the circadian rhythmicity of adrenal corticosteroid secretion. *Brain Research*. **195**: 373.
- Fuller, R.W. (1992). The involvement of serotonin in regulation of pituitary-adrenocortical function. *Frontiers in Neuroendocrinology*. **13**: 250.
- Furdon, P.J., Dominski, Z., and Kole, R. (1989). RNase H cleavage of RNA hybridised to oligonucleotides containing methylphosphonate, phosphorothioate and phosphodiester bonds. *Nucleic Acids Research*. **17**: 9193-9204.
- Gait, M.J., Misiura, K., Durrant, I., and Evans, M.R. (1991). A new multiple labelling method for synthetic oligo-nucleotides and increased sensitivity in DNA detection. *Nucleosides and Nucleotides*. **10**: 671-672.

- Garlow, S.J., Chin, A.C., Marinovitch, M.A., Heller, M.R., and Ciaranello, R.D. (1994). Cloning and functional promoter mapping of the rat serotonin-2 receptor gene. *Molecular and Cellular Neuroscience*. **5**: 291-300.
- Garlow, S.J., and Ciaranello, R.D. (1995). Transcriptional control of the rat serotonin-2 receptor gene. *Molecular Brain Research*. **31**: 201-209.
- Ge, L., Resnick, N.M., Ernst, L.K., Salvucci, L.A., Asman, D.C., and Cooper, D.L. (1995). Gene therapeutic approaches to primary and metastatic brain tumours: II. Ribozyme-mediated suppression of CD44 expression. *The Journal of Neuro-Oncology*. **26**: 251-257.
- Gibson, I. (1994). Antisense DNA and RNA strategies: New approaches to therapy. *The Journal of the Royal College of Physicians of London*. **28**: 507-511.
- Gillardon, F., Vogel, J., Hein, S., Zimmermann, M., and Uhlmann, E. (1997). Inhibition of carrageenan-induced spinal c-Fos activation by systemically administered c-fos antisense oligodeoxynucleotides may be facilitated by local opening of the blood-spinal cord barrier. *Journal of Neuroscience Research*. **47**: 582-589.
- Gill, G.N., and Lazar, C.S. (1981). Increased phosphotyrosine content and inhibition of proliferation of EGFR-treated A431 cells. *Nature*. **392**: 305-307.
- Glennon, R.A. (1990). Do classical hallucinogens act as 5-HT₂ agonists or antagonists? *Neuropsychopharmacology*. **3**: 509-517.
- Glennon, R.A., McKenney, J.D., Lyon, R.A., and Titeler, M. (1986). 5-HT₁ and 5-HT₂ binding characteristics of 1-(2,5-dimethoxy-4-bromophenyl)-2-aminopropane analogues. *Journal of Medicinal Chemistry*. **29**: 194-199.
- Green, A.R., and Curzon, G. (1968). Release of 5-hydroxytryptamine in the brain provoked by hydrocortisone and its prevention by allopurinol. *Nature*. **220**: 1095-1097.
- Grimaldi, S., Lisi, A., Pozzi, D., and Santoro, N. (1997). Attempts to use liposomes and RBC ghosts as vectors in drug and antisense therapy of virus infection. *Research in Virology*. **148**: 177-180.
- Guo, H.F., Tian, J., Wang, X., Fang, Y., Hou, Y., and Han, J. (1996). Brain substrates activated by electroacupuncture (EA) of different frequencies (II): Role of Fos/Jun proteins in EA-induced transcription of preproenkephalin and preprodynorphin genes. *Molecular Brain Research*. **43**: 167-173.
- Guy-Caffey, J.K., Bodepudi, V., Bishop, J.S., Jayaraman, K., and Chaudhary, N. (1995). Novel polyaminolipids enhance the cellular uptake of oligonucleotides. *Journal of Biological Chemistry*. **270**: 31391-31396.

- Guzowski, J.F., and McGaugh, J.L. (1997). Antisense oligodeoxynucleotide-mediated disruption of hippocampal cAMP response element binding protein levels impairs consolidation of memory for water maze training. *The Proceedings of the National Academy of Sciences of the USA*. **94**: 2693-2698.
- Handley, S.L., and Mithani, S. (1984). Effects of alpha-adrenoceptor agonists and antagonists in a maze-exploration model of fear-motivated behaviour. *Naunyn-Schmiedeberg's Archives of Pharmacology*. **327**: 1-5.
- Haque, N., and Isacson, O. (1997). Antisense gene therapy for neurodegenerative disease? *Experimental Neurology*. **144**: 139-146.
- Hawley, P., and Gibson, I. (1996). Interaction of oligodeoxynucleotides with mammalian cells. *Antisense and Nucleic Acid Drug Development*. **6**: 185-195.
- Heinrichs, S.C., Pich, E.M., Miczek, K.A., Britton, K.T., and Koob, G.F. (1992). Corticotrophin-releasing factor antagonist reduces emotionality in socially defeated rats via direct neurotropic action. *Brain Research*. **581**: 190-197.
- Helene, C., and Toulme, J.J. (1990). Specific regulation of gene expression by antisense, sense and antigene nucleic acids. *Biochimica et Biophysica Acta*. **1049**: 99-125.
- Herman, J.P., Cullinan, W.E., Morano, M.I., Akil, H., and Watson, S.J. (1995). Contribution of the ventral subiculum to inhibitory regulation of the hypothalamic-pituitary-adrenal axis. *Journal of Neuroendocrinology*. **7**: 475-482.
- Herz, J.M., Thomsen, W.J., and Yarbrough, G.G. (1997). Molecular approaches to receptors as targets for drug discovery. *Journal of Receptor and Signal Transduction Research*. **17**: 671-776.
- Ho, S.P., Bao, Y., Leshner, T., Malhotra, R., Ma, L.Y., Fluharty, S.J., and Sakai, R.R. (1998). Mapping of RNA accessible sites for antisense experiments with oligonucleotide libraries. *Nature Biotechnology*. **16**: 59-63.
- Ho, S.P., Britton, D.H.O., Stone, B.A., Behrens, D.L., Leffert, L.M., Hobbs, F.W., Miller, J.A., and Trainor, G.L. (1996). Potent antisense oligodeoxynucleotides to the human multidrug resistance-1 mRNA are rationally selected by mapping RNA-accessible sites with oligonucleotide libraries. *Nucleic Acids Research*. **24**: 1901-1907.
- Hoke, G.D., Draper, K., Freier, S., Gonzalez, C., Driver, V.B., Zounes, M.C., and Ecker, D. (1991). Effects of phosphorothioate capping on antisense oligonucleotide stability, hybridisation and antiviral efficacy versus Herpes Simplex Virus infection. *Nucleic Acids Research*. **19**: 5743-5748.
- Hooper, M.L., Chiasson, B.J., and Robertson, H.A. (1994). Infusion into the brain of an antisense oligonucleotide to the immediate-early gene *c-fos* suppresses production of fos and produces a behavioural effect. *Neuroscience*. **63**: 917-924.

- Hoyer, D., Clarke, D.E., Fozard, J.R., Hartig, P.R., Martin, G.R., Mylecharane, E.J., Saxena, P.R., and Humphrey, P.P.A. (1994). International union of pharmacology classification of receptors for 5-hydroxytryptamine (serotonin). *Pharmacological Reviews*. **46**: 157-203.
- Hrdina, P.D., Demeter, E., Vu, T.B., Sotonyi, P., and Palkovits, M. (1993). 5-HT uptake sites and 5-HT₂ receptors in brain of antidepressant-free suicide victims/depressives: Increase in 5-HT₂ sites in cortex and amygdala. *Brain Research*. **614**: 37-44.
- Hudson, A.J., Lewis, K.J., Rao, V.M., and Akhtar, S. (1996). Biodegradable polymer matrices for the sustained exogenous delivery of a biologically active c-myc hammerhead ribozyme. *International Journal of Pharmaceutics*. **136**: 23-29.
- Iversen, S.D. (1984). 5-HT and anxiety. *Neuropharmacology*. **23**: 1553-1560.
- Jacobs, B.L., and Azmitia, E.C. (1992). Structure and function of the brain serotonin system. *Physiological Reviews*. **72**: 165.
- Jacobson, L., Akana, S.F., Cascio, C.S., Scribner, K., Shinsako, J., and Dallman, M.F. (1989). The adrenocortical system responds slowly to removal of corticosterone in the absence of concurrent stress. *Endocrinology*. **124**: 2144.
- Jacobson, L., and Sapolsky, R. (1991). The role of the hippocampus in feedback regulation of the hypothalamo-pituitary-adrenocortical axis. *Endocrine Reviews*. **12**: 118-133.
- Joels, M., Heslen, W., and de Kloet, E.R. (1991). Mineralocorticoid hormones suppress serotonin-induced hyperpolarisation of rat hippocampal CA1 neurons. *Journal of Neuroscience*. **11**: 2288-2294.
- Jonat, C., Rahmsdorf, H.J., Park, K.K., Cato, A.C.B., Gebel, S., Ponta, H., and Herrlich, P. (1990). Antitumour promotion and anti-inflammation down-modulation of AP-1 (fos jun) activity by glucocorticoid hormone. *Cell*. **62**: 1189-1204.
- Karle, J., Witt, M.R., and Nielsen, M. (1997). The use of *in vivo* antisense oligonucleotide technology for the investigation of brain GABA receptors. *Neurochemistry-International*. **31**: 447-457.
- Keller-Wood, M.E., and Dallman, M.F. (1984). Corticosteroid inhibition of ACTH secretion. *Endocrine Reviews*. **5**: 1-24.
- Kennett, G.A., and Curzon, G. (1991). Potencies of antagonists indicate that 5-HT_{1C} receptors mediate the 1,3 (chlorophenyl) piperazine-induced hypophagia. *British Journal of Pharmacology*. **103**: 2016-2020.
- Kettle, C.J., Cheetham, S.C., Martin, K.F., Prow, M.R., and Heal, D.J. (1999). The effects of the peptide-coupling agent, EEDQ, on 5-HT_{2A} receptor binding and function in rat frontal cortex. *Neuropharmacology*. **38**: 1421-1430.

- Kiehntopf, M., Brach, M.A., Licht, T., Petschauer, S., Karawajew, S., Kirschning, C., and Herrmann, F. (1994). Ribozyme mediated cleavage of MDR-1 transcript restores chemosensitivity on previously resistant cancer cells. *EMBO Journal*. **13**: 4645-4652.
- Kisich, K.O., Stecha, P.F., Harter, H.A., and Stinchcomb, D.T. (1995). Inhibition of TNF- α secretion by murine macrophages following *in vivo* and *in vitro* ribozyme treatment. *The Journal of Cellular Biochemistry*. **19A**: 291.
- Kitayama, I., Cintra, A., Janson, A.M., Fuxe, K., Agnati, L.F., Aronsson, M., Harfstrand, A., Steinbusch, H.W.M., Visser, T.J., Goldstein, M., Vale, W., and Gustafsson, J-A. (1989). Chronic immobilisation stress: evidence for decrease of 5-hydroxytryptamine immunoreactivity and for increase of glucocorticoid receptor immunoreactivity in various brain regions of the male rat. *Journal of Neural Transmission*. **77**: 93.
- Kizer, J.S., Palkovits, M., Kopin, I.J., Saavedra, J.M., and Brownstein, M.J. (1976). Lack of effect of various endocrine manipulations on tryptophan hydroxylase activity of individual nuclei of the hypothalamus, limbic system and midbrain of the rat. *Endocrinology*. **98**: 743-747.
- Koello, W.P. (1988). Serotonin and sleep. In: *Neuronal Serotonin*. Osborne, N.N., and Hamon, M. (Eds). John Wiley and Sons Ltd, New York, USA, pp 153-170.
- Kole, R., Shukla, R.R., and Akhtar, S. (1991). Pre-mRNA splicing as a target for antisense oligonucleotides. *Advanced Drug Delivery Reviews*. **6**: 271-286.
- Korte, S.M., de Kloet, E.R., Buwalda, B., Bouman, S.D., and Bohus, B. (1996). Antisense to the glucocorticoid receptor in hippocampal dentate gyrus reduces immobility in forced swim test. *European Journal of Pharmacology*. **301**: 19-25.
- Kreig, A.M., Tonkinson, J., Matson, S., Zhao, Q., Saxon, M., Zhang, L., Bhanja, U., Yakubov, L., and Stein, C.A. (1993). Modification of antisense phosphodiester oligodeoxynucleotides by a 5' cholesterol moiety increases cellular association and improves efficacy. *The Proceedings of the National Academy of Sciences of the USA*. **90**: 1048-1052.
- Krieger, D.T. (1977). Rhythms in CRF, ACTH and corticosteroids. In: *Endocrine Rhythms*. Krieger, D.T. (Ed). Raven Press Ltd, New York, USA.
- Krystal, G.W. (1992). Regulation of eukaryotic gene expression by naturally occurring antisense RNA. In: *Gene Regulation. Biology of Antisense RNA and DNA*. Erickson, R.P. and Izant, J.G. (Eds). Raven Press Ltd, New York, USA.
- Kuroda, Y., Mikuni, M., Nomura, N., and Takahashi, K. (1993). Differential effect of subchronic dexamethasone treatment on serotonin-2 and β -adrenergic receptors in the rat cerebral cortex and hippocampus. *Neuroscience Letters*. **155**: 195-198.
- Kuroda, Y., Mikuni, M., Ogawa, T., and Takahashi, K. (1992). Effect of ACTH, adrenalectomy and the combination treatment on the density of 5-HT receptor binding sites in neocortex of rat forebrain and 5-HT₂ receptor-mediated wet-dog shake behaviours. *Psychopharmacology*. **108**: 27-32.

- Kuroda, Y., Watanabe, Y., Albeck, D.S., Hastings, N.B., and McEwen, B.S. (1994). Effects of adrenalectomy, Type I or Type II glucocorticoid receptor activation on 5-HT_{1A} and 5-HT₂ receptor binding and 5-HT transporter mRNA expression in rat brain. *Brain Research*. **648**: 157-161.
- Le Corre, S.M., Burnet, P.W.J., Meller, R., Sharp, T., and Harrison, P.J. (1997). Critical issues in the antisense inhibition of brain gene expression *in vivo*: Experiences targeting the 5-HT_{1A} receptor. *Neurochemistry International*. **31**: 349-362.
- Leonetti, J.P., Mechti, N., Degols, G., Gagnor, C., and Lebleu, B. (1991). Intracellular distribution of microinjected antisense oligonucleotides. *The Proceedings of the National Academy of Sciences of the USA*. **88**: 2702-2706.
- Lewis, K.J., Irwin, W.J., and Akhtar, S. (1995). Biodegradable poly (L-lactic acid) matrices for the sustained delivery of antisense oligonucleotides. *Journal of Controlled Release*. **37**: 173-183.
- Lewis, K.J., Irwin, W.J., and Akhtar, S. (1998). Development of a sustained release biodegradable polymer system for site-specific delivery of oligonucleotides: characterisation of P(LA-GA) copolymer microspheres *in vitro*. *Journal of Drug Targeting*, in press.
- Lieber, A., and Strauss, M. (1995). Selection of efficient cleavage sites in target RNAs by using a ribozyme expression library. *Molecular Cell Biology*. **15**: 540-551.
- Liebsch, G., Landgraf, R., Gerstberger, R., Probst, J.C., Wotjak, C.T., Engelmann, M., Holsboer, F., and Montkowski, A. (1995). Chronic infusion of a CRH₁ receptor antisense oligodeoxynucleotide into the central nucleus of the amygdala reduced anxiety behaviour in socially defeated rats. *Regulatory Peptides*. **59**: 229-239.
- Lima, W.F., Brown-Driver, V., Fox, M., Hanecak, R., and Brucie, T.W. (1997). Combinatorial screening and rational optimisation of hybridisation to folded hepatitis C virus RNA of oligonucleotides with biological antisense activity. *Journal of Biological Chemistry*. **272**: 626-638.
- Lima, W.F., Monia, B.P., Ecker, D.J., and Freier, S.M. (1992). Implication of RNA structure on antisense oligonucleotide hybridisation kinetics. *Biochemistry*. **31**: 12055-12061.
- Litzinger, D.C., Brown, J.M., Wala, I., Kaufman, S.A., Van, G.Y., Farrell, C.L., and Collins, D. (1996). Fate of cationic liposomes and their complex with oligonucleotide *in vivo*. *Biochimica et Biophysica Acta*. **1281**: 139-149.
- Liu, P.K., Salminen, A., He, Y.Y., Jiang, M.H., Xue, J.J., Liu, J.S., and Hsu, C.Y. (1994). Suppression of ischemia-induced fos expression and AP-1 activity by an antisense oligodeoxynucleotide to *c-fos* mRNA. *Annals Neurobiology*. **36**: 566-576.
- Loke, S.L., Stein, S.L., Zhang, X.H., Mori, K., Nakanishi, M., Subasinghe, C., Cohen, J., and Neckers, L.M. (1989). Characterisation of oligonucleotide transport in living cells. *The Proceedings of the National Academy of Sciences of the USA*. **86**: 3474-3478.

Long, J.B., and Holaday, J.W. (1985). Blood-brain barrier: endogenous modulation by adrenal-cortical function. *Science*. **227**: 1580-1583.

Lopez, J.F. (1994). Serotonin receptor regulation in chronic unpredictable stress: An animal model of depression? *Neuropsychopharmacology*. **10**: 751S (Abstract).

Lopez, J.F., Chalmers, D., Little, K.Y., and Watson, S.J. (1997). Regulation of 5-HT_{1A} receptor, glucocorticoid and mineralocorticoid receptor in rat and human hippocampus: implications for the neurobiology of depression. *Biological Psychiatry*. In press.

Lopez, J.F., Young, E.A., Herman, J.P., Akil, H., and Watson, S.J. (1991). Regulatory biology of the HPA axis: An integrative approach. *American Psychiatric Press, Inc.* Washington D.C. USA.

Lu, L., and Ordway, G.A. (1997). Reduced expression of alpha-2C adrenoceptors in rat striatum following antisense oligodeoxynucleotide infusion. *Brain Research and Molecular Brain Research*. **47**: 267-274.

Lucki, I., Nobler, M.S., and Frazer, A. (1984). Differential actions on two behavioural models of serotonin receptor activation in the rat. *Journal of Pharmacological and Experimental Therapy*. **228**: 133-139.

Mann, J.J., Arango, V., and Underwood, M.D. (1990). Serotonin and suicidal behaviour. *Annals New York Academy of Sciences*. **600**: 476-485.

Mann, J.J., Stanley, M., and McBride, P.A. (1986). Increased serotonin 2 and beta-adrenergic receptor binding in the frontal cortex of suicide victims. *Archives of General Psychiatry*. **43**: 954-959.

Mason, J.W. (1958). The central nervous system regulation of ACTH secretion. In: *The reticular formation of the brain*. Jasper, H.H., Proctor, L.D., Knighton, R.S., Noshay, W.C., Costello, R.T. (Eds). Brown and Co., Boston, USA, pp 645.

McDonnell, D.P., Clevenger, B., Dana, S., Santiso-Mere, D., Tzukerman, M.T., and Gleeson, A.G. (1993). The mechanism of action of steroid hormones: a new twist to an old tale. *Journal of Clinical Pharmacology*. **33**: 1165-1172.

McEwen, B.S. (1987). Glucocorticoid-biogenic amine interactions in relation to mood and behaviour. *Biochemistry and Pharmacology*. **36**: 1755-1763.

McEwen, B.S. (1998). Stress, adaptation, and disease. Allostasis and allostatic load. *Annals New York Academy of Sciences*. **860**: 33-44.

McEwen, B.S., De Kloet, E.R., and Rostene, W. (1986). Adrenal steroid receptors and actions in the nervous system. *Physiological Reviews*. **66**: 1121-1188.

McEwen, B.S., and Magarinos, A.M. (1997). Stress effects on morphology and function of the hippocampus. *Annals New York Academy of Sciences*. **821**: 271-284.

- McKittrick, C.R., Blanchard, D.C., Blanchard, R.J., McEwen, B.S., and Sakai, R.R. (1995). Serotonin receptor binding in a colony model of chronic social stress. *Biological Psychiatry*. **37**: 383-396.
- Meaney, M.J., Dioro, J., Francis, D., LaRoque, S., O'Donnell, D., Smythe, J.W., Sharma, S., and Tannenbaum, B. (1994). Environmental regulation of the development of glucocorticoid receptor systems in the rat forebrain: the role of serotonin. *Annals New York Academy of Sciences*. **746**: 260.
- Meaney, M.J., Viau, V., Aitken, D.H., and Bhatnagar, S. (1988). Stress-induced occupancy and translocation of hippocampal glucocorticoid receptors. *Brain Research*. **445**: 198-203.
- Meijer, O.C., and de Kloet, E.R. (1998). Corticosterone and serotonergic neurotransmission in the hippocampus: functional implications of central corticosteroid receptor diversity. *Critical Reviews in Neurobiology*. **12**: 1-20.
- Meijer, O.C., and De Kloet, E.R. (1994). Corticosterone suppresses the expression of 5-HT_{1A} receptor mRNA in rat dentate gyrus. *European Journal of Pharmacology*. **266**: 255-261.
- Meltzer, H.Y., and Lowry, M.T. (1987). The serotonin hypothesis of depression. In: *Psychopharmacology: The third generation of progress*. Meltzer, H.Y. (Ed). Raven Press, New York, USA, pp 513-526.
- Meltzer, H.Y., and Nash, J.F. (1991). Effects of antipsychotropic drugs on serotonin receptors. *Pharmacological Reviews*. **43**: 587-604.
- Miesfeld, R., Rusconi, S., Godowski, P.J., Maler, A., Okret, S., Wilkstrom, A-C., Gustafsson, J-A., and Yamamoto, K.R. (1986). Genetic complementation of a glucocorticoid receptor deficiency by expression of cloned receptor cDNA. *Cell*. **45**: 369-399.
- Miller, A.H., Spencer, R.L., Pulera, M., Kang, S., McEwen, B., and Stein, M. (1992). Adrenal steroid receptor activation in rat brain and pituitary following dexamethasone: implications for the dexamethasone suppression test. *Biological Psychiatry*. **32**: 850-869.
- Milligan, J.F., Matteucci, M.D., and Martin, J.C. (1993). Current concepts in antisense drug design. *The Journal of Medicinal Chemistry*. **36**: 1923-1931.
- Milner, N., Mir, K.U., and Southern, E.M. (1997). Selecting effective antisense reagents on combinatorial oligonucleotide arrays. *Nature Biotechnology*. **15**: 537-541.
- Minta, A., Kao, J.P.Y., and Tsien, R.Y. (1989). Fluorescent indicators for cytosolic calcium based on rhodamine and fluorescein chromophores. *Journal of Biological Chemistry*. **264**: 8171-8178.
- Mitchell, P.J., Rowe, W., Boksa, P., and Meany, M.J. (1990). Serotonin regulates type II corticosteroid receptor binding in hippocampal cell cultures. *Journal of Neuroscience*. **10**: 1745.

- Monia, B.P., Johnston, J.F., Geiger, T., Muller, M. and Fabbro, D. (1996). Antitumour-activity of a phosphorothioate antisense oligodeoxynucleotide targeted against c-raf kinase. *Nature Medicine*. **2**: 668-675.
- Munck, A., and Holbrook, N.J. (1984). Glucocorticoid-receptor complexes in rat thymus cells. *Journal of Biological Chemistry*. **259**: 820-831.
- Nauta, W.J.H., and Feirtag, M. (1986). *Fundamental Neuroanatomy*. Freeman and Co. Publications. New York, USA.
- Neckers, L., and Sze, P.Y. (1975). Regulation of 5-hydroxytryptamine metabolism in mouse brain by adrenal glucocorticoids. *Brain Research*. **93**: 123-132.
- Nicot, A., and Pfaff, D.W. (1997). Antisense oligodeoxynucleotides as specific tools for studying neuroendocrine and behavioural functions: Some prospects and problems. *Journal of Neuroscience Methods*. **71**: 45-53.
- Nutt, D.J., and George, D.T. (1990). Serotonin and anxiety. *Neurobiology of Anxiety*. **3**: 189-221.
- O'Donnell, D., Francis, D., Weaver, S., and Meaney, M.J. (1995). Effects of adrenalectomy and corticosterone replacement on glucocorticoid receptor levels in rat brain tissue: a comparison between Western blotting and receptor binding assays. *Brain Research*. **687**: 133-142.
- O'Driscoll, L., Daly, C., Saleh, M., and Clynes, M. (1993). The use of reverse transcriptase-polymerase chain reaction (RT-PCR) to investigate specific gene expression in multidrug-resistant cells. *Cytotechnology*. **12**: 289-314.
- Oitzl, M.S., Fluttert, M., and de Kloet, E.R. (1994). The effect of corticosterone on reactivity to spatial novelty is mediated by central mineralocorticosteroid receptors. *European Journal of Neuroscience*. **6**: 1072.
- Ogawa, S., Brown, H.E., Okano, H.J., and Pfaff, D.N. (1995). Cellular uptake of intracerebrally administered oligodeoxynucleotides in mouse brain. *Regulatory Peptides*. **59**: 143-149.
- Oleskevich, S., and Descarries, L. (1990). Quantified distribution of the serotonin innervation in the adult rat hippocampus. *Neuroscience*. **34**: 19.
- Ou, X.M., Storrington, J.M., Kushwaha, N., and Albert, P.R. (2000). A novel negative response element for transrepression of the 5-HT_{1A} receptor gene by mineralocorticoid/glucocorticoid receptor heterodimerisation. *Society for Neuroscience*. **26**: pp 120 (47.9-Abstract).
- Owens, M.J., Mulchahey, J.J., Kasckow, J.W., Plotsky, P.M., and Nemeroff, C.B. (1995). Exposure to an antisense oligonucleotide decreases corticotrophin-releasing factor receptor binding in rat pituitary cultures. *Journal of Neurochemistry*. **64**: 2358-2361.

- Pandey, G.N., Pandey, S.C., Janicak, P.G., Marks, R.C., and Davis, J.M. (1990). Platelet serotonin-2 receptor binding sites in depression and suicide. *Biological Psychiatry*. **28**: 215-222.
- Pardridge, W.M., Boado, R.J., and Kang, Y.S. (1995). Vector-mediated delivery of a polyamide ('peptide') nucleic acid analogue through the blood-brain barrier *in vivo*. *The Proceedings of the National Academy of Sciences of the USA*. **92**: 5592-5596.
- Paxinos, G., and Watson, C. (1986). *The rat brain stereotaxic co-ordinates*. New York: Academic Press, USA.
- Pellegrini, E., Bluet-Pajot, M.T., Mounier, F., Bennett, P., Kordon, C., Epelbaum, J. (1996). Central administration of a growth hormone (GH) receptor mRNA antisense increases GH pulsatility and decreases hypothalamic somatostatin expression in rats. *Journal of Neuroscience*. **16**: 8140-8148.
- Pellow, S., Chopin, P., File, S.E., and Briley, M. (1985). Validation of open: closed arm entries in an elevated plus-maze as a measure of anxiety in the rats. *Journal of Neuroscience Methods*. **14**: 149-167.
- Pepin, M.C., Pothier, F., and Barden, N. (1992). Impaired type II glucocorticoid-receptor function in mice bearing antisense RNA transgene. *Nature*. **355**: 725-728.
- Peroutka, S.J., and Snyder, S.H. (1980). Regulation of serotonin 2 (5-HT₂) receptors labelled with 3H-spiroperidol by chronic treatment with the antidepressant amitriptyline. *Journal of Pharmacology and Experimental Therapy*. **215**: 582-587.
- Pichon, C., Arar, K., Stewart, A.J., Dodon, M.D., Gazzolo, L., Courtoy, P.J., Mayer, R., Monsigny, M., and Roche, A.C. (1997). Intracellular routing and inhibitory activity of oligonucleotides containing a KDEL motif. *Molecular Pharmacology*. **51**: 431-438.
- Plotsky, P.M., Owens, M.J., and Nemeroff, C.B. (1998). Psychoneuroendocrinology of depression-Hypothalamic-pituitary-adrenal axis. *Psychiatric Clinics of North America*. **21**: 293.
- Puyal, C., Millhaud, P., Bienvenue, A., and Philippot, J.R. (1995). A new cationic liposome encapsulating genetic material. A potential delivery system for polynucleotides. *European Journal of Biochemistry*. **228**: 697-703.
- Quattrone, A., Papucci, L., Schiavone, N., Mini, E., and Capaccioli, S. (1994). Intracellular enhancement of intact antisense oligonucleotide steady-state levels by cationic lipids. *Anticancer Drug Design*. **9**: 549-553.
- Quercia, S., and Chang, S.L. (1996). Antisense oligodeoxynucleotide attenuates *in vivo* expression of c-fos in the paraventricular hypothalamic nucleus of the rat brain. *Neuroscience Letters*. **209**: 89-92.

- Qin, Z-H., Zhou, L-W., Zhang, S-P., Wang, Y., and Weiss, B. (1995). D₂ dopamine receptor antisense oligodeoxynucleotide inhibits the synthesis of a functional pool of D₂ dopamine receptors. *Molecular Pharmacology*. **48**: 730-737.
- Reddy, D.S. (1996). Antisense oligonucleotides: A new class of potential anti-AIDS and anticancer drugs. *Drugs of Today*. **32**: 113-137.
- Reichardt, H.M., and Schutz, G. (1998). Glucocorticoid signalling-multiple variations of a common theme. *Molecular and Cellular Endocrinology*. **146**: 1-6.
- Reul, J.M.H.M., and de Kloet, E.R. (1985). Two receptor systems for corticosterone in rat brain: microdistribution and differential occupation. *Endocrinology*. **117**: 2505-2511.
- Reul, J.M.H.M., Pearce, P.T., Funder, J.W., and Krozowski, Z.S. (1989). Type I and type II corticosteroid receptor gene expression in the rat: effect of adrenalectomy and dexamethasone administration. *Molecular Endocrinology*. **3**: 1674.
- Reul, J.M.H.M., Probst, J.C., Skutella, T., Hirschamann, M., Stec, I.S., Montkowski, A., Landgraf, R., and Holsboer, F. (1997). Increased stress-induced adrenocorticotrophin response after long term intracerebroventricular treatment of rats with antisense mineralocorticoid receptor oligodeoxynucleotides. *Neuroendocrinology*. **65**: 189-199.
- Reul, J.M.H.M., van den Bosch, F.R., and de Kloet, E.R. (1987). Differential response of type I and type II corticosteroid receptors to changes in plasma steroid level and circadian rhythmicity. *Neuroendocrinology*. **45**: 407.
- Rojanasakul, Y., Weissman, D.N., Shi, X.L., Castranova, V., Ma, J.K.H., and Liang, W.W. (1997). Antisense inhibition of silica-induced tumour necrosis factor in alveolar macrophages. *Journal of Biological Chemistry*. **272**: 3910-3914.
- Rossi, J.J. (1995). Controlled, targeted, intracellular expression of ribozymes: progress and problems. *Trends in Biotechnology*. **13**: 301-306.
- Sanchez-Blazquez, P., Garcia-Espana, A., and Garzon, J. (1997). Antisense oligodeoxynucleotides to opioid mu and delta receptors reduced morphine dependence in mice: Role of delta-2 opioid receptors. *Journal of Pharmacological Experimental Therapeutics*. **280**: 1423-1431.
- Saizieu, A., Certa, U., Warrington, J., Gray, C., Keck, W., and Mous, J. (1998). Bacterial transcript imaging by hybridisation of total RNA to oligonucleotide arrays. *Nature Biotechnology*. **16**: 45-48.
- Sambrook, J., Fritsch, E.F., and Maniatis, T. (1989). *Molecular cloning: a laboratory manual*. Second Edition. Cold Spring Harbor Laboratory Press, New York, USA, pp 11.20-11.28.
- Sapolsky, R.S., Armanini, M.P., Packan, D.R., Sutton, S.W., and Plotsky, P.M. (1990). Glucocorticoid feedback inhibition of adrenocorticotrophic hormone secretagogue release. *Neuroendocrinology*. **51**: 328.

- Sapolsky, R.S., and Plotsky, P.M. (1990). Hypercortisolism and its possible neural bases. *Biological Psychiatry*. **27**: 937.
- Scatton, B., Javoy-Agid, J., Rouquier, L., Dubois, B., Agid, Y. (1983). Reduction of cortical dopamine, noradrenaline, serotonin and their metabolites in parkinsons-disease. *Brain Research*. **275**: 321-328.
- Schwab, G., Chavany, C., Duroux, I., Goubin, G., Lebeau, J., Helene, C., and Saisonbehmoaras, T. (1994). Antisense oligonucleotides adsorbed to polyalkylcyanoacrylate nanoparticles specifically inhibit mutated Ha-ras-mediated cell proliferation and tumourigenicity in nude mice. *The Proceedings of the National Academy of Sciences of the USA*. **91**: 10460-10464.
- Schlingensiepen, K-H., and Heilig, M. (1997). Gene function analysis and therapeutic prospects in neurobiology. In: Antisense-from technology to therapy. Laboratory manual and textbook. Schlingensiepen, R., Brysch, W., and Schlingensiepen, K-H. (Eds). pp 186-223.
- Schobitz, B., Pezeshli, G., Probst, C.P., Reul, M.H.M., Skutella, T., Stohr, T., Holsboer, F., and Spanagel, R. (1997). Centrally administered oligonucleotides in rats: occurrence of non-specific effects. *European Journal of Pharmacology*. **331**: 97-107..
- Schweitzer, J.W., and Freidhoff, A.J. (1988). Gilles de la Tourette syndrome. In: *Receptors and Ligands in Neurological Disorders*. Sen, A.K., and Lee, T. (Eds). Cambridge University Press, Cambridge, UK, pp 64-79.
- Selye, H. (1952). The story of the adaptation syndrome. Montreal, Canada: Acta, Medical Publishers.
- Shea, R.G., Marsters, J.C., and Bischofberger, N. (1990). Synthesis, hybridisation properties and antiviral activity of lipid-oligodeoxynucleotide conjugates. *Nucleic Acids Research*. **18**: 3777-3783.
- Sherwood, L. (1989). The central nervous system. In: *Human Physiology, From Cells to Systems*. The West Publishing Company, St. Paul, Minnesota, USA.
- Shoji, Y., Akhtar, S., Periasamy, A., Herman, B., and Juliano, R.L. (1991). Mechanism of cellular uptake of modified oligodeoxynucleotides containing methylphosphonate linkages. *Nucleic Acids Research*. **19**: 5543-5550.
- Singh, V.B., Corley, K.C., Phan, T.C., and Boadle-Biber, M.C. (1989). Increases in the activity of tryptophan hydroxylase from rat cortex and midbrain in response to acute or repeated sound stress are blocked by adrenalectomy and restored by dexamethasone treatment. *Brain Research*. **516**: 66-76.
- Sioud, M. (1996). Ribozyme modulation of lipopolysaccharide-induced tumour necrosis factor- α production by peritoneal cells *in vitro* and *in vivo*. *The European Journal of Immunology*. **26**: 1026-1031.

- Sleight, A.J., Monsma, F.J. jr., Borroni, E., Austin, R.H., and Bourson, A. (1996). Effects of altered 5-HT₆ expression in the rat: functional studies using antisense oligonucleotides. *Behavioural Brain Research*. **73**: 245-248.
- Smith, D.F., and Toft, D.O. (1993). Steroid-receptors and their associated proteins. *Molecular Endocrinology*. **7**: 4-11.
- Sohail, M., Akhtar, S., and Southern, E.M. (1999). The folding of large RNA's studied by hybridisation to arrays of complementary oligonucleotides. *RNA-A Publication of the RNA Society*. **5**: 646-655.
- Southern, E.M. (1996). DNA chips: analysing sequence by hybridisation to oligonucleotides on a large scale. *Trends in Genetics*. **12**: 110-114.
- Southern, E.M., Case-Green, S.C., Elder, J., Johnson, M., Mir, K., Wang, L., and Williams, J.C. (1994). Arrays of complementary oligonucleotides for analysing the hybridisation behaviour of nucleic acids. *Nucleic Acids Research*. **22**: 1368-1373.
- Stanley, M., and Mann, J.J. (1983). Increased serotonin-2 binding sites in frontal cortex of suicide victims. *Lancet*. **1**: 214-216.
- Stec, I., Barden, N., and Reul, J.M., and Holsboer, F. (1994). Dexamethasone non-suppression in transgenic mice expressing antisense RNA to the glucocorticoid receptor. *Journal of Psychiatric Research*. **28**: 1-5.
- Stegmann, T., and Legendre, J-Y. (1997). Gene transfer mediated by cationic lipids: lack of correlation between lipid mixing and transfection. *Biochimica et Biophysica Acta*. **1325**: 71-79.
- Stein, C.A. (1997). Controversies in the cellular pharmacology of oligodeoxynucleotides. *Antisense and Nucleic Acid Drug Development*. **7**: 207-209.
- Stein, C.A., Tonkinson, J.L., Zhang, L-M., Yakubov, L., Gervasoni, J., Taub, R., and Rotenberg, S.A. (1993). Dynamics of the internalisation of phosphodiester oligodeoxynucleotides in HL60 cells. *Biochemistry*. **32**: 4855-4861.
- Stull, R.A., Taylor, L.A., and Szoka, F.C. (1992). Predicting antisense oligonucleotide inhibitory efficacy: a computational approach using histograms and thermodynamic indices. *Nucleic Acids Research*. **20**: 3501-3508.
- Stull, R.A., Zon, G., and Szoka, F.C. (1996). An *in vitro* mRNA binding assay as a tool for identifying hybridisation-competent antisense oligonucleotides. *Antisense and Nucleic Acid Drug Development*. **6**: 221-228.
- Swanson, J. (1989). Fluorescent labelling of endocytic compartments. *Methods in Cell Biology*. **29**: 137-151.

- Szklarczyk, A.W., and Kaczmarek, L. (1995). Antisense oligodeoxyribonucleotides: stability and distribution after intracerebral injection into rat brain. *Journal of Neuroscience Methods*. **60**: 181-187.
- Szklarczyk, A.W., and Kaczmarek, L. (1999). Brain as a unique antisense environment. *Antisense and Nucleic Acid Drug Development*. **9**: 105-116.
- Tarrason, G., Bellido, D., Eritja, R., Vilaro, S., and Piulats, J. (1995). Digoxigenin-labelled phosphorothioate oligonucleotides-A new tool for the study of cellular uptake. *Antisense Research and Development*. **5**: 193-201.
- Thierry, A., and Tackle, G.B. (1995). Liposomes as delivery system for antisense and ribozyme compounds. In: *Delivery Strategies for Antisense Oligonucleotide Therapeutics*. Akhtar, S. (Ed). CRC Press, Inc, London, UK.
- Tidd, D.M. (1996). Ribonuclease-H mediated antisense effects in intact human leukaemia cells. *Biochemical Society Transactions*. **24**: 619-623.
- Tonkinson, J.L., and Stein, C.A. (1994). Patterns of intracellular compartmentalisation, trafficking and acidification of 5²-fluorescein labelled phosphodiester and phosphorothioate oligodeoxynucleotides in HL-60 cells. *Nucleic Acids Research*. **22**: 4268-4275.
- Toulme, J.J. (1992). Artificial regulation of gene expression by complementary oligonucleotides- an overview. In: *Antisense RNA and DNA*. Wiley-Liss Inc, New York, pp 175-194.
- Towbin, H., Staehelin, T., and Gordon, J. (1979). Electrophoretic transfer of proteins from polyacrylamide gels to nitrocellulose sheets: procedure and some applications. *The Proceedings of the National Academy of Sciences of the USA*. **76**: 4350-4354.
- Tricklebank, M.D. (1985). The behavioural response to 5-HT receptor agonists and subtypes of the central 5-HT receptor. *Trends in Pharmacological Sciences*. **6**: 403-407.
- Turner, B.B. (1986). Tissue differences in the up-regulation of glucocorticoid-binding proteins in the rat. *Endocrinology*. **118**: 1211-1216.
- Uhlmann, E., and Peyman, A. (1990). Antisense oligonucleotides: a new therapeutic principle. *Chemical Reviews*. **90**: 543-584.
- Uhlmann, E., Rytte, A., and Peyman, A. (1997). Studies on the mechanism of stabilisation of partially phosphorothioated oligonucleotides against nucleolytic degradation. *Antisense and Nucleic Acid Drug Development*. **7**: 345-350.
- Udenfriend, S., Titus, E., and Weissbach, H. (1955). The identification of 5-hydroxy-3-indoleacetic acid in normal urine and a method for its assay. *Journal of Biological Chemistry*. **216**: 499-505.
- Van der Krol, A.R., Mol, J.N.M., and Stuitje, A.R. (1988). Modulation of eukaryotic gene expression by complementary RNA or DNA sequences. *BioTechniques*. **6**: 958-976.

- Van Dijken, H., de Goeij, D.C.E., Sutanto, W., Mos, J., de Kloet, E.R., and Tilders, F.J.H. (1993). Short inescapable stress produces long-lasting changes in the brain-pituitary-adrenal axis of adult male rats. *Neuroendocrinology*. **58**: 57.
- Van Loon, G.R., Shum, A., and Sole, M.J. (1981). Decreased brain serotonin turnover after short term (Two hour) adrenalectomy in rats: comparison of four turnover methods. *Endocrinology*. **108**: 1392-1402.
- Wagner, R.W. (1994). Gene inhibition using antisense oligodeoxynucleotides. *Nature*. **372**: 333-335.
- Wahlestedt, C. (1994). Antisense oligonucleotide strategies in neuropharmacology. *Trends in Pharmacological Sciences*. **15**: 42-46.
- Wahlestedt, C., Golanov, E., Yamamoto, S., Yee, F., Ericson, H., Yoo, H., Inturrisi, C.E., and Reis, D.J. (1993). Antisense oligodeoxynucleotides to NMDA-R1 receptor channel protect cortical neurones from excitotoxicity and reduce focal ischaemic infarctions. *Nature*. **363**: 260-263.
- Walker, I., Irwin, W.J., and Akhtar, S. (1995). Improved cellular delivery of antisense oligonucleotides using transferrin receptor antibody-oligonucleotide conjugates. *Pharmaceutical Research*. **12**: 1548-1553.
- Watanabe, Y., Sakai, R.R., McEwen, B.S., and Mendelson, S. (1993). Stress and antidepressant effects on hippocampal and cortical 5-HT_{1A} and 5-HT₂ receptors and transport sites for serotonin. *Brain Research*. **615**: 87-94.
- Weigel, N.L. (1996). Steroid hormone receptors and their regulation by phosphorylation. *Journal of Biochemistry*. **319**: 657-667.
- Weiss, B., Davidkova, G., and Zhang, S-P. (1997). Antisense strategies in neurobiology. *Neurochemistry International*. **31**: 321-348.
- Wetzler, S., Kahn, R.S., Asnis, G.M., Korn, M., and Van Praag, H.M. (1991). Serotonin receptor sensitivity and aggression. *Psychiatric Research*. **37**: 271-279.
- Whitesell, L., Geselowitz, D., Chavany, C., Fahmy, B., Walbridge, S., Alger, J.R., and Neckers, L.M. (1993). Stability, clearance and deposition of intraventricularly administered oligodeoxynucleotides: implications for therapeutic application within the central nervous system. *The Proceedings of the National Academy of Sciences of the USA*. **90**: 4665-4669.
- Wickstrom, E. (1986). Oligonucleotide stability in subcellular extracts and culture media. *The Journal of Biochemical and Biophysical Methods*. **13**: 97-102.
- Widnell, K.L., Self, D.W., Lane, S.B., Russell, D.S., Vaidya, V.A., Miserendino, M.J., Rubin, C.S., Duman, R.S., and Nestler, E.J. (1996). Regulation of CREB expression: *In vivo* evidence for a functional role in morphine action in the nucleus accumbens. *Journal of Pharmacology and Experimental Therapy*. **276**: 306-315.

- Wilchek, M., and Bayer, E.A. (1990). Application of avidin-biotin technology-Literature survey. *Methods in Enzymology*. **184**: 14-45.
- Williams, S.A., Chang, L., Buzby, J.S., Suen, Y., and Cairo, M.S. (1996). Cationic lipids reduce time and dose of c-myc antisense oligodeoxynucleotides required to specifically inhibit Burkitt's lymphoma cell growth. *Leukemia*. **10**: 1980-1989.
- Wilson, M., Greer, S.E., Greer, M.A., and Roberts, L. (1980). Hippocampal inhibition of pituitary-adrenocortical function in female rats. *Brain Research*. **197**: 433.
- Wohlpert, K.L., and Molinoff, P.B. (1997). Advances in serotonin receptor research. In: Regulation of levels of 5-HT_{2A} receptor mRNA. Martin, G.R., Eglén, R.M., Hoyer, D., Hamblin, M.W., Yocca, F. (Eds). *Annals New York Academy of Sciences*. **861**: 128-135.
- Wojcik, W.J., Swoveland, P., Zhang, X., and Vanguri, P. (1996). Chronic intrathecal infusion of phosphorothioate or phosphodiester antisense oligonucleotides against cytokine responsive gene-2/IP-10 in experimental allergic encephalomyelitis of Lewis rat. *Journal of Pharmacology and Experimental Therapy*. **278**: 404-410.
- Woolf, T.M., Jennings, C.G., Rebagliati, M., and Melton, D.A. (1990). The stability, toxicity and effectiveness of unmodified and phosphorothioate antisense oligodeoxynucleotides in *Xenopus* oocytes and embryos. *Nucleic Acids Research*. **18**: 1763-1769.
- Wrobel, I., and Collins, D. (1995). Fusion of cationic liposomes with mammalian-cells occurs after endocytosis. *Biochimica et Biophysica acta-Biomembranes*. **1235**: 296-304.
- Wu, H.C., Chen, K.Y., Lee, W.Y., and Lee, E.H. (1997). Antisense oligonucleotides to corticotrophin-releasing factor impair memory retention and increase exploration in rats. *Neuroscience*. **78**: 147-153.
- Wu-Pong, S., Weiss, T.L., and Hunt, C.A. (1994). Calcium dependent cellular uptake of a c-myc antisense oligonucleotide. *Cellular Molecular Biology*. **40**: 843-850.
- Wyman, T.B., Nicol, F., Zelphati, O., Scaria, P.V., Plank, C., and Szoka, F.C. (1997). Design, synthesis, and characterisation of a cationic peptide that binds to nucleic acids and permeabilises bilayers. *Biochemistry*. **36**: 3008-3017.
- Yaida, Y., and Nowak, T.S. Jnr. (1995). Distribution of phosphodiester and phosphorothioate oligonucleotides in rat brain after intraventricular and intrahippocampal administration determined by *in situ* hybridisation. *Regulatory Peptides*. **59**: 193-199.
- Yakubov, L.A., Deeva, E.A., Zarytova, V.F., Ivanova, E.M., Ryte, A.S., Yurchenko, L.V., and Vlassov, V.V. (1989). Mechanism of oligonucleotide uptake by cells: involvement of specific receptors? *The Proceedings of the National Academy of Sciences of the USA*. **86**: 6454-6458.

- Yamada, K., Moriguchi, A., Morishita, R., Aoki, M., Nakamura, Y., Mikami, H., Oshima, T., Ninomiya, M., Kaneda, Y., Higaki, J., and Ogihara, T. (1996). Efficient oligonucleotide delivery using the HVJ-Liposome method in the central nervous system. *American Journal of Physiology*. **40**: R1212-R1220.
- Yamamoto, T., Yamamoto, S., Kataoka, T., and Tokunaga, T. (1994). Ability of oligonucleotides with certain palindromes to induce interferon-production and augment natural killer-cell activity is associated with their base length. *Antisense Research and Development*. **4**: 119-122.
- Yamashiro, D.J., and Maxfield, F.R. (1987). Kinetics of endosome acidification in mutant and wild-type Chinese-hamster ovary cells. *Journal of Cellular Biology*. **105**: 2713-2721.
- Yaroslavov, A.A., Kulkov, V.E., Polinsky, A.S., Baibakov, B.A., and Kabanov, V.A. (1994). A polycation causes migration of negatively charged phospholipids from the inner to outer leaflet of the liposomal membrane. *FEBS Letters*. **340**: 121-123.
- Yates, M., Leake, A., Candy, J.M., Fairbairn, A.F., McKeith, I.G., and Ferrier, I.N. (1990). 5-HT₂ receptor changes in major depression. *Biological Psychology*. **27**: 489-496.
- Yee, F., Ericson, H., Reis, D.J., and Wahlestedt, C. (1994). Cellular uptake of intracerebroventricularly administered biotin- or digoxigenin-labelled antisense oligodeoxynucleotides in the rat. *Cellular Molecular Neurobiology*. **14**: 475-486.
- Young, E.A., Haskett, R.F., Murphy-Weinberg, V., Watson, S.J., and Akil, H. (1991). Loss of glucocorticoid fast feedback in depression. *Archives of General Psychiatry*. **48**: 693-699.
- Zabner, J. (1997). Cationic lipids used in gene transfer. *Advanced Drug Delivery Reviews*. **27**: 17-28.
- Zamecnik, P., and Stephenson, M. (1978). Inhibition of Rous sarcoma virus replication and cell transformation by a specific oligodeoxynucleotide. *The Proceedings of the National Academy of Sciences of the USA*. **75**: 280-284.
- Zapata, A., Capdevila, J.L., Tarrason, G., Adan, J., Martinez, J.M., Piulats, J., and Trullas, R. (1997). Effects of NMDA-R1 antisense oligodeoxynucleotide administration: Behavioural and radioligand binding studies. *Brain Research*. **745**: 114-120.
- Zelphati, O., Francis, C., and Szoka, Jr. (1996). Intracellular distribution and mechanisms of delivery of oligonucleotide mediated by cationic lipids. *Pharmaceutical Research*. **13**: 1367-1372.
- Zelphati, O., and Szoka, F.C. Jr. (1996). Mechanism of oligonucleotide release from cationic liposomes. *The Proceedings of the National Academy of Sciences of the USA*. **93**: 11943-11948.
- Zhang, M., and Creese, I. (1993). Antisense oligodeoxynucleotide reduces brain dopamine D₂ receptors: behaviour correlates. *Neuroscience Letters*. **161**: 223-226.

Zhang, S-P., Zhou, L-W., Morabito, M., Lin, R.C.S., and Weiss, B. (1996). Uptake and distribution of fluorescein-labelled D₂ dopamine antisense oligodeoxynucleotide in mouse brain. *Journal of Molecular Neuroscience*. **7**: 13-28.

Zhao, Q., Matson, S., Herrera, C.J., Fisher, E., Yu, H., and Krieg, A.M. (1993). Comparison of cellular binding and uptake of antisense phosphodiester, phosphorothioate and mixed phosphorothioate and methylphosphonate oligonucleotides. *Antisense Research and Development*. **3**: 53-66.

Zhou, X., and Huang, L. (1994). DNA transfection mediated by cationic liposomes containing lipopolylysine: characterisation and mechanism of action. *Biochimica et Biophysica Acta*. **1189**: 195-203.

Zhou, L.W., Zhang, S.P., and Weiss, B. (1996). Intrastratial administration of an oligodeoxynucleotide antisense to the D₂ dopamine receptor mRNA inhibits D₂ dopamine receptor-mediated behaviour and D₂ dopamine receptors in normal mice and in mice lesioned with 6-hydroxydopamine. *Neurochemistry-International*. **29**: 583-595.

Zon, G. (1995). Brief overview of control of genetic expression by antisense oligonucleotides and *in vivo* applications. *Molecular Neurobiology*. **10**: 219-229.

Zon, G., Iyer, R.P., Uznanski, B., Boal, J., Storm, C., Egan, W., Matsukura, M., Broder, S., Wilk, A., Koziolkiewicz, M., and Stec, W.J. (1990). A basic oligodeoxyribonucleoside phosphorothioates-synthesis and evaluation as anti-HIV-1 agents. *Nucleic Acids Research*. **18**: 2855-2859.